VISMEDERI

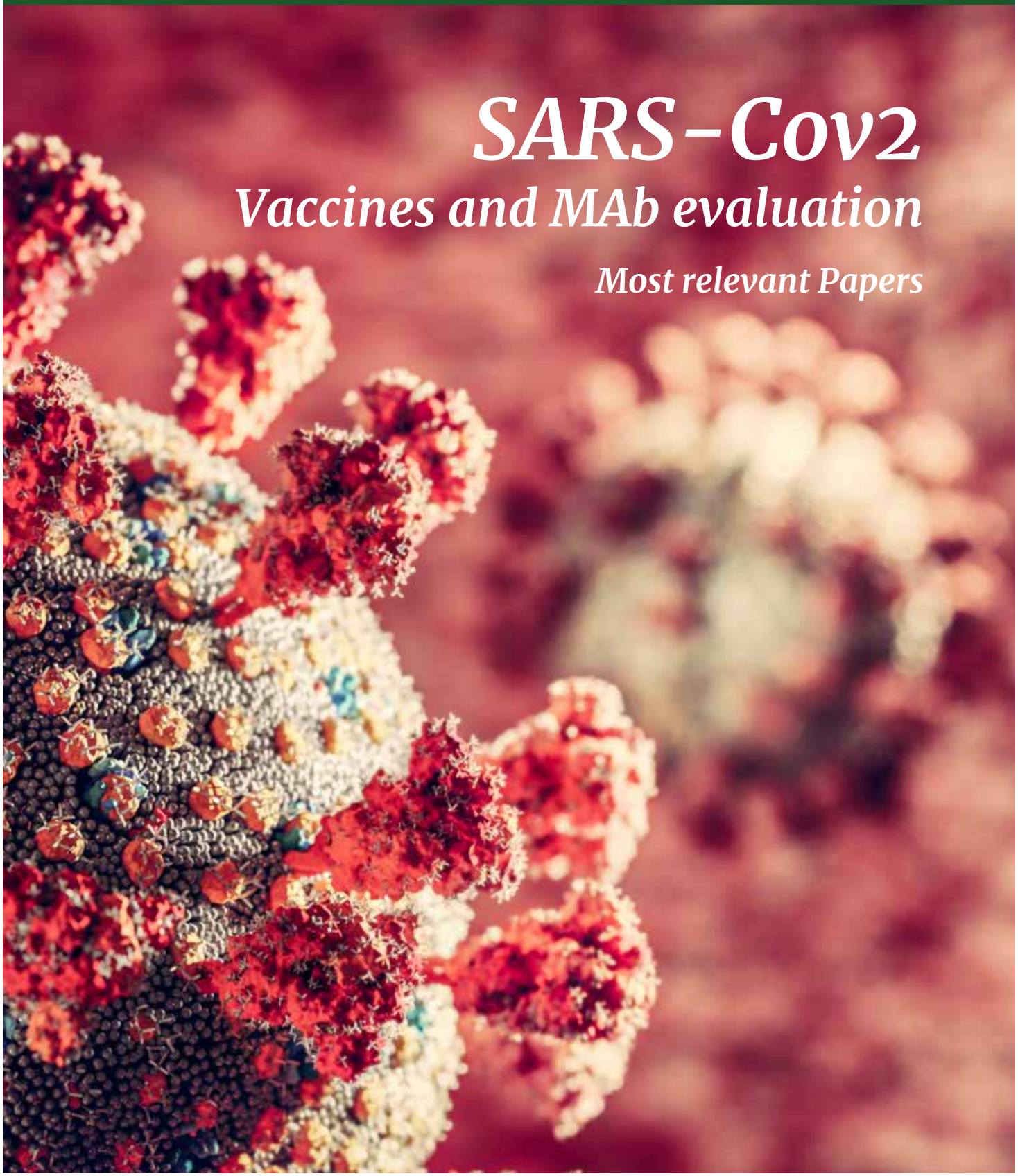

SARS-Cov2

Vaccines and MAb evaluation

Most relevant Papers

www.vismederi.com / info@vismederi.com

INDEX

frontiers in Public Health

ORIGINAL RESEARCH
published: 31 March 2022
doi: 10.3389/fpubh.2022.847384

Cellular and Humoral Immune Responses and Breakthrough Infections After Two Doses of BNT162b Vaccine in Healthcare Workers (HW) 180 Days After the Second Vaccine Dose

Alessandra Mangia[1]*, *Nicola Serra*[2], *Giovanna Cocomazzi*[1], *Vincenzo Giambra*[3], *Stefano Antinucci*[4], *Alberto Maiorana*[5], *Francesco Giuliani*[6], *Emanuele Montomoli*[7,8], *Paolo Cantaloni*[8], *Alessandro Manenti*[8] and *Valeria Piazzolla*[1]

[1] Liver Unit, Fondazione IRCCS "Casa Sollievo della Sofferenza", San Giovanni Rotondo, Italy, [2] Department of Public Health, University "Federico II", Naples, Italy, [3] Institute for Stem Cell Biology, Regenerative Medicine and Innovative Therapies (ISBReMIT), San Giovanni Rotondo, Italy, [4] Allergy Diagnostic Section Euroimmun, Italy Fondazione "Casa Sollievo della Sofferenza", San Giovanni Rotondo, Italy, [5] GSSL Unit, Fondazione "Casa Sollievo della Sofferenza", San Giovanni Rotondo, Italy, [6] ICT Innovation and Research Unit, Fondazione IRCCS "Casa Sollievo della Sofferenza", San Giovanni Rotondo, Italy, [7] Department of Molecular and Developmental Medicine, University of Siena, Siena, Italy, [8] VisMederi Srl, Siena, Italy

OPEN ACCESS

Edited by:
Marc Jean Struelens,
Université libre de Bruxelles, Belgium

Reviewed by:
Diego Cantoni,
University of Kent, United Kingdom
Riccardo Castagnoli,
National Institute of Allergy and Infectious Diseases (NIH), United States

***Correspondence:**
Alessandra Mangia
a.mangia@tin.it

Specialty section:
This article was submitted to Infectious Diseases - Surveillance, Prevention and Treatment, a section of the journal Frontiers in Public Health

Received: 16 January 2022
Accepted: 21 February 2022
Published: 31 March 2022

Citation:
Mangia A, Serra N, Cocomazzi G, Giambra V, Antinucci S, Maiorana A, Giuliani F, Montomoli E, Cantaloni P, Manenti A and Piazzolla V (2022) Cellular and Humoral Immune Responses and Breakthrough Infections After Two Doses of BNT162b Vaccine in Healthcare Workers (HW) 180 Days After the Second Vaccine Dose. Front. Public Health 10:847384. doi: 10.3389/fpubh.2022.847384

Background: Immunity and clinical protection induced by mRNA vaccines against SARS-CoV-2 have been shown to decline overtime. To gather information on the immunity profile deemed sufficient in protecting against hospitalization, we tested IgG levels, interferon-gamma (IFN-γ) secretion, and neutralizing antibodies 180 days (d180) after the second shot of BNT162b vaccine, in HW.

Methods: A total of 392 subjects were enrolled. All received BioNTech/Pfizer from February 2020 to April 2021. The vaccine-specific humoral response was quantitatively determined by testing for IgG anti-S1 domain of SARS-CoV-spike protein. Live virus microneutralization (MN) was evaluated by an assay performing incubation of serial 2-fold dilution of human serum samples, starting from 1:10 to 1:5120, with an equal volume of Wuhan strain and Delta VOC viral solution and assessing the presence/absence of a cytopathic effect. SARS-CoV-2-spike protein-specific T-cell response was determined by a commercial IFN-γ release assay.

Results: In 352 individuals, at d180, IgG levels decreased substantially but no results below the assay's positivity threshold were observed. Overall, 22 naive (8.1%) had values above the highest threshold. Among COVID-naive, the impact of age, which was observed at earlier stages, disappeared at d180, while it remained significant for 81 who had experienced a previous infection. Following the predictive model of protection by Khoury, we transformed the neutralizing titers in IU/ml and used a 54 IU/ml threshold to identify subjects with 50% protective immunity. Overall, live virus MN showed almost all subjects with previous exposure to SARS-CoV-2 neutralized the virus as compared to 33% of naive double-dosed subjects ($p < 0.0001$). All previously exposed subjects

had strong IFN-γ secretion (>200 mIU/ml); among 271 naive, 7 (2.58%) and 17 (6.27%) subjects did not show borderline or strong secretion, respectively.

Conclusions: In naive subjects, low IgG titers are relatively long-lasting. Only a third of naive subjects maintain neutralizing responses. After specific stimulation, a very limited number of naive were unable to produce IFN-γ. The results attained in the small group of subjects with breakthrough infection suggest that simultaneous neutralizing antibody titers <20, binding antibody levels/ml <200, and IFN-γ < 1,000 mIU/ml in subjects older than 58 may identify at-risk groups.

Keywords: SARS-CoV-2, mRNA vaccines, humoral response, IFN-γ, healthcare workers

INTRODUCTION

Several studies on the durability of humoral response in subjects recovered from SARS-CoV-2 infection showed that both binding and neutralizing antibody levels decrease only modestly at month 8 after the infection (1, 2). This evidence initially suggested that vaccinated persons and previously infected would experience a low number of breakthrough infections. However, the durability of immunity has been called into question by the mounting evidence of reinfections after natural recovery (3). Moreover, a progressive decline in humoral immune response has been shown after vaccination (4). In our experience, in a cohort of healthcare workers, this decline was shown to start from d90 after the first shot (5). These results were in agreement with larger cohort studies (4) and suggest that after vaccination or infection, several mechanisms of immunity exist both at the antibody level and at the level of cellular immunity.

Moderna and Pfizer vaccines using a mutated sequence of the receptor-binding domain (RDB) that contains two consecutive prolines, lysine 986, and valine 987 (6) have been associated with high protection rates (7). Accumulating evidence demonstrates that the two doses of the BNT162b vaccine elicit either high IgG or neutralizing antibody responses (8, 9). Neutralizing antibodies were shown to correlate with protection and may be used to assess effective vaccine-induced humoral response (10) However, there is scarce applicability of neutralizing assays in the routine practice as neutralizing tests are complex, time-consuming, and not always comparable across assays (11). In addition, a time-dependent neutralizing activity regression relationship with IgG levels has been demonstrated (4).

It has recently been shown that fully vaccinated people remain at the risk for SARS-CoV-2 infections and Pfizer's CEO announced in October 2021, the need for a booster within 12 months of the first dose (12–14). In a recent study from Israel, involving participants 60 years old, 5 months after two doses of BioNTech/Pfizer vaccine, rates of infection and severe illness were lower among those who received a booster injection as compared to participants who did not (15).

Evidence suggests that humoral response alone may not offer sufficient protection against either infection or disease, and SARS-CoV-2-specific cellular immunity may be more stable and longer-lasting than humoral immunity (1). It has been, therefore, hypothesized, based on experimental models, that CD4+ and CD8+ T-cells and production of IFN-γ play an important role in vaccination immune response (16).

We analyzed – by age, gender, and previous SARS-CoV-2 infection history –the binding and neutralizing antibody response induced by the BioNTech/Pfizer vaccine 180 days after the second vaccine shot in our cohort of almost 400 healthcare workers longitudinally followed up to 180 days after the second dose of BioNTech/Pfizer. The subjects' early humoral response had been previously reported to decline 90 days after the first vaccine dose (5). Spike-specific T-cell-mediated reactivity using an IFN-γ release assay, with the aim to gather information about cellular immune response, was also evaluated.

METHODS

Our analysis was based on the medical data from the multicenter longitudinal study (Covidiagnostix, funded by the Italian Ministry of Health) to investigate the antibody response in Healthcare workers vaccinated with BioNTech/Pfizer starting from February 11, 2020, and ending on April 11, 2021. All the subjects received two vaccine injections 21 days apart. The planned testing time for binding antibodies was day 0 (d0) (before the first dose), day 7 (d7), day 21 (d21), day 31 (d31) after the first shot, and day 90 (d90) 60 days after the second shot, day 180 (d180) days after the second shot corresponding to 210 days after the first shot, respectively.

We excluded the participants who do not have the complete set of blood sample collection. Blood samples were collected into clot activator BD vacutainer tubes (Becton Dickinson, Franklin Lakes, NJ, USA). The margin of sampling window for each time-point was of 2 days.

Antibody Evaluation

The vaccine-specific humoral immune response was quantitatively determined by testing for antiS1 and SARS-CoV-spike protein (EUROIMMUN, anti-SARS-CoV-2 QuantiVac enzyme-linked immunosorbent assay) with a positive cut-off of at least 3.2 Binding Arbitrary Unit (BAU) ml. This assay was designed to evaluate vaccine response and calibrated against WHO standards in order to provide results in BAU (17). The cut-off for positivity was 35.2 BAU, low quantitation limit 3.2 BAU/ml at 1:101 dilution, and range (3.2–384.0 BAU/ml). Results

25.6 but <35.2 were considered borderline (18). Specificity and sensitivity (>10 days after diagnosis) are 99.8 and 90.3%, respectively, when the manufacturer's suggested cut-off of 35.2 BAU/ml is used. A solution used for diluting samples above 348 U/ml was included in the measurement kits.

The SARS-CoV-2 spike protein-specific T-cell response was determined by a commercial, standardized interferon-gamma (IFN-γ) release assay (IGRA) using the EUROIMMUN SARS-CoV-2 IGRA stimulation tube set (product No. ET 2606-3003) and EUROIMMUN IFN-γ ELISA (product No. EQ 6841-960). The specific T-cell response was quantified according to the manufacturer's instructions and values >100 mIU/ml were interpreted as low positive, >200 mIU/ml as positive (19).

Cell Culture

VERO E6 C1008 cells (CRL-1586) were cultured in Dulbecco's Modified Eagle's Medium (DMEM), High Glucose (Euroclone), supplemented with 2 mM L-glutamine (Lonza), 100 units/ml Penicillin–Streptomycin mixture (Lonza), and 10% fetal bovine serum (FBS) (Euroclone), in 37°C and 5% CO2 humidified incubator. Adherent sub confluent cell monolayers of VERO E6 were prepared in DMEM high glucose containing 2% FBS in 96 well plates for virus titration and neutralization tests.

Micro-Neutralization Experiments

The micro-neutralization (MN) assay was performed as previously reported (20, 21). Briefly, serial 2-fold dilution of human serum samples, starting from 1:10 to 1: 5120, were incubated with an equal volume of SARS-CoV-2 (Wuhan Strain and Delta VOC) viral solution containing 25 tissue culture infective dose 50% (TCID50) for 1 h at RT (21). After incubation, 100 µl of the serum–virus mixture was transferred to a 96-well plate containing an 80% sub-confluent Vero E6 cell monolayer. The plates were incubated for 3 days (Wuhan strain) and 4 days (Delta strain) at 37°C and 5% CO_2. At the end of incubation, the presence/absence of cytopathic effect (CPE) was assessed by means of an inverted optical microscope. A CPE higher than 50% was indicative of infection. The MN titer was expressed as the reciprocal of the highest serum dilution showing protection from viral infection and CPE. The titer of 10 was considered as the lower limit of quantitation (LLOQ) and a titer equal to 5 was considered as negative. All experiments with live SARS-CoV-2 viruses were performed inside the Biosecurity Level 3 laboratories of VisMederi Srl. Standardization of neutralizing titers was made following the guidelines of the NIBSC 20/136 document[1].

COVID-19 Diagnostic Data

As part of preventive medicine practice, healthcare workers were subjected to routine RT-PCR swab testing using a Real-Time Reverse transcription PCR kit on a Roche Cobas Z480 thermocycler (Roche Diagnostic, Basel, Switzerland). RNA purification was performed using Roche Magna pure system (Roche Diagnostic, Basel, Switzerland). Both the results of the swab test and the clinical information collected in a dedicated questionnaire were used to confirm the previous SARS-CoV-2 infection and were compared to the results of the COVID-19 Regional Registry.

[1]https://www.nibsc.org/documents/ifu/20-136.pdf

Ethics Approval

All healthcare workers provided written consent in accordance with local review board requirements. Laboratory investigations and available clinical data were collected and analyzed according to the protocol COVIDIAGNOSTIX approved by the EC review board at our institution and funded by the Ministry of Health of Italy, "Bando Ricerca COVID-19," project number: COVID-2020-12371619; project title: COVIDIAGNOSTIX—Health Technology Assessment in COVID serological diagnostics.

Statistical Analysis

Data were presented as numbers and percentages for categorical variables. Continuous variables were expressed as mean ± *SD* or median with interquartile range (*IQR*). Test for Normal distribution was performed by Shapiro–Wilkson test. The *T*-test was used to compare the mean of unpaired samples. When the distribution of samples was not normal, a *T*-test with logarithmic transformation was performed. Alternative non-parametric tests such as Mann–Whitney test were used when distribution was not normal. Differences between groups were analyzed using the chi-square test or Fisher's exact test for categorical variables.

Linear regression was used to describe the relationship between two variables and to predict one variable from another. In a scatter diagram with a regression line, the relation between two variables was presented graphically, and the linear correlation coefficient and *p*-value were reported.

Tests with *p-value (p)* < 0.05 were considered significant. The statistical analysis was performed by Matlab statistical toolbox version 2008 (MathWorks, Natick, MA, USA) for Windows at 32 bit.

Logistic regression was used to find the best fitting model to describe the relationship between the dichotomous characteristic of interest (dependent variable) and a set of independent variables.

RESULTS

Serological Evaluation by the Previous History of SARS-CoV-2 Infection at day 180 After the Second Dose

Of 392 enrolled subjects, 352 were analyzed, as 40 (10.2%) had to be excluded because they did not complete the planned sample collection. The mean age was 47.7 years ± 11.8. Of the total participants, 57.2% were female; 271 had no experience of the previous infection and were defined as naive. Subjects infected before or immediately after the first vaccine dose ($n = 81$) were classified as experienced.

Of 271 naive, the female prevalence was 58.3%, and the mean age was 47.55 years ± 11.85. The mean values of IgG antibodies were 212.93 ± 182.98 BAU/ml (**Table 1**). None had results below the 35.2 BAU/ml positivity assay threshold. Overall, 22 individuals (8.1%) had antibody values above the highest

TABLE 1 | Baseline characteristics, antibody levels, neutralizing antibody titers, and IFN-γ concentration of vaccinated subjects.

	Prior COVID-19 experience		
	Yes (*n* = 81)	**No (*n* = 271)**	***p* value**
Age, mean (SD), years Median (IQR)	49.71 (12.32) 51 (40.75–59.25)	47.55 (11.85) 47 (39.0–57.0)	0.20
Sex: Male Female	38 (46.9) 43 (53.1)	113 (41.7) 158 (58.3)	0.41
Baseline SARS-CoV-2-IgG No (%)	79 (97.31)	0	$p < 0.0001$
Day 180 SARS-CoV-2-IgG, No (%)	81(100)	271 (100)	$p = 1$
Day 180 SARS-CoV2-IgG level Mean, (SD) BAU/ml Median (IQR)	418.81 ± 415.01 248.96 (140.48–610.0)	212.93 ± 182.98 179.79 (90.0–287.19)	$p < 0.0001$
Day 180* SARS-CoV2-IgG level >384 BAU/ml Mean, (SD) BAU/ml Median (IQR)	778.04 ± 40.15 630.41 (548.32–895.72)	630.50 ±361.46 489.93 (398.31–666.08)	$p = 0.092$
Day 180 Neutralizing antibody >10, No (%)	81 (100)	178 (65.89)	<0.0001
Day 180 Neutralizing antibody Mean (SD) Median (IQR)	419.08 ± 430.75 231.52 (138.46-612.16)	229.27 ± 213.92 200 (90.0–310–72)	$p = 0.0009$
Day 180** Neutralizing antibody >320 Mean, SD Median (IQR)	740.24 ± 588.37 663.36 (209.04–921.54)	246.09 ± 65.17 246.09 (200.0–292.17)	$p = 0.32$
Day 180 IFN-γ No (%) >100 mIU/ml	81 (100)	267 (98.52)	0.58
Day 180 IFN-γ No (%) >200 mIU/ml	81 (100)	254 (93.72)	0.0161
Day 180 IFN-γ >100 mIU/ml Mean (SD) Median (IQR)	2,299.97 ± 491.25 2,499.0 (2,400.0–2,500.0)	1,201.24 ± 846.24 926.0 (463.0–2,272.0)	$p < 0.0001$

IgG Mean values for subjects with results above the highest threshold of the assay; Mean titers of neutralizing antibodies among subjects with titers associated with strong neutralizing capacity.*

threshold. Their mean values were 630.50 ± 361.46 BAU/ml. No difference was observed by gender.

Among 81 experienced, the female was 53.1%. The mean age was 49.71 ± 12.32. At d180 after the second dose (210 days after the first vaccination), the mean values were 418.81 BAU/ml ± 415.01. None had results below the assay's threshold. Overall, 41.03% had results above the 384.0 BAU/ml (**Table 1**). Their mean values were 778.04 ± 40.15 BAU/ml. Values for men and women were not different regardless of the threshold used. Comparison between IgG levels in naive and experienced is depicted in a graph (**Figure 1**).

The impact of age on binding antibody levels was then investigated (**Table 2**). Within the naive group, stratification of

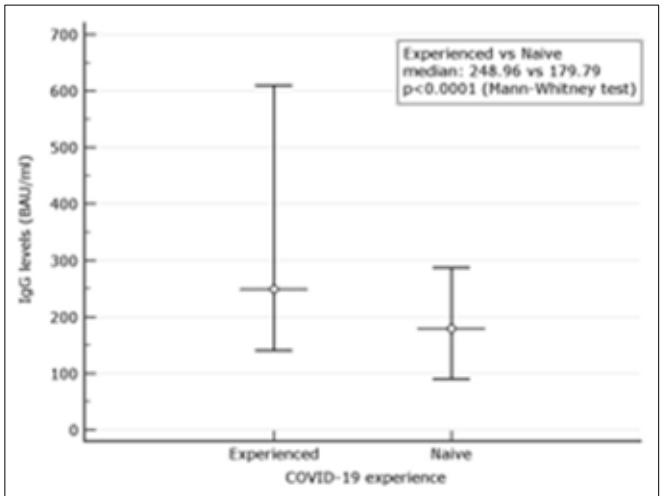

FIGURE 1 | Comparison between IgG levels in naive and experienced. Mean and Interquartile ranges (*IQR*) are reported ($p < 0.0001$).

TABLE 2 | Comparison of IgG levels in subjects previously infected or naive by age younger or older than 47 years.

IgG levels (age ≤47) Mean±SD Median (IQR)	224.58 ± 198.12 200.0(95.63;298.87)	274.11 ± 231.78 211.36 (126.40;310.0)	0.32
IgG levels (age >47) Mean±SD Median (IQR)	200.75 ± 165.55 169.84(90.0;268.87)	530.62 ± 487.68 412.82 (165.44;642.93)	<0.0001

SD, standard deviation; IQR, Interquartile range; Median and IQR were used for data with no normal distribution.

binding antibody levels by median age of 47 years revealed no difference. When subjects older than 47 years were compared to the younger patients, median levels of 169.84 (90.0–268.87) BAU/ml *vs.* 200.0 (95.63–298.87) BAU/ml ($p = 0.40$) were observed. At variance, within the experienced group, older had higher median age than younger 412.82 (165.44–642.93) *vs.* 211.36 (126.40–310.00) ($p = 0.0043$). This inverse relationship with the age within the experienced group was also observed although at a not significant level at d90, 60 days after the second shot ($p = 0.087$). At earlier time points, as reported in our previous experience (5), the difference between higher median IgG levels in younger *vs.* older was significant also within the naive group (median age of younger of 1026.0 (489.01 *vs.* 1690.01) *vs.* 720.12 (479.35–1251.02) ($p = 0.022$). Trend analysis of the three different time points IgG levels using median was performed ($p < 0.0001$ for both younger and older than 47 years) (**Figure 2**).

Neutralizing Antibodies Results

When the neutralizing titers were analyzed, 100% of previously infected patients and 178 (65.89%) of naive showed a titer of ≥10 (LLoQ). Individuals with titers associated with stronger neutralizing capacity associated to a dilution > 320 were 2 (0.73%) among naive and 25 (31.2%) among 80 experienced ($p < 0.0001$). Median neutralizing titers of 200 (90.0–310.72) were observed among 271 naive. The corresponding value among

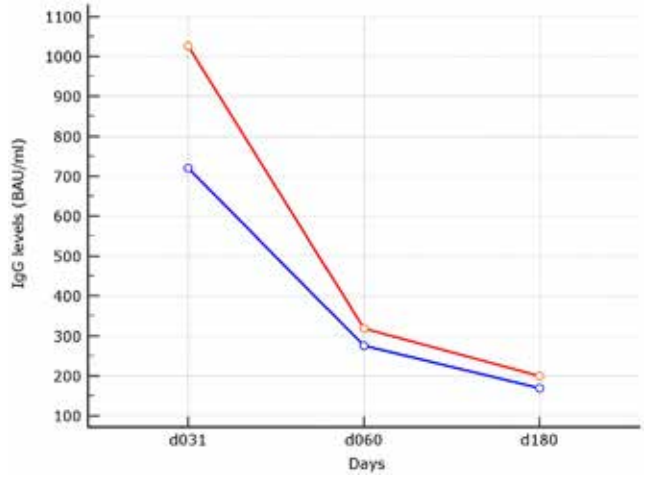

FIGURE 2 | Trend analysis of IgG levels at the different time points. In red median of IgG levels in subjects with median age ≤ 47 years. In blue median of IgG levels in subjects older than 47 years, linear trend was statistically significant for both ($p < 0.0001$).

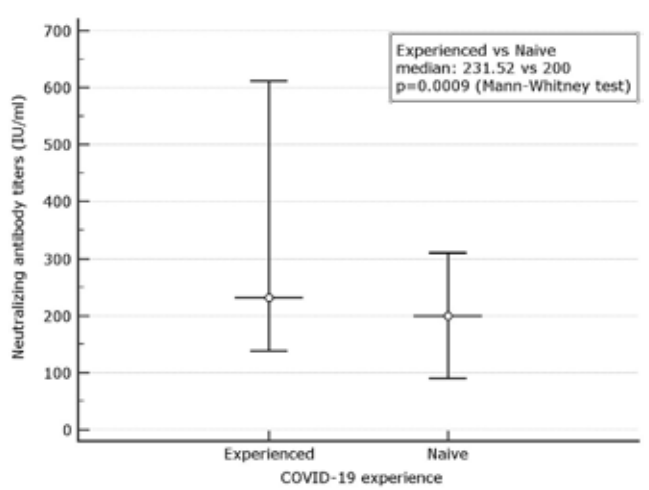

FIGURE 3 | Comparison between microneutralization results in naive and experienced. Mean and Interquartile ranges (*IQR*) are reported ($p = 0.0009$).

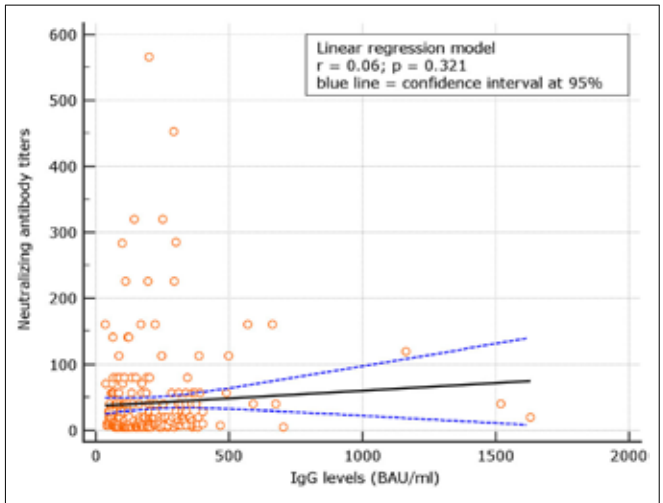

FIGURE 4 | Correlation between neutralizing antibody titers and IgG levels among naive.

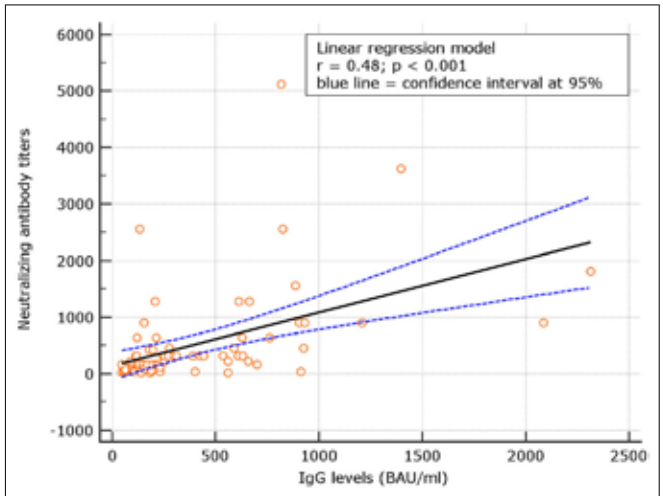

FIGURE 5 | Correlation between neutralizing antibody titers and IgG levels among experienced.

experienced was 231.52 (138.46–612.16) (**Figure 3**). When only subjects with strong neutralizing titers (>320) were analyzed, the median titers were 246.09 (200.0–292.17) for naive and 663.36 (209.04–921.54) for experienced. Following the predictive model of protection suggested by Khoury et al. (22) and using the standard IU/ml results suggested by WHO as a reference to normalize the different neutralizing testing[1], we transformed the neutralizing titers in IU/ml and used a 54 IU/ml threshold to identify subjects with 50% protective humoral immunity. Overall, 32.78% of naive and 91.89% of previously infected ($p < 0.0001$) showed protective neutralizing activity.

Correlation Between IgG and Neutralizing Antibodies

No correlation was observed between neutralizing antibody titers and IgG levels for naive ($r = 0.06$; $p = 0.321$), at d180. At variance, for experienced, the correlation was significant ($p = 0.48$; $p < 0.001$) (**Figures 4**, **5**). Despite the analysis of neutralizing antibody, IU/ml ≥54 conversions, we failed to observe correlation with binding antibody.

IFN-γ Results

The spike-specific T-cell response was assessed by semi-quantitative analysis of IFN-γ release. Overall, at d180, a borderline T-cell response (cutoff > 100 mIU/ml) as well as a stronger response (cutoff > 200 mIU/ml) was detectable in all the 81 experienced. Among 271 naive, 7 (2.58%) and 17 (6.27%) did

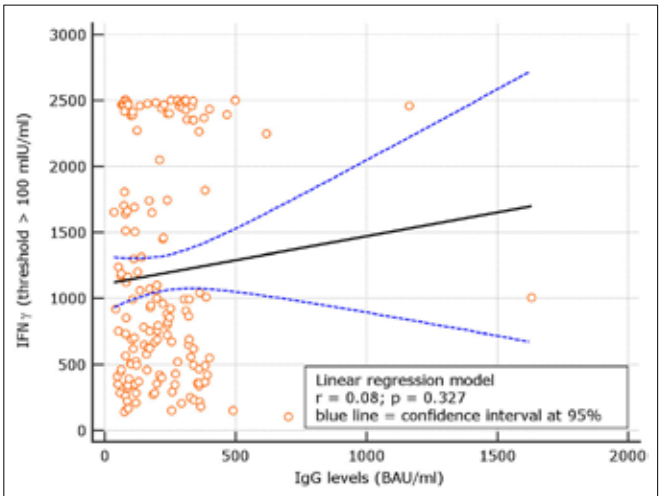

FIGURE 6 | Day 180, linear regression between IgG levels and IFN-γ concentration among naive group using the IFN-γ threshold of 100 mIU/ml.

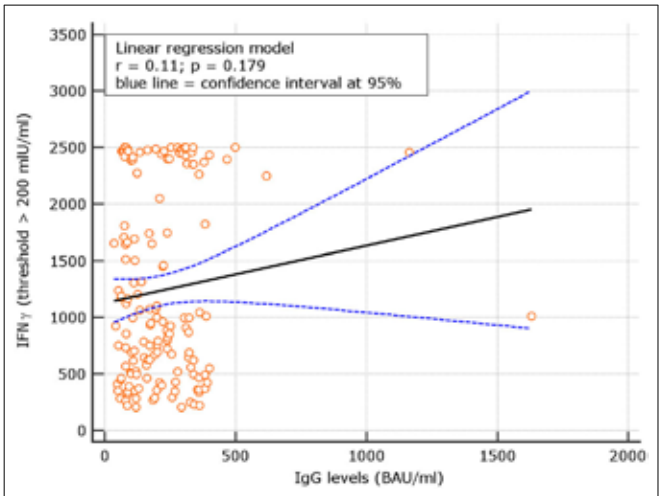

FIGURE 7 | Linear regression between IgG levels and IFN-g concentration among COVID naive group using the IFN-γ threshold of 200 mIU/ml.

not show borderline or strong responses, respectively (**Table 1**). The difference between median IFN-γ concentration of 254 (93.7%) naive and 81 (100%) previously experienced subjects was significant with values of 223.0 (463.0–2,272.0) mIU/ml vs. 2,499.0 (2,400.0–2,500.0) mIU/ml, respectively, ($p < 0.0001$) when IFN-γ concentration higher than 200 IU/ml was analyzed.

Correlation Between IgG Levels and IFN-γ in Naive

Levels of IgG at d180 were correlated with IFN-γ concentrations in subjects with results >100 IU/ml. A not significant correlation with $r = 0.08$, $p = 0.344$ was observed. Using a IFN-γ threshold > 200 IU/ml, a similar not significant correlation with $r = 0.11$, $p = 0.192$ was found (**Figures 6**, **7**). At variance, when levels of IgG at d60, 90 days after the first vaccine dose (5) were correlated with IFN-γ concentrations in subjects with results >100 IU/ml, at that time point, results were statistically significant $r = 0.28$, $p = 0.031$; similar results were attained using at d90 the threshold of >200 IU/ml (additional **Figures 1**, **3**). Thesedata support an overtime decline of humoral response but not of lymphocyte IFN-γ.

Correlation Between Neutralizing Antibodies and IFN-γ

An interesting correlation between neutralizing titers and IGRA levels was found for both naive and experienced. The results showed $r = 0.26$; $p = 0.001$ for naive and $r = 0.18$ $p = 0.134$, respectively (**Figures 8**, **9**). The significance of the correlation increased for naive when the IFN-γ positive threshold of 200 was used ($r = 0.25$; $p = 0.003$) and did not change for experience given the identical number of subjects with IFN-γ concentration >100 and >200 thresholds in this group (**Figure 10**). The regression curves for naive (at both

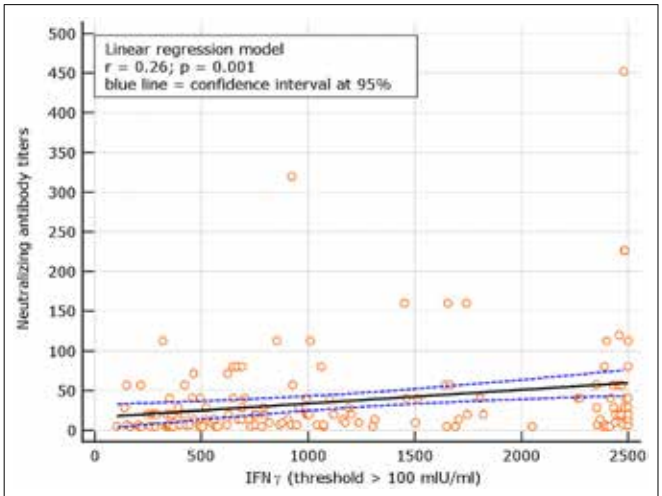

FIGURE 8 | Linear regression model between neutralizing antibody titers and IFN-γ concentration in naive (with IFN-γ threshold > 100 mIU/ml).

IFN-γ positivity thresholds) and experienced are reported in **Figures 8**–**10**.

Breakthrough Infections

Breakthrough infections were observed in 6 cases among naive fully vaccinated subjects (2.2%). Characteristics of subjects experiencing infection are shown in **Table 3**. In all the cases, the infection was mild, none of the subjects required hospitalization. A persistently positive swab result was observed in almost all (mean positivity duration 4.5 ± 2.3 weeks). For 4 out of 6, a common unvaccinated index case was identified. The remaining two cases came from the same household, where one of the individuals, a healthcare worker, was exposed and exposed to the second individual within the household. Demographic, virologic, and immunologic

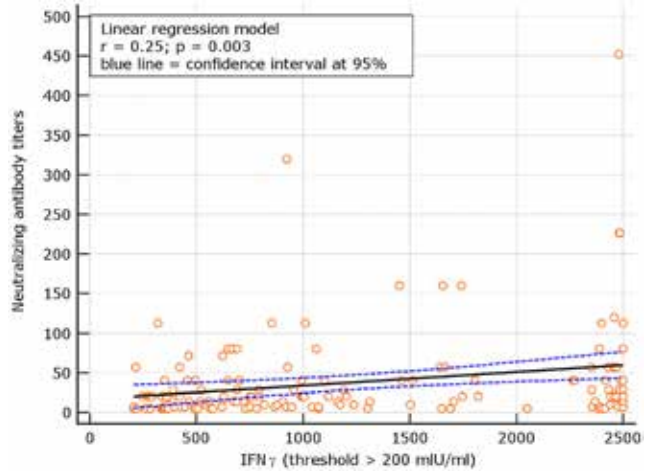

FIGURE 9 | Linear regression model for correlation between neutralizing antibody dilutions and IFN-γ concentration in naive (with IFN-γ concentration > 200 mIU/ml).

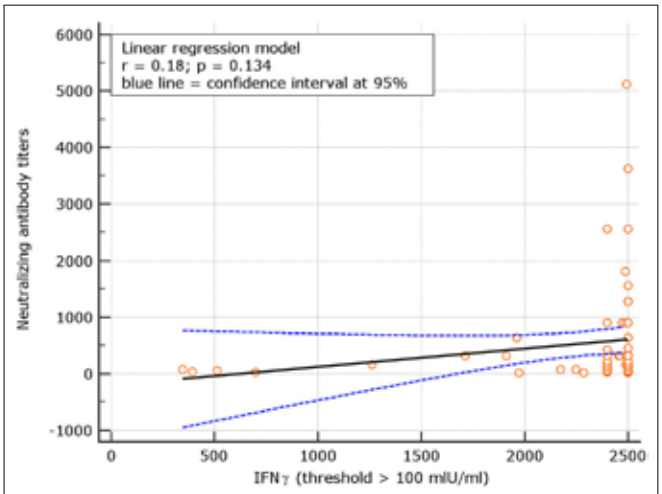

FIGURE 10 | Linear regression model for correlation between neutralizing antibody titers and IFN-γ concentration in experience (similar results for IFN-γ threshold of 100 and 200 mIU/ml given the identical number of subjects above these thresholds among experienced).

characteristics of these subjects were compared with those of the remaining not infected naive subjects (**Table 3**). Our small group of subjects with breakthrough infection showed simultaneous neutralizing antibody titers below 20, binding antibody levels below 200 BAU/ml and IFN-γ < 1,000. Similar results in subjects older than 58 years may be considered an alarming condition.

DISCUSSION

Our study investigated the IgG and neutralizing response in naive and experienced HW previously shown to be able to mount a strong IgG response at d31 (5). At d180 after the second BioNTech/Pfizer vaccine shot, among naive, all HW had binding antibody levels higher than the assay threshold, although only 8.1% had results higher than the highest assay threshold. At variance, 1/3 of subjects had neutralizing antibodies titers below LLoQ, while titers $\geq$ 320 generally associated with protection, were observed in very few cases (1.2%). Converting neutralizing antibody titers in International Unit (IU/ml) by running in the same neutralization assay, the first SARS-CoV-2 WHO International Standard (NIBSC 20/136)[1], we observed that only 32.78% of our patients had 50% protective neutralizing antibody. Our results appear in keeping with those reported in two studies from Israel, where the majority of the population was vaccinated using the BioNTech/Pfizer or Moderna vaccine. The first study on over 1,000,000 persons (596,618 vaccinated and 596,618 non-vaccinated) demonstrated high efficacy of vaccines, not only in disease prevention but also in infection transmission up to 42 days after the first vaccination (7). A second more recent study with longer follow up from the same Country, showed that 39 (2.6%) out of 1,497 fully vaccinated HW became infected during 14 weeks after their second dose of the BNT162b2 (BioNTech/Pfizer) vaccine; all the infected had lower neutralizing antibody levels than their uninfected colleagues during the peri-infection period (23). In our study, only 6 subjects (2.2%) experienced a breakthrough infection. All of them were older and had median neutralizing antibody levels lower than the median of the uninfected population. Although we are aware that our sample size is limited, our results appear in line with those reported in Israel.

The already known significant decline in BNT162b2 vaccine protection more than 120 days after the second dose, in our study, conducted in the region of Puglia with a low community incidence rate (positivity index on December 16, 2021, was 2.4%)[2], was associated with the rate of breakthrough infections comparable to those reported by Bergwek (23) and were significantly lower than the rates reported among unvaccinated subjects[3].

In keeping with the decreased severity of the disease in vaccinated individuals who acquire SARS-CoV-2 infection,

TABLE 3 | Characteristics of patients with breakthrough infection.

Pt initials	Gender	Age	IgG level BAU/ml	IGRA titers mIU/ml	Neutralizing antibody dilution
RF	M	35	311.14	905.1	14.1
VV	F	67	172.39	750	7.1
D'AG	M	57	105.53	420	5
VA	F	57	160	360	10
RG	F	59	200	620	20
CM	M	70	80.6	100	5

[2]https://bari.repubblica.it/argomenti/coronavirus_puglia (accessed December 16, 2021).

[3]https://www.epicentro.iss.it/coronavirus/bollettino/Bollettino-sorveglianza-integrata-COVID-19_7-dicembre-2021.pdf (accessed December 16, 2021).

all our patients with breakthrough infections were mild. A persistently positive swab result was observed in almost all (mean positivity duration 4.5 ± 2.3 weeks). Whether a possible further decrease in vaccine effectiveness against hospitalization after a longer interval from vaccination occurs was impossible to evaluate in our population given the mandatory administration of a third vaccine dose to the HW in Italy that started from November 22, 2021, based on the evidence that booster dose may mitigate the risk of transmission, disease, and deaths in all the age groups (24)[4].

Reliable detection of the T-cell-mediated immune response was explored in our study by IFN-γ production. Most of the subjects showed robust IFN-γ production after S-protein stimulation of peripheral blood cells. Results below the threshold of the assay were observed in only 12 (4.6%) naive, suggesting that lack of T-cell reactivity is a rare event even after a long interval from the second vaccine shot. This evidence was also confirmed by the cytoflorimetric analysis (manuscript in preparation). Moreover, as shown by the linear regression model, higher T-cell reactivity was observed in patients with higher neutralizing antibody levels. These results are in agreement with those reported by Schiffner et al. (25, 26). Consequently, the combination of these two assays seems to provide predictive information on protective immune reactions. Nevertheless, we need to keep in mind that neutralizing titers may be impractical to assess routinely, whereas IFN-γ evaluation as an expression of lymphocyte activity may be easier to use than other more complex CD4+ and CD8+ cellular response assessment methods.

Whether the decay of serum antibody levels is a good indicator for the timing of booster administration remains to be determined. Identifying immune correlates of protection (or lack thereof) from SARS-CoV-2 is critical in predicting how the expected antibody decay will affect clinical outcomes, if and when a booster dose will be needed, and whether vaccinated persons are protected (23, 26). Surely antibody decay represents one of the initial predisposing factors to breakthrough infections. However, while cellular and humoral immunity to SARS-CoV-2 is critical to control primary infection and correlates with severity of disease, the degree of vaccine protection from breakthrough infections may be an expression of the initial immune response rather than of the decay of antibody levels, since memory cells are expected to respond to future exposures. Moreover, while correlates of protection have been developed for other infections such as influenza (27) by challenge experiments in humans (28), no study has defined correlate of protection until a recent one that focused on correlates of protection against symptomatic COVID-19 (29, 30). This study highlights that there is no single threshold value for different assays (31). In our small group of subjects who experienced a breakthrough infection, we had the opportunity to both identify a common source of infection in an unvaccinated index case and to show low median neutralizing antibody titers and higher median age.

[4]https://www.salute.gov.it/portale/nuovocoronavirus/dettaglioComunicatiNuovoCoronavirus.jsp?menu=salastampa&id=5830 (accessed December 16, 2021).

The use of the same mRNA vaccine with a similar schedule and similar interval between vaccination and post-vaccination antibody assessment strengthen this study. Moreover, evaluating one of the longest delays between the second vaccine dose and both IgG and neutralizing antibody assessment has the advantage of using the IFN-γ spike-specific-induced T-cell immune response assay that allows simultaneous cellular responses evaluation. Finally, we had the opportunity to trace the incident breakthrough infection and to investigate its possible predictors. Limitations of our study are the relatively small sample size, the homogeneous demographic characteristics of our patients, young and healthy in the majority of cases. A further disadvantage is the relatively low prevalence of SARS-CoV-2 infection in our region as compared to others in Italy. This may prevent the exportability of our findings to the general population with different ages and co-morbidities.

In conclusion, our study shows that although the low humoral response is relatively long-lasting, high IgG levels are extremely rare in naive subjects. Only a third of subjects maintained neutralizing responses. In terms of T-cell, IFN-γ production after specific stimulation, a very limited number of subjects resulted unable to produce this cytokine over a period of 180 days after the second shot. IFN-γ testing could be used as surrogate testing for cellular immune responses. The results attained in our small group of subjects with breakthrough infection suggest that simultaneous neutralizing antibody titers below 20, binding antibody levels below 200 BAU/ml, and IFN-γ $<$1000 in subjects older than 58 years may be considered an alarming condition.

DATA AVAILABILITY STATEMENT

The datasets presented in this study can be found in online repositories. The names of the repository/repositories and accession number(s) can be found below: https://zenodo.org/record/5728042#.Ycy6BWnSJPw.

ETHICS STATEMENT

The studies involving human participants were reviewed and approved by EC IST Giovanni Paolo II IRCCS, BARI at Fondazione Casa Sollievo della Sofferenza San Giovanni Rotondo. The patients/participants provided their written informed consent to participate in this study.

AUTHOR CONTRIBUTIONS

AMang: conceptualization, data curation, formal analysis, investigation, methodology, project administration, supervision, validation, visualization, writing – original draft, and writing – review & editing. VP: data collection and writing – original draft. GC: formal analysis and data collection. VG: investigation and writing – original draft. AMane: formal analysis, investigation, writing – original draft, and writing – review & editing. PC: formal analysis and investigation. EM: writing – review & editing. FG: visualization. AMai: validation. SA: formal analysis and

investigation. All authors contributed to the article and approved the submitted version.

FUNDING

This study was partially funded by Ministry of Health of Italy, Bando Ricerca COVID-19; Project Number: COVID-2020-12371619; project title: COVIDIAGNOSTIX—Health Technology Assessment in COVID serological diagnostics.

SUPPLEMENTARY MATERIAL

The Supplementary Material for this article can be found online at: https://www.frontiersin.org/articles/10.3389/fpubh.2022.847384/full#supplementary-material

Supplementary Figure 1 | Day 60 Linear regression between IgG levels and IFN-γ concentration among COVID naïve group using the IFN-γ threshold of 100 mIU/ml.

Supplementary Figure 2 | Day 60 Linear regression between IgG levels and IFN-γ concentration among COVID naive group using the IFN-γ threshold of 200 mIU/ml.

REFERENCES

1. Dan J, Mateus J, Kato Y, Hastie KM, Faiti CE, Ramirez SI, et al. Immunological memory to SARS-CoV-2 assessed for greater than six months after infection. *Science*. (2021) 371:6529. doi: 10.1101/2020.11.15.383323
2. Vanshylla K, Di Cristanziano V, Kleipass F, Dewald F, Schmmers P, Gieselmann L et al. Kinetics and correlates of the neutralizing antibody response to SARS-CoV-2 infection. *Cell Host Microbe*. (2021) 29:917–29, doi: 10.1016/j.chom.2021.04.015
3. Letizia AG, Ge Y, Vangeti S, Goforth S, Weir DL, Kuzmina NA, et al. SARS-CoV-2 seropositivity and subsequent infection risk in healthy young adults: a prospective cohort study. *Lancet Resp Med*. (2021) 9:712–20. doi: 10.1016/S2213-2600(21)00158-2
4. Levin EG, Lustig Y, Cohen C, Fluss R, Indenbaum V, Amit S, et al. Waning Immune Humoral Response to BNT162b2 Covid-19 Vaccine over 6 Months. *N Engl J Med*. (2021) 385:e84. doi: 10.1056/NEJMoa2114583
5. Cocomazzi G, Piazzolla V, Squillante MM, Antinucci S, Giambra V, Giuliani F, et al. Early serological response to BNT162b2 mRNA Vaccine in healthcare workers. *Vaccines*. (2021) 9:913. doi: 10.3390/vaccines9080913
6. Pascolo S. Vaccines against COVID-19: Priority to mRNA-Based Formulations. *Cells*. (2021) 10:2716. doi: 10.3390/cells10102716
7. Dagan N, Barda N, Kepten E, Miron O, Perchick S, Katz MA, et al. BNT162b2 mRNA Covid-19 vaccine in a nationwide mass vaccination setting. *N Engl J Med*. (2021) 384:1412–23. doi: 10.1056/NEJMoa2101765
8. Doria-Rose N, Suthar MS. Antibody persistance through 6 months after the second dose of mRNA-1273 Vaccine for Covid-19. *N Engl J Med*. (2021) 384:2259-61. doi: 10.1056/NEJMc2103916
9. Bayart J, Douxfils J, Gillot C, David C, Mullier F, Elsen M, et al. Waning of IgG, Total and neutralizing antibodies 6 months post-vaccination with BNT162b2 in Healthcare workers. *Vaccines*. (2021) 9:1092. doi: 10.3390/vaccines9101092
10. Saadat S, Rikhtegaran Tehrani Z, Logue J, Newman M, Frieman MB, Harris AD, et al. Binding and neutralization antibody titers after single vaccine dose in Health Care Workers previously infected with SARS-CoV-2. *JAMA*. (2021) 325:1467–69. doi: 10.1101/2021.01.30.21250843
11. Ferrari D, Clementi N, Spanò MS, Albitar-Nehme S, Ranno S, Colombini A, et al. Harmonization of six quantitative SARS-COV-2 serological assays using era of vaccinated subjects. *Chimica Clinica Acta*. (2021) 522:141–52. doi: 10.1016/j.cca.2021.08.024
12. Berkley LJ. *Pfizer CEO Says Third Dose of Covid-19 Vaccine Likely Needed Within 12 months. CNBC*. (2021). Available online at: https://www.cnbc.com/2021/04/15/pfizer-ceo-says-third-dose-likely-needed-within-12months.htlm (accessed November 18, 2021).
13. Chemaitelly H, Tang P, Hasan MR, AlMukdad S, Yassine HM, Benslimane FM, et al. Waning of BNT162b2 vaccine protection against SARS-CoV-2 infection in Qatar. *N Engl J Med*. (2021) 385:e83. doi: 10.1101/2021.08.25.21262584
14. Robles Fontán MM, Nieves EG, Gerena IC, Irizarry RA. Time-varying effectiveness of three Covid-19 vaccines in Puerto Rico. *medRxiv*. (2021). doi: 10.1101/2021.10.17.21265101
15. Bar-On YM, Goldeberg Y, Mandel M, Bodenheimer O, Freedman L, Kalkstein N, et al. Protection of BNT162b2 Vaccine Booster against Covid-19 in Israel. *N Engl J Med*. (2021) 385:1393–400. doi: 10.1056/NEJMoa2114255
16. Hutzly D, Panning M, Smely F, Enders M, Komp J, Steinman D. Validation and performance evaluation of a novel interferon-γ release assay for the detection of SARS-CoV-2 specific T-cell response. *medRxiv*. (2021). doi: 10.1101/2021.07.17.21260316
17. Kristiansen A, Page P, Bernasconi M, Mattiuzzo V, Dull G, Makar P, et al. WHO International Standard for anti-SARS-CoV-2 immunoglobulin. *Lancet*. (2021) 397:1347–8. doi: 10.1016/S0140-6736(21)00527-4
18. Rikhtegaran Tehrani Z, Saadat S, Saleh E, Ouyang X, Constantine N, DeVico AL, et al. Performance of nucleocapsid and spike- based SARS-CoV-2 serologic assays. *PLoS ONE*. (2020) 15:e0237828. doi: 10.1371/journal.pone.0237828
19. Gimenez E, Albert E, Torres I, Remigia MJ, Alcaraz MJ, Galindo MJ. SARS-CoV-2-reactive interferon-γ-produducing CD8+ T vells in patients hospitalized with coronavirus disease 2019. *J Med Virol*. (2020) 93:375–82. doi: 10.1101/2020.05.18.20106245
20. Manenti A, Maggetti M, Casa E, Martinuzzi D, Torelli A, Trombetta CM, et al. Evaluation of SARS-CoV-2 neutralizing antibodies using a CPE-based colorimetric live virus micro-neutralization assay in human serum samples. *J Med Virol*. (2020) 92:2096–104. doi: 10.1002/jmv.25986
21. Manenti A, Molesti E, Maggetti M, Torelli A, Lapini G, Montomoli E. The theory and practice of the viral dose in neutralization assay: Insights on SARS-CoV-2 "doublethink" effect. *J Virol Methods*. (2021) 297:114261. doi: 10.1016/j.jviromet.2021.114261
22. Khoury DS, Cromer D, Reynaldi A, Schlub TE, Wheatley A, Wheatley AK, et al. Neutralizing antibody levels are highly predictive of immune protection from symptomatic SARS-CoV-2 infection. *Nat Med*. (2021) 27:1205–11. doi: 10.1038/s41591-021-01377-8
23. Bergwerk M, Gonen T, Lustig Y, Amit S, Lipsitch M, Cohen C, et al. Covid-19 Breakthrough Infections in Vaccinated Health Care Workers. *New Engl J Med*. (2021) 385:1630–1. doi: 10.1056/NEJMoa2109072
24. Barda N, Dagan N, Cohen C, Hernan MA, Lipsitch M, Kohane IS, et al. Effectiveness of a third dose of the BNT162b2 mRNA COVID-19 vaccine for preventing severe outcomes in Israel: an observational study. *Lancet*. (2021) 398:2093–100. doi: 10.1016/S0140-6736(21)02249-2
25. Schiffer J, Backhaus I, Rimmele J, Schulz S, Mohlenkamp T, Klemens JM. Long-term course of humoral and cellular immune responses in outpatients after SARS-CoV-2 infection. *Front Pubic Health*. (2021) 9:732787. doi: 10.3389/fpubh.2021.732787
26. Klompas M. Understanding Breakthrough Infections Following mRNA SARS-CoV-2 Vaccination. *JAMA*. (2021) 326:2018–20. doi: 10.1001/jama.2021.19063
27. Laurie KL, Engelhardt OG, Wood J, Heath A, Katz JM, Peiris M, et al. International laboratory comparison of infuenza microneutralization assays for A(H1N1)pdm09, A(H3N2), and A(H5N1) infuenza viruses by CONSISE. Clin. *Vac Immunol*. (2015) 22:957–64. doi: 10.1128/CVI.00278-15
28. Black S, Nicolay U, Vesikari T, Knuf M, Del Giudice G, Della Cioppa G, et al. Hemagglutination inhibition antibody titers as a correlate of protection for inactivated in uenza vaccines in children. *Pediatr Infect Dis J*. (2011) 30:1081–5. doi: 10.1097/INF.0b013e3182367662

29. Krammer F. Correlates of protection. *Lancet*. (2021) 397:1421–3. doi: 10.1016/S0140-6736(21)00782-0
30. Feng S, Phillips DJ, White T, Sayal H, Aley PK, Bibi S, et al. Correlates of protection against symptomatic and asymptomatic SARS-CoV-2 infection. *Nat Med*. (2021) 27:2032–40. doi: 10.1101/2021.06.21.21258528
31. Wall EC, Wu M, Harvey R, Kelly G, Warchal S, Sawyer C, et al. Neutralising antibody activity against SARS- CoV-2 VOCs B16172 and B1351 by BNT162b2 vaccination. *Lancet*. (2021) 397:2331–3. doi: 10.1016/S0140-6736(21)01290-3

Conflict of Interest: EM, PC, and AMane were employed by VisMederi Srl.

The remaining authors declare that the research was conducted in the absence of any commercial or financial relationships that could be construed as a potential conflict of interest.

Publisher's Note: All claims expressed in this article are solely those of the authors and do not necessarily represent those of their affiliated organizations, or those of the publisher, the editors and the reviewers. Any product that may be evaluated in this article, or claim that may be made by its manufacturer, is not guaranteed or endorsed by the publisher.

Article

Hybrid immunity improves B cells and antibodies against SARS-CoV-2 variants

https://doi.org/10.1038/s41586-021-04117-7

Received: 19 August 2021

Accepted: 8 October 2021

Published online: 20 October 2021

Open access

Check for updates

Emanuele Andreano[1], Ida Paciello[1], Giulia Piccini[2], Noemi Manganaro[1], Piero Pileri[1], Inesa Hyseni[2,3], Margherita Leonardi[2,3], Elisa Pantano[1], Valentina Abbiento[1], Linda Benincasa[3], Ginevra Giglioli[3], Concetta De Santi[1], Massimiliano Fabbiani[4], Ilaria Rancan[4,5], Mario Tumbarello[4,5], Francesca Montagnani[4,5], Claudia Sala[1], Emanuele Montomoli[2,3,6] & Rino Rappuoli[1,7]✉

The emergence of SARS-CoV-2 variants is jeopardizing the effectiveness of current vaccines and limiting the application of monoclonal antibody-based therapy for COVID-19 (refs. [1,2]). Here we analysed the memory B cells of five naive and five convalescent people vaccinated with the BNT162b2 mRNA vaccine to investigate the nature of the B cell and antibody response at the single-cell level. Almost 6,000 cells were sorted, over 3,000 cells produced monoclonal antibodies against the spike protein and more than 400 cells neutralized the original SARS-CoV-2 virus first identified in Wuhan, China. The B.1.351 (Beta) and B.1.1.248 (Gamma) variants escaped almost 70% of these antibodies, while a much smaller portion was impacted by the B.1.1.7 (Alpha) and B.1.617.2 (Delta) variants. The overall loss of neutralization was always significantly higher in the antibodies from naive people. In part, this was due to the IGHV2-5;IGHJ4-1 germline, which was found only in people who were convalescent and generated potent and broadly neutralizing antibodies. Our data suggest that people who are seropositive following infection or primary vaccination will produce antibodies with increased potency and breadth and will be able to better control emerging SARS-CoV-2 variants.

Twenty months after the beginning of the COVID-19 pandemic, with 252 million people infected, 5 million deaths and 7.2 billion vaccine doses administered, the world is still struggling to control the virus. In most developed countries, vaccines have vastly reduced severe disease, hospitalization and deaths, but they have not been able to control the infections that are fuelled by new and more infectious variants. A large number of studies so far have shown that protection from infection is linked to the production of neutralizing antibodies against the spike (S) protein of the virus[3–6]. This is a metastable, trimeric class 1 fusion glycoprotein, composed of the S1 and S2 subunits, and mediates virus entry, changing from a prefusion to postfusion conformation after binding to the human angiotensin-converting enzyme 2 (ACE2) receptor and heparan sulfates on the host cells[7]. Potent neutralizing antibodies recognize the S1 subunit of each monomer, which includes the receptor-binding domain (RBD) and N-terminal domain (NTD) immunodominant sites[8]. The large majority of neutralizing antibodies bind to the receptor-binding motif, within the RBD, and a smaller fraction targets the NTD[5,9]. Neutralizing antibodies against the S2 subunit have been described; however, they have very low potency[5,10]. Neutralizing antibodies generated after infection derive in large part from germline IGHV3-53 and the closely related IGHV3-66 with very few somatic mutations[11,12]. From June 2020, the virus started to generate mutations that allowed the virus to evade neutralizing antibodies, to become more infectious, or both. Some of the mutant viruses completely replaced the original SARS-CoV-2 first detected in Wuhan, China. The most successful variant viruses are B.1.1.7 (Alpha), B.1.351 (Beta), B.1.1.248 (Gamma) and B.1.617.2 (Delta), which have been named variants of concern (VoCs)[13]. The Delta variant is currently spreading across the globe and causing large concerns also in fully vaccinated populations. It is therefore imperative to understand the molecular mechanisms of the immune response to vaccination to design better vaccines and vaccination policies. Several investigators have shown that vaccination of people who are convalescent can yield neutralizing antibodies that can be up to a thousand-fold higher than those induced by infection or vaccination, suggesting that one way of controlling the pandemic may be the induction of a hybrid immunity-like response using a third booster dose[14–18]. At the single-cell level, here we compared the nature of the neutralizing antibody response against the original virus first detected in Wuhan and the VoCs in naive and convalescent participants who were immunized with the BNT162b2 mRNA vaccine.

B cell response in COVID-19 vaccinees

We enrolled ten donors who were vaccinated with the BNT162b2 mRNA vaccine: five of them were healthy people who were naive to SARS-CoV-2 infection at vaccination (seronegative) and the other five had recovered

[1]Monoclonal Antibody Discovery (MAD) Lab, Fondazione Toscana Life Sciences, Siena, Italy. [2]VisMederi S.r.l, Siena, Italy. [3]VisMederi Research S.r.l., Siena, Italy. [4]Department of Medical Sciences, Infectious and Tropical Diseases Unit, Siena University Hospital, Siena, Italy. [5]Department of Medical Biotechnologies, University of Siena, Siena, Italy. [6]Department of Molecular and Developmental Medicine, University of Siena, Siena, Italy. [7]Department of Biotechnology, Chemistry and Pharmacy, University of Siena, Siena, Italy. ✉e-mail: rino.r.rappuoli@gsk.com

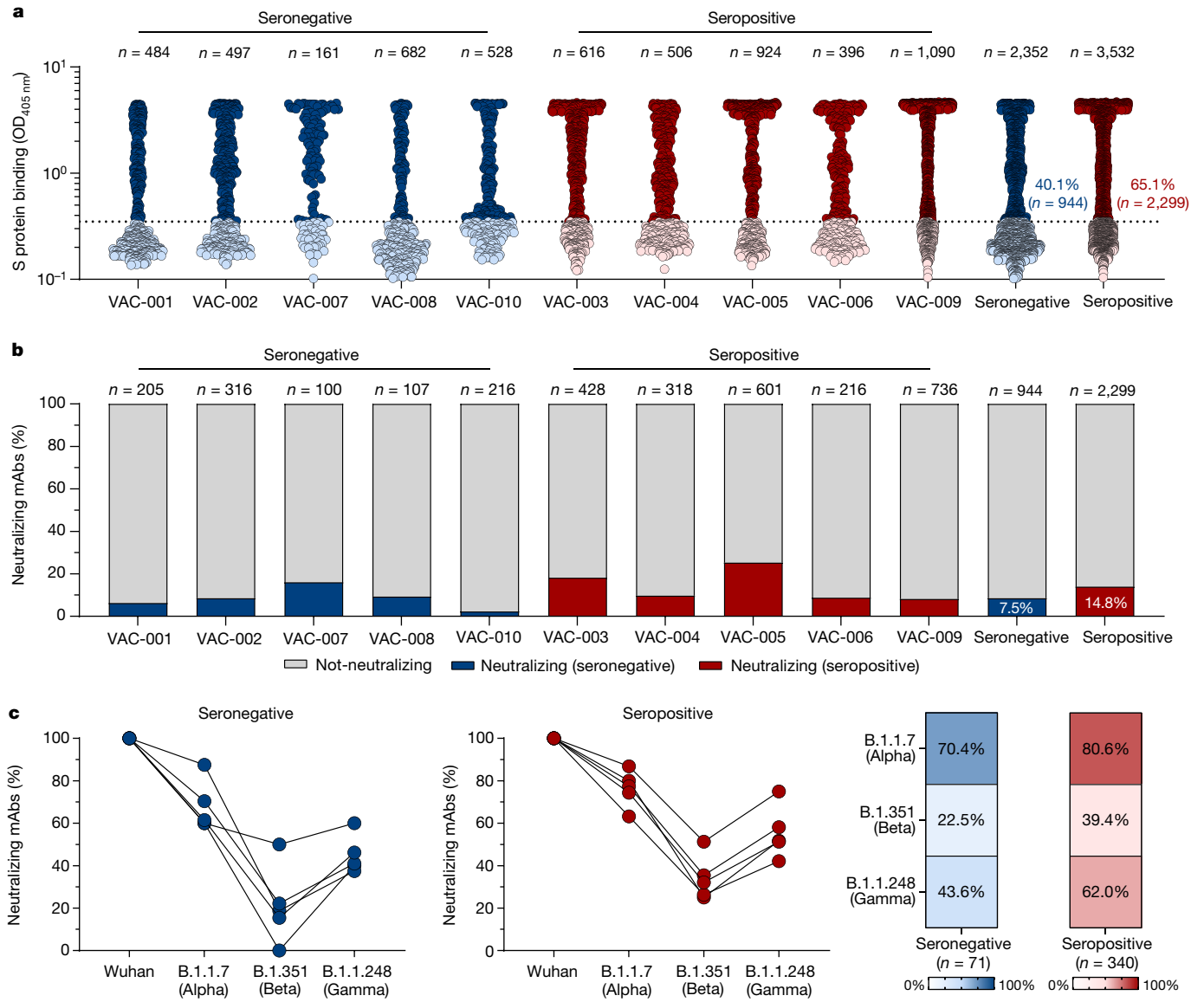

Fig. 1 | Identification of cross-neutralizing SARS-CoV-2 S protein-specific nAbs. a, The graph shows supernatants that were tested for binding to the SARS-CoV-2 S protein antigen first detected in Wuhan, China. The threshold of positivity was set as two times the value of the blank (dotted line). The dark blue and dark red dots represent mAbs that bind to the S protein for vaccinees who were seronegative and seropositive, respectively. The light blue and light red dots represent mAbs that do not bind to the S protein for vaccinees who were seronegative and seropositive, respectively. OD, optical density. **b**, The bar graph shows the percentage of not-neutralizing antibodies (grey), nAbs from individuals who were seronegative (dark blue) and nAbs for individuals who were seropositive (dark red). The total number (*n*) of antibodies tested per individual is shown on the top of each bar in **a**, **b**. **c**, The graphs show the fold-change percentage of nAbs in individuals who were seronegative (left) and seropositive (right) against the Alpha, Beta and Gamma VoCs compared with the original SARS-CoV-2 virus detected in Wuhan. The heat maps show the overall percentage of the SARS-CoV-2 nAbs detected in Wuhan that are able to neutralize the tested VoCs.

from SARS-CoV-2 infection before vaccination (seropositive). Participant details are summarized in Extended Data Table 1. Blood collection occurred at an average of 48 and 21 days after the last vaccination dose for participants who were seronegative and seropositive, respectively (Extended Data Table 1). This difference may affect the frequency of circulating B cells and the serum activity of participants who are seronegative and seropositive analysed in this study. We initially analysed the frequency of circulating B cell populations between our groups. Participants who were seropositive showed a 2.46-fold increase in S-protein-specific $CD19^+CD27^+IgD^-IgM^-$ memory B cells compared with participants who were seronegative and an overall 10% higher count of $CD19^+CD27^+IgD^-IgM^-$ memory B cells (Extended Data Fig. 1a–c). Conversely, participants who were seronegative showed a 2.3-fold higher frequency of $CD19^+CD27^+IgD^-IgM^+$ memory B cells than participants who were seropositive. No differences were found in the numbers of $CD19^+CD27^+IgD^-IgM^+$ S protein$^+$ memory B cells between the two groups assessed in this study (Extended Data Fig. 1a–c). Following the analyses of memory B cells, we characterized the polyclonal response of these donors by testing their binding response to the S protein trimer, RBD, NTD and the S2 domain, and subsequently by testing their neutralization activity against the original SARS-CoV-2 virus first detected in Wuhan (Extended Data Fig. 2). Plasma from participants who were seropositive showed a higher binding activity to the S protein and all tested domains than plasma from participants who were seronegative (Extended Data Fig. 2a–d). In addition, participants who were seropositive showed a tenfold-higher neutralization activity against the original SARS-CoV-2 virus detected in Wuhan than in participants who were seronegative (Extended Data Fig. 2e, f).

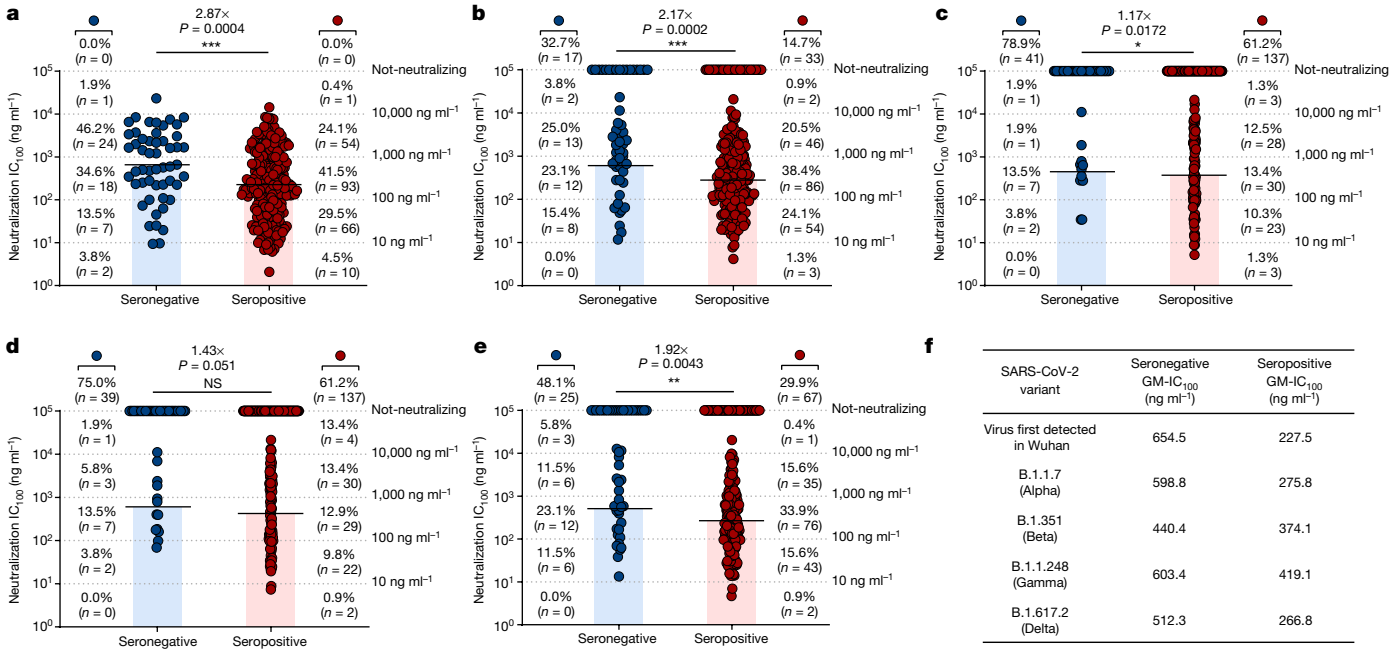

f

SARS-CoV-2 variant	Seronegative GM-IC_{100} (ng ml^{-1})	Seropositive GM-IC_{100} (ng ml^{-1})
Virus first detected in Wuhan	654.5	227.5
B.1.1.7 (Alpha)	598.8	275.8
B.1.351 (Beta)	440.4	374.1
B.1.1.248 (Gamma)	603.4	419.1
B.1.617.2 (Delta)	512.3	266.8

Fig. 2 | Potency and breadth of neutralization of nAbs against SARS-CoV-2 and VoCs. a–e, Scatter dot charts show the neutralization potency, reported as IC_{100} (ng ml^{-1}), of nAbs tested against the original SARS-CoV-2 virus first detected in Wuhan (**a**) and the B.1.1.7 (**b**), B.1.351 (**c**), B.1.1.248 (**d**) and B.1.617.2 (**e**) VoCs. The number and percentage of nAbs from individuals who were seronegative versus seropositive, fold change, neutralization IC_{100} geometric mean (black lines, blue and red bars) and statistical significance are denoted on each graph. A non-parametric Mann–Whitney *t*-test was used to evaluate statistical significances between groups. Two-tailed *P* value significances are shown as $*P < 0.05$, $**P < 0.01$, $***P < 0.001$. NS, not significant. **f**, The table shows the IC_{100} geometric mean (GM) of all nAbs pulled together from each group against all SARS-CoV-2 viruses tested. Technical duplicates were performed for each experiment.

Isolation of neutralizing antibodies

To better characterize the B cell immune response, we single-cell-sorted antigen-specific memory B cells using the SARS-CoV-2 S protein antigen identified in Wuhan as bait, which was encoded by the mRNA vaccine. The single-cell sorting strategy was performed as previously described[5]. In brief, the prefusion S protein trimer-specific (S protein$^+$), class-switched memory B cells ($CD19^+CD27^+IgD^-IgM^-$) were single-cell-sorted and then incubated for 2 weeks to naturally produce and release monoclonal antibodies (mAbs) into the supernatant. A total of 2,352 and 3,532 S protein$^+$ memory B cells were sorted from vaccinees who were seronegative and seropositive, respectively (Extended Data Table 2). Of these, 944 (40.1%) and 2,299 (65.1%), respectively, were released in the supernatant mAbs, recognizing the S protein prefusion trimer in enzyme-linked immunosorbent assay (ELISA) (Fig. 1a, Extended Data Table 2). These mAbs were then tested in a cytopathic effect-based microneutralization assay (CPE-MN) with the original live SARS-CoV-2 virus detected in Wuhan at a single point dilution (1:5) to identify SARS-CoV-2 neutralizing human monoclonal antibodies (nAbs). This first screening identified a total of 411 nAbs, of which 71 derived from participants who were seronegative and 340 were from participants who were seropositive (Fig. 1b, Extended Data Table 2). Overall, the fraction of S-protein-specific B cells producing nAbs were 7.5% for participants who were seronegative and 14.8% for participants who were seropositive. Following this first screening, all nAbs that were able to neutralize the SARS-CoV-2 virus detected in Wuhan were tested by CPE-MN against major VoCs, including B.1.1.7 (Alpha), B.1.351 (Beta) and B.1.1.248 (Gamma) to understand the breadth of neutralization of nAbs elicited by the BNT162b2 mRNA vaccine. At the time of this assessment the B.1.617.2 (Delta) variant had not yet spread globally and therefore was not available for screening. Participants who were seropositive had an overall higher percentage of nAbs neutralizing the VoCs than participants who were seronegative. The average frequency of nAbs from participants who were seropositive neutralizing the Alpha, Beta and Gamma variants was 80.6% ($n = 274$), 39.4% ($n = 134$) and 62.0% ($n = 211$), respectively, compared with 70.4% ($n = 50$), 22.5% ($n = 16$) and 43.6% ($n = 31$), respectively, in participants who were seronegative (Fig. 1c, Extended Data Table 2).

Potency and breadth against variants

To better characterize and understand the potency and breadth of coverage of all nAbs against the SARS-CoV-2 virus detected in Wuhan, we aimed to express all the 411 nAbs previously identified as IgG1. We were able to recover and express 276 antibodies for further characterization, 224 (89.8%) from participants who were seropositive and 52 (10.2%) from participants who were seronegative. Initially, antibodies were tested for binding against the RBD, NTD and the S2 domain of the original SARS-CoV-2 Sprotein identified in Wuhan. Overall, no major differences were observed in nAbs that recognized the RBD and NTD, whereas nAbs that were able to bind to the S protein only in its trimeric conformation (that is, not able to bind single domains) were almost threefold higher in participants who were seronegative than in participants who were seropositive (Extended Data Fig. 3). None of the tested nAbs targeted the S2 domain. nAbs were then tested by CPE-MN in serial dilution to evaluate their 100% inhibitory concentration (IC_{100}) against the SARS-CoV-2 virus detected in Wuhan and the VoCs. At this stage of the study, the B.1.617.2 (Delta) virus had spread globally, and we were able to obtain the live virus for our experiments. Overall, nAbs isolated from vaccinees who were seropositive had a significantly higher potency than those isolated from vaccinees who were seronegative. The IC_{100} geometric mean in participants who were seropositive was 2.87-fold, 2.17-fold, 1.17-fold, 1.43-fold and 1.92-fold lower than in participants who were seronegative for the virus detected in Wuhan, and the Alpha, Beta, Gamma and Delta VoCs, respectively (Fig. 2). In addition, a bigger fraction of nAbs from participants who were seropositive retained the

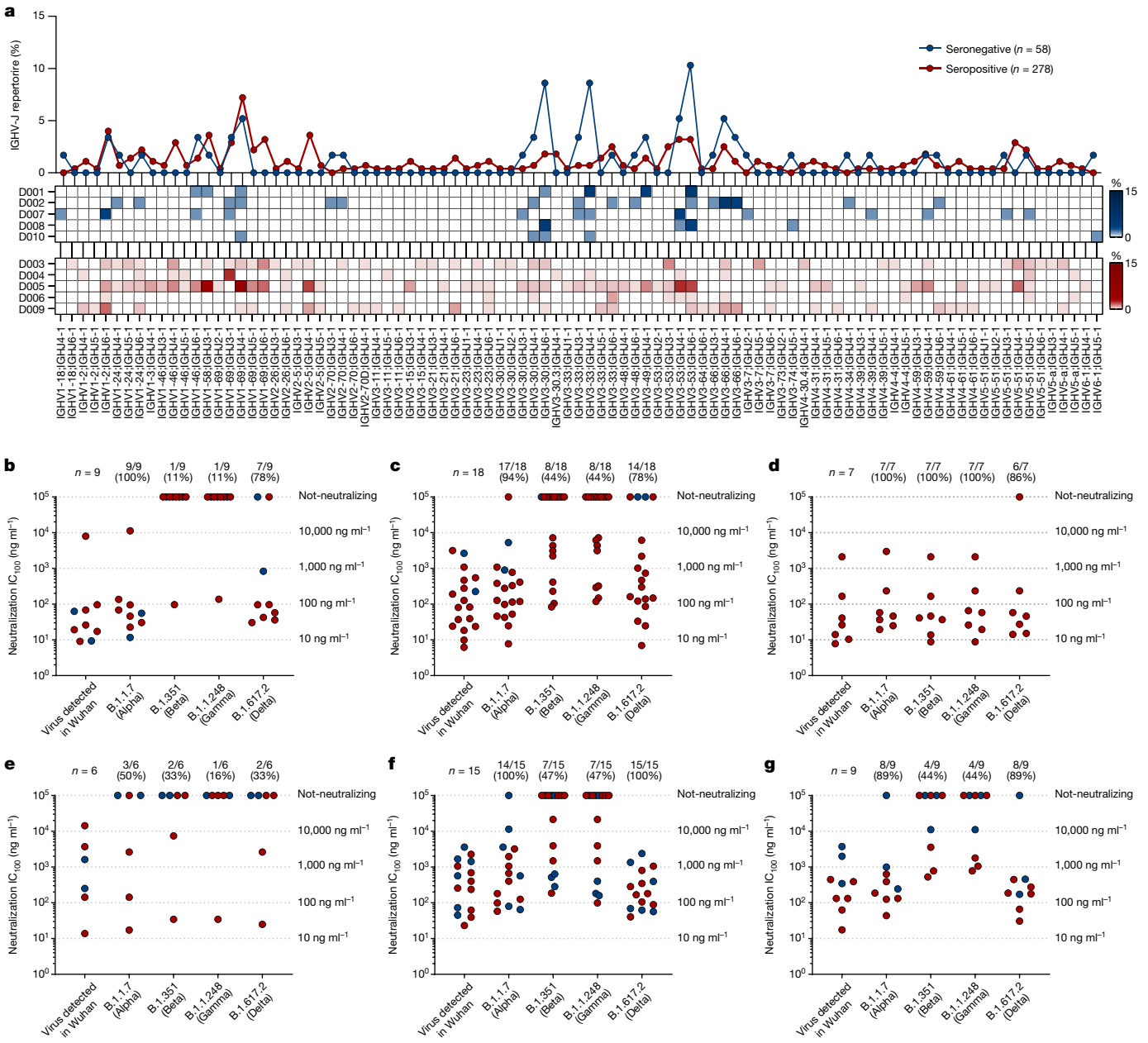

Fig. 3 | Repertoire analyses and functional characterization of predominant gene-derived nAbs. a, The graph shows the IGHV-J rearrangement frequencies between vaccinees who were seronegative and seropositive (top), and the frequency within seronegative (middle) and seropositive (bottom) participants. **b**–**g**, The graphs show the neutralization potency (IC_{100}) of predominant gene-derived nAbs from the IGHV1-2;IGHJ6-1 (**b**), IGHV1-69;IGHJ4-1 (**c**), IGHV2-5;IGHJ4-1 (**d**), IGHV3-30;IGHJ6-1 (**e**), IGHV3-53;IGHJ6-1 (**f**) and IGHV3-66;IGHJ4-1 (**g**) families, against the original SARS-CoV-2 virus first detected in Wuhan and the B.1.1.7, B.1.351, B.1.1.248 and B.1.617.2 VoCs.

ability to neutralize the VoCs. Indeed, when nAbs were individually tested against all VoCs, the ability to neutralize the Alpha, Beta, Gamma and Delta variants was lost by 14%, 61%, 61% and 29% of the antibodies from participants who were seropositive versus 32%, 78%, 75% and 46% of those from participants who were seronegative, respectively (Fig. 2). Finally, a major difference between participants who were seronegative and seropositive was found in the class of nAbs with medium/high potency (IC_{100} of 11–100 ng ml^{-1} and 101–1,000 ng ml^{-1}) against all variants. Indeed, nAbs in these ranges from participants who were seropositive constitute 71.0%, 62.5%, 23.7%, 22.8% and 53.1% of the whole nAb repertoire, whereas nAbs from seronegative donors were 48.1%, 38.5%, 17.3%, 17.3% and 34.6% against the SARS-CoV-2 virus detected in Wuhan and the Alpha, Beta, Gamma and Delta VoCs respectively (Fig. 2).

Functional gene repertoire

The analysis of the immunoglobulin G heavy chain variable (IGHV) and joining (IGHJ) gene rearrangements of 58 and 278 sequences recovered from participants who were seronegative and seropositive, respectively, showed that they use a broad range of germlines and share the most abundant germlines. In particular, both groups predominantly used the IGHV1-69;IGHJ4-1 and IGHV3-53;IGHJ6-1 germlines, which were shared by three out five participants per group (Fig. 3a). In addition, the IGHV3-30;IGHJ6-1 and IGHV3-33;IGHJ4-1 germlines, which were more abundant in donors who were seronegative, and the IGHV1-2;IGHJ6-1 germline, which was mainly expanded in vacinees who were seropositive, were also used with high frequency in both groups. Only the IGHV2-5;IGHJ4-1

germline was seen to be predominantly expanded only in donors who were seropositive (Fig. 3a). Despite the fact that selected germlines were boosted following vaccination, no major clonal families were identified, and the biggest family observed contained only four antibodies. To better characterize these predominant gene families, we evaluated their neutralization potency and breadth against SARS-CoV-2 and VoCs. In this analysis, we could not evaluate IGHV3-33;IGHJ4-1 nAbs, as only three of these antibodies were expressed, but we included the IGHV3-53 closely related family IGHV3-66;IGHJ4-1, as this family was previously described to be mainly involved in the neutralization of the SARS-CoV-2 virus[11,19]. A large part of nAbs deriving from these predominant germlines had a very broad range of neutralization potency against the original SARS-CoV-2 virus detected in Wuhan, with the IC_{100} spanning from less than 10 to over 10,000 ng ml^{-1} (Fig. 3b–g). However, many of them lost the ability to neutralize SARS-CoV-2 VoCs. The loss of neutralizing activity occurred for most germlines and it was moderate against the Alpha and Delta variants, whereas the loss was marked against the Beta and Gamma variants (Fig. 3b–g). A notable exception was the IGHV2-5;IGHJ4-1 germline, which was present only in nAbs of participants who were seropositive, that showed potent antibodies able to equally neutralize all SARS-CoV-2 VoCs (Fig. 3d). Finally, we evaluated the CDRH3 length and V-gene somatic hypermutation levels for all nAbs retrieved from participants who were seronegative and seropositive and for predominant germlines. Overall, the two groups show a similar average CDRH3 length (15.0 amino acids and 15.1 amino acids for participants who were seronegative and seropositive, respectively); however, participants who were seropositive showed almost twofold-higher V-gene mutation levels than participants who were seronegative (Extended Data Fig. 4). As for predominant gene-derived nAbs, we observed heterogenous CDRH3 length, with the only exception of IGHV3-53;IGHJ6-1 nAbs, and higher V-gene mutation levels in predominant germlines from participants who were seropositive than in germlines from participants who were seronegative (Extended Data Fig. 5).

S protein epitope mapping

To map the regions of the S protein recognized by the identified nAbs, we used a competition assay with four known antibodies: J08, which targets the top loop of the receptor-binding motif[5]; S309, which binds to the RBD but outside of the RMB region[20]; 4A8, which recognizes the NTD[21]; and L19, which binds to the S2 domain[5] (Extended Data Fig. 6). The nAbs identified in this study were pre-incubated with the original SARS-CoV-2 S protein detected in Wuhan, and subsequently the four nAbs labelled with different fluorophores were added as a single mix. For one of the four fluorescently labelled nAbs, 50% signal reduction was used as a threshold for positive competition. The vast majority of nAbs from both seronegative (50.0%; $n = 26$) and seropositive (51.3%; $n = 115$) vaccinees competed with J08 (Extended Data Fig. 7a, Extended Data Table 3). For vaccinees who were seronegative, the second most abundant population was composed of nAbs that did not compete with any of the four fluorescently labelled nAbs (25.0%; $n = 13$), followed by nAbs targeting the NTD (17.3%; $n = 9$). As for vaccinees who were seropositive, the second most abundant population was composed of nAbs that competed with S309 (21.4%; $n = 48$), followed by nAbs that competed with 4A8 (15.6%; $n = 35$) and not-competing nAbs (11.6%; $n = 26$). None of our nAbs competed with the S2-targeting antibody L19 (Extended Data Fig. 7a, Extended Data Table 3). nAbs that competed with J08, which are likely to bind to the receptor-binding motif, derived from several germlines, including the predominant IGHV3-53;IGHJ6-1 (10.6%; $n = 14$), IGHV1-69;IGHJ4-1 (8.3%; $n = 11$) and IGHV1-2;IGHJ6-1 (6.8%; $n = 9$) germlines (Extended Data Fig. 7b). By contrast, those that competed with S309 derived mostly from the IGHV2-5;IGHJ4-1 germline (13.7%; $n = 7$), which were isolated exclusively from vaccinees who were seropositive (Extended Data Fig. 7c). As for NTD-directed nAbs, the non-predominant gene family IGHV1-24;IGHJ6-1 was the most abundant, confirming what was reported in previous studies[22] (Extended Data Fig. 7d). Finally, for nAbs that did not compete with any of the known antibodies used in our competition assay, the non-predominant gene families IGHV1-69;IGHJ3-1 (9.7%; $n = 3$) and IGHV1-69;IGHJ6-1 (9.7%; $n = 3$) were the most abundant (Extended Data Fig. 7e).

Discussion

Our study analysed the repertoire of B cells producing neutralizing antibodies following vaccination of naive and previously infected people at the single-cell level. The most important conclusion from this work is that people who are previously exposed to SARS-CoV-2 infection respond to vaccination with more B-cell-producing antibodies that are not susceptible to escape variants and that have higher neutralization potency. This can be explained in part by the increased number of somatic mutations and by the fact that participants who are seropositive expand potent antibodies derived from the IGHV2-5;IGHJ4-1 germline, which were not described in naive vaccinees[18]. One limitation of our study is that we did not include people who received a third booster dose of vaccine. Despite this limitation, we believe that our conclusions are likely to be extendable to people who are seronegative, as a third vaccine dose could lead to a hybrid immunity-like response as neutralizing antibodies following infection and vaccination derive mostly from the same immunodominant germlines[11,12,17–19]. Our analysis suggests that a booster dose of vaccine will increase the frequency of memory B cells producing potent neutralizing antibodies that are not susceptible to escape variants and will allow better control of this pandemic. The massive variant escape from predominant germlines, such as IGHV3-53, IGHV3-66, IGHV3-30 and IGHV1-69, and the presence of antibodies deriving from the IGHV2-5 germline that are resistant to variants, suggest that the design of vaccines that preferentially promote or avoid the expansion of selected germlines can generate broad protection against SARS-CoV-2 variants. Germline-targeting vaccination, which has been pioneered in the HIV field[23,24], may be a promising strategy to fight the COVID-19 pandemic.

Online content

Any methods, additional references, Nature Research reporting summaries, source data, extended data, supplementary information, acknowledgements, peer review information; details of author contributions and competing interests; and statements of data and code availability are available at https://doi.org/10.1038/s41586-021-04117-7.

1. Krause, P. R. et al. SARS-CoV-2 variants and vaccines. *N. Engl. J. Med.* **385**, 179–186 (2021).
2. Starr, T. N. et al. Prospective mapping of viral mutations that escape antibodies used to treat COVID-19. *Science* **371**, 850–854 (2021).
3. Wajnberg, A. et al. Robust neutralizing antibodies to SARS-CoV-2 infection persist for months. *Science* **370**, 1227–1230 (2020).
4. Xiaojie, S., Yu, L., Lei, Y., Guang, Y. & Min, Q. Neutralizing antibodies targeting SARS-CoV-2 spike protein. *Stem Cell Res.* **50**, 102125 (2021).
5. Andreano, E. et al. Extremely potent human monoclonal antibodies from COVID-19 convalescent patients. *Cell* **184**, 1821–1835.e16 (2021).
6. Yang, Y. & Du, L. SARS-CoV-2 spike protein: a key target for eliciting persistent neutralizing antibodies. *Signal Transduct. Target. Ther.* **6**, 95 (2021).
7. Clausen, T. M., et al. SARS-CoV-2 infection depends on cellular heparan sulfate and ACE2. *Cell* **183**, 1043-1057.e15 (2020).
8. Wrapp, D. et al. Cryo-EM structure of the 2019-nCoV spike in the prefusion conformation. *Science* **367**, 1260–1263 (2020).
9. Piccoli, L. et al. Mapping neutralizing and immunodominant sites on the SARS-CoV-2 spike receptor-binding domain by structure-guided high-resolution serology. *Cell* **183**, 1024–1042.e21 (2020).
10. Tortorici, M. A. et al. Broad sarbecovirus neutralization by a human monoclonal antibody. *Nature* **597**, 103–108 (2021).
11. Andreano, E. & Rappuoli, R. Immunodominant antibody germlines in COVID-19. *J. Exp. Med.* **218**, e20210281 (2021).
12. Yuan, M. et al. Structural basis of a shared antibody response to SARS-CoV-2. *Science* **369**, 1119–1123 (2020).
13. Callaway, E. Coronavirus variants get Greek names — but will scientists use them? *Nature* **594**, 162 (2021).

14. Stamatatos, L. et al. mRNA vaccination boosts cross-variant neutralizing antibodies elicited by SARS-CoV-2 infection. *Science* **372**, 1413–1418 (2021).
15. Goel, R. R. et al. Distinct antibody and memory B cell responses in SARS-CoV-2 naïve and recovered individuals after mRNA vaccination. *Sci. Immunol.* **6**, eabi6950 (2021).
16. Urbanowicz, R. A. et al. Two doses of the SARS-CoV-2 BNT162b2 vaccine enhances antibody responses to variants in individuals with prior SARS-CoV-2 infection. *Sci. Transl. Med.* **13**, eabj0847 (2021).
17. Crotty, S. Hybrid immunity. *Science* **372**, 1392–1393 (2021).
18. Wang, Z. et al. Naturally enhanced neutralizing breadth against SARS-CoV-2 one year after infection. *Nature* **595**, 426–431 (2021).
19. Zhang, Q. et al. Potent and protective IGHV3-53/3-66 public antibodies and their shared escape mutant on the spike of SARS-CoV-2. *Nat. Commun.* **12**, 4210 (2021).
20. Pinto, D. et al. Cross-neutralization of SARS-CoV-2 by a human monoclonal SARS-CoV antibody. *Nature* **583**, 290–295 (2020).
21. Chi, X. et al. A neutralizing human antibody binds to the N-terminal domain of the spike protein of SARS-CoV-2. *Science* **369**, 650–655 (2020).
22. Voss, W. N. et al. Prevalent, protective, and convergent IgG recognition of SARS-CoV-2 non-RBD spike epitopes. *Science* **372**, 1108–1112 (2021).
23. Steichen, J. M. et al. A generalized HIV vaccine design strategy for priming of broadly neutralizing antibody responses. *Science* **366**, eaax4380 (2019).
24. Havenar-Daughton, C., Abbott, R. K., Schief, W. R. & Crotty, S. When designing vaccines, consider the starting material: the human B cell repertoire. *Curr. Opin. Immunol.* **53**, 209–216 (2018).

Article

Methods

Enrolment of COVID-19 vaccinees and human sample collection

This work results from a collaboration with the Azienda Ospedaliera Universitaria Senese, Siena (IT) that provided samples from donors vaccinated against COVID-19, of both sexes, who gave their written consent. The study was approved by the Comitato Etico di Area Vasta Sud Est (CEAVSE) ethics committees (Parere 17065 in Siena) and conducted according to good clinical practice in accordance with the declaration of Helsinki (European Council 2001, US Code of Federal Regulations, ICH 1997). This study was unblinded and not randomized. No statistical methods were used to predetermine sample size.

Single-cell sorting of SARS-CoV-2 S protein$^+$ memory B cells from COVID-19 vaccinees

Peripheral blood mononuclear cells (PBMCs) and the single-cell sorting strategy were performed as previously described[5]. In brief, PBMCs were isolated from heparin-treated whole blood by density gradient centrifugation (Ficoll-Paque PREMIUM, Sigma-Aldrich). After separation, PBMCs were stained with Live/Dead Fixable Aqua (Invitrogen; Thermo Scientific) diluted 1:500 at room temperature. After 20 min of incubation, cells were washed with PBS and unspecific bindings were saturated with 20% normal rabbit serum (Life Technologies). Following 20 min of incubation at 4 °C, cells were washed with PBS and stained with SARS-CoV-2 S protein labelled with Strep-Tactin XT DY-488 (2-1562-050, iba-lifesciences) for 30 min at 4 °C. After incubation, the following staining mix was used CD19 V421 (1:320; 562440, BD), IgM PerCP-Cy5.5 (1:50; 561285, BD), CD27 PE (1:30; 340425, BD), IgD-A700 (1:15; 561302, BD), CD3 PE-Cy7 (1:100; 300420, BioLegend), CD14 PE-Cy7 (1:320; 301814, BioLegend), CD56 PE-Cy7 (1:80; 318318, BioLegend) and cells were incubated at 4 °C for an additional 30 min. Stained memory B cells were single-cell-sorted with a BD FACS Aria III (BD Biosciences) into 384-well plates containing 3T3-CD40L feeder cells and were incubated with IL-2 and IL-21 for 14 days as previously described[25].

ELISA assay with SARS-CoV-2 S protein prefusion trimer

mAbs and plasma binding specificity against the S protein trimer was detected by ELISA as previously described[5]. In brief, 384-well plates (microplate clear, Greiner Bio-one) were coated with 3 µg/ml of streptavidin (Thermo Fisher) diluted in carbonate-bicarbonate buffer (E107, Bethyl Laboratories) and incubated at room temperature overnight. The next day, plates were incubated for 1 h at room temperature with 3 µg/ml of SARS-CoV-2 S protein diluted in PBS. Plates were then saturated with 50 µl per well of blocking buffer (phosphate-buffered saline and 1% BSA) for 1 h at 37 °C. After blocking, 25 µl per well of mAbs diluted 1:5 in sample buffer (phosphate-buffered saline, 1% BSA and 0.05% Tween-20) was added to the plates and was incubated at 37 °C. Plasma samples derived from vaccinees were tested (starting dilution of 1:10; step dilution of 1:2 in sample buffer) in a final volume of 25 µl per well and were incubated at 37 °C. After 1 h of incubation, 25 µl per well of alkaline phosphatase-conjugated goat anti-human IgG and IgA (Southern Biotech) diluted 1:2,000 in sample buffer was added. Finally, S protein binding was detected using 25 µl per well of PNPP (p-nitrophenyl phosphate; Thermo Fisher) and the reaction was measured at a wavelength of 405 nm by the Varioskan Lux Reader (Thermo Fisher Scientific). After each incubation step, plates were washed three times with 100 µl per well of washing buffer (phosphate-buffered saline and 0.05% Tween-20). Sample buffer was used as a blank and the threshold for sample positivity was set at twofold the optical density (OD) of the blank. Technical duplicates were performed for mAbs and technical triplicates were performed for sera samples.

ELISA assay with RBD, NTD and S2 subunits

Identification of mAbs and plasma screening of vaccinees against RBD, NTD or S2 SARS-CoV-2 protein were performed by ELISA. In brief, 3 µg/ml of RBD, NTD or S2 SARS-CoV-2 protein diluted in carbonate-bicarbonate buffer (E107, Bethyl Laboratories) was coated in 384-well plates (microplate clear, Greiner Bio-one). After overnight incubation at 4 °C, plates were washed three times with washing buffer (phosphate-buffered saline and 0.05% Tween-20) and blocked with 50 µl per well of blocking buffer (phosphate-buffered saline and 1% BSA) for 1 h at 37 °C. After washing, plates were incubated 1 h at 37 °C with mAbs diluted 1:5 in sample buffer (phosphate-buffered saline, 1% BSA and 0.05% Tween-20) or with plasma at a starting dilution of 1:10 and step diluted of 1:2 in sample buffer. Wells with no sample added were consider blank controls. Anti-human IgG–peroxidase antibody (Fab specific) produced in goat (Sigma) diluted 1:45,000 in sample buffer was then added and samples were incubated for 1 h at 37 °C. Plates were then washed, incubated with TMB substrate (Sigma) for 15 min before adding the stop solution (H_2SO_4 0.2 M). The OD values were identified using the Varioskan Lux Reader (Thermo Fisher Scientific) at 450 nm. Each condition was tested in triplicate and samples tested were considered positive if the OD value was twofold the blank.

Flow cytometry-based competition assay

To classify mAb candidates on the basis of their interaction with S epitopes, we performed a flow cytometry-based competition assay. In detail, magnetic beads (Dynabeads His-Tag, Invitrogen) were coated with histidine-tagged S protein according to the manufacturer's instructions. Then, 20 µg/ml of coated S protein beads were pre-incubated with unlabelled nAb candidates diluted 1:2 in PBS for 40 min at room temperature. After incubation, the mix beads–antibodies was washed with 100 µl of 1% PBS-BSA. Then, to analyse epitope competition, mAbs that are able to bind to the RBD (J08 and S309), NTD (4A8) or S2 domain (L19) of the S protein were labelled with four different fluorophores (Alexa Fluor 647, 488, 594 and 405) using the Alexa Fluor NHS Ester kit (Thermo Scientific), were mixed and incubated with S protein beads. Following 40 min of incubation at room temperature, the mix beads–antibodies was washed with PBS, resuspended in 150 µl of 1% PBS-BSA and analysed using the BD LSR II flow cytometer (Becton Dickinson). Beads with or without S protein incubated with labelled antibodies mix were used as positive and negative controls, respectively. FACSDiva Software (version 9) was used for data acquisition and analysis was performed using FlowJo (version 10).

SARS-CoV-2 authentic viruses neutralization assay

All SARS-CoV-2 authentic virus neutralization assays were performed in the biosafety level 3 (BSL3) laboratories at Toscana Life Sciences in Siena (Italy) and Vismederi Srl, Siena (Italy). BSL3 laboratories are approved by a certified biosafety professional and are inspected every year by local authorities. To evaluate the neutralization activity of identified nAbs against SARS-CoV-2 and all VoCs and to evaluate the breadth of neutralization of this antibody, CPE-MN was performed[5]. In brief, for the CPE-based neutralization assay, we co-incubated J08 with a SARS-CoV-2 viral solution containing 100 median tissue culture infectious dose (100 $TCID_{50}$) of virus, and after 1 h of incubation at 37 °C, 5% CO_2. The mixture was then added to the wells of a 96-well plate containing a sub-confluent Vero E6 cell monolayer. Plates were incubated for 3–4 days at 37 °C in a humidified environment with 5% CO_2, then examined for CPE by means of an inverted optical microscope by two independent operators. All nAbs were tested at a starting dilution of 1:5 and the IC_{100} was evaluated based on their initial concentration, while plasma samples were tested starting at a 1:10 dilution. Both nAbs and plasma samples were then step diluted 1:2. Technical duplicates were performed for both nAbs and plasma samples. In each plate, positive and negative controls were used as previously described[5].

SARS-CoV-2 virus variants CPE-MN neutralization assay

The SARS-CoV-2 viruses used to perform the CPE-MN neutralization assay were the original SARS-CoV-2 virus first detected in Wuhan

(SARS-CoV-2/INMI1-Isolate/2020/Italy: MT066156), SARS-CoV-2 B.1.1.7 (INMI GISAID accession number: EPI_ISL_736997), SARS-CoV-2 B.1.351 (EVAg Cod: 014V-04058), B.1.1.248 (EVAg CoD: 014V-04089) and B.1.617.2 (GISAID ID: EPI_ISL_2029113)[26].

Single-cell RT–PCR and Ig gene amplification and transcriptionally active PCR expression

The whole process for nAbs heavy and light chain recovery, amplification and transcriptionally active PCR (TAP) expression was performed as previously described[5]. In brief, 5 µl of cell lysate was mixed with 1 µl of random hexamer primers (50 ng/µl), 1 µl of dNTP-Mix (10 mM), 2 µl of 0.1 M DTT, 40 U/µl of RNAse OUT, $MgCl_2$ (25 mM), 5× FS buffer and Superscript IV reverse transcriptase (Invitrogen) to perform RT–PCR. Reverse transcription (RT) reaction was performed at 42 °C for 10 min, 25 °C for 10 min, 50 °C for 60 min and 94 °C for 5 min. Two rounds of PCR were performed to obtain the heavy (VH) and light (VL) chain amplicons. All PCRs were performed in a nuclease-free water (DEPC) in a total volume of 25 µl per well. For PCR I, 4 µl of cDNA were mixed with 10 µM of VH and 10 µM of VL primer-mix, 10 mM of dNTP mix, 0.125 µl of Kapa Long Range Polymerase (Sigma), 1.5 µl of MgCl2 and 5 µl of 5× Kapa Long Range Buffer. The PCR I reaction was performed at 95 °C for 3 min, 5 cycles at 95 °C for 30 s, 57 °C for 30 s, 72 °C for 30 s and 30 cycles at 95 °C for 30 s, 60 °C for 30 s, 72 °C for 30 s and a final extension of 72 °C for 2 min. Nested PCR II was performed as above starting from 3.5 µl of unpurified PCR I product. PCR II products were purified by the Millipore MultiScreen PCRµ96 plate according to manufacturer's instructions and eluted in 30 µl of nuclease-free water (DEPC). As for TAP expression, vectors were initially digested using restriction enzymes AgeI, SalI and Xho as previously described and PCR II products ligated by using the Gibson Assembly NEB into 25 ng of respective human Igγ1, Igκ and Igλ expression vectors[27,28]. TAP reaction was performed using 5 µl of Q5 polymerase (NEB), 5 µl of GC Enhancer (NEB), 5 µl of 5X buffer, 10 mM of dNTPs, 0.125 µl of forward/reverse primers and 3 µl of ligation product, using the following cycles: 98 °C for 2 min, 35 cycles 98 °C for 10 s, 61 °C for 20 s, 72 °C for 1 min and 72 °C for 5 min. TAP products were purified under the same PCR II conditions, quantified by the Qubit Fluorometric Quantitation assay (Invitrogen) and used for transient transfection in the Expi293F cell line following the manufacturer's instructions.

Functional repertoire analyses

The VH and VL sequence reads of nAbs were manually curated and retrieved using CLC sequence viewer (Qiagen). Aberrant sequences were removed from the dataset. Analysed reads were saved in FASTA format and the repertoire analyses were performed using Cloanalyst (http://www.bu.edu/computationalimmunology/research/software/)[29,30].

Statistical analysis

Statistical analysis was assessed with GraphPad Prism Version 8.0.2 (GraphPad Software). Non-parametric Mann–Whitney *t*-test was used to evaluate statistical significance between the two groups analysed in this study. Statistical significance was shown as $^{*}P \leq 0.05$, $^{**}P \leq 0.01$, $^{***}P \leq 0.001$, $^{****}P \leq 0.0001$.

Reporting summary

Further information on research design is available in the Nature Research Reporting Summary linked to this paper.

Data availability

Source data are provided with this paper. All data supporting the findings in this study are available within the article or can be obtained from the corresponding author on request. Source data are provided with this paper.

25. Huang, J. et al. Isolation of human monoclonal antibodies from peripheral blood B cells. *Nat. Protoc.* **8**, 1907–1915 (2013).
26. Planas, D. et al. Sensitivity of infectious SARS-CoV-2 B.1.1.7 and B.1.351 variants to neutralizing antibodies. *Nat. Med.* **27**, 917–924 (2021).
27. Tiller, T. et al. Efficient generation of monoclonal antibodies from single human B cells by single cell RT-PCR and expression vector cloning. *J. Immunol. Methods* **329**, 112–124 (2008).
28. Wardemann, H. & Busse, C. E. Expression cloning of antibodies from single human B cells. *Methods Mol. Biol.* **1956**, 105–125 (2019).
29. Kepler, T. B. Reconstructing a B-cell clonal lineage. I. Statistical inference of unobserved ancestors. *F1000Res.* **2**, 103 (2013).
30. Kepler, T. B. et al. Reconstructing a B-cell clonal lineage. II. Mutation, selection, and affinity maturation. *Front. Immunol.* **5**, 170 (2014).

Acknowledgements This work was funded by the European Research Council (ERC) advanced grant agreement number 787552 (vAMRes). This publication was supported by funds from the 'Centro Regionale Medicina di Precisione' and by all of the people who answered the call to fight with us in the battle against SARS-CoV-2 with their kind donations on the platform ForFunding (https://www.forfunding.intesasanpaolo.com/DonationPlatform-ISP/nav/progetto/id/3380). This work was funded by COOP ITALIA Soc. Coop. This publication was supported by the European Virus Archive goes Global (EVAg) project, which has received funding from the European Union's Horizon 2020 research and innovation programme under grant agreement number 653316. This publication was supported by the COVID-2020-12371817 project, which has received funding from the Italian Ministry of Health. We also acknowledge J. McLellan, for kindly providing the S protein trimer, RBD, NTD and S2 constructs; O. Schwartz, for providing the B.1.617.2 (Delta) SARS-CoV-2 variant; the nursing staff of the operative unit of the department of Medical Sciences, Infectious and Tropical Diseases Unit, Siena University Hospital, Siena, Italy; and all of the donors who are vaccinated against COVID-19 for participating to this study.

Author contributions E.A. and R.R. conceived the study. F.M., M.F., I.R. and M.T. enrolled the COVID-19 vaccinees. E.A. and I.P. performed PBMC isolation and single-cell sorting. I.P. performed ELISAs and competition assays. I.P. and N.M. recovered nAbs expressing VH and VL and antibodies. P.P. and E.A. recovered the VH and VL sequences and performed the repertoire analyses. E.P. and V.A. produced and purified the SARS-CoV-2 S protein constructs. E.A., G.P., I.H., M.L., L.B. and G.G. performed the neutralization assays in the BSL3 facilities. C.D.S. supported day-to-day laboratory activities and management. E.A. and R.R. wrote the manuscript. E.A., I.P., G.P., N.M., P.P., I.H., M.L., E.P., V.A., L.B., G.G., C.D.S., M.F., I.R., M.T., F.M., C.S., E.M. and R.R. undertook the final revision of the manuscript. E.A., C.S., E.M. and R.R. coordinated the project.

Competing interests R.R. is an employee of the GSK group of companies. E.A., I.P., N.M., P.P., E.P., C.D.S., C.S. and R.R. are listed as inventors of full-length human mAbs described in Italian patent applications no. 102020000015754 filed on 30 June 2020, 102020000018955 filed on 3 August 2020 and 102020000029969 filed on 4 December 2020, and the international patent system number PCT/IB2021/055755 filed on 28 June 2021. All patents were submitted by Fondazione Toscana Life Sciences, Siena, Italy. The remaining authors declare no competing interests.

Additional information
Supplementary information The online version contains supplementary material available at https://doi.org/10.1038/s41586-021-04117-7.
Correspondence and requests for materials should be addressed to Rino Rappuoli.
Peer review information *Nature* thanks the anonymous reviewer(s) for their contribution to the peer review of this work. Peer reviewer reports are available.
Reprints and permissions information is available at http://www.nature.com/reprints.

Article

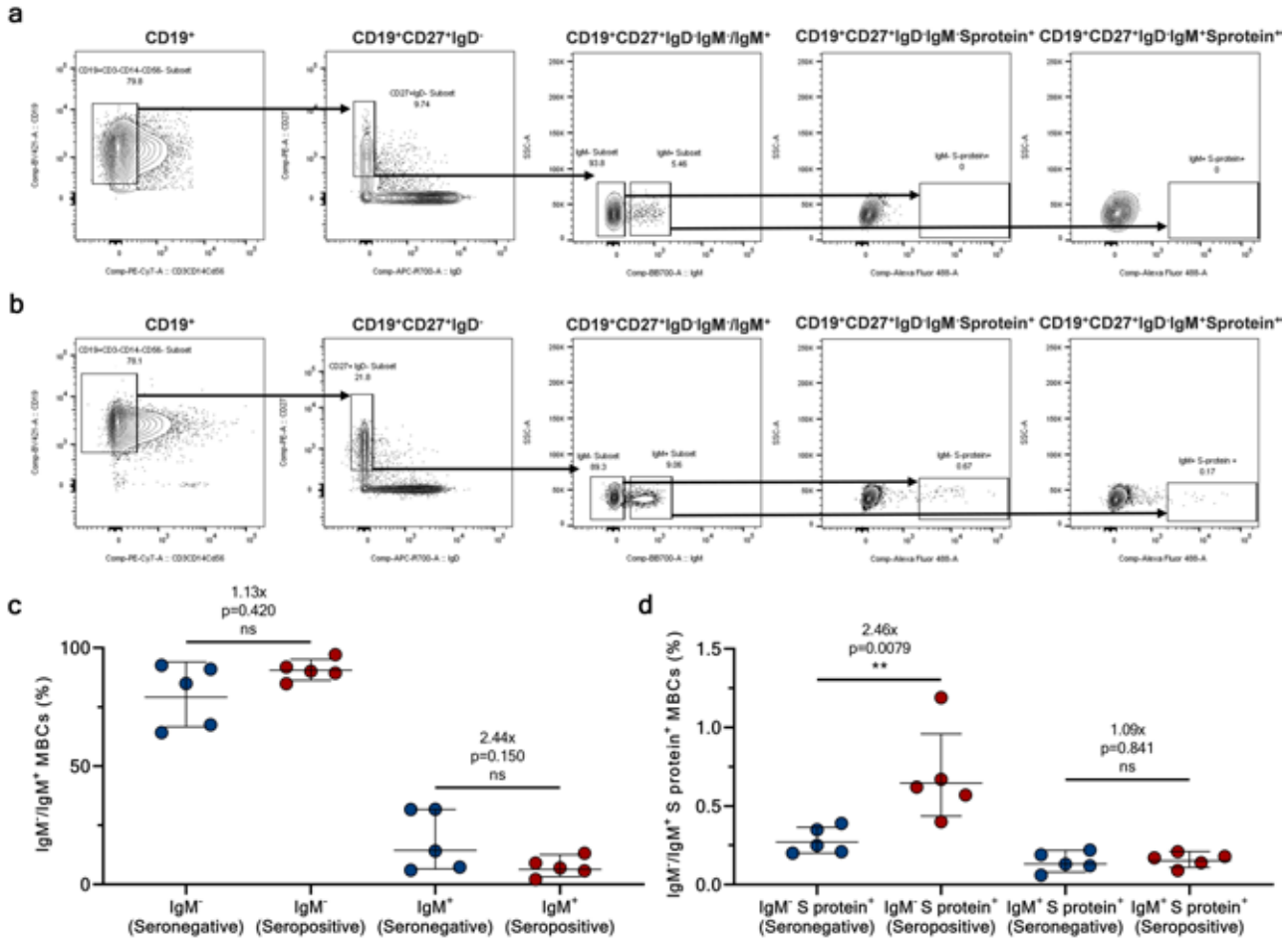

e

Subject	SARS-CoV-2 serology	IgM- Subset (%)	IgM- S protein+ Subset (%)	IgM+ Subset (%)	IgM+ S protein+ Subset (%)
VAC-001	Seronegative	67.50	0.21	31.70	0.13
VAC-002	Seronegative	64.20	0.25	31.80	0.06
VAC-007	Seronegative	92.60	0.35	6.02	0.22
VAC-008	Seronegative	84.90	0.39	14.10	0.12
VAC-010	Seronegative	91.00	0.20	7.27	0.19
VAC-003	Seropositive	91.80	0.57	5.77	0.21
VAC-004	Seropositive	97.10	0.62	2.14	0.14
VAC-005	Seropositive	89.30	0.67	9.06	0.17
VAC-006	Seropositive	90.10	0.40	6.94	0.18
VAC-009	Seropositive	84.80	1.19	13.20	0.09

Extended Data Fig. 1 | Single cell sorting and memory B cell frequencies. **a**, **b**, The gating strategy shows from left to right: $CD19^+$ B cells; $CD19^+CD27^+IgD^-$; $CD19^+CD27^+IgD^-IgM^-/IgM^+$; $CD19^+CD27^+IgD^-IgM^-Sprotein^+$; $CD19^+CD27^+IgD^-IgM^+Sprotein^+$ for a healthy donor (used as negative control for S protein staining) and a vaccinated subject. **c**, The graph shows the frequency of $CD19^+CD27^+IgD^-IgM^-$ and IgM^+ in seronegative (n=5) and seropositive donors (n=5). **d**, The graph shows the frequency of $CD19^+CD27^+IgD^-IgM^-$ and IgM^+ able to bind the SARS-CoV-2 S protein trimer (S protein$^+$) in seronegative (n=5) and seropositive (n=5) donors. Geometric mean and standard deviation are denoted on the graphs. A nonparametric Mann–Whitney t test was used to evaluate statistical significances between groups. Two-tailed p-value significances are shown as $^*p < 0.05$, $^{**}p < 0.01$, $^{***}p < 0.001$, and $^{****}p < 0.0001$. **e**, The table summarizes the frequencies of the cell population above described for all subjects enrolled in our study.

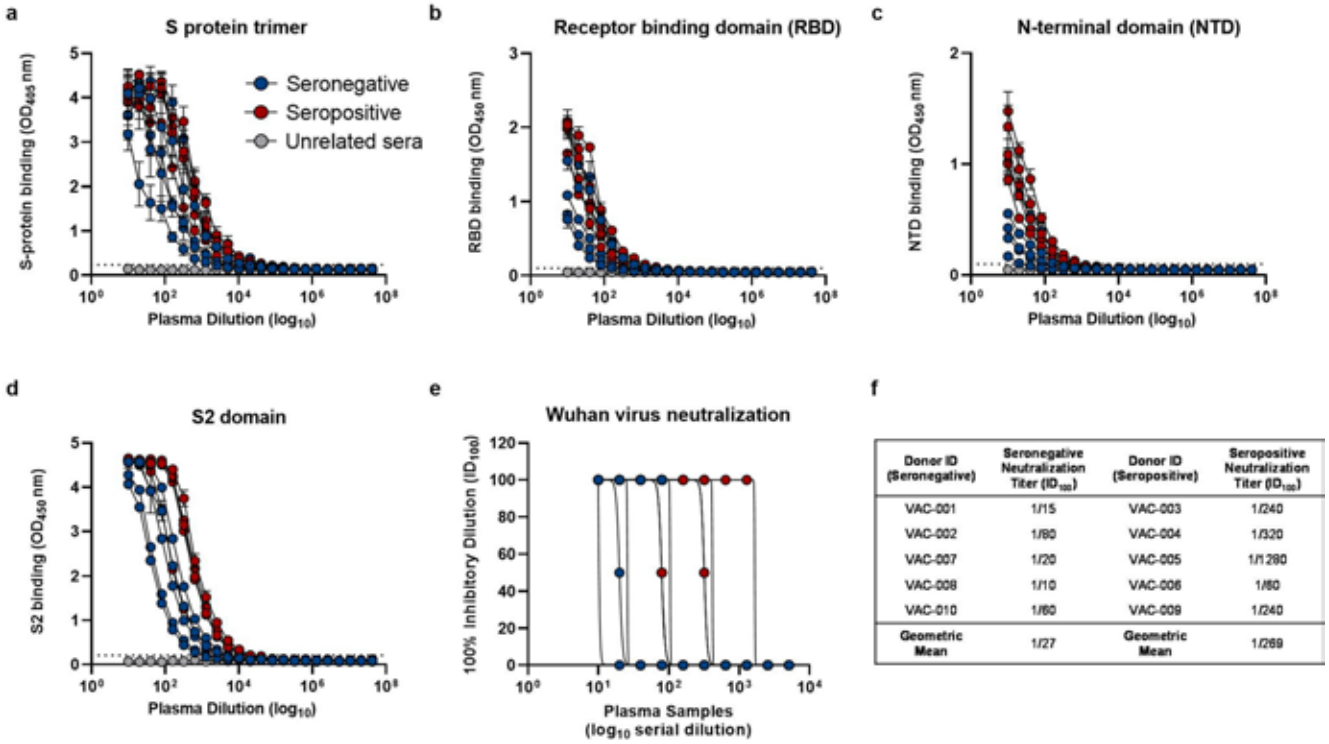

f

Donor ID (Seronegative)	Seronegative Neutralization Titer (ID_{100})	Donor ID (Seropositive)	Seropositive Neutralization Titer (ID_{100})
VAC-001	1/15	VAC-003	1/240
VAC-002	1/80	VAC-004	1/320
VAC-007	1/20	VAC-005	1/1280
VAC-008	1/10	VAC-006	1/60
VAC-010	1/60	VAC-009	1/240
Geometric Mean	1/27	Geometric Mean	1/269

Extended Data Fig. 2 | Plasma response of COVID-19 vaccinees. a–**d**, Graphs show the ability of plasma samples from seronegative and seropositive vaccinees to bind the S protein trimer, RBD, NTD and S2 domain. Mean and standard deviation are denoted on each graph. Technical triplicates were performed for each experiment. **e**, The graph shows the neutralizing activity of plasma samples against the original Wuhan SARS-CoV-2 virus. Technical duplicates were performed for each experiment. **f**, The table summarizes the 100% inhibitory dilution (ID_{100}) of each COVID-19 vaccinee and the geometric mean for seronegative and seropositive donors.

Article

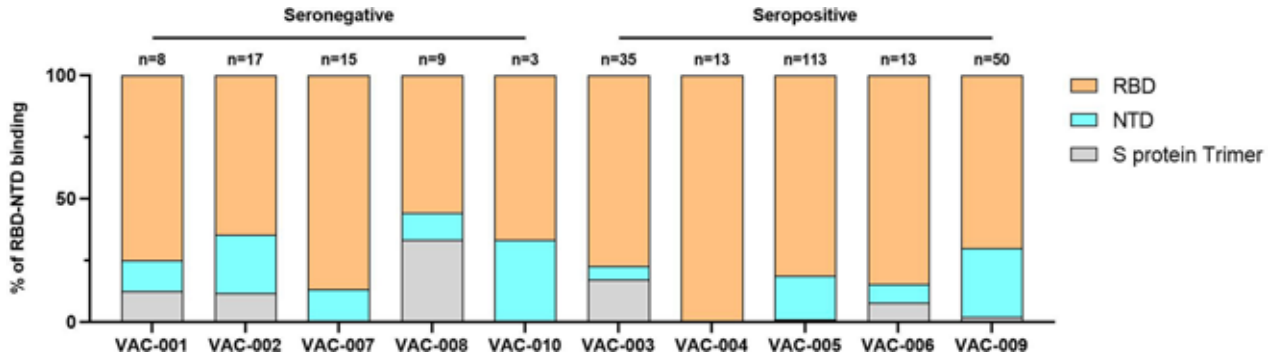

Extended Data Fig. 3 | RBD and NTD binding distribution of nAbs. The graph shows the percentage of antibodies that bind specifically the RBD (light orange) or the NTD (cyan) or that did not bind single domains but recognized exclusively the S protein in its trimetric conformation (gray). The number (n) of tested nAbs per donor is reported on top of each bar. Technical duplicates were performed for each experiment.

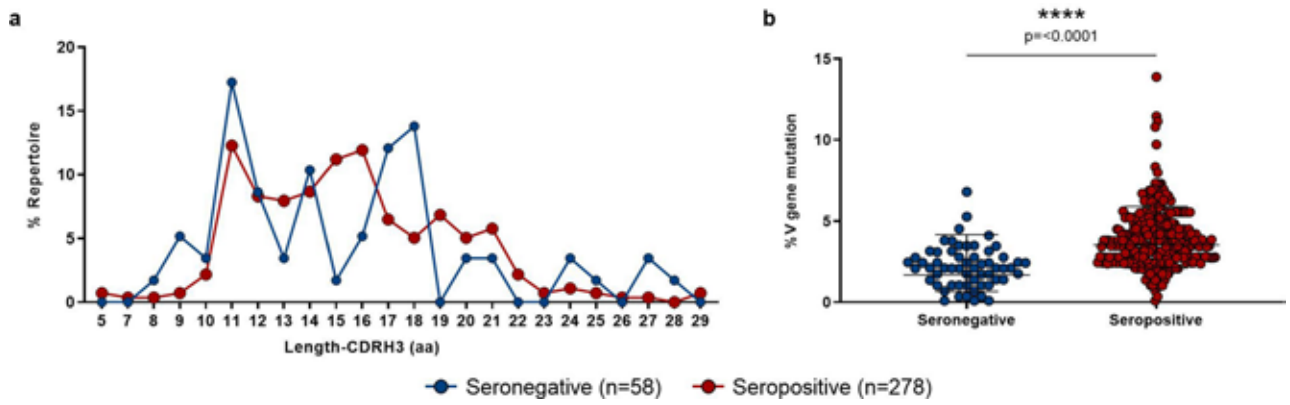

Extended Data Fig. 4 | Heavy chain CDR3 length and somatic hypermutation levels in seronegative and seropositive vaccinees. a, The graph shows the heavy chain CDR3 length represented in amino acids (aa). **b**, The graph shows the overall somatic hypermutation level of nAbs isolated from seronegative and seropositive vaccinees. Geometric mean and standard deviation are denoted on the graphs. A nonparametric Mann–Whitney t test was used to evaluate statistical significances between groups. Two-tailed p-value significances are shown as *p < 0.05, **p < 0.01, ***p < 0.001, and ****p < 0.0001.

Article

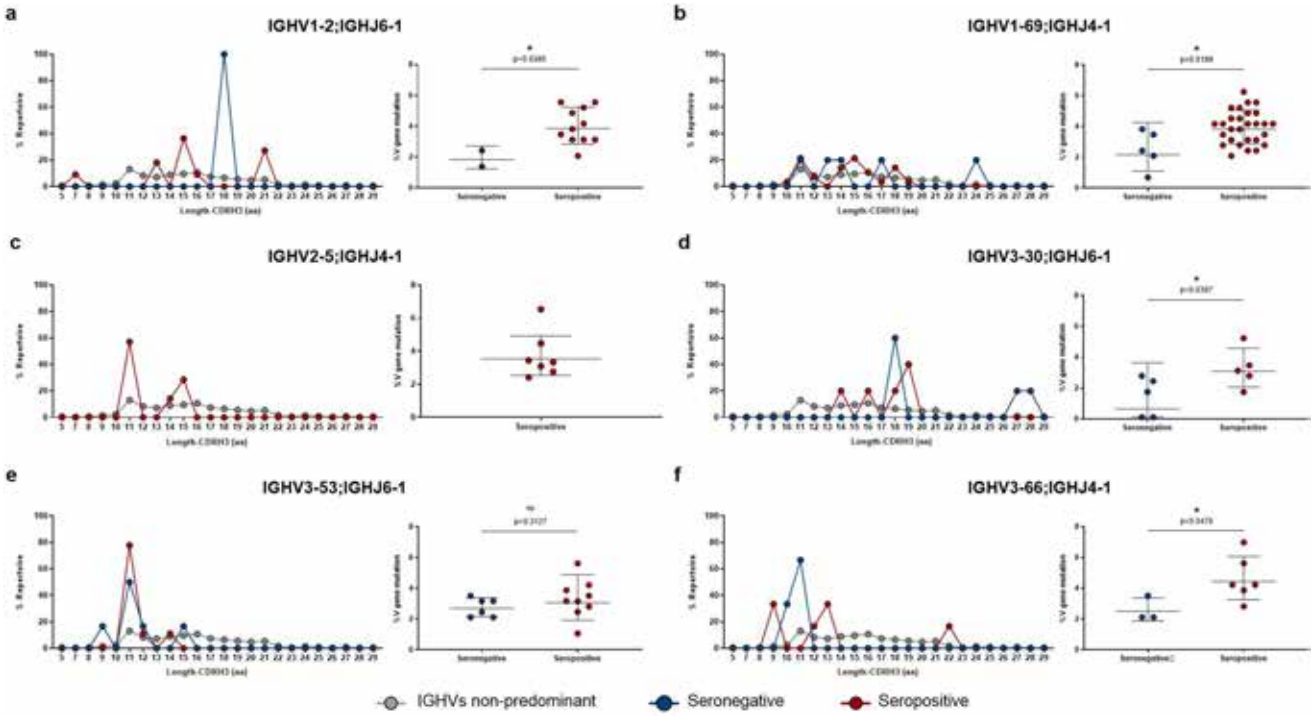

Extended Data Fig. 5 | Heavy chain CDR3 length and somatic hypermutation levels of predominant gene derived nAbs. a–**f**, Graphs show the amino acidic heavy chain CDR3 length (left panel) and the somatic hypermutation level (right panel) of nAbs derived from the IGHV1-2;IGHJ6-1 (*n* = 13), IGHV1-69;IGHJ4-1 (*n* = 33), IGHV2-5;IGHJ4-1 (*n* = 7), IGHV3-30;IGHJ6-1 (*n* = 10), IGHV3-53;IGHJ6-1 (*n* = 15) and IGHV3-66;IGHJ4-1 (*n* = 9) gene families. Geometric mean and standard deviation are denoted on the graphs. A nonparametric Mann–Whitney t test was used to evaluate statistical significances between groups. Two-tailed p-value significances are shown as *$p < 0.05$, **$p < 0.01$, ***$p < 0.001$, and ****$p < 0.0001$.

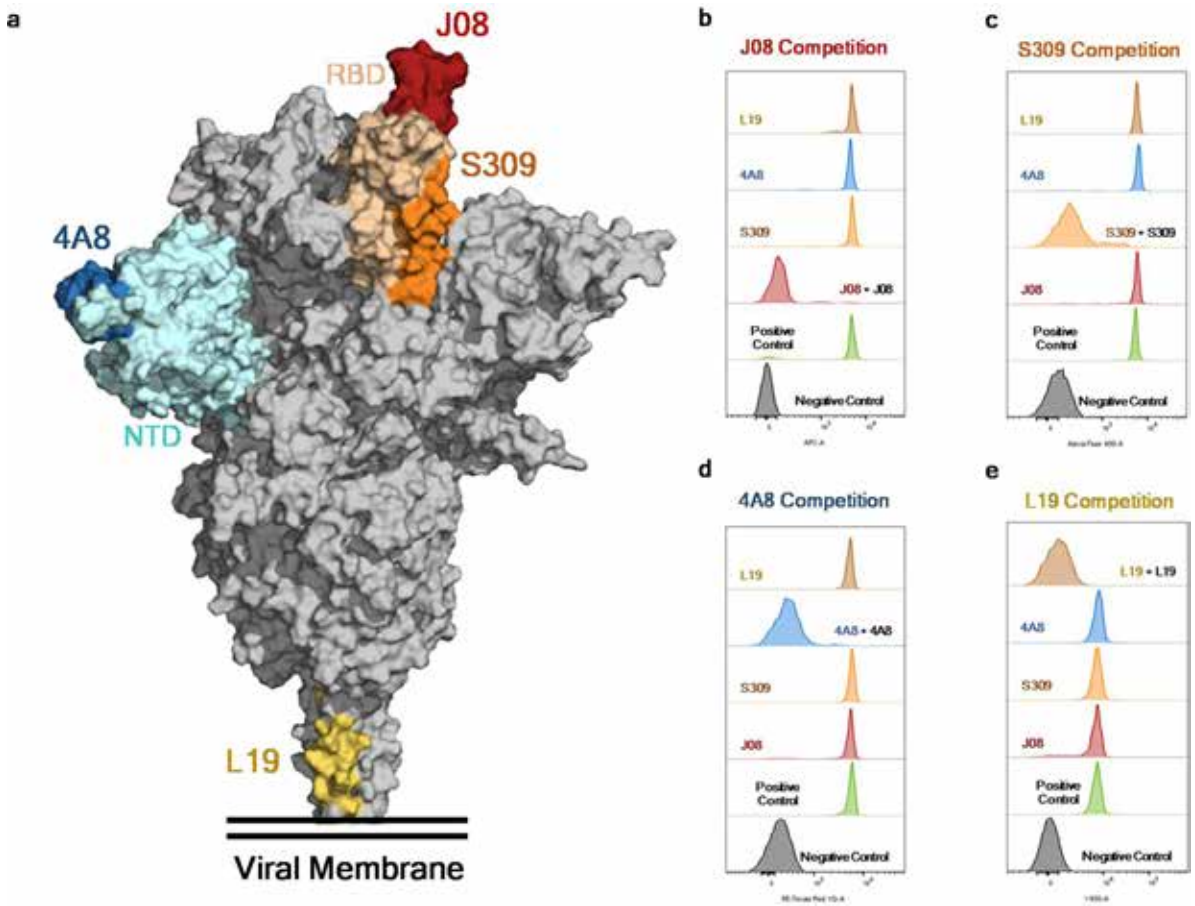

Extended Data Fig. 6 | Epitope binning assay. a, Schematic representation of the epitopes recognized by J08 (dark red), S309 (orange), 4A8 (dark blue) and L19 (gold), mAbs on the S protein surface. **b**–**e**, Representative cytometer peaks per each of the four mAbs used for the competition assay. Positive (beads conjugated with only primary labeled antibody) and negative (un-conjugated beads) controls are shown as green and gray peaks, respectively.

Article

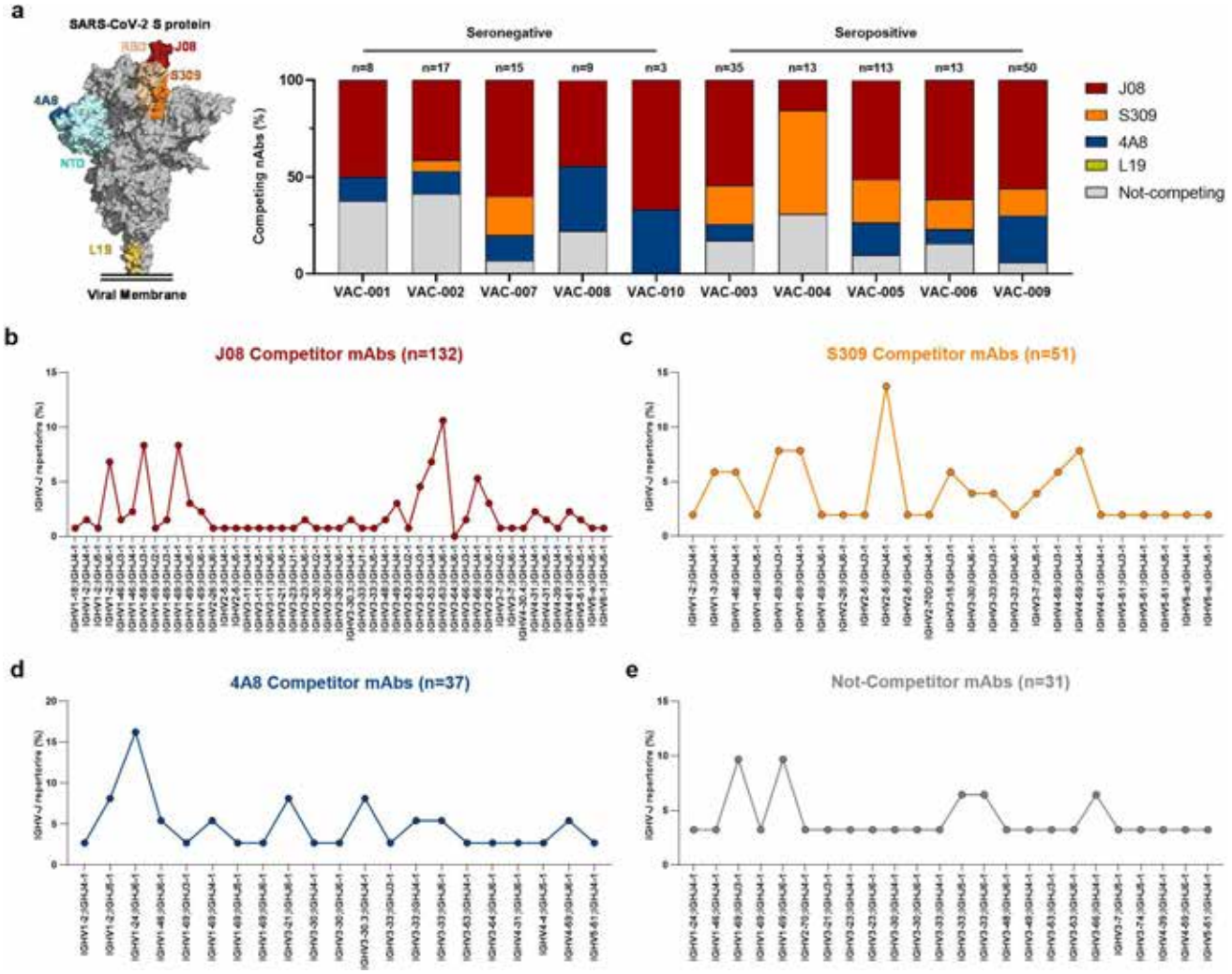

Extended Data Fig. 7 | Epitope binning and genetic characterization of competing nAbs. a, The bar graph shows the percentage (%) of nAbs competing with J08 (dark red), S309 (orange), 4A8 (dark blue) and L19 (gold), or antibodies that did not compete with any of the previous mAbs (gray). A schematic representation of J08, S309, 4A8 and L19 epitopes on the S protein surface is shown on the left side of the panel. **b**–**e**, Graphs show the IGHV-J rearrangement percentage for nAbs that competed against J08, S309, 4A8, or that did not compete with any of these mAbs. The total number (n) of competing nAbs per group is shown on top of each graph.

Extended Data Table 1 | Clinical details of COVID-19 vaccinees

Subject ID	Gender	Age	Previous COVID-19 negative test	COVID-19 positive test	Type of test	Severity of Infection	SARS-CoV-2 Serology	First Dose (dd/mm/yy)	Second Dose (dd/mm/yy)	Blood Collection (dd/mm/yy)	Days from Infection to First Dose	Days from Last Dose to Blood Collection
VAC-001	M	38	16/12/2020	Not-applicable	Swab	Not-applicable	Seronegative	27/12/2020	18/01/2021	02/03/2021	Not-applicable	43
VAC-002	F	38	31/12/2020	Not-applicable	Swab	Not-applicable	Seronegative	01/01/2021	22/01/2021	02/03/2021	Not-applicable	39
VAC-007	M	38	29/12/2020	Not-applicable	Swab	Not-applicable	Seronegative	04/01/2021	25/01/2021	31/03/2021	Not-applicable	65
VAC-008	M	43	28/12/2020	Not-applicable	Swab	Not-applicable	Seronegative	03/01/2021	24/01/2021	31/03/2021	Not-applicable	66
VAC-010	F	51	15/02/2021	Not-applicable	Swab	Not-applicable	Seronegative	18/02/2021	11/03/2021	07/04/2021	Not-applicable	27
VAC-003	M	38	15/10/2020	26/10/2020	Swab	Asymptomatic	Seropositive	08/01/2021	15/02/2021	09/03/2021	74	22
VAC-004	F	25	Not-applicable	22/10/2020	Swab	Mild	Seropositive	08/02/2021	01/03/2021	09/03/2021	78	8
VAC-005	M	25	01/08/2020	02/11/2020	Serological	Mild	Seropositive	11/01/2021	16/02/2021	16/03/2021	71	28
VAC-006	F	57	27/04/2020	24/10/2020	Swab	Asymptomatic	Seropositive	16/01/2021	11/02/2021	16/03/2021	79	33
VAC-009	M	46	29/09/2020	06/11/2020	Serological	Moderate	Seropositive	20/03/2021	Not-applicable	07/04/2021	134	18

Article

Extended Data Table 2 | Summary of B cell frequencies and antibodies of COVID-19 vaccinees

Subject	SARS-CoV-2 serology	S protein+ MBCs Sorted	S protein+ mAbs (n)	S protein+ mAbs (%)	Wuhan - Neutralizing antibodies (n)	Wuhan - Neutralizing antibodies (%)	B.1.1.7 - Neutralizing antibodies (n)	B.1.1.7 - Neutralizing antibodies (%)	B.1.351 - Neutralizing antibodies (n)	B.1.351 - Neutralizing antibodies (%)	B.1.1.248 - Neutralizing antibodies (n)	B.1.1.248 - Neutralizing antibodies (%)
VAC-001	Seronegative	484	205	42.3	13	6.3	8	61.5	2	15.4	6	46.2
VAC-002	Seronegative	497	316	63.6	27	8.5	19	70.4	6	22.2	11	40.7
VAC-007	Seronegative	161	100	62.1	16	16.0	14	87.5	3	18.8	6	37.5
VAC-008	Seronegative	682	107	15.7	10	9.3	6	60.0	5	50.0	6	60.0
VAC-010	Seronegative	528	216	40.9	5	2.3	3	60.0	0	0.0	2	40.0
Total (Seronegative)		2,352	944	40.1	71	7.5	50	70.4	16	22.5	31	43.6
VAC-003	Seropositive	616	428	69.5	78	18.2	58	74.4	25	32.1	40	51.3
VAC-004	Seropositive	506	318	62.8	31	9.7	24	77.4	11	35.5	18	58.1
VAC-005	Seropositive	924	601	65.0	152	25.3	132	86.8	78	51.3	114	75.0
VAC-006	Seropositive	396	216	55.8	19	8.8	12	63.2	5	26.3	8	42.1
VAC-009	Seropositive	1,090	736	67.5	60	8.1	48	80.0	15	25.0	31	51.7
Total (Seropositive)		3,532	2,299	65.1	340	14.8	274	80.6	134	39.4	211	62.0

Extended Data Table 3 | Competition assay summary

Subject	SARS-CoV-2 serology	Distribution Competition J08 (n)	Distribution Competition J08 (%)	Distribution Competition S309 (n)	Distribution Competition S309 (%)	Distribution Competition 4A8 (n)	Distribution Competition 4A8 (%)	Distribution Competition L19 (n)	Distribution Competition L19 (%)	Distribution Competition Not-competing (n)	Distribution Competition Not-competing (%)
VAC-001	Seronegative	4	50.0	0	0.0	1	12.5	0	0.0	3	37.5
VAC-002	Seronegative	7	41.2	1	5.9	2	11.8	0	0.0	7	41.2
VAC-007	Seronegative	9	60.0	3	20.0	2	13.3	0	0.0	1	6.7
VAC-008	Seronegative	4	44.4	0	0.0	3	33.3	0	0.0	2	22.2
VAC-010	Seronegative	2	66.7	0	0.0	1	33.3	0	0.0	0	0.0
Total (Seronegative)		26	50.0	4	7.7	9	17.3	0	0.0	13	25.0
VAC-003	Seropositive	19	54.3	7	20.0	3	8.6	0	0.0	6	17.1
VAC-004	Seropositive	2	15.4	7	53.8	0	0.0	0	0.0	4	30.8
VAC-005	Seropositive	58	51.3	25	22.1	19	16.8	0	0.0	11	9.7
VAC-006	Seropositive	8	61.5	2	15.4	1	7.7	0	0.0	2	15.4
VAC-009	Seropositive	28	56.0	7	14.0	12	24.0	0	0.0	3	6.0
Total (Seropositive)		115	51.3	48	21.4	35	15.6	0	0.0	26	11.6

nature portfolio

Corresponding author(s): Rino Rappuoli

Last updated by author(s): Oct 3, 2021

Reporting Summary

Nature Portfolio wishes to improve the reproducibility of the work that we publish. This form provides structure for consistency and transparency in reporting. For further information on Nature Portfolio policies, see our Editorial Policies and the Editorial Policy Checklist.

Statistics

For all statistical analyses, confirm that the following items are present in the figure legend, table legend, main text, or Methods section.

n/a	Confirmed	
☐	☒	The exact sample size (*n*) for each experimental group/condition, given as a discrete number and unit of measurement
☐	☒	A statement on whether measurements were taken from distinct samples or whether the same sample was measured repeatedly
☐	☒	The statistical test(s) used AND whether they are one- or two-sided *Only common tests should be described solely by name; describe more complex techniques in the Methods section.*
☒	☐	A description of all covariates tested
☒	☐	A description of any assumptions or corrections, such as tests of normality and adjustment for multiple comparisons
☐	☒	A full description of the statistical parameters including central tendency (e.g. means) or other basic estimates (e.g. regression coefficient) AND variation (e.g. standard deviation) or associated estimates of uncertainty (e.g. confidence intervals)
☐	☒	For null hypothesis testing, the test statistic (e.g. *F*, *t*, *r*) with confidence intervals, effect sizes, degrees of freedom and *P* value noted *Give P values as exact values whenever suitable.*
☒	☐	For Bayesian analysis, information on the choice of priors and Markov chain Monte Carlo settings
☒	☐	For hierarchical and complex designs, identification of the appropriate level for tests and full reporting of outcomes
☒	☐	Estimates of effect sizes (e.g. Cohen's *d*, Pearson's *r*), indicating how they were calculated

Our web collection on statistics for biologists contains articles on many of the points above.

Software and code

Policy information about availability of computer code

Data collection	- Thermo Fisher SkanIt Software Microplate Readers 6.0.1 - BD Biosciences BD FACSDiva Software v9.0
Data analysis	- GraphPad Prism 8.0.2 was used to perform statistical analyses - BD FlowJo 10.5.3 - Qiagen CLC sequence viewer 350 8.0.0 - Boston University, Cloanalyst (http://www.bu.edu/computationalimmunology/research/software/)

For manuscripts utilizing custom algorithms or software that are central to the research but not yet described in published literature, software must be made available to editors and reviewers. We strongly encourage code deposition in a community repository (e.g. GitHub). See the Nature Portfolio guidelines for submitting code & software for further information.

Data

Policy information about availability of data

All manuscripts must include a data availability statement. This statement should provide the following information, where applicable:

- Accession codes, unique identifiers, or web links for publicly available datasets
- A description of any restrictions on data availability
- For clinical datasets or third party data, please ensure that the statement adheres to our policy

Source data are provided with this paper. All data supporting the findings in this study are available within the article or can be obtained from the corresponding author upon request.

Field-specific reporting

Please select the one below that is the best fit for your research. If you are not sure, read the appropriate sections before making your selection.

☒ Life sciences ☐ Behavioural & social sciences ☐ Ecological, evolutionary & environmental sciences

For a reference copy of the document with all sections, see nature.com/documents/nr-reporting-summary-flat.pdf

Life sciences study design

All studies must disclose on these points even when the disclosure is negative.

Sample size	10 subjects in total, 5 seronegative and 5 seropositive, were analyzed in this study. A total of 2,352 and 3,532 spike protein specific memory B cells from seronegative and seropositive subjects were tested in this study. Given the exploratory nature of the study, we did not use statistical methods to predetermine sample size. Sample size was based on previous studies that applied a similar technology. The authors believed that 5 subjects/group were a good balance between feasibility of analyzing at single cell level several thousands of memory B cells and the ability to represent the antibody response of seronegative and seropositve people.
Data exclusions	No data was excluded.
Replication	All experiments were performed in technical duplicates or triplicates as indicated in the figure legends and methods section.
Randomization	The experiments were not randomized and all available samples were tested. The authors aimed to specifically assess the antibody response of seronegative and seropositve subjects. Donors were specifically recruited based on their previous infection and vaccination history. Randomization would have not allowed to enroll 5 subjects/group which was our technical limit for single cell analysis of the antibody response. Based on what stated above, the authors believed that randomization was not appropriate.
Blinding	The investigators were not blinded during group allocation, data collection and analyses. The clinical protocol established to enroll subjects in this study reports information regarding previous infection and vaccination in order to allocate 5 subjects/group. Pseudonymized information received in the lab reports the same information and therefore blinding for group allocation was not possible.

Reporting for specific materials, systems and methods

We require information from authors about some types of materials, experimental systems and methods used in many studies. Here, indicate whether each material, system or method listed is relevant to your study. If you are not sure if a list item applies to your research, read the appropriate section before selecting a response.

Materials & experimental systems

n/a	Involved in the study
☐	☒ Antibodies
☐	☒ Eukaryotic cell lines
☒	☐ Palaeontology and archaeology
☒	☐ Animals and other organisms
☐	☒ Human research participants
☒	☐ Clinical data
☒	☐ Dual use research of concern

Methods

n/a	Involved in the study
☒	☐ ChIP-seq
☐	☒ Flow cytometry
☒	☐ MRI-based neuroimaging

Antibodies

Antibodies used	BD Biosciences CD19 BV421, Cat#562440, Clone ID HIB19, Lot#8270584 BD Biosciences IgM PerCP-Cy5.5, Cat#561285, Clone ID G20-127, Lot#9269055 BD Biosciences CD27 PE, Cat#340425, Clone ID L128, Lot#9288842 BD Biosciences IgD-A700, Cat#561302, Clone ID IA6-2, Lot#9199226 BioLegend CD3 PE-Cy7, Cat#300420, Clone ID UCHT1, Lot#B303315 BioLegend CD14 PE-Cy7, Cat#301814, Clone ID M5E2, Lot#B272337 BioLegend CD56 PE-Cy7, Cat#318318, Clone ID HCD56, Lot#B297987 Southern Biotech Goat Anti-Human IgG-Alkaline Phosphatase, Cat#2040-04, polyclonal, Lot#K2119-XG00B Southern Biotech Goat Anti-Human IgA-Alkaline Phosphatase, Cat#2050-04, polyclonal, Lot#G0919-W620C Sigma-Aldrich Anti-Human IgG (Fab specific)–Peroxidase antibody produced in goat, Cat#A0293, polyclonal, Lot#019M4876V
Validation	BD Biosciences CD19 BV421, Cat#562440, Clone ID HIB19, QC testing, reactivity human, application flow cytometry (https://www.bdbiosciences.com/content/bdb/paths/generate-tds-document.us.562440.pdf). BD Biosciences IgM PerCP-Cy5.5, Cat#561285, Clone ID G20-127, QC testing, reactivity human, application flow cytometry (https://www.bdbiosciences.com/content/bdb/paths/generate-tds-document.us.561285.pdf). BD Biosciences CD27 PE, Cat#340425, Clone ID L128, QC testing, reactivity human, application flow cytometry (https://

www.bdbiosciences.com/en-us/products/reagents/flow-cytometry-reagents/clinical-discovery-research/single-color-antibodies-ruo-gmp/pe-mouse-anti-human-cd27.340425)
BD Biosciences IgD-A700, Cat#561302, Clone ID IA6-2, QC testing, reactivity human, application flow cytometry (https://www.bdbiosciences.com/content/bdb/paths/generate-tds-document.us.561302.pdf)
BioLegend CD3 PE-Cy7, Cat#300420, Clone ID UCHT1, reactivity human and cross-reactivity with chimpanzee, application flow cytometry (https://www.biolegend.com/en-us/global-elements/pdf-popup/pe-cyanine7-anti-human-cd3-antibody-3070?filename=PECyanine7%20anti-human%20CD3%20Antibody.pdf&pdfgen=true)
BioLegend CD14 PE-Cy7, Cat#301814, Clone ID M5E2, Reactivity Human, African Green, Capuchin Monkey, Cattle (Bovine, Cow), Chimpanzee, Common Marmoset, Cotton-topped Tamarin, Cynomolgus, Dog (Canine), Rhesus, Pigtailed Macaque, Squirrel Monkey, application flow cytometry (https://www.biolegend.com/en-us/global-elements/pdf-popup/pe-cyanine7-anti-human-cd14-antibody-2729?filename=PECyanine7%20anti-human%20CD14%20Antibody.pdf&pdfgen=true)
BioLegend CD56 PE-Cy7, Cat#318318, Clone ID HCD56, Reactivity Human, African Green, Baboon, Cynomolgus, Rhesus, application flow cytometry (https://www.biolegend.com/en-us/global-elements/pdf-popup/pe-cyanine7-anti-human-cd56-ncam-antibody-3802?filename=PECyanine7%20anti-human%20CD56%20NCAM%20Antibody.pdf&pdfgen=true)
Southern Biotech Goat Anti-Human IgG-Alkaline Phosphatase, Cat#2040-04, polyclonal, reactivity heavy chain of human IgG, application ELISA (https://www.southernbiotech.com/techbul/2040.pdf)
Southern Biotech Goat Anti-Human IgA-Alkaline Phosphatase, Cat#2050-04, polyclonal, reactivity heavy chain of human IgA, application ELISA (https://www.southernbiotech.com/techbul/2050.pdf)
Sigma-Aldrich Anti-Human IgG (Fab specific)–Peroxidase antibody produced in goat, Cat#A0293, polyclonal, reactivity human, application ELISA (https://www.sigmaaldrich.com/IT/en/product/sigma/a0293#)

Eukaryotic cell lines

Policy information about cell lines

Cell line source(s)	VERO E6 cell line ATCC Cat#CRL-1586; Expi293F cells Thermo Fisher Cat#A14527; 3T3-msCD40L Cells NIH AIDS Reagent Program Cat#12535.
Authentication	These cell lines were obtained from vendors that sell authenticated cell lines, they grew, performed and showed morphology as expected. No additional specific authentication was performed.
Mycoplasma contamination	Vero E6 cell lines are routinely tested on a monthly basis and tested negative for mycoplasma. 3T3-msCD40L cell line was tested negative to mycoplasma by the provider and Expi293F cells were not tested for mycoplasma contamination.
Commonly misidentified lines (See ICLAC register)	No commonly misidentified cell lines were used in this study.

Human research participants

Policy information about studies involving human research participants

Population characteristics	This work results from a collaboration with the Azienda Ospedaliera Universitaria Senese, Siena (IT) that provided samples from COVID-19 vaccinated donors, of both sexes (4 females and 6 males), who gave their written consent. All data relevant to enrolled subjects are reported in this study. Subjects elegible for this study were of all sexes (aged 18-85) naïve or previously infected by SARS-CoV-2 and then vaccinated with the COVID-19 BNT162b2 mRNA vaccine.
Recruitment	Individuals with or without previous SARS-CoV-2 infection vaccinated with the COVID-19 BNT162b2 mRNA vaccine were enrolled by the clinicians involved in the study entitled "Isolamento di anticorpi monoclonali umani contro SARS-CoV-2 per lo sviluppo di nuove terapie e vaccini", Prot. n. TLS_SARS-CoV-2, at the Azienda Ospedaliera Universitaria Senese, Siena (IT). The authors do not see any potential bias in the generation or interpretation of the data reported in this study.
Ethics oversight	The study was approved by the Comitato Etico di Area Vasta Sud Est (CEAVSE) ethics committees (Parere 17065 in Siena) and conducted according to good clinical practice in accordance with the declaration of Helsinki (European Council 2001, US Code of Federal Regulations, ICH 1997). This study was unblinded and not randomized. No statistical methods were used to predetermine sample size.

Note that full information on the approval of the study protocol must also be provided in the manuscript.

Flow Cytometry

Plots

Confirm that:

☒ The axis labels state the marker and fluorochrome used (e.g. CD4-FITC).

☒ The axis scales are clearly visible. Include numbers along axes only for bottom left plot of group (a 'group' is an analysis of identical markers).

☒ All plots are contour plots with outliers or pseudocolor plots.

☒ A numerical value for number of cells or percentage (with statistics) is provided.

Methodology

Sample preparation	Human PBMC were isolated from heparin-treated whole blood by density gradient centrifugation (Ficoll-Paque™ PREMIUM,

Sample preparation	Sigma-Aldrich). After separation, PBMC were stained with Live/Dead Fixable Aqua (Invitrogen; Thermo Scientific) diluted 1:500 at room temperature RT. After 20 min incubation cells were washed with PBS and unspecific bindings were saturated with 20% normal rabbit serum (Life technologies). Following 20 min incubation at 4°C cells were washed with PBS and stained with SARS-CoV-2 S-protein labeled with Strep-Tactin®XT DY-488 (iba-lifesciences cat# 2-1562-050) for 30 min at 4°C. After incubation the following staining mix was used CD19 V421 (BD cat# 562440, 1:320), IgM PerCP-Cy5.5 (BD cat# 561285, 1:50), CD27 PE (BD cat# 340425, 1:30), IgD-A700 (BD cat# 561302, 1:15), CD3 PE-Cy7 (BioLegend cat# 300420, 1:100), CD14 PE-Cy7 (BioLegend cat# 301814, 1:320), CD56 PE-Cy7 (BioLegend cat# 318318, 1:80) and cells were incubated at 4°C for additional 30 min. Stained MBCs were single cell-sorted with a BD FACS Aria III (BD Biosciences).
Instrument	BD FACS Aria III Cell Sorter BD Biosciences
Software	BD Biosciences BD FACSDiva Software v9.0
Cell population abundance	Single cell sorted S protein trimer-specific (S protein+), class-switched memory B cells (CD19+CD27+IgD-IgM-) were 0.21, 0.25, 0.35, 0.39, 0.20, 0.57, 0.62, 0.67, 0.40 and 1.19% for subject VAC-001, VAC-002, VAC-007, VAC-008, VAC-010, VAC-003, VAC-004, VAC-005, VAC-006 and VAC-009 respectively. Sorted cells were gated on the CD19+CD27+IgD-IgM-S protein+ population based on the negative control as reported in the Extended Data (Extended Data Figure 1a,b).
Gating strategy	The gating strategy used for the single cell sorting of spike protein specific memory B cells is shown in the Extended Data (Extended Data Figure 1). Boundaries between “positive” and “negative” cells are defined and denoted on each graph.

☒ Tick this box to confirm that a figure exemplifying the gating strategy is provided in the Supplementary Information.

Journal of Virological Methods 297 (2021) 114261

Contents lists available at ScienceDirect

Journal of Virological Methods

journal homepage: www.elsevier.com/locate/jviromet

Short communication

The theory and practice of the viral dose in neutralization assay: Insights on SARS-CoV-2 "doublethink" effect

Alessandro Manenti [a,*], Eleonora Molesti [b], Marta Maggetti [a], Alessandro Torelli [a], Giulia Lapini [a], Emanuele Montomoli [a,b,c]

[a] VisMederi s.r.l., Siena, Italy
[b] VisMederi Research s.r.l., Siena, Italy
[c] Department of Molecular and Developmental Medicine, University of Siena, Siena, Italy

ARTICLE INFO

Keywords:
SARS-CoV-2
Infective dose
Live virus
Micro-neutralisation
Immunological responses

ABSTRACT

The neutralization assays are considered the gold-standard being capable of evaluating and detecting, functional antibodies. To date, many different protocols exist for micro-neutralization (MN) assay which varies in several steps: cell number and seeding conditions, virus amount used in the infection step, virus-serum-cells incubation time and read out.

The aim of the present preliminary study was to carry out SARS-CoV-2 wild type MN assay in order to investigate which optimal tissue culture infective dose 50 ($TCID_{50}$) infective dose in use is the most adequate choice for implementation in terms of reproducibility, standardization possibilities and comparability of results. Therefore, we assessed the MN by using two viral infective doses: the "standard" dose of 100 $TCID_{50}$/well and a reduced dose of 25 $TCID_{50}$/well. The results obtained, yielded by MN on using the lower infective dose (25 TCID50), were higher respect to those obtained with the standard infective dose. This suggests that the lower dose can potentially have a positive impact on the detection and estimation of real amount of neutralizing antibodies present in a given sample, showing higher sensitivity maintaining high specificity.

The detection and quantitation of serum antibodies to different viral antigens, after natural infection and/or immunization, has long been used to assess the likelihood of protection against a specific pathogen (Petherick, 2020). The Enzyme Linked-immunosorbent assay (ELISA) is one of the most used method for total antibodies detection. This method is able to detect all the immunoglobulins (class and subclass) present in a given sample able to bind the specific antigen of interest coated in a dedicated plate. It is fast, cheap and safe because it does not require the handling of live pathogens. Another classical way of measuring antibody response for agglutinating viruses such as Influenza, is the Haemagglutination Inhibition assay (HAI). This method is considered as the gold standard in Influenza field (Hirst, 1942; Salk, 1944) and correlates of protection have been established. It is based upon the principle that antibody able to bind the globular head of the haemagglutinin (HA) can inhibit the HA's ability to agglutinate red blood cells (RBCs) by prevent the binding between the head domain (HA1) and the sialic acids (SA) present on the RBC surface. Both, ELISA and HAI suffer from the fact that they are not able to give a precise indication about the functionality of the antibodies detected. Given these limitations, the neutralization assays are an attractive alternative for the assessment of baseline sero-status and the evaluation of the humoral responses following natural infection and/or vaccination (Klimov et al., 2012). MN assays were developed in 1990 (Okuno et al., 1990; Bachmann et al., 1999). This is a functional assay, and it is able to detect neutralizing antibodies capable of prevent the virus infection of different mammalian cell lines and the neutralization activity is measured as the ability of the sera to reduce the cytopathic effect (CPE) due to inhibition of viral entry and subsequent replication (WHO, 2011). Compared to the ELISA-based methods, the results derived by the MN represent a more precise and relevant estimation of antibody-mediated protection in-vitro (Sicca et al., 2020).

On the other hand, MN is more complex to manage due to some requirements: the need of live viruses and biosecurity level 4, 3 or 2+ laboratories (in case of class IV, III or II pathogens), the costs associated with the assay and the difficulties in protocol standardization across laboratories (e.g. cell lines, infective dose, days of incubation and read-out).

* Corresponding author at: Strada del Petriccio e Belriguardo, 35 – 53100, Siena, Italy.
E-mail address: alessandro.manenti@vismederi.com (A. Manenti).

https://doi.org/10.1016/j.jviromet.2021.114261
Received 5 May 2021; Received in revised form 6 August 2021; Accepted 7 August 2021
Available online 14 August 2021

In the present small and investigative study, we focused our attention on the performance of the MN assay with SARS-CoV-2 wild type virus using two different input of viral dose: the standard 100 Tissue Culture Infective Dose 50 % (TCID50) and the 25 TCID50 infective dose. As it is well known in the field of enzymology and enzyme kinetics (Adamczyk et al., 2011), there is a close bond between the half maximum inhibitory concentration (IC50) value and the chosen concentration of the enzyme/molecule in a given system. In this case, by lowering the SARS−COV-2 viral input we expect to observe a general improve in antibody titers and, the focus of this work was to try to evaluate what is the most appropriate value of viral dose to perform the MN in order to have strong sensitivity and specificity as well. Regarding this, a total of 102 human serum samples, anonymously collected in compliance with Italian ethics law, were collected as part of an epidemiological study performed at the University of Siena, Italy (Marchi et al., 2019). The human monoclonal antibody (mAb) IgG1 SAD-S35 (Acrobiosystem) was tested along with the serum samples in the MN assay and ELISA Kit (Euroimmun) as positive control. Human serum minus IgA/IgM/IgG (S5393−1VL) (Sigma, St. Louis, MO, USA) was used as a negative control. SARS-CoV 2 Italy-INMI1, Clade V - wild type virus was purchased from the European Virus Archive goes Global (EVAg, Spallanzani Institute, Rome). The virus was propagated and titrated as previously reported (Manenti et al., 2020). The plates were observed daily for a total of four days for the presence of CPE by means of an inverted optical microscope. The 102 human serum samples were heat-inactivated for 30 min at 56 °C then tested in MN as already reported (Manenti et al., 2020).

After four days of incubation, the plates were inspected by an inverted optical microscope. The highest serum dilution protecting more than the 50 % of cells from CPE was taken as the neutralization titre.

The data obtained have been evaluated to investigate the optimal viral dose that could be effectively used for SARS-CoV-2 strain in the MN assay.

Among various serological tests, the MN is the only assay that can offer a high throughput in processing samples along with the information regarding the capability of the antibodies to prevent the attachment/entry of the virus into the target cells. To date, MN assay is considered the reference standard method for detection of neutralizing antibodies, which may be used as a correlate of protective immunity. Although alternative BSL2 protocols using SARS CoV-2 pseudotyped viruses are being developed to obviate culture of live SARS-CoV-2 virus (Hyseni et al., 2020; Crawford et al., 2020; Nie et al., 2020) these methods remain in the research area.

Historically, such as for Influenza virus, the MN assay is routinely carried out in 96-micro-well plates, by mixing different 2-fold serial dilutions of a serum-containing antibodies with a well-defined viral dose containing 100 $TCID_{50}$/well. However, for newly emerging viruses such as SARS-CoV-2, the viral dose needs to be accurately evaluated necessitating agreement on a consensus assay protocol for future studies.

The viral load equal to 100 $TCID_{50}$, in accordance with the empirical formula obtained by applying the Poisson distribution, should be equal to approximately 70 plaque-forming units (pfu), which represents the measure of the infectious viral particles in a certain volume of medium used in each well of the microplate. Clearly, this is valid if the same cell system is used and the virus is able to form plaques on the cells monolayer.

All the 102 serum samples screened have been assayed by Commercial ELISA test in order to assess more specifically the presence/absence of anti-SARS-CoV-2 binding antibodies. Among the ELISA positive sample 19.8–20 % of sera were found positive in MN assay with 100 $TCID_{50}$ and 25 $TCID_{50}$ of viral dose.

Our results show that, with the lower dose (25 $TCID_{50}$) in the majority of the cases the MN titres are higher of one or two dilution steps (Fig. 1A and B). This is also confirmed for the neutralizing mAb, used as a positive control sample for the assay, with a titre equal of 320 using 100 $TCID_{50}$ and 640 using 25 $TCID_{50}$. More interestingly, one sample (Fig. 1B; ELISA POS 5) with ELISA positive signal but tested negative in MN 100$TCID_{50}$ resulted to be low positive for the presence of neutralizing antibodies with 25 $TCID_{50}$ with a titre of 20. All the ELISA negative samples were also confirmed negative by MN 25$TCID_{50}$.

Although it has already been studied by others (Magnus, 2013; Klasse, 2014), these results are of considerable importance supporting the evidence that even if a lower infective dose is used, the possibility to have false positives in ELISA and MN 100 $TCID_{50}$ confirmed-negative samples is low. Indeed, the sensitivity of the assay to detect functional antibodies could be improved by reducing the viral dose.

Thus, confirming that even with a lower infective dose the cell monolayer is able to results in high percentage of CPE after 4 days (128 h) of incubation, avoiding the possibility to have false positive outcomes due to non-specific inhibition of the viral infection by the high serum concentration at the first sample dilution.

This aspect could be crucial in order to evaluate the immune response against new emerging viruses, such as the SARS-CoV-2, for which immunological and serological data need to be well interpreted. In fact, a variety of in vitro assays for the detection of SARS-CoV-2 neutralizing antibodies has been described but there is no doubt that

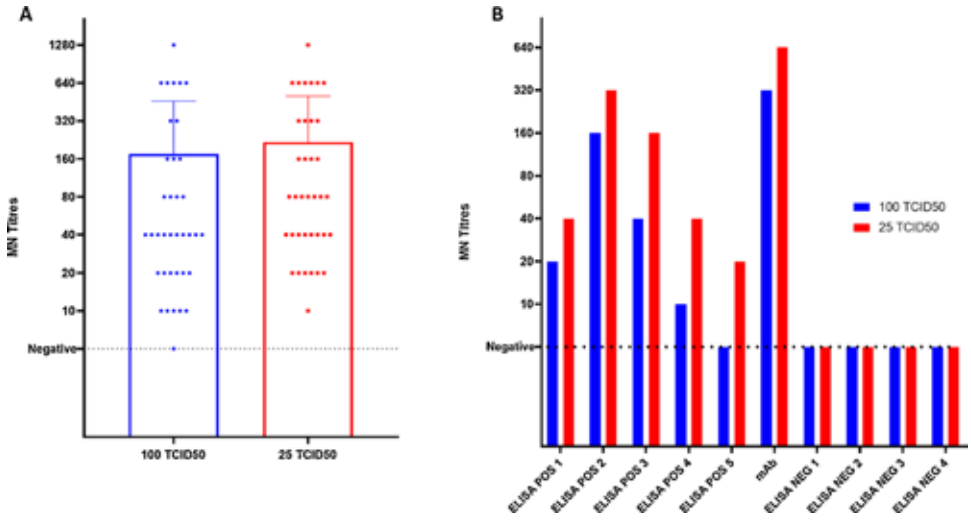

Fig. 1. A) ELISA and MN positive CPE- viral titres obtained when 102 samples were tested against 100 $TCID_{50}$ and 25 $TCID_{50}$ SARS-CoV-2 analysed by GraphPad using Kruskal-Wallis non-parametric test; B) impact of the viral load on the neutralization titre in different samples (5 ELISA positive, the neutralizing mAb, 4 ELISA negative sample).

the absence of oversight and standardisation of serologic tests is a concern. Given that, the available serologic assays are highly variable, differing in their format, the antibody class detected, the selected antigen, and the acceptable sample types (Laurie et al., 2015).

As evidenced before (Petherick, 1942; Theel et al., 2020) it is fundamental to note how serological assays able to detect neutralizing antibody responses could be crucial to provide the most accurate and precise results for vaccine immunogenicity trials. There are many topics of discussion involving antibody responses to SARS-CoV-2 (Chvatal-Medina et al., 2021), and plenty of research is yet to be done in some of these fields (e.g. kinetics and antibody-dependent enhancement mechanisms). However, confirming that the viral dose is not able to compromise the specificity of the neutralisation profiles it would definitely be of great importance for the successful development (design and pre-clinical stage) and assessment of new vaccines platform, such as RNA, DNA or nasal vaccine. Especially for the latter, it is extremely important to have tests able to detect even extremely low levels of Immunoglobulin A (IgA) with neutralizing capability generally present in high diluted human specimens such as nasal wash/swab or saliva (Gianchecchi et al., 2019). Noteworthy was the application of this MN method using 25$TCID_{50}$ in the first phase of discovery of the extremely potent monoclonal antibody as reported and described in detail in the paper of (Andreano et al., 2021). The use of the lower infective dose allowed us to detect even very low concentration of neutralizing immunoglobulin after the sorting and culturing of single B cells.

As stated before, our observations are in line with the enzymology and competition kinetics laws: decrease in the viral titres lead to an increase in antibody titres, but we believe that the most important point is that the specificity of this assay remain higher. This highlights how the such viral input should be taken as the most appropriate one to perform the MN assay for SARS-CoV-2 virus, since no precise indications or protocols have been established yet.

Even if small and preliminary, this study aims to encourage further international collaborations towards the standardization of the SARS-CoV-2 neutralization assays, maximizing the yield in terms of sensitivity. Said that, albeit at present the ability of a give antibody to neutralize SARS-CoV-2 virus remains the main target for vaccine design and their subsequent approval, more studies are focusing the attention on some mechanisms that could be crucial in Covid-19 pathologies, such as the antibody-dependent cellular cytotoxicity (ADCC). Due to the countless functions of antibodies in immune responses, it is possible that they could mediate protection from disease though different more hidden effector mechanisms (Tso et al., 2021; Tauzin et al., 2021).

Author statement

Conceptualization: AM, EMO; Data curation; AM, EMO, MM, AT. Formal analysis: AM, EMO, MM; Funding acquisition: EM; Investigation; AM, MM, GL, AT Methodology: AM, MM, EMO; Resources: EM; Supervision: EM, AT; Validation:AM, MM; Visualization; AM, EMO; Roles/Writing - original draft: AM, EMO; Writing - review & editing: all authors have approved the final version of the manuscript.

Declaration of Competing Interest

The authors report no declarations of interest.

Acknowledgements

This publication was supported by the European Virus Archive goes Global (EVAg) project which has received founding from the European Union's Horizon 2020 research and Innovation Programme under grant agreement No 653316. We would like to thank the Department of Molecular Epidemiology of the University of Siena for providing the human serum samples.

References

Adamczyk, M., van Eunen, K., Bakker, B.M., Westerhoff, H.V., 2011. Enzyme kinetics for systems biology when, why and how. Methods Enzymol. 500, 233–257. https://doi.org/10.1016/B978-0-12-385118-5.00013-X. PMID: 21943901.

Andreano, E., Nicastri, E., Paciello, I., et al., 2021. Extremely potent human monoclonal antibodies from COVID-19 convalescent patients. Cell. 184 (7), 1821–1835. https://doi.org/10.1016/j.cell.2021.02.035 e16.

Bachmann, M.F., Ecabert, B., Kopf, M., 1999. Influenza virus: a novel method to assess viral and neutralizing antibody titers in vitro. J. Immunol. Methods 225 (1), 105–111. https://doi.org/10.1016/S0022-1759(99)00034-4.

Chvatal-Medina, M., Mendez-Cortina, Y., Patiño, P.J., Velilla, P.A., Rugeles, M.T., 2021. Antibody responses in COVID-19: a review. Front. Immunol. (April 12), 633184 https://doi.org/10.3389/fimmu.2021.633184. PMID: 33936045; PMCID: PMC8081880.doi:10.1136/bmjopen-2019-032987.

Crawford, K.H.D., Eguia, R., Dingens, A.S., et al., 2020. Protocol and reagents for pseudotyping lentiviral particles with SARS-CoV-2 spike protein for neutralization assays. Viruses. 12 (5) https://doi.org/10.3390/v12050513.

Gianchecchi, E., Manenti, A., Kistner, O., Trombetta, C., Manini, I., Montomoli, E., 2019. How to assess the effectiveness of nasal influenza vaccines? Role and measurement of sIgA in mucosal secretions. Influenza Other Respir. Viruses 13 (September (5)), 429–437. https://doi.org/10.1111/irv.12664. Epub 2019 Jun 21. PMID: 31225704; PMCID: PMC6692539.

Hirst, G.K., 1942. The quantitative determination of influenza virus and antibodies by means of red cell agglutination. J. Exp. Med. 75 (1), 49–64. https://doi.org/10.1084/jem.75.1.49.

Hyseni, I., Molesti, E., Benincasa, L., et al., 2020. Characterisation of SARS-CoV-2 lentiviral pseudotypes and correlation between pseudotype-based neutralisation assays and live virus-based Micro neutralisation assays. Viruses. 12 (9) https://doi.org/10.3390/v12091011.

Klasse, P.J., 2014. Neutralization of virus infectivity by antibodies: old problems in new perspectives. Adv. Biol. 2014, 157895 https://doi.org/10.1155/2014/157895. Epub 2014 Sep 9. PMID: 27099867; PMCID: PMC4835181.

Klimov, A., Balish, A., Veguilla, V., et al., 2012. Influenza virus titration, antigenic characterization, and serological methods for antibody detection. In: Kawaoka, Y., Neumann, G. (Eds.), Influenza Virus. Methods in Molecular Biology (Methods and Protocols), Volume 865. Humana Press. https://doi.org/10.1007/978-1-61779-621-0_3.

Laurie, K.L., Engelhardt, O.G., Wood, J., et al., 2015. International laboratory comparison of influenza microneutralization assays for a(H1N1)pdm09, a(H3N2), and a(H5N1) influenza viruses by CONSISE. Clin Vaccine Immunol CVI. 22 (8), 957–964. https://doi.org/10.1128/CVI.00278-15.

Magnus, C., 2013. Virus neutralisation: new insights from kinetic neutralisation curves. PLoS Comput. Biol. 9 (2), e1002900 https://doi.org/10.1371/journal.pcbi.1002900. Epub 2013 Feb 28. PMID: 23468602; PMCID: PMC3585397.

Manenti, A., Maggetti, M., Casa, E., et al., 2020. Evaluation of SARS-CoV-2 neutralizing antibodies using a CPE-based colorimetric live virus micro-neutralization assay in human serum samples. J Med Virol. Published online May 8. https://doi.org/10.1002/jmv.25986.

Marchi, S., Montomoli, E., Remarque, E.J., et al., 2019. Pertussis over two decades: seroepidemiological study in a large population of the Siena Province, Tuscany Region, Central Italy. BMJ Open 9 (10), e032987.

Nie, J., Li, Q., Wu, J., et al., 2020. Establishment and validation of a pseudovirus neutralization assay for SARS-CoV-2. Emerg. Microbes Infect. 9 (1), 680–686. https://doi.org/10.1080/22221751.2020.1743767.

Okuno, Y., Tanaka, K., Baba, K., Maeda, A., Kunita, N., Ueda, S., 1990. Rapid focus reduction neutralization test of influenza A and B viruses in microtiter system. J. Clin. Microbiol. 28 (6), 1308.

Petherick, A., 2020. Developing antibody tests for SARS-CoV-2. Developing Antibody Tests for SARS-CoV-2, pp. 1101–1102. April 4.

Salk, 1944. A simplified procedure for titrating hemagglutinating capacity of influenza-virus and the corresponding antibody. J. Immunol. 49 (2), 87.

Sicca, F., Martinuzzi, D., Montomoli, E., Hukriede, A., 2020. Comparison of Influenza-specific Neutralizing Antibody Titers Determined Using Different Assay Readouts and Hemagglutination Inhibition Titers: Good Correlation but Poor Agreement, pp. 2527–2541.

Tauzin, A., Nayrac, M., Benlarbi, M., et al., 2021. A single dose of the SARS-CoV-2 vaccine BNT162b2 elicits Fc-mediated antibody effector functions and T cell responses. Cell Host Microbe 29 (July (7)), 1137–1150. https://doi.org/10.1016/j.chom.2021.06.001 e6 Epub 2021 Jun 4. PMID: 34133950; PMCID: PMC8175625.

Theel, E.S., Slev, Patricia, Wheeler, S., Couturier, Marc Roger, Wong, S.J., Kadkhodaf, Kamran, 2020. The Role of Antibody Testing for SARS-CoV-2: Is There One? The Role of Antibody Testing for SARS-CoV-2: Is There One? July 23.

Tso, F.Y., Lidenge, S.J., Poppe, L.K., et al., 2021. Presence of antibody-dependent cellular cytotoxicity (ADCC) against SARS-CoV-2 in COVID-19 plasma. PLoS One 16 (March (3)), e0247640. https://doi.org/10.1371/journal.pone.0247640. PMID: 33661923; PMCID: PMC7932539.

World Health Organization, 2011. Manual for the laboratory diagnosis and virological surveillance of influenza. Manual for the Laboratory Diagnosis and Virological Surveillance of Influenza. WHO Press, pp. 63–77.

SARS-CoV-2 escape from a highly neutralizing COVID-19 convalescent plasma

Emanuele Andreano[a], Giulia Piccini[b], Danilo Licastro[c], Lorenzo Casalino[d], Nicole V. Johnson[e], Ida Paciello[a], Simeone Dal Monego[c], Elisa Pantano[a], Noemi Manganaro[a], Alessandro Manenti[b,f], Rachele Manna[b], Elisa Casa[b,f], Inesa Hyseni[b,f], Linda Benincasa[f], Emanuele Montomoli[b,f,g], Rommie E. Amaro[d], Jason S. McLellan[e], and Rino Rappuoli[a,h,1]

[a]Monoclonal Antibody Discovery Lab, Fondazione Toscana Life Sciences, 53100 Siena, Italy; [b]VisMederi S.r.l., 53100 Siena, Italy; [c]ARGO Open Lab Platform for Genome Sequencing, 34149 Trieste, Italy; [d]Department of Chemistry and Biochemistry, University of California San Diego, La Jolla, CA 92093; [e]Department of Molecular Biosciences, The University of Texas at Austin, Austin, TX 78712; [f]VisMederi Research S.r.l., 53100 Siena, Italy; [g]Department of Molecular and Developmental Medicine, University of Siena, 53100 Siena, Italy; and [h]Faculty of Medicine, Imperial College, SW7 2DD London, United Kingdom

Contributed by Rino Rappuoli, June 7, 2021 (sent for review February 16, 2021; reviewed by Rafi Ahmed and Shane Crotty)

To investigate the evolution of severe acute respiratory syndrome coronavirus 2 (SARS-CoV-2) in the immune population, we coincupi bated the authentic virus with a highly neutralizing plasma from a COVID-19 convalescent patient. The plasma fully neutralized the virus for seven passages, but, after 45 d, the deletion of F140 in the spike N-terminal domain (NTD) N3 loop led to partial breakthrough. At day 73, an E484K substitution in the receptor-binding domain (RBD) occurred, followed, at day 80, by an insertion in the NTD N5 loop containing a new glycan sequon, which generated a variant completely resistant to plasma neutralization. Computational modeling predicts that the deletion and insertion in loops N3 and N5 prevent binding of neutralizing antibodies. The recent emergence in the United Kingdom, South Africa, Brazil, and Japan of natural variants with similar changes suggests that SARS-CoV-2 has the potential to escape an effective immune response and that vaccines and antibodies able to control emerging variants should be developed.

SARS-CoV-2 | COVID-19 | emerging variants | immune evasion | antibody response

Severe acute respiratory syndrome coronavirus 2 (SARS-CoV-2), causative agent of COVID-19, accounts for over 105 million cases of infections and more than 2.3 million deaths worldwide. Thanks to an incredible scientific and financial effort, several prophylactic and therapeutic tools, such as vaccines and monoclonal antibodies (mAbs), have been developed in less than 1 y to combat this pandemic (1–4). The main target of vaccines and mAbs is the SARS-CoV-2 spike protein (S protein), a large class I trimeric fusion protein which plays a key role in viral pathogenesis (3, 5, 6). The SARS-CoV-2 S protein is composed of two subunits: S1, which contains the receptor-binding domain (RBD) responsible for the interaction with receptors on the host cells, and S2, which mediates membrane fusion and viral entry (7, 8). The S1 subunit presents two highly immunogenic domains, the N-terminal domain (NTD) and the RBD, which are the major targets of polyclonal and monoclonal neutralizing antibodies (4, 9, 10). The continued spread in immune-competent populations has led to adaptations of the virus to the host and generation of new SARS-CoV-2 variants. Indeed, S-protein variants have been recently described in the United Kingdom, South Africa, Brazil, and Japan (11–13), and the Global Initiative on Sharing All Influenza Data (GISAID) database reports more than 1,100 amino acid changes in the S protein (14, 15).

An important question for vaccine development is whether the authentic virus, under the selective pressure of the polyclonal immune response in convalescent or vaccinated people, can evolve to fully escape immunity and antibody treatment. To address this question, we incubated the authentic SARS-CoV-2 wild-type (WT) virus for more than 90 d in the presence of a potent neutralizing plasma.

Results

Characterization of COVID-19 Convalescent Donor Plasma Samples. Plasma samples from 20 convalescent patients with confirmed COVID-19 infection were collected for this study. All plasmas were collected between March and May 2020 where only the original Wuhan virus and D614G variants were circulating. All plasmas, tested by enzyme-linked immunosorbent assay (ELISA), were found to bind the SARS-CoV-2 S-protein trimer, and most of them also bound the S1 and S2 subunits, and the RBD. However, a broad range of reactivity profiles were noticed, ranging from weak binders with titers of 1/10 to strong binders with titers of 1/10,240 (Table 1 and *SI Appendix*, Fig. S1*A*). PT008, PT009, PT015, PT122, and PT188 showed the strongest binding toward the S trimer, and, among them, PT188 had also the highest binding to the S1–S2 subunits and among the highest binding titers against the RBD (1/1,280). All but one plasma sample (PT103) were able to bind the S-protein S1 subunit, while three plasma samples (PT103, PT200, and PT276) were negative for binding to

Significance

This work shows that, under strong immune pressure, SARS-CoV-2 can use mutations in both the N-terminal domain and the receptor-binding domain to escape potent polyclonal neutralizing responses. Indeed, after a long period under immune selective pressure, SARS-CoV-2 evolved to evade the immunity of a potent polyclonal serum from a COVID-19 convalescent donor. Only three mutations were sufficient to generate this escape variant. The new virus was resistant to 70% of the neutralizing antibodies tested and had a decreased susceptibility to all convalescent sera. Our data predict that, as the immunity in the population increases, following infection and vaccination, new variants will emerge, and therefore vaccines and monoclonal antibodies need to be developed to address them.

Author contributions: E.A. and R.R. designed research; E.A., G.P., D.L., L.C., N.V.J., I.P., S.D.M., E.P., N.M., A.M., R.M., E.C., I.H., L.B., and R.E.A. performed research; E.A., D.L., L.C., N.V.J., E.M., R.E.A., J.S.M. and R.R. analyzed data; and E.A. and R.R. wrote the paper.

Reviewers: R.A., Emory University; and S.C., La Jolla Institute for Allergy & Immunology.

Competing interest statement: R.R. is an employee of the GSK group of companies. E.A., I.P., E.P., N.M., and R.R. are listed as inventors of full-length human monoclonal antibodies described in Italian patent applications 102020000015754 filed on June 30, 2020 and 102020000018955 filed on August 3, 2020.

This article is a PNAS Direct Submission.

[1]To whom correspondence may be addressed. Email: rino.r.rappuoli@gsk.com.

This article contains supporting information online at https://www.pnas.org/lookup/suppl/doi:10.1073/pnas.2103154118/-/DCSupplemental.

Published August 20, 2021.

Table 1. Summary of COVID-19 convalescent plasma characteristics

Sample ID	S-protein trimer-binding titer	RBD-binding titer	S1-binding titer	S2-binding titer	Neutralization titer WT	Neutralization titer D614G	Neutralization titer PT188-EM
PT003	1/320	1/10	1/80	1/320	1/15	Not neutralizing	Not neutralizing
PT004	1/2,560	1/80	1/320	1/2,560	1/120	1/60	1/20
PT005	1/320	1/80	1/160	1/1,280	1/80	1/30	1/10
PT006	1/640	1/160	1/1,280	1/640	1/120	1/20	1/10
PT008	1/10,240	1/80	1/640	1/640	1/120	1/80	1/40
PT009	1/10,240	1/2,560	1/1,280	1/2,560	1/640	1/320	1/120
PT010	1/320	1/80	1/80	1/2,560	1/15	1/10	1/10
PT012	1/1,280	1/160	1/320	1/320	1/120	1/80	1/15
PT014	1/1,280	1/80	1/160	1/1,280	1/120	1/40	1/20
PT015	1/10,240	1/10,240	1/2,560	1/5,120	1/640	1/320	1/160
PT041	1/640	1/40	1/160	1/80	1/40	1/10	1/10
PT042	1/5,120	1/320	1/1,280	1/5,120	1/960	1/320	1/60
PT100	1/1,280	1/80	1/160	1/1,280	1/80	1/30	1/40
PT101	1/640	1/40	1/160	1/320	1/20	1/10	1/10
PT102	1/160	1/20	1/80	1/640	1/10	Not neutralizing	Not neutralizing
PT103	1/160	Not binder	Not binder	1/160	Not neutralizing	Not neutralizing	Not neutralizing
PT122	1/10,240	1/1,280	1/1,280	1/2,560	1/640	1/480	1/320
PT188	1/10,240	1/1,280	1/5,120	1/5,120	1/10,240	1/10,240	1/40
PT200	1/1,280	Not binder	1/160	1/10,240	1/60	1/30	Not neutralizing
PT276	1/80	Not binder	1/80	1/320	Not neutralizing	Not neutralizing	Not neutralizing

The table shows the binding profile and neutralization activities of 20 COVID-19 convalescent plasma samples.

the RBD. Neutralization activity tested against the SARS-CoV-2 WT and D614G variant also showed variable titers. Most of the plasma samples neutralized the viruses with titers ranging from 1/20 to 1/320. Four samples had extremely low titers (1/10), whereas sample PT188 showed extremely high titers (1/10,240). Four plasma samples did not show neutralization activity against the SARS-CoV-2 WT and SARS-CoV-2 D614G variant. Plasma from subject PT188, which had the highest neutralizing titer and ELISA binding reactivity (Table 1 and *SI Appendix*, Fig. S1 *B–D*), was selected to test whether SARS-CoV-2 can evolve to escape a potent humoral immunity.

Evolution of SARS-CoV-2 Convalescent Plasma Escape Mutant. Two-fold dilutions of plasma PT188 ranging from 1/10 to 1/20,480 were coincubated with 10^5 median tissue culture infectious dose ($TCID_{50}$) of the WT virus in a 24-well plate. This viral titer was approximately 3 logs more than what is conventionally used in microneutralization assays (16–20). The plasma/virus mixture was coincubated for 5 d to 8 d. Then, the first well showing cytopathic effect (CPE) was diluted 1:100 and incubated again with serial dilutions of plasma PT188 (Fig. 1*A* and *SI Appendix*, Table S1). For six passages and 38 d, PT188 plasma neutralized the virus with a titer of 1/640 and did not show any sign of escape. However, after seven passages and 45 d, the neutralizing titer decreased to 1/320. Sequence analyses revealed a deletion of the phenylalanine in position 140 (F140) on the S-protein NTD N3 loop in 36% of the virions (Fig. 1 *B* and *C* and *SI Appendix*, Table S1). In the subsequent passage (P8), this mutation was observed in 100% of the sequenced virions, and an additional twofold decrease in neutralization activity was observed, reaching an overall neutralization titer of 1/160. Following this initial breakthrough, a second mutation occurred after 12 passages and 80 d of plasma/virus coincubation (P12). This time, the glutamic acid in position 484 of the RBD was substituted with a lysine (E484K). This mutation occurred in 100% of sequenced virions and led to a fourfold decrease in neutralization activity which reached a titer of 1/40 (Fig. 1 *B* and *C* and *SI Appendix*, Table S1). The E484K substitution was rapidly followed by a third and final change comprising an 11-amino acid insertion between Y248 and L249 in the NTD N5 loop ($_{248a}$KTRNKSTSRRE$_{248k}$). The insertion contained an N-linked glycan sequon ($_{248d}$NKS$_{248f}$), and this viral variant resulted in complete abrogation of neutralization activity by the PT188 plasma sample. Initially, this insertion was observed in only 49% of the virions, but, when the virus was kept in culture for another passage (P14), the insertion was fully acquired by the virus (Fig. 1 *B* and *C* and *SI Appendix*, Table S1).

Reduced Susceptibility to Convalescent Plasma and Monoclonal Antibodies. To evaluate the ability of the SARS-CoV-2 PT188 escape mutant (PT188-EM) to evade the polyclonal antibody response, all 20 plasma samples from COVID-19 convalescent patients were tested in a traditional CPE-based neutralization assay against this viral variant using the virus at 100 $TCID_{50}$. All samples showed at least a twofold decrease in neutralization activity against SARS-CoV-2 PT188-EM (Fig. 2*A*, Table 1, and *SI Appendix*, Fig. S1 *B–D*). As expected, the plasma used to select the escape mutant showed the biggest neutralization decrease against this escape mutant with a 256-fold decrease compared to WT SARS-CoV-2. Plasma PT042, PT006, PT005, PT012, and PT041 also showed a substantial drop in neutralization efficacy (Table 1). In addition, we observed that a higher response toward the S-protein S1 subunit correlates with loss of neutralization activity against SARS-CoV-2 PT188-EM (see *SI Appendix*, Fig. S2*A*), whereas a high response toward the S-protein S2 subunit did not show correlation (see *SI Appendix*, Fig. S2*B*).

We also tested a previously identified panel of 13 neutralizing mAbs (nAbs) by CPE-based neutralization assay to assess their neutralization efficacy against SARS-CoV-2 PT188-EM. These antibodies were classified into three groups based on their binding profiles to the S protein. Group I nAbs were able to bind the S1-RBD, group II targeted the S1 subunit but not the RBD, and group III nAbs were specific for the S-protein trimer (Table 2). These antibodies also showed a variable neutralization potency against the SARS-CoV-2 WT and D614G viruses ranging from 3.9 ng/mL to 500.0 ng/mL (Fig. 2*B*, Table 2, and *SI Appendix*, Fig. S1 *E–G*). The three mutations selected by SARS-CoV-2 PT188-EM to escape the highly neutralizing plasma completely abrogated the neutralization activity of two of the six tested RBD-directed antibodies (F05 and G12) (Fig. 2*B*, Table 2, and *SI Appendix*, Fig. S1 *E–G*), suggesting that their epitopes include E484. In contrast, the extremely potent neutralizing antibody J08 was the most potently

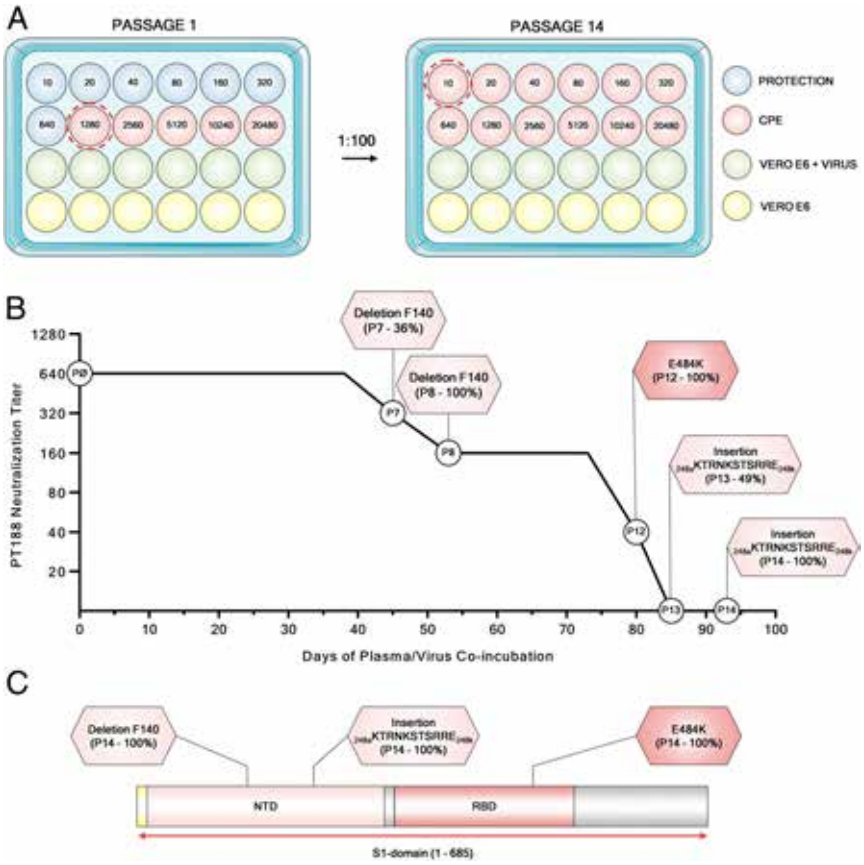

Fig. 1. Evolution of an authentic SARS-CoV-2 escape mutant. (*A*) Schematic representation of the 24-well plate format used to select the authentic SARS-CoV-2 escape mutant. Blue, red, green, and yellow wells show feeder cells protect from PT188 neutralization, CPE, authentic virus on Vero E6 cells, and Vero E6 alone, respectively. (*B*) The graph shows the PT188 neutralization titer after each mutation acquired by the authentic virus. Specific mutations, fold decrease, and days on which the mutations occur are reported in the figure. (*C*) SARS-CoV-2 S-protein gene showing type, position of mutations, and frequency of mutations.

neutralizing antibody against this escape mutant, with an IC_{100} of 22.1 ng/mL. Interestingly, the S1-RBD–directed antibody C14 showed a twofold increase in neutralization activity compared to the SARS-CoV-2 WT virus, whereas I14 and B07 showed a 16-fold and twofold decrease, respectively. All tested antibodies derived from group II (S1-specific not RBD) and group III (S-protein trimer specific) completely lost their neutralization ability against SARS-CoV-2 PT188-EM (Fig. 2*B*, Table 2, and *SI Appendix*, Fig. S1 *E*–*G*). To better understand the abrogation of activity of some of the tested antibodies, J13, I21, and H20 were cocomplexed with SARS-CoV-2 WT S protein and structurally evaluated by negative-stain EM. Two-dimensional (2D) class averages of the three tested antibodies showed that they all bind to the NTD of the S protein (Fig. 2*C*). A 3D reconstruction for the J13 Fab complex provided further evidence that this antibody binds to the NTD (Fig. 2*D*).

Putative Structural Effects Enabling Viral Escape. Computational modeling and simulation of the WT and PT188-EM spikes provides a putative structural basis for understanding antibody escape. The highly antigenic NTD is more extensively mutated, containing the F140 deletion as well as the 11-amino acid insertion in loop N5 that introduces a novel N-glycan sequon at position N248d (Fig. 3 *A*–*C*). In contrast, the single mutation in the RBD (E484K) swaps the charge of the sidechain, which would significantly alter the electrostatic complementarity of antibody binding to this region (Fig. 3*D*). Upon inspection of molecular dynamics (MD) simulations of the NTD escape mutant model, we hypothesize that the F140 deletion alters the packing of the N1, N3, and N5 loops (see *SI Appendix*, Fig. S3), where the loss of the bulky aromatic sidechain would overall reduce the stability of this region (Table 1). Subsequently, the extensive insertion within the N5 loop appears to remodel this critical antigenic region, predicting substantial steric occlusion with antibodies targeting this epitope, such as antibody 4A8 (Fig. 3*B*) (21). Furthermore, introduction of a new N-glycan at position N248d (mutant numbering scheme) would effectively eliminate neutralization by such antibodies (Fig. 3*B* and *SI Appendix*, Fig. S4).

Escape Mutant Shows Similar Viral Fitness Compared to the WT Virus. To determine the extent to which the escape mutations were detrimental to the infectivity of SARS-CoV-2 PT188-EM, the viral fitness was evaluated. Four different measures were assessed: visible CPE, viral titer, RNA-dependent RNA polymerase (RdRp), and nucleocapsid (N) RNA detection by RT-PCR (see *SI Appendix*, Fig. S5). Initially, the SARS-CoV-2 WT virus and the PT188-EM variant were inoculated at a multiplicity of infection of 0.001 on Vero E6 cells. Every day, for four consecutive days, a titration plate was prepared and optically assessed after 72 h of incubation to evaluate the CPE effect on Vero E6 cells and viral titer. Furthermore, the RNA was extracted to assess RdRp and N-gene levels in the supernatant. We collected pictures at 72 h postinfection to evaluate the morphological status of noninfected Vero E6 cells and the CPE on infected feeder cells. Vero E6 cells were confluent at 72 h, and no sign of CPE was optically detectable (see *SI Appendix*, Fig. S5*A*). Conversely, SARS-CoV-2 WT and PT188-EM showed significant and comparable amounts of CPE (see *SI Appendix*, Fig.

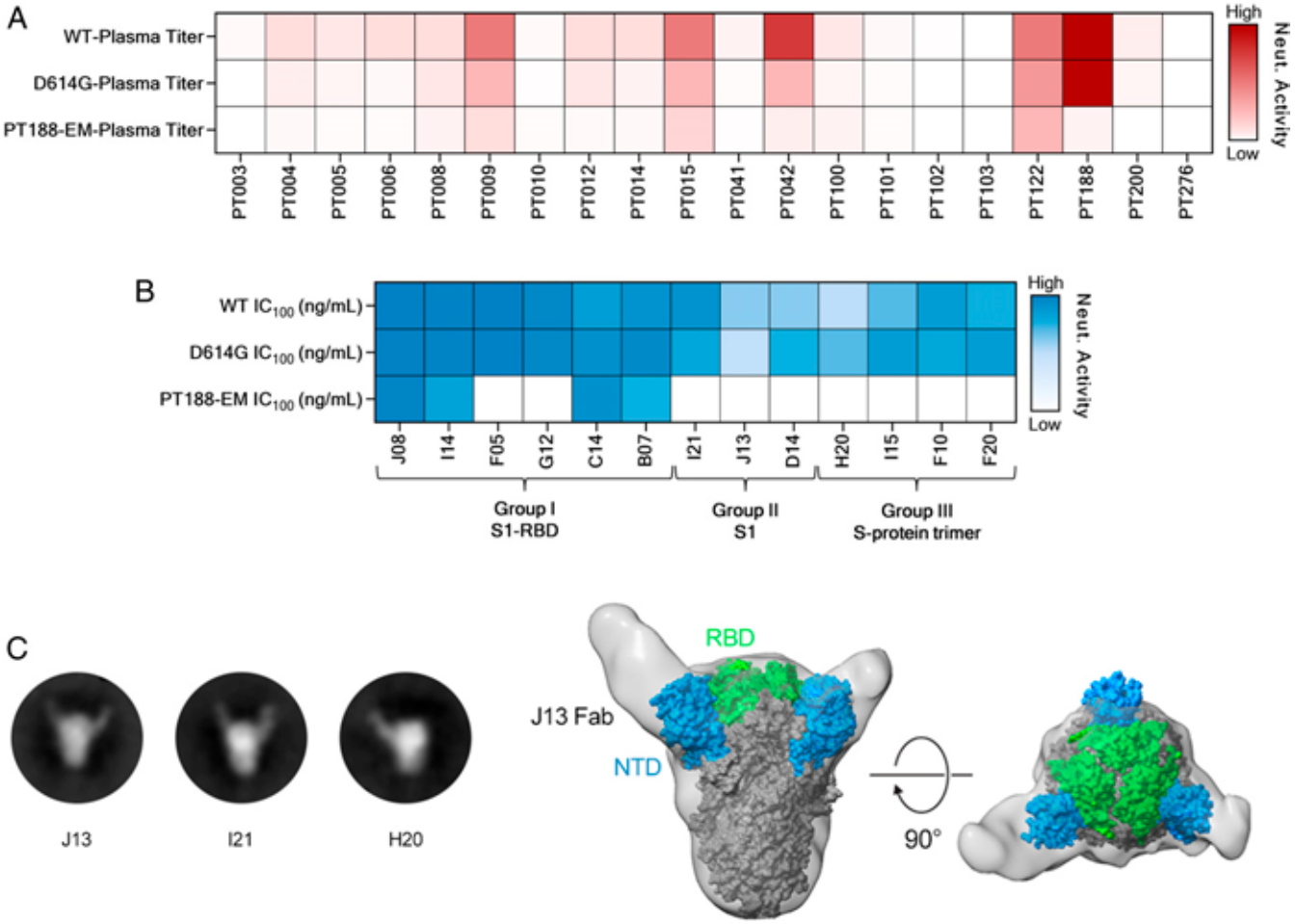

Fig. 2. Neutralization (Neut.) efficacy of plasma and 13 mAbs against SARS-CoV-2 PT188-EM. (*A*) Heat map showing the neutralization activity of tested plasma samples to the SARS-CoV-2 WT and D614G and PT188-EM variants. (*B*) Heat maps showing neutralization profiles of tested mAbs. (*C*) Negative stain EM 2D class averages showing J13, I21, and H20 Fabs bound to the SARS-CoV-2 S protein. (*D*) A 3D reconstruction of J13 bound to the NTD domain of the S protein viewed looking along (*Left*) or toward (*Right*) the viral membrane.

S5*A*). Viral titers were evaluated for both SARS-CoV-2 WT and PT188-EM, and no significant differences were observed, as the viruses showed almost identical growth curves (see *SI Appendix*, Fig. S5*B*). A similar trend was observed when RdRp and N-gene levels in the supernatant were detected, even if slightly higher levels of RdRp and N gene were detectable for SARS-CoV-2 PT188-EM

Table 2. Features of 13 SARS-CoV-2 neutralizing antibodies

mAb ID	Binding specificity*	Neutralization WT IC_{100} (ng:mL)*	Neutralization D614G IC_{100} (ng:mL)*	Neutralization PT188-EM IC_{100} (ng:mL)
J08	S1-RBD	3.9	7.8	22.1
I14	S1-RBD	11.0	19.7	176.8
F05	S1-RBD	3.9	4.9	Not neutralizing
G12	S1-RBD	39.4	39.4	Not neutralizing
C14	S1-RBD	157.5	78.7	88.4
B07	S1-RBD	99.2	49.6	250.0
I21	S1	99.2	198.4	Not neutralizing
J13	S1	396.8	500.0	Not neutralizing
D14	S1	396.8	250.0	Not neutralizing
H20	S protein	492.2	310.0	Not neutralizing
I15	S protein	310.0	155.0	Not neutralizing
F10	S protein	155.0	195.3	Not neutralizing
F20	S protein	246.1	155.0	Not neutralizing

The table shows the binding and neutralization profile of 13 previously identified SARS-CoV-2 nAbs.
*Column refers to previously published data (1).

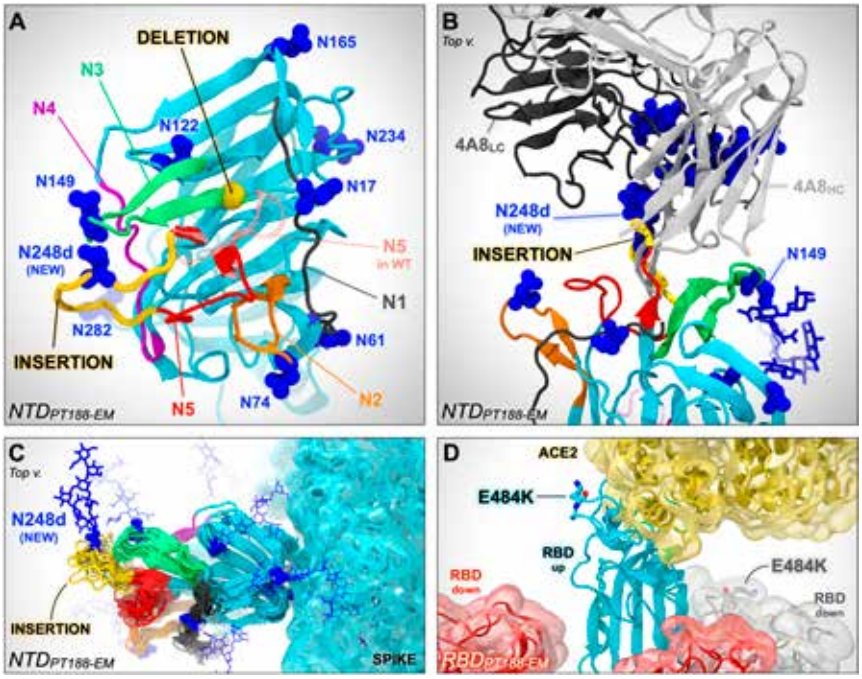

Fig. 3. In silico modeling of the PT188-EM spike NTD and RBD. (*A*) In silico model of the NTD of the SARS-CoV-2 PT188-EM spike protein based on PDB ID code 7JJI. This model accounts for the 11-amino acid insertion (yellow ribbon) and F140 deletion (highlighted with a yellow bead). N5 loop as in the WT cryo-EM structure (PDB ID code 7JJI) is shown as a transparent red ribbon. (*B*) Close-up of the PT188-EM spike NTD model in complex with antibody 4A8. Both heavy chain (HC, light gray) and light chain (LC, dark gray) of 4A8 are shown. The 11-amino acid insertion (yellow ribbon) within N5 loop introduces a new N-linked glycan (N248d) that sterically clashes with 4A8, therefore disrupting the binding interface. The N-glycan at position N149 is, however, compatible with 4A8 binding. (*C*) Conformational dynamics of the PT188-EM spike NTD model resulting from 100 ns of MD simulation is shown by overlaying multiple frames along the generated trajectory. (*D*) In silico model of the PT188-EM spike RBD based on PDB ID code 6M17, where the E484K mutation is shown with licorice representation.

at day 0 and day 1 (see *SI Appendix*, Fig. S5*C*). Finally, strong correlations between viral titers and RdRp/N-gene levels were observed for both SARS-CoV-2 WT and PT188-EM (see *SI Appendix*, Fig. S5 *D* and *E*).

Discussion

We have shown that the authentic SARS-CoV-2, if constantly pressured, has the ability to escape even a potent polyclonal serum targeting multiple neutralizing epitopes. These results are remarkable because SARS-CoV-2 shows a very low estimated evolutionary rate of mutation, as this virus encodes a proofreading exoribonuclease machinery, and, therefore, while escape mutants can be easily isolated when viruses are incubated with single mAbs, it is usually believed that a combination of two mAbs is sufficient to eliminate the evolution of escape variants (22–25). The recent isolation of SARS-CoV-2 variants in the United Kingdom, South Africa, Brazil, and Japan with deletions in or near the NTD loops shows that what we describe here can occur in the real world. The ability of the virus to adapt to the host immune system was also observed in clinical settings where an immunocompromised COVID-19 patient, after 154 d of infection, presented different variants of the virus, including the E484K substitution (26). Therefore, we should be prepared to deal with virus variants that may be selected by the immunity acquired from infection or vaccination. This can be achieved by developing second-generation vaccines and mAbs, possibly targeting universal epitopes and able to neutralize emerging variants of the virus.

A limitation of this study is that viral evolution of SARS-CoV-2 was evaluated only for one plasma sample, limiting the observation of possible spike protein mutations only to a specific polyclonal response. In fact, PT188-EM impacted our plasma samples differently, where PT188, used to pressure the virus in vitro, was the most impacted sample (256-fold decrease), while the remaining 15 neutralizing plasmas showed a median neutralization titer reduction of ∼sevenfold.

Our data also confirm that the SARS-CoV-2 neutralizing antibodies acquired during infection target almost entirely the NTD and the RBD. In the RBD, the possibility to escape is limited, and the mutation E484K that we found is one of the most frequent mutations to escape mAbs (22) and among the most common RBD mutations described in experimental settings (27). Remarkably, the evolution of the E484K substitution observed in our experimental setting was replicated a few months later in the real world by the emergence of E484K variants in South Africa, Brazil, and Japan (14). This is likely due to residue E484 being targeted by antibodies derived from IGHV3-53 and closely related IGHV3-66 genes, which are the most common germlines for antibodies directed against the RBD (28). Recently, this mutation has also been shown to reduce considerably the neutralizing potency of vaccine-induced immunity and to escape mAbs already approved for emergency use by the Food and Drug Administration (29–31).

On the other hand, the NTD loops can accommodate many different changes, such as insertions, deletions, and amino acid alterations. Interestingly, in our case, the final mutation contained an insertion carrying an N-glycosylation site which has the potential to hide or obstruct the binding to neutralizing epitopes. The introduction of a glycan is a well-known immunogenic escape strategy described in influenza (32), HIV-1, and other viruses (33–35), although this finding presents a patient-derived escape mutant utilizing this mechanism for SARS-CoV-2. Surprisingly, only three mutations, which led to complete rearrangement of NTD N3 and N5 loops and substitution to a key residue on the RBD, were sufficient to eliminate the neutralization ability of a

potent polyclonal serum. Fortunately, not all plasma and mAbs tested were equally affected by the three mutations, suggesting that natural immunity to infection can target additional epitopes that can still neutralize the PT188-EM variant. Vaccine-induced immunity, which is more robust than natural immunity, is likely to be less susceptible to emerging variants. Indeed, so far, the virus has not mutated sufficiently to completely avoid the antibody response raised by current vaccines (36, 37).

Going forward, it will be important to continue to closely monitor which epitopes on the S protein are targeted by the vaccines against SARS-CoV-2 that are being deployed in hundreds of millions of people around the world.

Materials and Methods

Enrollment of SARS-CoV-2 Convalescent Donors and Human Sample Collection. COVID-19 convalescent plasma samples were provided by the National Institute for Infectious Diseases, Institute for Scientific Based Recovery and Cure—Lazzaro Spallanzani Rome (Italy) and Azienda Ospedaliera Universitaria Senese, Siena (Italy). Samples were collected from convalescent donors who gave their written consent. The study was approved by local ethics committees (Parere 18_2020 in Rome and Parere 17065 in Siena) and conducted according to good clinical practice in accordance with the Declaration of Helsinki (European Council 2001, US Code of Federal Regulations, International Conference on Harmonization 1997). This study was unblinded and not randomized.

SARS-CoV-2 Authentic Virus Neutralization Assay. The mAbs and plasma neutralization activity was evaluated using a CPE-based assay as previously described (17, 20). Further details are available in *SI Appendix, Materials and Methods*.

Viral Escape Assay Using Authentic SARS-CoV-2. All SARS-CoV-2 authentic virus procedures were performed in the biosafety level 3 (BSL3) laboratories at Toscana Life Sciences in Siena (Italy) and Vismederi S.r.l., Siena (Italy). BSL3 laboratories are approved by a certified biosafety professional and are inspected every year by local authorities. To detect neutralization-resistant SARS-CoV-2 escape variants, a standard concentration of the virus was sequentially passaged in cell cultures in the presence of serially diluted samples containing SARS-CoV-2-specific antibodies. Briefly, 12 serial twofold dilutions of PT188 plasma prepared in complete Dulbecco's modified Eagle's medium 2% fetal bovine serum (starting dilution 1:10) were added to the wells of one 24-well plate. Virus solution containing 10^5 $TCID_{50}$ of authentic SARS-CoV-2 was dispensed in each antibody-containing well, and the plates were incubated for 1 h at 37 °C, 5% CO_2. The mixture was then added to the wells of a 24-well plate containing a subconfluent Vero E6 cell monolayer. Plates were incubated for 5 d to 7 d at 37 °C, 5% CO_2 and examined for the presence of CPE using an inverted optical microscope. A virus-only control and a cell-only control were included in each plate to assist in distinguishing absence or presence of CPE. At each virus passage, the content of the well corresponding to the lowest sample dilution that showed complete CPE was diluted 1:100 and transferred to the antibody-containing wells of the predilution 24-well plate prepared for the subsequent virus passage. At each passage, both the virus pressured with PT188 and the virus-only control were harvested, propagated in 25-cm^2 flasks, and aliquoted at −80 °C to be used for RNA extraction, RT-PCR, and sequencing.

Negative Stain Electron Microscopy. SARS-CoV-2 S protein was expressed and purified as previously described (38). Purified spike was combined with individual Fabs at final concentrations of 0.04 mg/mL and 0.16 mg/mL, respectively. Following a 30-min incubation on ice, each complex was deposited on plasma cleaned CF-400 grids (EMS) and stained using methylamine tungstate (Nanoprobes). Grids were imaged at 92,000× magnification in a Talos F200C transmission electron microscope (TEM) equipped with a Ceta 16M detector (Thermo Fisher Scientific). Contrast transfer function estimation and particle picking were performed using cisTEM (39), and particle stacks were exported to cryoSPARC v2 (40) for 2D classification, ab initio 3D reconstruction, and heterogeneous refinement.

Computational Methods. The PT188-EM spike escape mutant was modeled using in silico approaches. As the mutations are localized in two different domains of the spike, namely the NTD and the RBD, separate models were generated for each domain. In detail, two models of the PT188-EM spike NTD (residues 13 to 308) were built starting from two different cryoelectron microscopy (cryo-EM) structures of the WT S protein as templates: 1) one bearing a completely resolved NTD [Protein Data Bank (PDB) ID code 7JJI (41)], which includes all the loops from N1 to N5, and 2) one bound to the antibody 4A8 [PDB ID code 7C2L (21)], which presents only one small gap within the N5 loop. The model of the PT188-EM spike RBD was based on the cryo-EM structure of the spike's RBD in complex with ACE2 [PDB ID code 6M17 (42)]. The generated models were subsequently refined using explicitly solvated all-atom MD simulations. The systems and the simulations were visually inspected with visual molecular dynamics, which was also used for image rendering (43). Further details on the computational method analyses are reported in *SI Appendix, Materials and Methods*.

Data Availability. All study data are included in the article and *SI Appendix*.

ACKNOWLEDGMENTS. This work was funded by European Research Council Advanced Grant Agreement 787552 (vaccines as a remedy for antimicrobial resistant bacterial infections [vAMRes]). This publication was supported by funds from the "Centro Regionale Medicina di Precisione" and by all the people who answered the call to fight with us the battle against SARS-CoV-2 with their kind donations on the platform ForFunding (https://www.forfunding.intesasanpaolo.com/DonationPlatform-ISP/nav/progetto/id/3380). This publication was supported by the European Virus Archive Goes Global project, which has received funding from the European Union's Horizon 2020 Research and Innovation Programme under Grant Agreement 653316. This publication was supported by the COVID-2020-12371817 project, which has received funding from the Italian Ministry of Health. This work was supported by NIH Grant GM132826, NSF Grants for Rapid Response Research Grant MCB-2032054, an award from the Research Corporation for Science Advancement, and a University of California San Diego Moore's Cancer Center 2020 SARS-CoV-2 seed grant to R.E.A and National Institute of Allergy and Infectious Diseases Grant R01-AI127521 awarded to J.S.M. We are grateful for the efforts of the Texas Advanced Computing Center Frontera team and for the compute time made available through a Director's Discretionary Allocation (made possible by NSF Award OAC-1818253). We also thank Dr. Fiona Kearns for assistance with the NTD glycan modeling.

1. S. Jiang, C. Hillyer, L. Du, Neutralizing antibodies against SARS-CoV-2 and other human coronaviruses. *Trends Immunol.* **41**, 355–359 (2020).
2. F. Krammer, SARS-CoV-2 vaccines in development. *Nature* **586**, 516–527 (2020).
3. Y. Dong *et al.*, A systematic review of SARS-CoV-2 vaccine candidates. *Signal Transduct. Target. Ther.* **5**, 237 (2020).
4. E. Gavor, Y. K. Choong, S. Y. Er, H. Sivaraman, J. Sivaraman, Structural basis of SARS-CoV-2 and SARS-CoV antibody interactions. *Trends Immunol.* **41**, 1006–1022 (2020).
5. Z. Ke *et al.*, Structures and distributions of SARS-CoV-2 spike proteins on intact virions. *Nature* **588**, 498–502 (2020).
6. A. C. Walls *et al.*, Structure, function, and antigenicity of the SARS-CoV-2 spike glycoprotein. *Cell* **181**, 281–292.e6 (2020).
7. T. M. Clausen *et al.*, SARS-CoV-2 infection depends on cellular heparan sulfate and ACE2. *Cell* **183**, 1043–1057.e15 (2020).
8. T. F. Rogers *et al.*, Isolation of potent SARS-CoV-2 neutralizing antibodies and protection from disease in a small animal model. *Science* **369**, 956–963 (2020).
9. Q. Wang *et al.*, Structural and functional basis of SARS-CoV-2 entry by using human ACE2. *Cell* **181**, 894–904.e9 (2020).
10. J. Lan *et al.*, Structure of the SARS-CoV-2 spike receptor-binding domain bound to the ACE2 receptor. *Nature* **581**, 215–220 (2020).
11. COG-UK, "COG-UK update on SARS-CoV-2 Spike mutations of special interest" (Rep. 1, COG-UK, 2020).
12. H. Tegally *et al.*, Emergence and rapid spread of a new severe acute respiratory syndrome-related coronavirus 2 (SARS-CoV-2) lineage with multiple spike mutations in South Africa. *medRxiv* [Preprint] (2020). https://doi.org/10.1101/2020.12.21.20248640 (Accessed 22 December 2020).
13. E. C. Sabino *et al.*, Resurgence of COVID-19 in Manaus, Brazil, despite high seroprevalence. *Lancet* **397**, 452–455 (2021).
14. S. Elbe, G. Buckland-Merrett, Data, disease and diplomacy: GISAID's innovative contribution to global health. *Glob. Chall.* **1**, 33–46 (2017).
15. Y. Shu, J. McCauley, GISAID: Global initiative on sharing all influenza data—From vision to reality. *Eurosurveillance* **22**, 30494 (2017).
16. L. A. Jackson *et al.*, An mRNA vaccine against SARS-CoV-2—Preliminary report. *N. Engl. J. Med.* **383**, 1920–1931 (2020).
17. A. Manenti *et al.*, Evaluation of SARS-CoV-2 neutralizing antibodies using a CPE-based colorimetric live virus micro-neutralization assay in human serum samples. *J. Med. Virol.* **92**, 2096–2104 (2020).
18. P. M. Folegatti *et al.*, Safety and immunogenicity of the ChAdOx1 nCoV-19 vaccine against SARS-CoV-2: A preliminary report of a phase 1/2, single-blind, randomised controlled trial. *Lancet* **396**, 467–478 (2020).
19. S. J. Zost *et al.*, Potently neutralizing and protective human antibodies against SARS-CoV-2. *Nature* **584**, 443–449 (2020).

20. E. Andreano *et al*., Extremely potent human monoclonal antibodies from COVID-19 convalescent patients. *Cell* **184**, 1821–1835.e1816 (2021).
21. X. Chi *et al*., A neutralizing human antibody binds to the N-terminal domain of the Spike protein of SARS-CoV-2. *Science* **369**, 650–655 (2020).
22. A. Baum *et al*., Antibody cocktail to SARS-CoV-2 spike protein prevents rapid mutational escape seen with individual antibodies. *Science* **369**, 1014–1018 (2020).
23. Y. Bar-On *et al*., Safety and antiviral activity of combination HIV-1 broadly neutralizing antibodies in viremic individuals. *Nat. Med.* **24**, 1701–1707 (2018).
24. S. Nakagawa, T. Miyazawa, Genome evolution of SARS-CoV-2 and its virological characteristics. *Inflamm. Regen.* **40**, 17 (2020).
25. F. Robson *et al*., Coronavirus RNA proofreading: Molecular basis and therapeutic targeting. *Mol. Cell* **79**, 710–727 (2020).
26. B. Choi *et al*., Persistence and evolution of SARS-CoV-2 in an immunocompromised host. *N. Engl. J. Med.* **383**, 2291–2293 (2020).
27. A. J. Greaney *et al*., Complete mapping of mutations to the SARS-CoV-2 spike receptor-binding domain that escape antibody recognition. *Cell Host Microbe* **29**, 44–57 (2021).
28. F. Fagiani, M. Catanzaro, C. Lanni, Molecular features of IGHV3-53-encoded antibodies elicited by SARS-CoV-2. *Signal Transduct. Target. Ther.* **5**, 170 (2020).
29. Z. Wang *et al*., mRNA vaccine-elicited antibodies to SARS-CoV-2 and circulating variants. *Nature* **592**, 616–622 (2021).
30. P. Wang *et al*., Increased resistance of SARS-CoV-2 variants B.1.351 and B.1.1.7 to antibody neutralization. *bioRxiv* [Preprint] (2021). https://doi.org/10.1101/2021.01.25.428137 (Accessed 12 February 2021).
31. R. L. Gottlieb *et al*., Effect of bamlanivimab as monotherapy or in combination with etesevimab on viral load in patients with mild to moderate COVID-19: A randomized clinical trial. *JAMA* **325**, 632–644 (2021).
32. M. O. Altman *et al*., Human Influenza A virus hemagglutinin glycan evolution follows a temporal pattern to a glycan limit. *mBio* **10**, e00204–e00219 (2019).
33. M. Zhang *et al*., Tracking global patterns of N-linked glycosylation site variation in highly variable viral glycoproteins: HIV, SIV, and HCV envelopes and influenza hemagglutinin. *Glycobiology* **14**, 1229–1246 (2004).
34. W. Wang *et al*., A systematic study of the N-glycosylation sites of HIV-1 envelope protein on infectivity and antibody-mediated neutralization. *Retrovirology* **10**, 14 (2013).
35. Wang W, *et al*. (2015) N463 glycosylation site on V5 loop of a mutant gp120 regulates the sensitivity of HIV-1 to neutralizing monoclonal antibodies VRC01/03. *J. Acquired Immune Defic. Syndr. (1999)* **69**, 270–277.
36. S. Crotty, Hybrid immunity. *Science* **372**, 1392–1393 (2021).
37. E. Andreano, R. Rappuoli, SARS-CoV-2 escaped natural immunity, raising questions about vaccines and therapies. *Nat. Med.* **27**, 759–761 (2021).
38. C.-L. Hsieh *et al*. Structure-based design of prefusion-stabilized SARS-CoV-2 spikes. *Science* **369**, 1501–1505 (2020).
39. T. Grant, A. Rohou, N. Grigorieff, *cis*TEM, user-friendly software for single-particle image processing. *eLife* **7**, 7 (2018).
40. A. Punjani, J. L. Rubinstein, D. J. Fleet, M. A. Brubaker, cryoSPARC: Algorithms for rapid unsupervised cryo-EM structure determination. *Nat. Methods* **14**, 290–296 (2017).
41. S. Bangaru *et al*., Structural analysis of full-length SARS-CoV-2 spike protein from an advanced vaccine candidate. *Science* **370**, 1089–1094 (2020).
42. R. Yan *et al*. Structural basis for the recognition of SARS-CoV-2 by full-length human ACE2. *Science* **367**, 1444–1448 (2020).
43. W. Humphrey, A. Dalke, K. Schulten, VMD: Visual molecular dynamics. *J. Mol. Graph.* **14**, 27–38 (1996).

viruses

MDPI

Communication

Serum Neutralizing Activity against B.1.1.7, B.1.351, and P.1 SARS-CoV-2 Variants of Concern in Hospitalized COVID-19 Patients

Claudia Maria Trombetta [1,*], Serena Marchi [1], Simonetta Viviani [1], Alessandro Manenti [2], Linda Benincasa [3], Antonella Ruello [4], Emilio Bombardieri [4], Ilaria Vicenti [5], Maurizio Zazzi [5] and Emanuele Montomoli [1,2,3]

[1] Department of Molecular and Developmental Medicine, University of Siena, 53100 Siena, Italy; serena.marchi2@unisi.it (S.M.); simonetta.viviani@unisi.it (S.V.); emanuele.montomoli@unisi.it (E.M.)
[2] VisMederi srl, Strada del Petriccio e Belriguardo 35, 53100 Siena, Italy; alessandro.manenti@vismederi.com
[3] VisMederi Research srl, Strada del Petriccio e Belriguardo 35, 53100 Siena, Italy; linda.benincasa@vismederiresearch.com
[4] Humanitas Gavazzeni, Via Mauro Gavazzeni 21, 24125 Bergamo, Italy; antonella.ruello@gavazzeni.it (A.R.); emilio.bombardieri@gavazzeni.it (E.B.)
[5] Department of Medical Biotechnologies, University of Siena, 53100 Siena, Italy; ilariavicenti@gmail.com (I.V.); maurizio.zazzi@gmail.com (M.Z.)
* Correspondence: trombetta@unisi.it

Citation: Trombetta, C.M.; Marchi, S.; Viviani, S.; Manenti, A.; Benincasa, L.; Ruello, A.; Bombardieri, E.; Vicenti, I.; Zazzi, M.; Montomoli, E. Serum Neutralizing Activity against B.1.1.7, B.1.351, and P.1 SARS-CoV-2 Variants of Concern in Hospitalized COVID-19 Patients. *Viruses* **2021**, *13*, 1347. https://doi.org/10.3390/v13071347

Academic Editor: Luis Martinez-Sobrido and Fernando Almazan Toral

Received: 6 May 2021
Accepted: 8 July 2021
Published: 12 July 2021

Abstract: The recent spreading of new SARS-CoV-2 variants, carrying several mutations in the spike protein, could impact immune protection elicited by natural infection or conferred by vaccination. In this study, we evaluated the neutralizing activity against the viral variants that emerged in the United Kingdom (B.1.1.7), Brazil (P.1), and South Africa (B.1.351) in human serum samples from hospitalized patients infected by SARS-CoV-2 during the first pandemic wave in Italy in 2020. Of the patients studied, 59.5% showed a decrease (≥2 fold) in neutralizing antibody titer against B.1.1.7, 83.3% against P.1, and 90.5% against B.1.351 with respect to the original strain. The reduction in antibody titers against all analyzed variants, and in particular P.1 and B.1.351, suggests that previous symptomatic infection might be not fully protective against exposure to SARS-CoV-2 variants carrying a set of relevant spike mutations.

Keywords: neutralizing activity; SARS-CoV-2; variants of concern

1. Introduction

One year ago, the Director-General of the World Health Organization declared the first pandemic caused by a coronavirus named severe acute respiratory syndrome coronavirus 2 (SARS-CoV-2) [1]. Neutralizing antibodies, targeting the viral spike (S) protein and its receptor-binding domain (RBD), are considered a surrogate of protection against COVID-19 [2], the disease caused by SARS-CoV-2, although no formal correlates of protection have been established so far. In fact, available COVID-19 vaccines that have shown high efficacy are developed with the concept that the S protein is the immunodominant antigen. These vaccines are designed based on the Wuhan strain, the original strain that since January 2020 has been at the origin of the worldwide pandemic.

In the last months, different variants of concern (VOCs) [3] of SARS-CoV-2 emerged around the world, initially as occasional isolates; however, in some settings, the most efficient variants are rapidly replacing the original Wuhan strain.

One new variant emerged in the United Kingdom (UK), affecting people under 60 years of age. Retrospective analyses have dated the first identification as occurring in

September 2020 in South East England [4,5]. This variant, called B.1.1.7, spread in several countries around the world (i.e., Italy, Denmark, the United States, the Netherlands, Australia, Iceland), and it has been associated with 50% increased transmission [6] and increased risk of death [4,7–9]. Seventeen mutations/deletions in the viral genome characterize the B.1.1.7, including eight in the S protein (Δ69–70, ΔY144, N501Y, A570D, P681H, T716I, S982A, D118H) [5,8]. Three mutations are of biological significance, namely Δ69–70, N501Y, and P681H. The first one is related to an increased viral infectivity and a potential impact on PCR assays targeting the S gene [4,8,10]; however, this mutation is not restricted to this variant [10]. The N501Y is a mutation in the RBD resulting in an increased binding affinity to its cellular ACE-2 receptor [7,8,11]. The last one, P681H, is supposed to be related to an improved transmissibility of the virus [12].

Two new variants emerged in Brazil, both originating from the B.1.1.28 clade [13]. The first variant (named B.1.1.28.2), detected in October 2020, was characterized by the E484K mutation in the S protein, related to a possible escape from neutralizing antibodies [14]. The second variant (named B.1.1.28.1) was reported by the National Institute of Infectious Diseases in Japan after sampling of Brazilian travelers to Japan. Since this variant presents other substantial mutations such as H655Y, L18F, D138Y, and N501Y, in addition to the E484K [7,13,15], it was classified as a "variant of concern" [16]. Notably, the E484K mutation is in common with the B.1.351 variant first identified in the Republic of South Africa but not with B.1.1.7 [13]. The P.1 and B.1.351 variants share common mutations in the S protein, increasing the possibility of evasion of the humoral response and enhanced transmissibility [13,17].

As of 2 March 2021, B.1.1.7 accounts for 54.0% of Italian cases nationwide, ranging from 0 to 93.3% between regions, and is becoming the most widely present variant in the country. The P.1 variant is less prevalent for now, accounting for 4.3% of all new local COVID-19 cases, while B.1.351 is involved in just 0.4% of new cases [18]. Recently, a new VOC emerged, the SARS-CoV-2 B.1.617.2, also named Delta, first detected in India and now dominant in the UK [19,20]. The new variant has overtaken B.1.1.7 in the UK, and it is estimated that it will represent 90% of all viruses circulating in Europe by the end of August [19,21]. Additionally, it seems to be characterized by a higher risk of hospital admission and increased transmissibility [19,20,22]. Here we assess the neutralization activity against B.1.1.7, P.1, and B.1.351 variants in a panel of human serum samples from hospitalized infected COVID-19 patients, previously tested by 2019-nCov/Italy-INMI1, clade V strain (Wuhan strain).

2. Materials and Methods

2.1. Study Population

Sera of 42 COVID-19 patients (35 recovered and 7 with fatal outcome), hospitalized at Humanitas Gavazzeni (Bergamo, Italy) during the first epidemic wave that occurred in Italy between March and May 2020, were included in the present study. Subject characteristics and study procedures were described in detail elsewhere (approval number 17373—Ethics Committee of the University of Siena; approval number 17/20—Ethics Committee of Humanitas Gavazzeni) [23].

For the purpose of the present study, sera available for each patient at three time points were selected: the hospital admission sample (baseline), the sample showing the highest neutralizing antibody titer against 2019-nCov/Italy-INMI1 strain (hereafter referred to as wild-type (wt) strain) found in the previous study [23] and defined as "peak", and the last sample available during hospital stay. For 22 patients, the "peak" sample was the last sample available during the hospital stay. Samples of deceased/recovered patients were pulled together for the purpose of this study, as in the original study no difference was found between the 2 groups in terms of neutralizing antibody titers with respect to the wt strain.

2.2. Cell Culture and Viral Growth

VERO E6 cells (ATCC—CRL 1586) were cultured in Dulbecco's Modified Eagle's Medium (DMEM), High Glucose (Euroclone, Pero, Italy), supplemented with 2 mM L-glutamine (Lonza, Milano, Italy), 100 units/mL penicillin–streptomycin mixture (Lonza, Milano, Italy) and 10% fetal bovine serum (FBS) (Euroclone, Pero, Italy), in a 37 °C and 5% CO_2 humidified incubator.

Adherent subconfluent cell monolayers of VERO E6 were prepared in growth medium (DMEM High Glucose containing 2% FBS, 2 mM L-glutamine, 100 units/mL penicillin–streptomycin) in 175 cm^2 flasks or 96-well plates for propagation or titration and neutralization tests of SARS-CoV-2, respectively.

Cells were seeded in a 175 cm^2 flask at a density of 1×10^6 cells/mL. After 18–20 h, the subconfluent cell monolayer was washed twice with sterile Dulbecco's phosphate-buffered saline (DPBS). After the DPBS was removed, cells were infected with 3.5 mL of DMEM 2% FBS containing the SARS-CoV-2 virus at a multiplicity of infection (MOI) of 0.01. After 1 h of incubation at 37 °C in a humidified atmosphere with 5% CO_2, 50 mL of DMEM containing 2% FBS was added. The flasks were observed daily, and the virus was harvested when 80–90% of the cells manifested cytopathic effect (CPE). The culture medium was centrifuged at +4 °C and 469× *g* for 8 min, aliquoted, and stored at −80 °C.

2.3. SARS-CoV-2 Viruses

The SARS-CoV-2 (nCoV strain 2019-nCov/Italy-INMI1 strain) wt virus was purchased from the European Virus Archive goes Global (EVAg, Spallanzani Institute, Rome). Notably, the used strain did not carry the S protein amino acid change D614G.

The B.1.1.7 named England/MIG457/2020 and the B.1.351 variant named hCoV-19/Netherlands/NoordHolland_10159/2021, next strain clade 20H, wt viruses were purchased from EVAg.

The P.1 variant (next strain 20J/501Y.V3) (lineage B.1.1.28.1) was kindly provided by the University of Siena, Department of Medical Biotechnology.

2.4. Virus Neutralization Assay

The virus neutralization (VN) assay was performed as previously reported [24]. Briefly, after heat-inactivation for 30 min at 56 °C, serum samples, starting from 1:10 dilution, were mixed with an equal volume of SARS-CoV-2 (B.1.1.7, P.1, and B.1.351) viral solution containing 100 tissue culture infective dose 50% (TCID50). After 1 h of incubation at room temperature, 100 µL of virus–serum mixture was added to a 96-well plate containing an 80% confluent Vero E6 cell monolayer. Plates were incubated for 4 days at 37 °C and 5% CO_2 in humidified atmosphere and then checked for presence/absence of CPE by an inverted optical microscope. A CPE higher than 50% indicated infection. The VN titer was expressed as the reciprocal of the highest serum dilution showing protection from viral infection and CPE.

2.5. Statistical Analysis

All statistical analyses were performed using GraphPad Prism version 6.01 for Windows (GraphPad Software, San Diego, CA, USA [25]. For each variant, the mean fold decrease in antibody levels with respect to the *wt* strain was calculated along with its standard deviation (SD). Antibody levels were expressed as log and statistically evaluated with respect to the wt strain using a paired t-tests. Statistical significance was set at $p < 0.05$, two-tailed.

3. Results

Neutralizing antibody titers of each patient by time point and variant are shown in Figure 1 with statistically significant titer decrease for all three variants at any time point at hospital admission (baseline); 10 patients (23.8%) were negative for neutralizing

antibodies against the wt strain as well as for all the variants. In total, 16 patients (38.1%) were negative for B.1.1.7, 20 (47.6%) were negative for P.1, and 30 (71.4%) were negative for B.1.351 at baseline. Twenty-three (54.8%) and 30 (71.4%) patients showed a ≥2-fold decrease in neutralizing antibody titer when tested against B.1.1.7 and P.1, respectively (Table 1a, b). Thirty-two patients (76.2%) showed a ≥2-fold decrease in neutralizing antibody titer against B.1.351 (Table 1c). A significant decrease in neutralizing antibody titers against all three variants ($p < 0.0001$) was observed with respect to the wt strain.

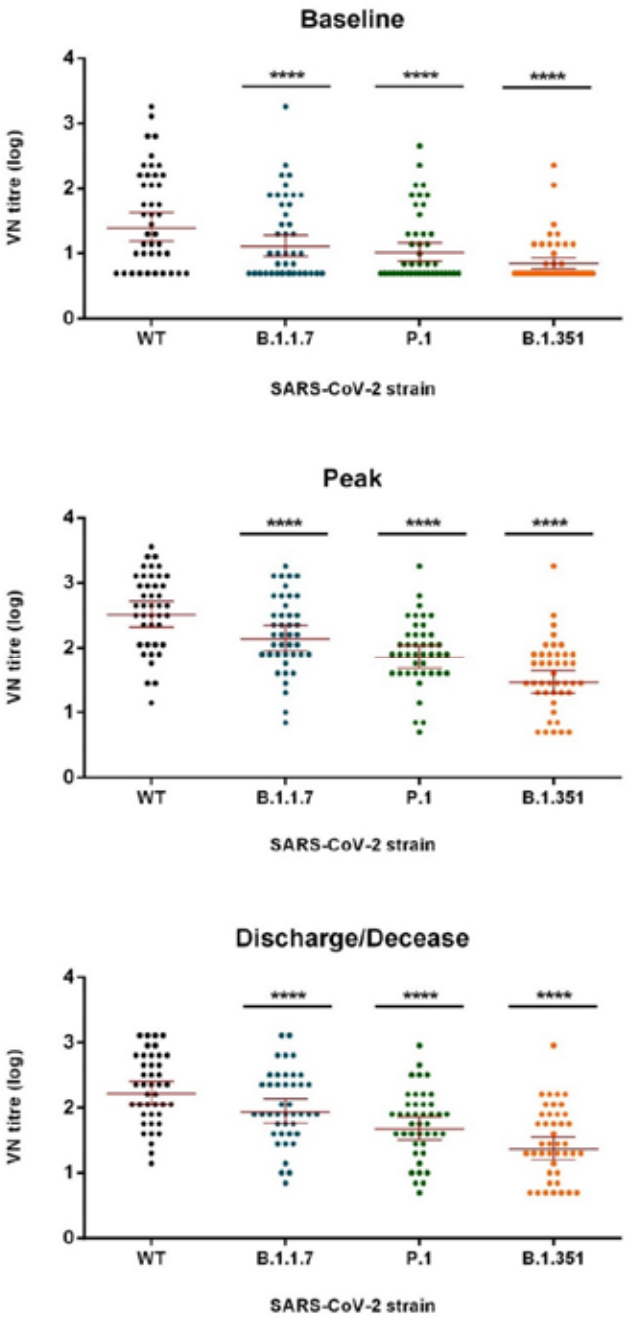

Figure 1. SARS-CoV-2 virus-neutralization (VN) titers with geometric mean and 95% confidence intervals, by time point and strain. For each variant, VN titers were compared with respect to the wt strain using a paired t-test (**** $p \leq 0.0001$).

Table 1. Fold decrease in neutralizing antibody titers of B.1.1.7 (a), P.1 (b) and B.1.351 (c) variants with respect to the wt strain by time point (baseline, peak, and discharge/decease).

(a) B.1.1.7 Variant						
	Baseline		**Peak**		**Discharge/Decease**	
	N	**%**	**N**	**%**	**N**	**%**
-	19	45.2%	16	38.1%	17	40.5%
2-fold	12	28.6%	14	33.3%	16	38.1%
4- fold	7	16.7%	8	19.0%	9	21.4%
>4- fold	4	9.5%	4	9.5%	0	0.0%
Total	42	100%	42	100%	42	100%
Mean fold (SD)	3.0 (3.1)		3.5 (5.0)		2.3 (1.4)	
(b) P.1 Variant						
	Baseline		**Peak**		**Discharge/Decease**	
	N	**%**	**N**	**%**	**N**	**%**
-	12	28.6%	5	11.9%	7	16.7%
2-fold	15	35.7%	10	23.8%	14	33.3%
4- fold	6	14.3%	12	28.6%	14	33.3%
>4- fold	9	21.4%	15	35.7%	7	16.7%
Total	42	100%	42	100%	42	100%
Mean fold (SD)	4.3 (4.5)		6.0 (4.3)		4.4 (3.4)	
(c) B.1.351 Variant						
	Baseline		**Peak**		**Discharge/Decease**	
	N	**%**	**N**	**%**	**N**	**%**
-	10	23.8%	4	9.5%	4	9.5%
2-fold	10	23.8%	5	11.9%	9	21.4%
4- fold	2	4.8%	5	11.9%	6	14.3%
>4- fold	20	47.6%	28	66.7%	23	54.8%
Total	42	100%	42	100%	42	100%
Mean fold (SD)	10.2 (14.9)		18.5 (18.9)		11.0 (12.3)	

– means a decrease less than 2-fold; SD: standard deviation.

Twenty-six samples (61.9%) with peak neutralizing titers for the wt strain had a ≥2-fold decrease in neutralizing antibody titer against B.1.1.7, with a mean decrease of 3.5-fold (SD 5.0). In particular, 14 (33.3%) showed a 2-fold decrease, 8 (19.0%) showed a 4-fold decrease, and 4 (9.5%) showed a >4-fold decrease (Table 1a). When tested for P.1, 37 (88.1%) had a ≥2-fold decrease with a mean decrease of 6.0-fold (SD 4.3). Ten (23.8%) showed a 2-fold decrease, 12 (28.6%) showed a 4-fold decrease, and 15 (35.7%) showed a >4-fold decrease (Table 1b). When tested for B.1.351, 38 (90.5%) showed a ≥2-fold decrease with a mean decrease of 18.5-fold (SD 18.9); 5 (11.9%) showed a 2-fold decrease, 5 (11.9%) showed a 4-fold decrease, and 28 (66.7%) showed a ≥4-fold decrease (Table 1c). The decrease in neutralizing antibody titer with respect to the wt strain was significant for all three variants ($p < 0.0001$).

At discharge/decease, all patients showed neutralizing antibody against the wt strain, although a decline in titer was observed as deeply described elsewhere [23]. When tested against B.1.1.7, one patient (2.4%) was found negative. A ≥2-fold decrease was observed in 25 (59.5%) patients: 16 (38.1%) and 9 (21.4%) showed a 2-fold and 4-fold decrease, respectively (mean decrease 2.3-fold (SD 1.4)) (Table 1a). Three patients (7.1%) were found negative when tested against P.1, and a ≥2-fold decrease was observed in 35 (83.3%) patients. In particular, 14 (33.3%) showed a 2-fold decrease, 14 (33.3%) showed a 4-fold decrease, and 7 (16.7%) showed a >4-fold decrease, with a mean decrease of 4.4-fold (SD 3.4) (Table 1b).

Nine patients (21.4%) were found negative when tested against B.1.351, and a ≥2-fold decrease was observed in 38 (90.5%) patients. In particular, 9 (21.4%) showed a 2-fold decrease, 6 (14.3%) showed a 4-fold decrease, and 23 (54.8%) showed a >4-fold decrease, with a mean decrease of 11.0-fold (SD 12.3). The decrease in neutralizing antibody titer was statistically significant for all three variants ($p < 0.0001$) with respect to the wt strain.

4. Discussion

Recently, different variants of SARS-CoV-2 with mutations in the S protein have emerged, raising concerns about the protection elicited by natural infection or conferred by vaccination.

In this study, we evaluated the neutralizing activity against B.1.1.7, P.1, and B.1.351 VOCs in a panel of human serum samples from hospitalized patients infected by SARS-CoV-2 between March and May 2020 during the first wave of the pandemic in Italy [23].

Although we assessed the neutralizing activity at three time points for each patient, namely hospital admission (baseline), neutralizing antibody titer peak, and the last time point available (at discharge or decease), here we mainly discuss the last one since it may represent the "antibody baggage".

In our study, 59.5% of the patients had a decrease (≥2-fold) in neutralizing antibody titer against B.1.1.7, and 21.4% showed a 4-fold decrease, as shown in a similar study [26]. On the contrary, other studies have reported that samples from convalescent or hospitalized patients are able to neutralize the B.1.1.7 variant, either maintaining similar levels of neutralizing activity or exhibiting a modest decrease compared to the original antibody titer [27–29]. We can hypothesize that the decrease in neutralizing antibody titer found in our study may be ascribed to the wt virus used, lacking D614G mutation. In general, the modest change in the potency of neutralization against this variant could be related to the N501Y mutation that, even though related to an increased binding to the ACE-2 receptor, does not appear to have a significant implication for neutralizing activity [28].

Regarding the P.1 variant, 83.3% of the patients involved in the study showed significantly reduced neutralizing activity (a ≥2-fold decrease), and 16.7% had a decrease higher than 4-fold, almost twice that reported for B.1.1.7. The reduction in neutralizing activity was even higher against the B.1.351 variant, with 90.5% of patients showing a fold decrease of ≥2 with a mean decrease almost 3 times higher than that against the P.1 variant. These findings are consistent with other studies [27,28,30,31] in which a reduced neutralizing potency of antibodies against these variants has been reported, although convalescent and vaccinated sera seem to better neutralize P.1 than B.1.351. The reduced neutralization could be ascribed to the E484K mutation shared between P.1 and B.1.351 and related to a possible escape from neutralizing antibodies. Considering that some mutations of P.1 are in common with B.1.351, such as the E484K mutation, it is very likely that a similar or higher reduction in neutralizing antibodies may be caused by variants carrying the same mutation. The immunoevasion could lead to reinfection of subjects who recovered from a previous infection [16] and could reduce the protection induced by vaccination and/or natural infection [27]. However, recent studies have proven that boosting pre-existing immunity against SARS-CoV-2 with one dose of mRNA vaccine induces a strong neutralizing response even against divergent variants (i.e., B.1.351) [8,32]. In Italy, subjects naturally infected by SARS-CoV-2 receive just one dose of vaccine from 3 to 6 months after infection [33]. In addition, a recent study [34] reported that neutralizing antibodies after natural infection by SARS-CoV-2 can last for at least 9 months.

Notably, one serum sample was not able to neutralize the B.1.1.7 variant, three were not able to neutralize the P.1 variant, and nine were not able to neutralize the B.1.351 variant, suggesting that symptomatic subjects previously infected by SARS-CoV-2 wt virus might not be fully protected against the emerging variants.

A key strength of the study is that the neutralizing activity has been assessed using authentic live SARS-CoV-2 viruses and not surrogate VN assay.

This study has some limitations. First, the cohort only included hospitalized patients, which may not be representative of the general population. The lack of follow-up samples after discharge does not allow the assessment of the full breadth of cross-neutralization potential that can be reached following more extended affinity maturation.

Overall, our findings provide evidence of a remarkable lower neutralization capacity of SARS-CoV-2 antibodies acquired during the first wave of the pandemic against the B.1.351 variant, and to a lesser extent against P.1 and B.1.1.7. This might suggest the possibility of reinfection or that previously infected individuals may be partially protected against current and new emerging variants with relevant mutations. However, the immune response induced by natural infection may protect from severe disease [35]. The emergence of the Delta VOC is also raising concern; however, so far, it appears that vaccines remain effective, especially after two doses [21,22,36]. Our study highlights the importance of evaluating SARS-CoV-2 pre-existing immunity against emerging variants as a tool to foresee the immune escape and the extent of vaccine efficacy.

Author Contributions: C.M.T., conceptualization, funding acquisition, investigation, project administration, writing—original draft preparation; S.M., investigation, data curation, formal analysis, writing—review and editing; S.V., writing— review and editing; A.M., methodology, writing—review and editing; L.B., methodology, writing—review and editing; A.R., resources, writing—review & editing; E.B., resources, writing—review & editing; I.V., resources, methodology, writing—review and editing; M.Z., resources, methodology, writing—review and editing; E.M., methodology, writing—review and editing. All authors have read and agreed to the published version of the manuscript.

Funding: This research received no external funding.

Institutional Review Board Statement: The study was conducted according to the guidelines of the Declaration of Helsinki and approved by the Ethics Committee of the University of Siena (approval number 17373, approval date 1 June 2020) and by the Ethics Committee of Humanitas Gavazzeni (approval number 236 Protocol 670/20, approval date 22 September 2020).

Informed Consent Statement: Patient consent was waived since all serum samples have been fully anonymized before testing.

Data Availability Statement: Data is contained within the article.

Acknowledgments: This study was supported by the European Virus Archive goes Global (EVAg) project, which has received funding from the European Union's Horizon 2020 research and innovation programme under grant agreement No. 653316.

Conflicts of Interest: The authors declare no conflict of interest.

References

1. World Health Organization. WHO Director-General's Opening Remarks at the Media Briefing on COVID-19—11 March 2020. 2020. Available online: https://www.who.int/dg/speeches/detail/who-director-general-s-opening-remarks-at-the-media-briefing-on-covid-19---11-march-2020 (accessed on 4 May 2021).
2. Algaissi, A.; Alfaleh, M.A.; Hala, S.; Abujamel, T.S.; Alamri, S.S.; Almahboub, S.A.; Alluhaybi, K.A.; Hobani, H.I.; Alsulaiman, R.M.; AlHarbi, R.H.; et al. SARS-CoV-2 S1 and N-based serological assays reveal rapid seroconversion and induction of specific antibody response in COVID-19 patients. *Sci. Rep.* **2020**, *10*, 16561.
3. CDC. SARS-CoV-2 Variant Classifications and Definitions. 2021. Available online: https://www.cdc.gov/coronavirus/2019-ncov/cases-updates/variant-surveillance/variant-info.html#Concern (accessed on 6 April 2021).
4. WHO. SARS-CoV-2 Variant—United Kingdom of Great Britain and Northern Ireland. 2020. Available online: https://www.who.int/csr/don/21-december-2020-sars-cov2-variant-united-kingdom/en/ (accessed on 6 April 2021).
5. Burki, T. Understanding variants of SARS-CoV-2. *Lancet* **2021**, *397*, 462.
6. Davies, N.G.; Abbott, S.; Barnard, R.C.; Jarvis, C.I.; Kucharski, A.J.; Munday, J.D.; Pearson, C.A.B.; Russell, T.W.; Tully, D.C.; Washburne, A.D.; et al. Estimated transmissibility and impact of SARS-CoV-2 lineage B.1.1.7 in England. *Science* **2021**, *372*, eabg3055.
7. CDC. Science Brief: Emerging SARS-CoV-2 Variants. 2021. Available online: https://www.cdc.gov/coronavirus/2019-ncov/science/science-briefs/scientific-brief-emerging-variants.html (accessed on 6 April 2021).

8. Wu, K.; Werner, A.P.; Moliva, J.I.; Koch, M.; Choi, A.; Stewart-Jones, G.B.E.; Bennett, H.; Boyoglu-Barnum, S.; Shi, W.; Graham, B.S.; et al. mRNA-1273 vaccine induces neutralizing antibodies against spike mutants from global SARS-CoV-2 variants. *bioRxiv* **2021**, doi:10.1101/2021.01.25.427948.
9. Davies, N.G.; Jarvis, C.I.; CMMID COVID-19 Working Group; Edmunds, J.W.; Jewell, N.P.; Diaz-Ordaz, K.; Keogh, R.H. Increased mortality in community-tested cases of SARS-CoV-2 lineage B.1.1.7. *Nature* **2021**, *593*, 270–274.
10. eCDC. *Rapid Increase of a SARS-CoV-2 Variant with Multiple Spike Protein Mutations Observed in the United Kingdom*; 2020; pp. 1–13. Available online: https://www.ecdc.europa.eu/sites/default/files/documents/SARS-CoV-2-variant-multiple-spike-protein-mutations-United-Kingdom.pdf (accessed on 12 July 2021).
11. Muik, A.; Wallisch, A.K.; Sanger, B.; Swanson, K.A.; Muhl, J.; Chen, W.; Cai, H.; Maurus, D.; Sarkar, R.; Tureci, O.; et al. Neutralization of SARS-CoV-2 lineage B.1.1.7 pseudovirus by BNT162b2 vaccine-elicited human sera. *Science* **2021**, *371*, 1152–1153.
12. Zuckerman, N.S.; Fleishon, S.; Bucris, E.; Bar-Ilan, D.; Linial, M.; Bar-Or, I.; Mor, O. A unique SARS-CoV-2 spike protein P681H strain detected in Israel. *medRxiv* **2021**, doi:10.1101/2021.03.25.21253908.
13. Toovey, O.T.R.; Harvey, K.N.; Bird, P.W.; Tang, J.W.W. Introduction of Brazilian SARS-CoV-2 484K.V2 related variants into the UK. *J. Infect.* **2021**, doi:10.1016/j.jinf.2021.01.025.
14. Nonaka, C.K.V.; Franco, M.M.; Graf, T.; de Lorenzo Barcia, C.A.; de Avila Mendonca, R.N.; de Sousa, K.A.F.; Neiva, L.M.C.; Fosenca, V.; Mendes, A.V.A.; de Aguiar, R.S. Genomic Evidence of SARS-CoV-2 Reinfection Involving E484K Spike Mutation, Brazil. *Emerg. Infect. Dis.* **2021**, *27*, 1522–1524.
15. Sabino, E.C.; Buss, L.F.; Carvalho, M.P.S.; Prete, C.A., Jr; Crispim, M.A.E.; Fraiji, N.A.; Pereira, R.H.M.; Parag, K.V.; da Silva Peixoto, P.; Kraemer, M.U.G.; et al. Resurgence of COVID-19 in Manaus, Brazil, despite high seroprevalence. *Lancet* **2021**, *397*, 452–455.
16. Naveca, F.; da Costa, C.; Nascimento, V.; Souza, V.; Corado, A.; Nascimento, F.; Costa, A.; Duarte, D.; Silva, G.; Mejía, M.; et al. *SARS-CoV-2 Reinfection by the New Variant of Concern (VOC) P.1 in Amazonas, Brazil*; 2021. Available online: https://virological.org/t/sars-cov-2-reinfection-by-the-new-variant-of-concern-voc-p-1-in-amazonas-brazil/596 (accessed on 12 July 2021).
17. Fontanet, A.; Autran, B.; Lina, B.; Kieny, M.P.; Karim, S.S.A.; Sridhar, D. SARS-CoV-2 variants and ending the COVID-19 pandemic. *Lancet* **2021**, *397*, 952–954.
18. ISS. CS N° 14/2021—In Italia il 54% Delle Infezioni Dovute a 'Variante Inglese', il 4,3% a Quella 'Brasiliana' e lo 0,4% a Quella 'Sudafricana'. 2021. Available online: https://www.iss.it/comunicati-stampa/-/asset_publisher/fjTKmjJgSgdK/content/id/5647546?_com_liferay_asset_publisher_web_portlet_AssetPublisherPortlet_INSTANCE_fjTKmjJgSgdK_redirect=https%3A%2F%2Fwww.iss.it%2Fcomunicatistampa%3Fp_p_id%3Dcom_liferay_asset_publisher_web_portlet_AssetPublisherPortlet_INSTANCE_fjTKmjJgSgdK%26p_p_lifecycle%3D0%26p_p_state%3Dnormal%26p_p_mode%3Dview%26_com_liferay_asset_publisher_web_portlet_AssetPublisherPortlet_INSTANCE_fjTKmjJgSgdK_cur%3D0%26p_r_p_resetCur%3Dfalse%26_com_liferay_asset_publisher_web_portlet_AssetPublisherPortlet_INSTANCE_fjTKmjJgSgdK_assetEntryId%3D5647546 (accessed on 6 April 2021).
19. Torjesen, I. Covid-19: Delta variant is now UK's most dominant strain and spreading through schools. *BMJ* **2021**, *373*, n1445.
20. Wall, E.C.; Wu, M.; Harvey, R.; Kelly, G.; Warchal, S.; Sawyer, C.; Bauer, D.L. Neutralising antibody activity against SARS-CoV-2 VOCs B.1.617.2 and B.1.351 by BNT162b2 vaccination. *Lancet* **2021**, *397*, 2331–2332.
21. eCDC. ECDC Statement on the SARS-CoV-2 Delta Variant in the EU/EEA. Available online: https://www.ecdc.europa.eu/en/news-events/ecdc-statement-sars-cov-2-delta-variant-eueea (accessed on 24 June 2021).
22. Bernal, J.L.; Andrews, N.; Gower, C.; Gallagher, E.; Simmons, R.; Thelwall, S.; Ramsay, M. Effectiveness of COVID-19 vaccines against the B.1.617.2 variant. *MedRxiv* **2021**, doi:10.1101/2021.05.22.21257658.
23. Marchi, S.; Simonetta, V.; Remarque, E.; Ruello, A.; Bombardieri, E.; Bollati, V.; Trombetta, C. Characterization of antibody response in asymptomatic and symptomatic SARS-CoV-2 infection. *PLoS ONE* **2021**, doi:10.1371/journal.pone.0253977.
24. Manenti, A.; Maggetti, M.; Casa, E.; Martinuzzi, D.; Torelli, A.; Trombetta, C.M.; Marchi, S.; Montomoli, E. Evaluation of SARS-CoV-2 neutralizing antibodies using a CPE-based colorimetric live virus micro-neutralization assay in human serum samples. *J. Med. Virol.* **2020**, *92*, 2096–2104.
25. GraphPad Software. Available online: www.graphpad.com. (accessed on 17 June 2021).
26. Supasa, P.; Zhou, D.; Dejnirattisai, W.; Liu, C.; Mentzer, A.J.; Ginn, H.M.; Screaton, G.R. Reduced neutralization of SARS-CoV-2 B.1.1.7 variant by convalescent and vaccine sera. *Cell* **2021**, *184*, 2201–2211.
27. Tada, T.; Dcosta, B.M.; Samanovic-Golden, M.; Herati, R.S.; Cornelius, A.; Mulligan, M.J.; Landau, N.R. Neutralization of viruses with European, South African, and United States SARS-CoV-2 variant spike proteins by convalescent sera and BNT162b2 mRNA vaccine-elicited antibodies. *bioRxiv* **2021**, doi:10.1101/2021.02.05.430003.
28. Wang, P.; Nair, M.S.; Liu, L.; Iketani, S.; Luo, Y.; Guo, Y.; Wang, M.; Yu, J.; Zhang, B.; Kwong, P.D.; et al. Antibody resistance of SARS-CoV-2 variants B.1.351 and B.1.1.7. *Nature* **2021**, *593*, 130–135.
29. Rees-Spear, C.; Muir, L.; Griffith, S.A. The impact of Spike mutations on SARS-CoV-2 neutralization. *BioRxiv* **2021**, 1–26, doi:10.1101/2021.01.15.426849.
30. Chen, R.E.; Zhang, X.; Case, J.B.; Winkler, E.S.; Liu, Y.; VanBlargan, L.A.; Liu, J.; Errico, J.M.; Xie, X.; Suryadevara, N.; et al. Resistance of SARS-CoV-2 variants to neutralization by monoclonal and serum-derived polyclonal antibodies. *Nat. Med.* **2021**, *27*, 717–726.

31. Stamatatos, L.; Czartoski, J.; Wan, Y.H.; Homad, L.J.; Rubin, V.; Glantz, H.; Neradilek, M.; Seydoux, E.; Jennewein, M.F.; MacCamy, A.J.; et al. mRNA vaccination boosts cross-variant neutralizing antibodies elicited by SARS-CoV-2 infection. *Science* **2021**, doi:10.1126/science.abg9175.
32. Ebinger, J.E.; Fert-Bober, J.; Printsev, I.; Wu, M.; Sun, N.; Prostko, J.C.; Frias, E.C.; Stewart, J.L.; van Eyk, J.E.; Braun, J.G.; et al. Antibody responses to the BNT162b2 mRNA vaccine in individuals previously infected with SARS-CoV-2. *Nat. Med*. **2021**, doi:10.1038/s41591-021-01325-6.
33. Ministero Della SALUTE. OGGETTO: Vaccinazione dei Soggetti che Hanno Avuto Un'infezione da SARS-CoV-2. 2021. Available online: http://www.regioni.it/sanita/2021/03/04/ministero-della-salute-circolare-vaccinazione-dei-soggetti-che-hanno-avuto-uninfezione-da-sars-cov-2-03-03-2021-630251/ (accessed on 1 April 2021).
34. He, Z.Y.; Ren, L.L.; Yang, J.T.; Guo, L.; Feng, L.Z.; Ma, C.; Wang, X.; Leng, Z.W.; Tong, X.L.; Zhou, W.; et al. Seroprevalence and humoral immune durability of anti-SARS-CoV-2 antibodies in Wuhan, China: A longitudinal, population-level, cross-sectional study. *Lancet* **2021**, *397*, 1075–1084.
35. Naveca, F.; da Costa, C.; Nascimento, V.; Souza, V.; Corado, A.; Nascimento, F.; Resende, P.C. Three SARS-CoV-2 reinfection cases by the new Variant of Concern (VOC) P.1/501Y.V3. *Res. Sq.* **2021**, 1–13, doi:10.21203/rs.3.rs-318392/v1.
36. Stowe, J.; Andrews, N.; Gower, C.; Gallagher, E.; Utsi, L.; Simmons, R. Effectiveness of COVID-19 Vaccines against Hospital Admission with the Delta (B.1.617.2) Variant. Available online: https://media.tghn.org/articles/Effectiveness_of_COVID-19_vaccines_against_hospital_admission_with_the_Delta_B._G6gnnqJ.pdf (accessed on 23 June 2021).

PLOS ONE

RESEARCH ARTICLE

Characterization of antibody response in asymptomatic and symptomatic SARS-CoV-2 infection

Serena Marchi[1☯], Simonetta Viviani[1☯], Edmond J. Remarque[2], Antonella Ruello[3], Emilio Bombardieri[3], Valentina Bollati[4], Gregorio P. Milani[4,5], Alessandro Manenti[6,7], Giulia Lapini[6], Annunziata Rebuffat[8], Emanuele Montomoli[1,6,7], Claudia M. Trombetta[1]*

1 Department of Molecular and Developmental Medicine, University of Siena, Siena, Italy, **2** Department of Virology, Biomedical Primate Research Centre, Rijswijk, The Netherlands, **3** Humanitas Gavazzeni, Bergamo, Italy, **4** Department of Clinical Sciences and Community Health, University of Milan, Milan, Italy, **5** Pediatric Unit, Fondazione IRCCS Ca' Granda Ospedale Maggiore Policlinico, Milan, Italy, **6** VisMederi srl, Siena, Italy, **7** VisMederi Research srl, Siena, Italy, **8** Presidio Ospedaliero di Campostaggia, Località Campostaggia, Poggibonsi, Italy

☯ These authors contributed equally to this work.
* trombetta@unisi.it

OPEN ACCESS

Citation: Marchi S, Viviani S, Remarque EJ, Ruello A, Bombardieri E, Bollati V, et al. (2021) Characterization of antibody response in asymptomatic and symptomatic SARS-CoV-2 infection. PLoS ONE 16(7): e0253977. https://doi.org/10.1371/journal.pone.0253977

Editor: Wenbin Tan, University of South Carolina, UNITED STATES

Received: March 10, 2021

Accepted: June 16, 2021

Published: July 2, 2021

Data Availability Statement: All relevant data are within the manuscript.

Funding: This study was funded by a research grant (Pfizer Tracking Number 60353289). The Principal Investigator (Grant Recipient) is CMT. The funders had no role in study design, data collection and analysis, decision to publish, or preparation of the manuscript. Author AM was employed by VisMederi Research srl. Authors AM and GL are employed by VisMederi srl. EM is the Chief Scientific Officer of VisMederi srl and VisMederi

Abstract

SARS-CoV-2 pandemic is causing high morbidity and mortality burden worldwide with unprecedented strain on health care systems. To investigate the time course of the antibody response in relation to the outcome we performed a study in hospitalized COVID-19 patients. As comparison we also investigated the time course of the antibody response in SARS-CoV-2 asymptomatic subjects. Study results show that patients produce a strong antibody response to SARS-CoV-2 with high correlation between different viral antigens (spike protein and nucleoprotein) and among antibody classes (IgA, IgG, and IgM and neutralizing antibodies). The antibody peak is reached by 3 weeks from hospital admission followed by a sharp decrease. No difference was observed in any parameter of the antibody classes, including neutralizing antibodies, between subjects who recovered or with fatal outcome. Only few asymptomatic subjects developed antibodies at detectable levels.

Introduction

On March 11, 2020, the World Health Organization (WHO) Director General declared a pandemic situation due to a novel coronavirus causing a Severe Acute Respiratory Syndrome (SARS) rapidly spreading worldwide [1]. The novel coronavirus (CoV) SARS-CoV-2 has been firstly identified in Wuhan, Hubei Province, China, at the end of 2019 when a cluster of atypical pneumonia occurred [1, 2]. In January 2020, SARS-CoV-2 was isolated and sequenced as a CoV genetically related to the highly pathogenic CoV (SARS-CoV-1) responsible for the 2003 SARS epidemic that spread mainly in Asia with approximately 10% case fatality rate (CFR) [3]. Since 2004 SARS-CoV-1 circulation in humans ended whereas a third highly pathogenic CoV emerged in 2012 in Saudi Arabia causing the Middle East Respiratory Syndrome (MERS) [2, 4–7]. Since then MERS-CoV has spread to 27 countries with limited human-to-human

Research srl. VisMederi srl and VisMederi Research srl provided support in the form of salaries for authors AM, and GL, but did not have any additional role in the study design, data collection and analysis, decision to publish, or preparation of the manuscript. The specific roles of these authors are articulated in the 'author contributions' section.

Competing interests: We have the following interests: This study was funded by a research grant (Pfizer Tracking Number 60353289). Authors AM and GL are employed by VisMederi srl. EM is the Chief Scientific Officer of VisMederi srl and VisMederi Research srl. This does not alter our adherence to PLOS ONE policies on sharing data and materials.

transmission, and a CFR of approximately 34.4%, according to the most recent WHO report [7]. As SARS-CoV-1 and MERS-CoV, the SARS-CoV-2 virus is an enveloped, single-stranded, and positive-sense RNA virus belonging to the Betacoronavirus Genus, *Coronaviridae* family. SARS-CoV-2 genome, as the other emerging pathogenic human CoVs, encodes four major structural proteins: spike (S), envelope (E), membrane (M), nucleocapsid (N); approximately 16 nonstructural proteins (nsp1–16), and five to eight accessory proteins. Among them, the S protein plays an essential role in viral attachment, fusion, entry, and transmission. The S protein is the common target antigen for antibodies and vaccine development [8–11]. After SARS-CoV-2 infection, different categories of antibodies are circulating in serum as Immunoglobulin G (IgG), Immunoglobulin M (IgM) and Immunoglobulin A (IgA) mainly targeting two viral proteins, the S protein and the nucleoprotein (NP). The latter is abundant and highly expressed however, due to its biological function, it seems to be unlikely that antibodies against NP have neutralizing activity. The S protein contains the receptor binding domain (RBD), which mediates the binding to the host cell through the human Angiotensin-Converting Enzyme 2 (ACE2) and the fusion of viral and cellular membranes. Based on SARS-CoV-2 evidence as well as for other CoVs, the S protein seems to be the main target for neutralizing antibodies [12–14]. In COVID-19 patients, the levels of IgM and IgG increased at least 10 days after the onset of symptoms, most patients showed seroconversion within the first 3 weeks and the median time to seroconversion was 20 days [15, 16]. IgG and IgM seroconversion can occur simultaneously or sequentially [17] while IgA timing seems to be the most variable [15–18]. Common serological tests used are ELISA-based with different combinations of coatings on the S protein (S1, S1+S2, S1-S2, extracellular domain, RBD). The NP-based ELISA- is also used [19]. ELISAs have some advantages, such as high readout, speed of testing, and a BSL2 laboratory [20] (24). However, the Virus-Neutralization assay (VN) is currently considered the gold-standard as capable of measuring neutralizing antibodies that mimic in vitro the in vivo functional activity of blocking the virus [21].

SARS-CoV-2 predominant way of transmission is human-to-human through respiratory droplets, however, close contact with infected surfaces or objects may also be an occasional way of transmission as the virus is excreted and detectable in saliva and stool [6, 9, 22]. SARS-CoV-2 disease, or COVID-19, ranges from a mild upper/lower respiratory tract infection that resolves in a few days without sequelae to more serious disease with fever, cough, shortness of breath, myalgias, fatigue, confusion, headache, sore throat, acute respiratory distress syndrome, leading to respiratory or multiorgan failure [6, 9, 22]. The fatality rate is high in people with underlying comorbidities, such as diabetes, hypertension, chronic respiratory disease, or cardiovascular disease and in the elderly [9, 22]. Almost one year after the first COVID-19 cases were reported in Wuhan, as of 13 December 2020, there have been over 70 million cases and over 1.5 million deaths reported to WHO [23] with Europe being one of the most affected areas. COVID-19 pandemic is causing high morbidity and mortality burden worldwide, an unprecedented strain on health care systems, and social and economic disruption [24].

Italy has been affected by COVID-19 as early as February 2020 with the first SARS-CoV-2 case identified in Codogno at the end of February 2020, considered as the Italian index case. However, some evidence has later emerged that the virus had been circulating in Italy and Europe since autumn 2019 [25–28]. Italy suffered the first epidemic wave from February 2020 until June 2020 when the whole country was under strict lockdown. The most affected areas were in the Northern and, to a less extent, in Central Italy, while the Southern part of the country was relatively unaffected [29, 30]. During the summer COVID-19 remained endemic, with a second epidemic wave starting in October 2020 that led to a subsequent nationwide lockdown in November 2020. As of the 13th of December 2020, more than 1.8 million confirmed cases and more than 64.000 deaths due to SARS-CoV-2 were reported to ISS (Istituto

Superiore di Sanità), Rome [29]. The mean age of fatalities from COVID-19 was 80 years, 42,4% were women and more than 90% had one or more co-morbidity as ischemic heart disease, diabetes, active cancer, atrial fibrillation, dementia, and a history of stroke [31].

The emerging and rapid diffusion of COVID-19 has risen the calls for more targeted research in the field [32] helping to elucidate the mechanism of infection, protection, or rapid evolution until fatal outcome. We present here a study performed in hospitalized COVID-19 patients to investigate the time course of the antibody response in relation to the outcome, and as explorative comparison, to investigate the time course of the antibody response in SARS-CoV-2 asymptomatic subjects.

Material and methods

Study population

This was a retrospective study on COVID-19 patients and SARS-CoV-2 asymptomatic subjects collected between March and May 2020 during the first epidemic wave occurred in Italy.

A total of 42 COVID-19 patients, hospitalized at Humanitas Gavazzeni (Bergamo, Italy), were retrospectively selected for this study, of whom 35 (22 males and 13 females) recovered and 7 (3 males and 4 females) had a fatal outcome. All subjects were admitted to hospital with a diagnosis of interstitial pneumonia confirmed by chest radiograph or a CAT (computerized axial tomography) and had rhino-pharyngeal swab positive to SARS-CoV-2 (Real-Time PCR Thermo Fisher Scientific). Six (6) patients required care in the intensive care unit (ICU), the others were hospitalized in the general medicine unit. Out of 7 deceased patients, 3 were hospitalized in ICU and 4 in the general medicine unit.

Serum samples were collected at different time points from March to April 2020 for diagnostic/therapeutic purposes. We selected patients who had at least 5 blood samples available during the period of hospital stay (baseline, day 2, day 6, day 12–14, day 18–20, day 27–30). Demographic and clinical variables reported in this study were those collected at hospital admission. For the purpose of this study patients were categorized according to the outcome: recovered or deceased.

During the first phase of the COVID-19 epidemic, little was known about this novel CoV and there was no standard therapy, so the management changed over time. The Italian Society of Infectious and Tropical Diseases recommended as therapy hydroxychloroquine, antiviral agents, steroids, low molecular weight heparin and oxygen support in different combinations according to the clinician's evaluation. The antibiotic therapy was adopted only in case of suspected or confirmed bacterial superinfection.

Serum samples from 25 asymptomatic subjects who presented a positive rhino-pharyngeal swab for SARS-CoV-2 were collected as part of the UNICORN project and were analysed in the present study [33].

This study was approved by the Ethics Committee of the University of Siena (approval number 17373, approval date June 1, 2020), by the Ethics Committee of Humanitas Gavazzeni (approval number 236, approval date September 22, 2020 Protocol 670/20). All serum samples have been fully anonymized before testing. The UNICORN study was approved by the Ethics Committee of the University of Milan (approval number 17/20, approval date March 6, 2020). All participants signed an informed consent form.

Serological assay

ELISA. All serum samples were tested by commercial ELISA for the detection of IgA, IgG, and IgM against the S1 of SARS-CoV-2 (Aeskulisa® SARS-CoV-2 S1 IgA, IgM, IgG,

Aesku. Diagnostics, Wendelsheim, Germany) and for the detection of IgG against the NP of SARS-CoV-2 (Aeskulisa® SARS-CoV-2 NP IgG, Aesku.Diagnostics, Wendelsheim, Germany).

According to the manufacturer's instructions, quantitative analysis was performed by use of a 4-parameter logistic standard curve obtained by plotting the optical density (OD) values measured for 4 calibrators against their antibody activity (U/ml) using logarithmic/linear coordinates. Antibody activities of the samples were evaluated from OD values using the generated curve and considered positive if >12 U/ml.

Virus neutralization assay. The virus neutralization (VN) assay has been performed as previously reported [20]. Briefly, serum samples were heat-inactivated for 30 minutes at 56˚C and, starting from 1:10 dilution, were mixed with an equal volume of SARS-CoV-2 (2019-nCov/Italy-INMI1 strain) viral solution containing 100 Tissue Culture Infective Dose 50% (TCID50). After 1 hour of incubation at room temperature, 100μl of virus-serum mixture were added to a 96-well plate containing VERO E6 cells with 80% confluency. Plates were incubated for 3 days at 37˚C, 5% CO_2 in humidified atmosphere, then inspected for presence/absence of cytopathic effect (CPE) by means of an inverted optical microscope. A CPE higher than 50% indicated infection. The VN titer was expressed as the reciprocal of the highest serum dilution showing protection from viral infection and CPE.

Statistical analysis

All statistical analyses were performed using Microsoft R-Open version 3.5.0 (R Core Team (2018). R: A language and environment for statistical computing. R Foundation for Statistical Computing, Vienna, Austria. URL https://www.R-project.org/). For patient baseline characteristics continuous variables were evaluated using Mann-Whitney tests and for categorical variables Chi-square tests were used. Seroconversion rates were compared using Fisher's exact test. Antibody levels were statistically evaluated using t-tests. Statistical significance was set at $p<0.05$, two tailed.

Results

COVID-19 patients

Between March and April 2020, a total of 42 subjects were retrospectively selected, of whom 35 recovered and 7 had a fatal outcome. The median age at admission was 64.0 years (interquartile range (IQR) 56.0–71.5) for those who recovered and 69.0 years (IQR 64.5–72.0) for deceased patients. The median length of stay in the hospital was similar in both groups with 11.0 days (IQR 9.0–24.5) and 10.0 (IQR 6.0–15.59) for recovered and deceased patients, respectively. The mean number of pre-existing conditions in recovered and deceased was 1.53 (standard deviation (SD) 1.25) and 2.0 (SD 1.41), respectively, and comorbidities were indicated in 1.88 (SD 1.36) and 3.5 (SD 3.54) of recovered and deceased patients, respectively. Forty-five per cent (45%) of patients had at least one comorbidity. Main co-morbidities were cardiovascular disease, diabetes, cerebrovascular disease, hypertension and COPD (Chronic Obstructive Pulmonary Disease). No differences were found between recovered and deceased patients when compared for symptoms at admission (fever, cough, diarrhea, dyspnea) or presence/absence of comorbidities and/or preexisting conditions. The other demographic, clinical, and blood chemistry variables collected at baseline were similar between the two groups, with exception of ALT that showed to be statistically significantly higher (p-value 0.021) in subjects who recovered (Table 1).

At hospital admission, 15 patients (35.7%) were negative for S1 IgM, 11 (26.2%) for S1 IgA, 13 (30.9%) for S1 IgG, 15 (35.7%) for NP IgG, and 10 (23.8%) for neutralizing antibodies. Five

Table 1. Baseline characteristics of COVID-19 patients according to outcome. Median (IQR).

Parameter	*Recovered*	*Deceased*	*P-value*
Sex	22 M / 13 F	3 M / 4 F	0.574
Age	64.0 (56.0 to 71.5)	69.0 (64.5 to 72.0)	0.279
Length of stay	11.0 (9.0 to 24.5)	10.0 (6.0 to 15.5)	0.498
ICU	3 yes / 32 no	3 yes / 4 no	0.076
WBC	7.1 (5.8 to 9.7)	8.8 (5.5 to 11.6)	0.800
RBC	4.2 (3.9 to 4.6)	4.6 (4.1 to 4.9)	0.273
Hb	13.2 (12.2 to 14.3)	13.9 (13.2 to 14.0)	0.649
PLT	202.0 (152.5 to 298.0)	165.0 (134.0 to 283.0)	0.673
Neutrophils	6.2 (4.2 to 8.1)	6.9 (4.5 to 10.2)	0.673
Lymphocytes	0.9 (0.7 to 1.3)	0.4 (0.4 to 0.7)	0.075
AST	52.0 (31.5 to 80.0)	46.0 (35.0 to 52.0)	0.418
ALT	40.0 (25.5 to 64.5)	23.0 (22.5 to 29.0)	0.021
LDH	382.0 (279.0 to 527.5)	602.0 (400.5 to 680.5)	0.147
GGT	46.0 (34.0 to 96.5)	60.0 (23.0 to 73.0)	0.566
Creatinine	0.9 (0.8 to 1.0)	1.0 (0.9 to 1.1)	0.380
CRP	12.6 (7.9 to 16.1)	10.6 (7.9 to 13.5)	0.716
Ferritin	544.0 (315.5 to 1310.0)	1079.0 (967.5 to 1301.0)	0.224
Fibrinogen	591.0 (446.0 to 650.5)	577.0 (447.0 to 602.0)	0.500
D-Dimer	1383.0 (669.0 to 2261.5)	1137.0 (962.5 to 1733.5)	1.000
Fever*	33 yes / 2 no	7 yes / 0 no	1.000
Cough*	7 yes / 28 no	3 yes / 4 no	0.418
Diarrhea*	5 yes / 30 no	1 yes / 6 no	1.000
Dyspnea*	26 yes / 9 no	6 yes / 1 no	0.871
Comorbidities	17 yes / 18 no	2 yes / 5 no	0.579
Preexisting conditions	15 yes / 20 no	2 yes / 5 no	0.779

ICU, Intensive care unit; WBC, white blood cells (103/mmc); RBC, red blood cells (106/mmc); Hb, haemoglobin (gr/dl); PLT, platelets (103/mmc); AST, Aspartate aminotransferase (UI/l); ALT, Alanine aminotransferase (UI/l); LDH, lactate dehydrogenase (U/l); GGT, Gamma Glutamyl Transferase (UI/l); CRP, C reactive protein (mg/l). Neutrophils (103/mmc); Lymphocytes (103/mmc); Creatinine (mg/dl); Ferritin (ug/l); Fibrinogen (g/l); D-Dimer (mcg/ml).

*Fever: A measured temperature of 100.4˚ F (38˚ C) or greater, or with a history of feeling feverish.; Cough: Continuous cough for more than an hour, or 3 or more coughing episodes in 24 hours; Diarrhea: Loose, watery stools that occur more frequently than usual (at least 3 episodes within a 24-hour period); Dyspnea: Difficult or labored breathing; shortness of breath.

https://doi.org/10.1371/journal.pone.0253977.t001

patients (11.9%) were negative to any antibody assay at the time of admission; of these, 2 died and 3 recovered. Two days after admission, 6 patients (14.3%) were still negative for S1 IgM, 7 (16.7%) for S1 IgA, 4 (9.5%) for S1 IgG, 3 (7.1%) for NP IgG, and 5 (11.9%) for neutralizing antibodies. Two patients (4.8%) were still negative to any antibody assay; of these, 1 died and 1 recovered. At 6 days of sample collection, all subjects except one (97.6%) were positive to all assays (Figs 1–5). The exception was a 40-year-old male patient, positive to S1 IgG at any time point, and borderline for NP IgG only at admission and at day 2. This patient had neutralizing antibody titers less or equal than 40 at any time point. At admission, he had fever and dyspnea with no comorbidities or preexisting conditions and recovered in 12 days.

Two patients, one recovered and one deceased both within 6 days after admission, were both negative to NP IgG at admission and at day 2. Two subjects, both recovered, were positive

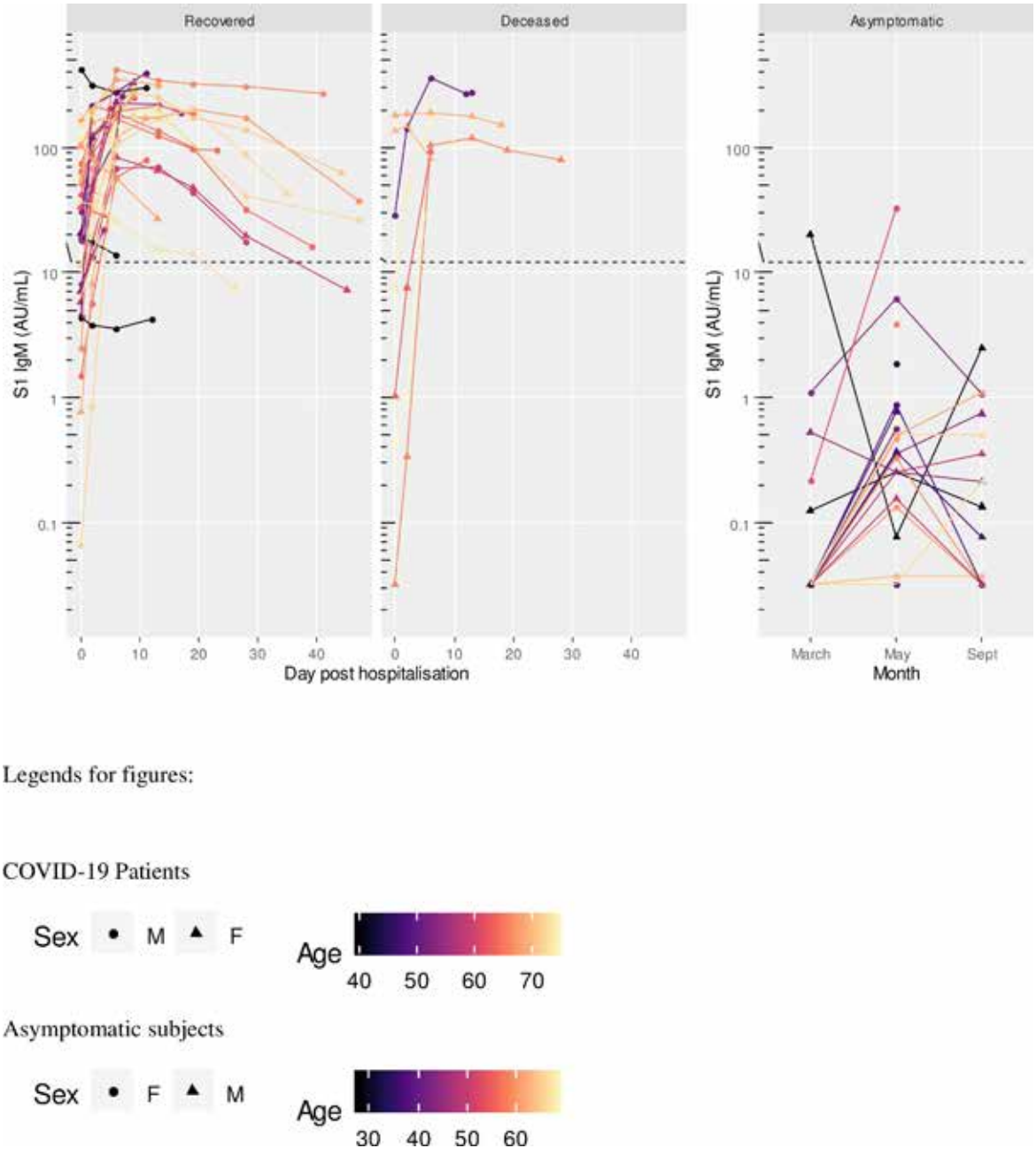

Fig 1. S1 IgM titres in COVID-19 patients (recovered and deceased) and asymptomatic subjects. Black dashed line indicates positivity threshold at 12 U/ml.

https://doi.org/10.1371/journal.pone.0253977.g001

only for neutralizing antibodies at admission, with titers less or equal to 40. They became positive to all antibodies from day 2 onward (Figs 1–5).

Neutralizing antibodies were found in all patients, with a range from 10 to 5120.

Antibody titers for patients are presented in Table 2. S1 and NP antibodies started increasing at day 2 and again at day 6. A decrease for all antibodies was observed in recovered patients at day 27–30. S1 antibody increase was similar in both recovered and deceased patients, while NP IgG titers were significantly higher in deceased patients at day 6 (p-value 0.044). At

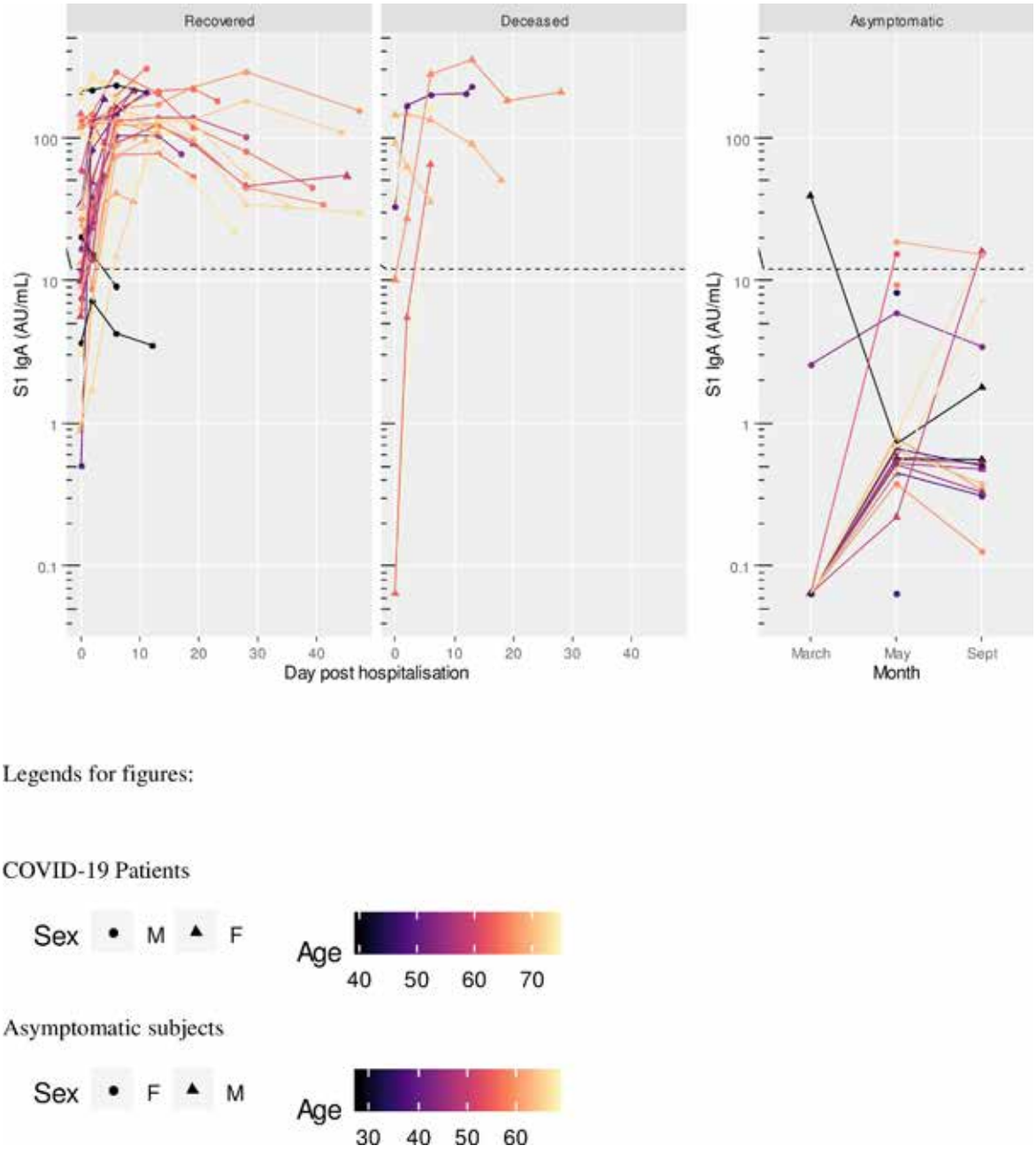

Fig 2. S1 IgA titres in COVID-19 patients (recovered and deceased) and asymptomatic subjects. Black dashed line indicates positivity threshold at 12 U/ml.

https://doi.org/10.1371/journal.pone.0253977.g002

baseline, neutralizing antibody titers were 40.8 (95%CI 1.3–1296.4) in recovered patients and 24.4 (95%CI 0.2–3093.8) in those deceased. Already at day 6, neutralizing antibody titers had increased steadily with 427.9 (95% CI 29.0–6321.5) in recovered patients and 226.3 (95% CI 12.1–4228.2) in those deceased. In recovered patients, a plateau of neutralizing antibody titers was observed until day 18–20, followed by a decline at day 27–30. No significant difference was found between the two groups at any time point. However, the comparison at day 27–30 was not possible as only 2 subjects were in the deceased group (Table 2).

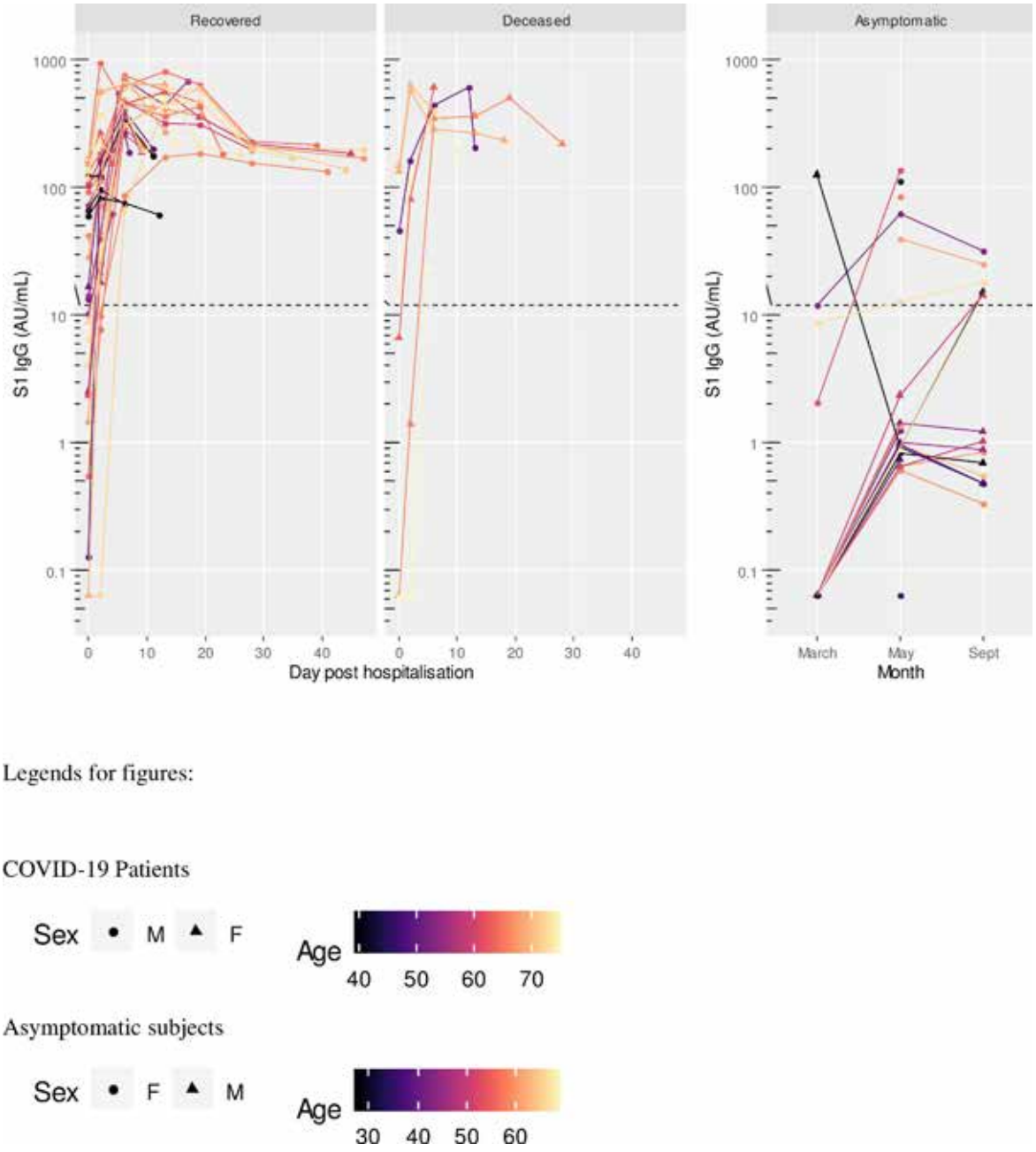

Fig 3. S1 IgG titres in COVID-19 patients (recovered and deceased) and asymptomatic subjects. Black dashed line indicates positivity threshold at 12 U/ml.

https://doi.org/10.1371/journal.pone.0253977.g003

IgM seroconversion rates were higher in the deceased at day 2 (p-value 0.043), whereas seroconversion rates for the other antibody classes were similar (Table 3).

No significant difference in antibody titers at baseline and by peak antibody level (all 5 assays combined) was found between those who survived and those deceased by using the Cox proportional hazard model. A good correlation was found among all assays as shown in Fig 6. Overall, the level of S1 specific response was well correlated among antibody types (r = 0.781 and r = 0.794, S1 IgG correlating with S1 IgA and S1 IgM, respectively; r = 0.760 S1 IgA correlating with S1 IgM). S1 IgG response was highly correlated with NP IgG (r = 0.834).

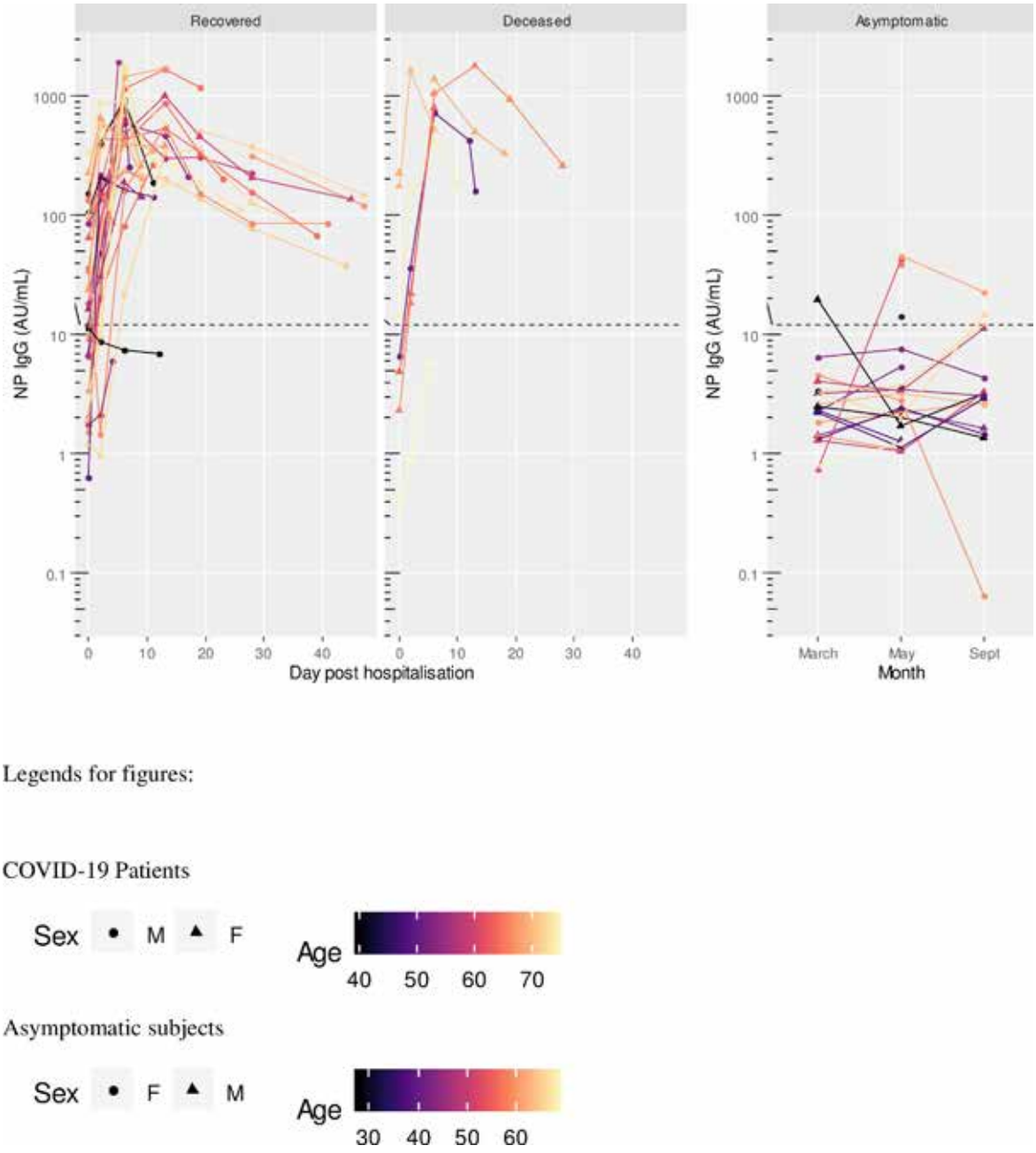

Fig 4. NP IgG titres in COVID-19 patients (recovered and deceased) and asymptomatic subjects. Black dashed line indicates positivity threshold at 12 U/ml.

https://doi.org/10.1371/journal.pone.0253977.g004

Neutralizing antibodies well correlated with all ELISA antibodies tested (r = 0.722 with S1 IgA, r = 0.798 with S1 IgM, r = 0.739 with S1 IgG, and r = 0.730 with NP IgG).

Asymptomatic SARS-CoV-2 infected subjects

Asymptomatic subjects were part of the UNICORN project [33] and serum samples of 25 subjects were kindly provided for the present study. Their median age was 45.0 years (IQR 36.0–60.0), 8 were males and 17 females (Table 4). Twenty-one (21) subjects had the

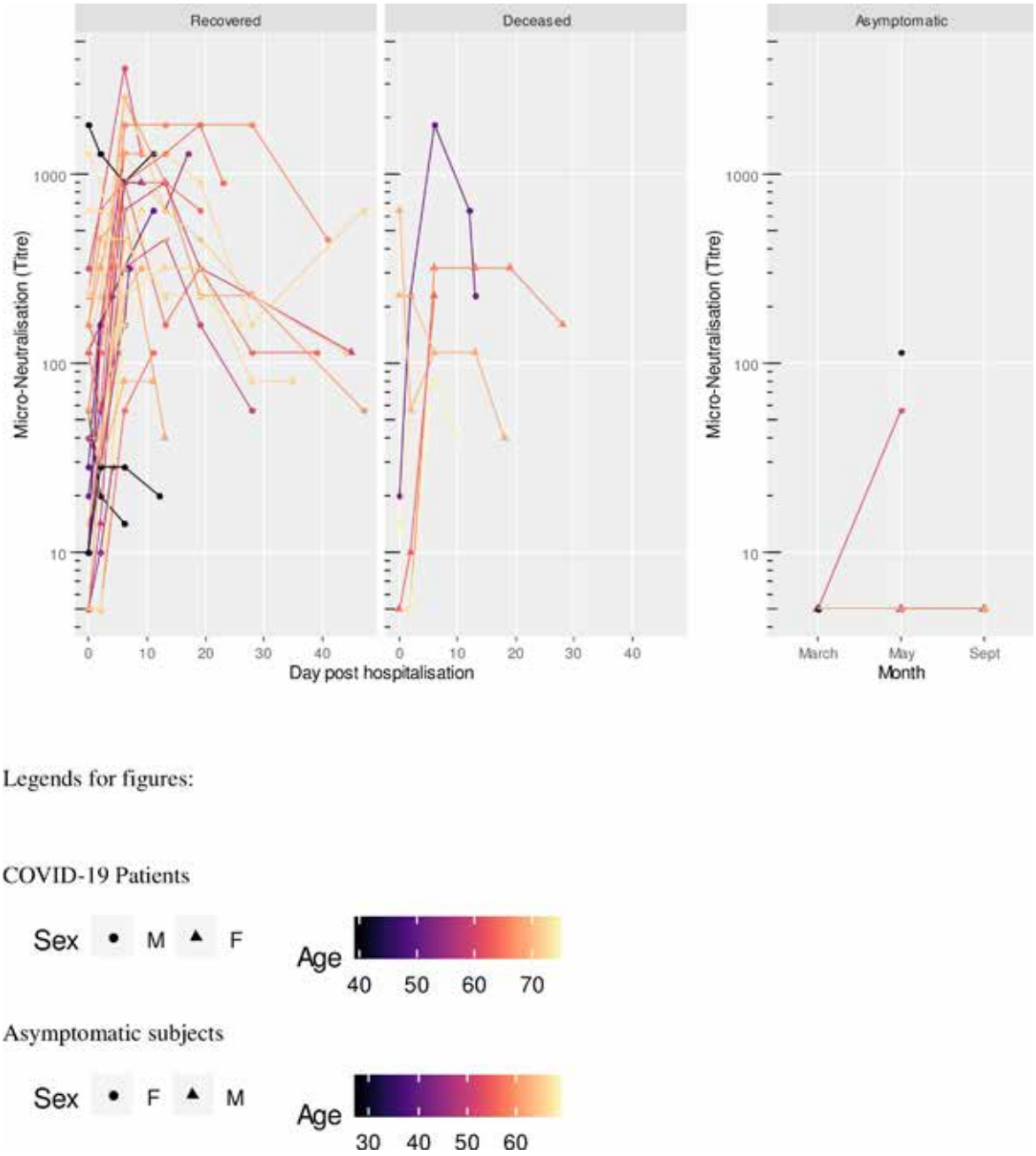

Fig 5. Neutralizing antibody (NAb) titres in COVID-19 patients (recovered and deceased) and asymptomatic subjects.

https://doi.org/10.1371/journal.pone.0253977.g005

rhino-pharyngeal swab positive to SARS-CoV-2 in March 2020 and a blood draw at the same time, 19 out of the 21 subjects had a second blood draw in May, and 14 of them a third blood draw in September. Four (4) subjects had the rhino-pharyngeal swab positive in May and a blood draw at the same time, of whom 1 subject had a second blood draw in September. Asymptomatic subjects did not receive any medication during the study period that may have interfered with antibody response. Out of 25 asymptomatic subjects, 16 (64.0%) were negative to any antibody at any time point. Nine (9) subjects (36.0%) had at least one detectable antibody type at least at one time point. At the first time point, 6 subjects (24.0%)

Table 2. Comparison of immune responses in recovered versus deceased COVID-19 patients.

		Recovered		Deceased			
Antibody	*Day*	*N*	*GMT (95% CI)*	*N*	*GMT (95% CI)*	*Ratio D/R*	*P-value*
S1 IgM	Baseline	35	19.6 (0.5 to 718.5)	7	5.0 (0.0 to 12159.3)	0.25 (0.01 to 4.89)	0.308
	Day 2	35	46.9 (3.0 to 732.2)	7	17.4 (0.0 to 9381.0)	0.37 (0.03 to 4.03)	0.356
	Day 6	31	126.7 (16.9 to 951.6)	6	146.4 (34.5 to 621.4)	1.16 (0.61 to 2.17)	0.627
	Day 12–14	18	111.5 (9.7 to 1284.4)	3	177.7 (29.9 to 1057.1)	1.59 (0.70 to 3.63)	0.232
	Day 18–20	12	107.3 (15.6 to 737.9)	2	119.4 (1.7 to 8251.2)	1.00 (1.00 to 1.00)	
	Day 27–30	8	64.4 (5.3 to 788.3)	1	79.2 (0.0 to 0.0)	1.00 (1.00 to 1.00)	
S1 IgA	Baseline	35	17.8 (0.6 to 497.5)	7	6.8 (0.0 to 21390.7)	0.38 (0.02 to 8.03)	0.473
	Day 2	35	42.9 (3.2 to 571.6)	7	34.6 (0.5 to 2510.1)	0.81 (0.16 to 4.13)	0.768
	Day 6	31	96.4 (14.1 to 659.6)	6	118.3 (16.4 to 854.9)	1.23 (0.54 to 2.78)	0.581
	Day 12–14	18	100.2 (15.5 to 646.2)	3	187.0 (10.0 to 3493.1)	1.87 (0.48 to 7.23)	0.249
	Day 18–20	12	108.0 (38.2 to 305.2)	2	95.8 (0.0 to 10573636.2)	1.00 (1.00 to 1.00)	
	Day 27–30	8	79.7 (13.6 to 465.8)	1	206.7 (0.0 to 0.0)	1.00 (1.00 to 1.00)	
S1 IgG	Baseline	35	16.8 (0.1 to 1966.3)	7	6.2 (0.0 to 21044.6)	0.37 (0.02 to 8.18)	0.476
	Day 2	35	66.3 (2.2 to 1956.6)	7	33.5 (0.0 to 147927.2)	0.50 (0.02 to 12.13)	0.623
	Day 6	31	355.8 (90.2 to 1403.1)	6	403.3 (212.0 to 767.1)	1.13 (0.82 to 1.57)	0.436
	Day 12–14	18	397.6 (115.7 to 1366.9)	3	392.4 (65.8 to 2339.2)	0.99 (0.44 to 2.22)	0.964
	Day 18–20	12	408.9 (160.9 to 1038.9)	2	344.5 (0.4 to 335188.3)	1.00 (1.00 to 1.00)	
	Day 27–30	8	202.7 (151.6 to 271.0)	1	220.8 (0.0 to 0.0)	1.00 (1.00 to 1.00)	
NP IgG	Baseline	35	18.1 (0.5 to 647.9)	7	10.8 (0.0 to 2898.3)	0.60 (0.07 to 5.03)	0.588
	Day 2	35	70.3 (2.0 to 2416.5)	7	71.7 (0.1 to 68291.3)	1.02 (0.08 to 13.77)	0.987
	Day 6	31	411.9 (32.3 to 5248.2)	6	756.0 (246.1 to 2323.1)	1.84 (1.02 to 3.32)	0.044
	Day 12–14	18	466.7 (30.1 to 7248.5)	3	725.4 (24.0 to 21884.1)	1.55 (0.34 to 7.06)	0.467
	Day 18–20	12	371.8 (59.2 to 2333.6)	2	550.5 (0.0 to 6914416.1)	1.00 (1.00 to 1.00)	
	Day 27–30	8	171.3 (43.6 to 672.3)	1	262.0 (0.0 to 0.0)	1.00 (1.00 to 1.00)	
NAb	Baseline	35	40.8 (1.3 to 1296.4)	7	24.4 (0.2 to 3093.8)	0.60 (0.09 to 3.81)	0.539
	Day 2	35	75.4 (3.2 to 1754.7)	7	32.8 (0.6 to 1907.7)	0.44 (0.09 to 2.07)	0.255
	Day 6	31	427.9 (29.0 to 6321.5)	6	226.3 (12.1 to 4228.2)	0.53 (0.16 to 1.77)	0.257
	Day 12–14	18	373.3 (27.5 to 5071.8)	3	285.1 (6.7 to 12155.4)	0.76 (0.14 to 4.21)	0.670
	Day 18–20	12	508.0 (79.9 to 3229.0)	2	113.1 (0.0 to 14707762061.6)	1.00 (1.00 to 1.00)	
	Day 27–30	8	190.3 (16.0 to 2267.5)	1	160.0 (0.0 to 0.0)	1.00 (1.00 to 1.00)	

ELISA titres are expressed as U/ml.

NAb, neutralizing antibody.

https://doi.org/10.1371/journal.pone.0253977.t002

had positive S1 IgG, of whom 2 also had S1 IgA and NP IgG, 1 subject also had S1 IgM, S1 IgA and NP IgG, and 1 subject had S1 IgA, NP IgG and positive neutralizing antibodies. Three (3) subjects, who were negative at any antibody at the first time point, had antibodies at one of the subsequent time points. One (1) of these subjects was positive to all antibody assays at the second time point including to neutralizing antibodies. The other 2 subjects had S1 IgA, S1 IgG and NP IgG at the third time point. One subject was positive to all ELISA antibodies (S1 IgM, S1 IgA, S1 IgG, and NP IgG) at the first time point, negative at the second time point, and positive again only to S1 IgG at the third time point. Detectable neutralizing antibodies were found only in 2 subjects (8.0%): in one subject at the first and only time point available, and in the other one at the second time point, as the third time point was not available. Both subjects were positive also to S1 IgA, S1 IgG, and NP IgG, and only the first subject was positive to S1 IgM.

Table 3. Seroconversion in COVID-19 patients according to outcome.

		Recovered		*Deceased*		
Antibody	***Day***	***SC Yes***	***SC No***	***SC Yes***	***SC No***	***P-value***
S1 IgM	Day 2	6	29	4	3	0.043
	Day 6	19	12	4	2	1.000
	Day 12–14	11	7	2	1	1.000
	Day 18–20	7	5	1	1	1.000
	Day 27–30	4	4	1	0	1.000
S1 IgA	Day 2	8	27	3	4	0.353
	Day 6	20	11	4	2	1.000
	Day 12–14	12	6	2	1	1.000
	Day 18–20	8	4	1	1	1.000
	Day 27–30	5	3	1	0	1.000
S1 IgG	Day 2	11	24	5	2	0.085
	Day 6	23	8	4	2	0.653
	Day 12–14	13	5	2	1	1.000
	Day 18–20	9	3	1	1	0.505
	Day 27–30	4	4	1	0	1.000
NP IgG	Day 2	16	19	6	1	0.096
	Day 6	24	7	5	1	1.000
	Day 12–14	14	4	2	1	1.000
	Day 18–20	9	3	1	1	0.505
	Day 27–30	7	1	1	0	1.000
NAb	Day 2	5	30	1	6	1.000
	Day 6	22	9	4	2	1.000
	Day 12–14	13	5	2	1	1.000
	Day 18–20	9	3	1	1	0.505
	Day 27–30	6	2	1	0	1.000

Seroconversion (SC) was calculated as 4-fold increase in titre compared to baseline.
NAb, neutralizing antibody.

https://doi.org/10.1371/journal.pone.0253977.t003

Asymptomatic subjects with positive antibody levels in any of the assays had titers well below the level found in patients as shown in Figs 1–5 and Table 5.

Discussion

In this study we primarily evaluated the time course of the antibody response to different antigens of SARS-CoV-2 (IgG, IgM, and IgA against S1, IgG against NP, and neutralizing antibodies) in COVID-19 patients admitted to hospital for interstitial pneumonia during the first epidemic wave in March and April 2020 in Italy. No significant difference in titers was observed in any of the S1 antibody class at any time point between patients who survived and who did not survive.

The only significant difference was the higher S1 IgM seroconversion rate observed in the deceased group that may suggest an early admission to hospital after infection. In other similar studies early antibody response to S1 IgA or IgM or difference in the magnitude of the immune response to SARS-CoV-2 infection was a predictor of disease severity or progression or outcome [34–37]. In this study, IgG antibody titers against NP at day 6 were significantly higher in the deceased group, as reported in other studies where an early response to NP during the first 15 days after disease onset was predictive of fatal outcome [34, 36]. No difference

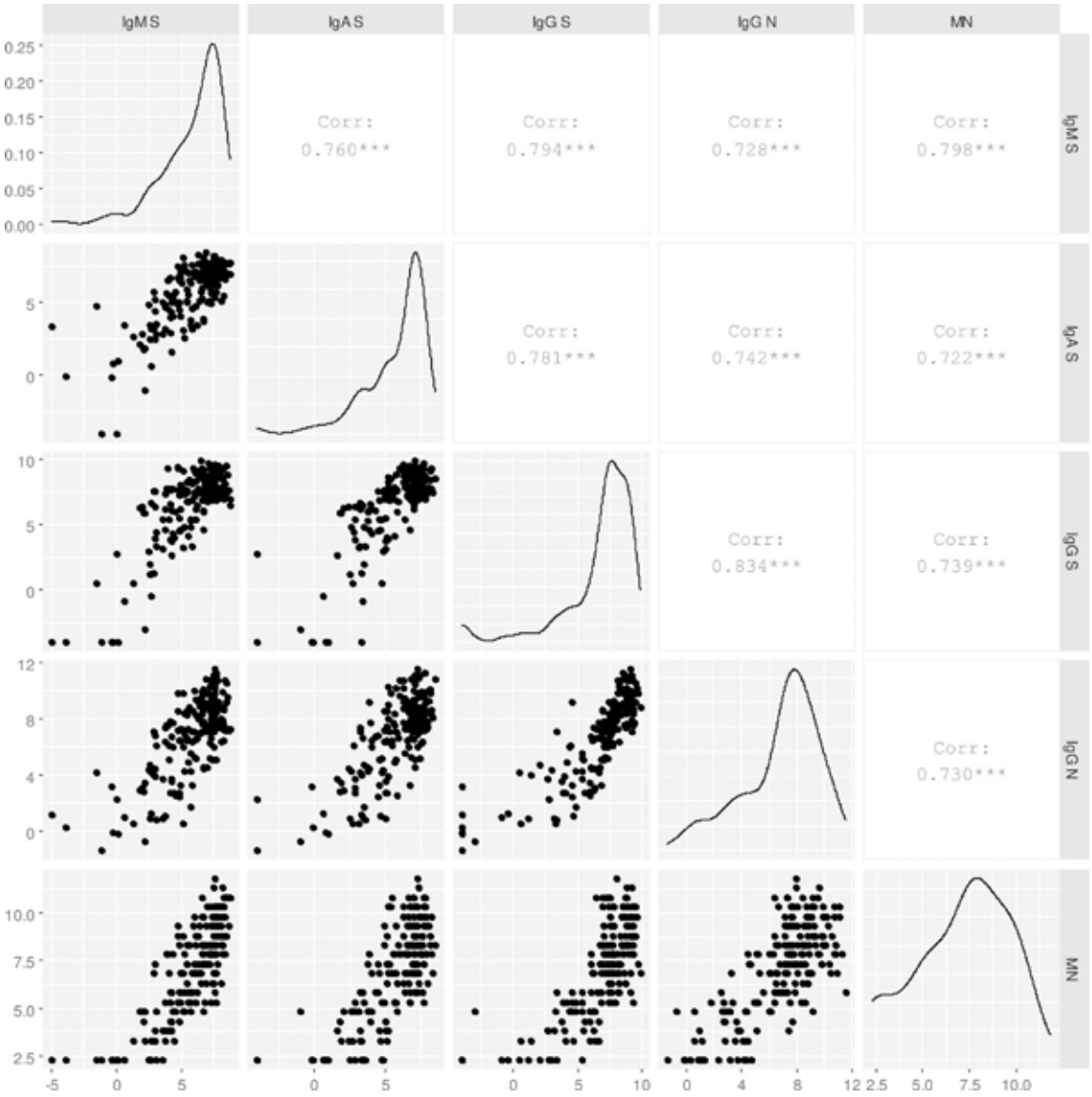

Fig 6. Correlations between antibody for COVID-19 patients. Titres are shown as log-2 transformed.

https://doi.org/10.1371/journal.pone.0253977.g006

was observed for neutralizing antibodies between the recovered and deceased patients as, on the contrary, reported in other studies where neutralizing antibodies were significantly higher in patients who required ICU or died [36]. One possible explanation for the similar immune

Table 4. Baseline characteristics of SARS-CoV-2 asymptomatic subjects. Median (IQR).

Parameter	*Statistics*
Sex	8 M / 17 F
Smoke	14 never, 5 stopped, 5 active
Age	45.0 (36.0 to 60.0)
BMI	22.8 (21.5 to 24.6)

BMI, Body Mass Index.

https://doi.org/10.1371/journal.pone.0253977.t004

Table 5. Comparison of baseline immune responses for recovered or deceased versus asymptomatic controls.

Antibody	Recovered/ Asymptomatic	P value	Deceased / Asymptomatic	P value
S1 IgM	286 (111 to 734)	1.42E-15	73 (4 to 1448)	0.0111
S1 IgA	172 (71 to 422)	6.05E-15	65 (3 to 1351)	0.0145
S1 IgG	96 (27 to 338)	4.86e- 9	36 (2 to 798)	0.0295
NP IgG	7.3 (3.7 to 14.3)	3.22e- 7	4.3 (0.5 to 36.3)	0.142
NAb	8.2 (4.6 to 14.6)	1.88e- 8	4.9 (0.8 to 30.5)	0.0785

https://doi.org/10.1371/journal.pone.0253977.t005

response observed in this study in both survived and deceased patients can be the fact that at admission COVID-19 patients had similar clinical and demographic characteristics. In addition, other factors may contribute to the specific immune response against SARS-CoV-2 infection that need to be considered, as the cellular-mediated immunity that may play a role in protection and disease progression.

The kinetics of the antibody response showed an increase starting from day 2 and reaching the peak between days 6 and 18–20. At day 27–30, a decline in titers was observed for any of the antibody classes. In other studies, the antibody kinetic in COVID-19 patients showed the peak at the 4^{th} and 5^{th} week after disease onset, followed by antibody decay starting at the 6^{th} week [37, 38]. This observation differs from our findings most likely due to the fact that our study period started at hospital admission when the severity of the disease was already in an advanced stage.

In this study, almost two-thirds of asymptomatic subjects were negative at any time point for any antibody class, including neutralizing antibodies. Among the few subjects with detectable antibodies, all were positive to S1 IgG, and, none of these subjects was positive to any of the other antibody classes if not positive to S1 IgG. This is difficult to explain. It may be due to the fact that the S protein is deemed the immunodominant antigen of SARS-CoV-2. In accordance with a similar study, antibody titres in asymptomatic subjects were sensibly lower as compared to COVID-19 patients [39]. It has been reported that asymptomatic subjects have a low viral load in the nasopharynges as assessed by RT-PCR, and most likely a lack or a defective viral replication that induces a weak or any antibody response [40]. Although memory B and T cells are likely to be primed in SARS-CoV-2 infected subjects with undetectable antibodies, the question of whether they should be vaccinated is critical now that effective vaccines are available against COVID-19.In this study, a good correlation between S1 and NP protein-based ELISA and the VN assay was observed in COVID-19 patients, although less evident in asymptomatic subjects since only 2 of them had detectable neutralizing antibodies in addition to other ELISA antibody classes. It is acknowledged that antibodies with neutralizing activity should retain enough avidity or have a sufficient concentration or both [41, 42]. In fact, ELISA detects antibody against individual antigens that may not retain neutralizing properties if not in quantity. This may explain the difference in the correlation between ELISA-based assays and neutralizing antibodies in COVID-19 patients and asymptomatic subjects observed in this study.

This study has some limitations. The sample size was small due to the availability of subjects with severe COVID-19 disease who had a sufficient number of blood samples for measuring the time course of antibody for at least one month. This may introduce a bias. However, the ratio between deceased and recovered patients (7 out of 42, 16,6%) falls in the acceptable range (from 5.7% to 30.4%) described in the literature [18, 43]. The retrospective nature of the study and the collection of COVID-19 samples carried out in a single center introduce some limitations. The findings from this study do not allow to predict the kinetics of the antibody decay over time in patients who recovered from COVID-19, and who may be susceptible to reinfection over time, since no follow-up samples after discharge were available.

In conclusion, the results of this study show that COVID-19 patients produce a strong antibody response to SARS-CoV-2 with high correlation between different viral antigens (S1 and NP) and among antibody classes (IgA, IgG, and IgM and neutralizing antibodies). The peak is reached by three weeks from hospital admission followed by a sharp decrease. On the contrary, only few asymptomatic subjects develop antibodies at detectable levels, and significantly lower compared to COVID-19 patients. Currently, no correlates of protection are established for COVID-19. As cases of reinfection are reported [44–47] and since neutralizing antibodies are rarely produced in asymptomatic subjects, the findings of this study support the current recommendation to vaccinate subjects with a previous SARS-CoV-2 infection as well as those who recovered from COVID-1.

Acknowledgments

This study was supported by the European Virus Archive goes Global (EVAg) project, which has received funding from the European Union's Horizon 2020 research and innovation programme under grant agreement No 653316.

The UNICORN population was recruited thanks to the Funding Action "Ricerche Emergenza coronavirus", University of Milan, 2020.

The authors thank Linda Benincasa for technical support.

Author Contributions

Conceptualization: Simonetta Viviani, Claudia M. Trombetta.

Data curation: Serena Marchi, Antonella Ruello, Emilio Bombardieri, Valentina Bollati, Gregorio P. Milani.

Formal analysis: Edmond J. Remarque.

Funding acquisition: Simonetta Viviani, Claudia M. Trombetta.

Investigation: Serena Marchi, Claudia M. Trombetta.

Methodology: Alessandro Manenti, Giulia Lapini, Annunziata Rebuffat, Emanuele Montomoli.

Project administration: Claudia M. Trombetta.

Resources: Antonella Ruello, Emilio Bombardieri, Valentina Bollati, Gregorio P. Milani.

Writing – original draft: Simonetta Viviani.

Writing – review & editing: Serena Marchi, Edmond J. Remarque, Antonella Ruello, Emilio Bombardieri, Valentina Bollati, Gregorio P. Milani, Alessandro Manenti, Giulia Lapini, Annunziata Rebuffat, Emanuele Montomoli, Claudia M. Trombetta.

References

1. World Health Organization. WHO Director-General's opening remarks at the media briefing on COVID-19–11 March 2020. 2020; Available from: https://www.who.int/dg/speeches/detail/who-director-general-s-opening-remarks-at-the-media-briefing-on-covid-19—11-march-2020.
2. Lu R., Zhao X., Li J., Niu P., Yang B., Wu H., et al., Genomic characterisation and epidemiology of 2019 novel coronavirus: implications for virus origins and receptor binding. Lancet, 2020. 395(10224): p. 565–574. https://doi.org/10.1016/S0140-6736(20)30251-8 PMID: 32007145
3. Tay M.Z., Poh C.M., Renia L., MacAry P.A., and Ng L.F.P., The trinity of COVID-19: immunity, inflammation and intervention. Nat Rev Immunol, 2020. 20(6): p. 363–374. https://doi.org/10.1038/s41577-020-0311-8 PMID: 32346093

4. Amanat F. and Krammer F., SARS-CoV-2 Vaccines: Status Report. Immunity, 2020. 52(4): p. 583–589. https://doi.org/10.1016/j.immuni.2020.03.007 PMID: 32259480

5. Chan J.F., Yuan S., Kok K.H., To K.K., Chu H., Yang J., et al., A familial cluster of pneumonia associated with the 2019 novel coronavirus indicating person-to-person transmission: a study of a family cluster. Lancet, 2020. 395(10223): p. 514–523. https://doi.org/10.1016/S0140-6736(20)30154-9 PMID: 31986261

6. Zhu N., Zhang D., Wang W., Li X., Yang B., Song J., et al. China Novel Coronavirus, and T. Research, A Novel Coronavirus from Patients with Pneumonia in China, 2019. N Engl J Med, 2020. 382(8): p. 727–733. https://doi.org/10.1056/NEJMoa2001017 PMID: 31978945

7. World Health Organization. MERS SITUATION UPDATE. 2019 02/16/2021]; Available from: https://applications.emro.who.int/docs/EMRPUB-CSR-241-2019-EN.pdf?ua=1&ua=1&ua=1.

8. Du L.Y., He Y.X., Zhou Y.S., Liu S.W., Zheng B.J., and Jiang S.B., The spike protein of SARS-CoV—a target for vaccine and therapeutic development. Nature Reviews Microbiology, 2009. 7(3): p. 226–236. https://doi.org/10.1038/nrmicro2090 PMID: 19198616

9. Huang C., Wang Y., Li X., Ren L., Zhao J., Hu Y., et al., Clinical features of patients infected with 2019 novel coronavirus in Wuhan, China. Lancet, 2020. 395(10223): p. 497–506. https://doi.org/10.1016/S0140-6736(20)30183-5 PMID: 31986264

10. Jiang S., Hillyer C., and Du L., Neutralizing Antibodies against SARS-CoV-2 and Other Human Coronaviruses: (Trends in Immunology 41, 355–359; 2020). Trends Immunol, 2020. 41(6): p. 545. https://doi.org/10.1016/j.it.2020.04.008 PMID: 32362491

11. Du L., Yang Y., Zhou Y., Lu L., Li F., and Jiang S., MERS-CoV spike protein: a key target for antivirals. Expert Opin Ther Targets, 2017. 21(2): p. 131–143. https://doi.org/10.1080/14728222.2017.1271415 PMID: 27936982

12. Wajnberg A., Amanat F., Firpo A., Altman D.R., Bailey M.J., Mansour M., et al, Robust neutralizing antibodies to SARS-CoV-2 infection persist for months. Science, 2020. https://doi.org/10.1126/science.abd7728 PMID: 33115920

13. Seow J., Graham C., Merrick B., Acors S., Pickering S., Steel K.J.A., et al., Longitudinal observation and decline of neutralizing antibody responses in the three months following SARS-CoV-2 infection in humans. Nat Microbiol, 2020. https://doi.org/10.1038/s41564-020-00813-8 PMID: 33106674

14. Amanat F., Stadlbauer D., Strohmeier S., Nguyen T.H.O., Chromikova V., McMahon M., et al., A serological assay to detect SARS-CoV-2 seroconversion in humans. Nat Med, 2020. 26(7): p. 1033–1036. https://doi.org/10.1038/s41591-020-0913-5 PMID: 32398876

15. To K.K., Tsang O.T., Leung W.S., Tam A.R., Wu T.C., Lung D.C., et al., Temporal profiles of viral load in posterior oropharyngeal saliva samples and serum antibody responses during infection by SARS-CoV-2: an observational cohort study. Lancet Infect Dis, 2020. https://doi.org/10.1016/S1473-3099(20)30196-1 PMID: 32213337

16. Haveri A., Smura T., Kuivanen S., Osterlund P., Hepojoki J., Ikonen N., et al., Serological and molecular findings during SARS-CoV-2 infection: the first case study in Finland, January to February 2020. Euro Surveill, 2020. 25(11). https://doi.org/10.2807/1560-7917.ES.2020.25.11.2000266 PMID: 32209163

17. Long Q.X., Liu B.Z., Deng H.J., Wu G.C., Deng K., Chen Y.K., et al., Antibody responses to SARS-CoV-2 in patients with COVID-19. Nat Med, 2020. 26(6): p. 845–848. https://doi.org/10.1038/s41591-020-0897-1 PMID: 32350462

18. Roltgen K., Powell A.E., Wirz O.F., Stevens B.A., Hogan C.A., Najeeb J., et al., Defining the features and duration of antibody responses to SARS-CoV-2 infection associated with disease severity and outcome. Sci Immunol, 2020. 5(54). https://doi.org/10.1126/sciimmunol.abe0240 PMID: 33288645

19. Heald-Sargent T. and Gallagher T., Ready, set, fuse! The coronavirus spike protein and acquisition of fusion competence. Viruses, 2012. 4(4): p. 557–80. https://doi.org/10.3390/v4040557 PMID: 22590686

20. Manenti A., Maggetti M., Casa E., Martinuzzi D., Torelli A., Trombetta C.M., et al., Evaluation of SARS-CoV-2 neutralizing antibodies using a CPE-based colorimetric live virus micro-neutralization assay in human serum samples. J Med Virol, 2020. 92(10): p. 2096–2104. https://doi.org/10.1002/jmv.25986 PMID: 32383254

21. WHO, Manual for the laboratory diagnosis and virological surveillance of influenza. 2011. p. 1–153.

22. Young B.E., Ong S.W.X., Kalimuddin S., Low J.G., Tan S.Y., Loh J., et al., Epidemiologic Features and Clinical Course of Patients Infected With SARS-CoV-2 in Singapore. JAMA, 2020. 323(15): p. 1488–1494. https://doi.org/10.1001/jama.2020.3204 PMID: 32125362

23. World Health Organization. WHO Coronavirus Disease (COVID-19) Dashboard. 2021 12/13/2020]; Available from: https://covid19.who.int/.

24. Food and Agriculture Organization of the United Nations. Impact of COVID-19 on people's livelihoods, their health and our food systems. 2020 02/1672021]; Available from: http://www.fao.org/news/story/en/item/1313598/icode/.

25. Apolone G., Montomoli E., Manenti A., Boeri M., Sabia F., Hyseni I., et al., Unexpected detection of SARS-CoV-2 antibodies in the prepandemic period in Italy. Tumori, 2020: p. 300891620974755. https://doi.org/10.1177/0300891620974755 PMID: 33176598

26. Deslandes A., Berti V., Tandjaoui-Lambotte Y., Alloui C., Carbonnelle E., Zahar J.R., et al., SARS-CoV-2 was already spreading in France in late December 2019. Int J Antimicrob Agents, 2020. 55(6): p. 106006. https://doi.org/10.1016/j.ijantimicag.2020.106006 PMID: 32371096

27. Amendola A., Bianchi S., Gori M., Colzani D., Canuti M., Borghi E., et al., Evidence of SARS-CoV-2 RNA in an Oropharyngeal Swab Specimen, Milan, Italy, Early December 2019. Emerg Infect Dis, 2021. 27(2): p. 648–650. https://doi.org/10.3201/eid2702.204632 PMID: 33292923

28. Gianotti R., Barberis M., Fellegara G., Galvan-Casas C., and Gianotti E., COVID-19-related dermatosis in November 2019: could this case be Italy's patient zero? Br J Dermatol, 2021. https://doi.org/10.1111/bjd.19804 PMID: 33410129

29. Istituto Superiore di Sanità, Caratteristiche dei pazienti deceduti positivi all'infezione da SARS-CoV-2 in Italia. 2020.

30. Onder G., Rezza G., and Brusaferro S., Case-Fatality Rate and Characteristics of Patients Dying in Relation to COVID-19 in Italy. JAMA, 2020. 323(18): p. 1775–1776. https://doi.org/10.1001/jama.2020.4683 PMID: 32203977

31. Istituto Superiore di Sanità, EPIDEMIA COVID-19. Aggiornamento nazionale 2 Aprile 2020. 2020.

32. Lipsitch M., Swerdlow D.L., and Finelli L., Defining the Epidemiology of Covid-19—Studies Needed. N Engl J Med, 2020. 382(13): p. 1194–1196. https://doi.org/10.1056/NEJMp2002125 PMID: 32074416

33. Milani G.P., Dioni L., Favero C., Cantone L., Macchi C., Delbue S., et al., Serological follow-up of SARS-CoV-2 asymptomatic subjects. Sci Rep, 2020. 10(1): p. 20048. https://doi.org/10.1038/s41598-020-77125-8 PMID: 33208819

34. Atyeo C., Fischinger S., Zohar T., Slein M.D., Burke J., Loos C., et al., Distinct Early Serological Signatures Track with SARS-CoV-2 Survival. Immunity, 2020. 53(3): p. 524–+. https://doi.org/10.1016/j.immuni.2020.07.020 PMID: 32783920

35. Wang Y.Q., Zhang L., Sang L., Ye F., Ruan S.C., Zhong B., et al., Kinetics of viral load and antibody response in relation to COVID-19 severity. Journal of Clinical Investigation, 2020. 130(10): p. 5235–5244. https://doi.org/10.1172/JCI138759 PMID: 32634129

36. Hashem A.M., Algaissi A., Almahboub S.A., Alfaleh M.A., Abujamel T.S., Alamri S.S., et al., Early Humoral Response Correlates with Disease Severity and Outcomes in COVID-19 Patients. Viruses, 2020. 12(12). https://doi.org/10.3390/v12121390 PMID: 33291713

37. Chen Y., Tong X., Li Y., Gu B., Yan J., Liu Y., et al., A comprehensive, longitudinal analysis of humoral responses specific to four recombinant antigens of SARS-CoV-2 in severe and non-severe COVID-19 patients. PLoS Pathog, 2020. 16(9): p. e1008796. https://doi.org/10.1371/journal.ppat.1008796 PMID: 32913364

38. Okba N.M.A., Muller M.A., Li W., Wang C., GeurtsvanKessel C.H., Corman V.M., et al., Severe Acute Respiratory Syndrome Coronavirus 2-Specific Antibody Responses in Coronavirus Disease Patients. Emerg Infect Dis, 2020. 26(7): p. 1478–1488. https://doi.org/10.3201/eid2607.200841 PMID: 32267220

39. Algaissi A., Alfaleh M.A., Hala S., Abujamel T.S., Alamri S.S., Almahboub S.A., et al., SARS-CoV-2 S1 and N-based serological assays reveal rapid seroconversion and induction of specific antibody response in COVID-19 patients. Sci Rep, 2020. 10(1): p. 16561. https://doi.org/10.1038/s41598-020-73491-5 PMID: 33024213

40. Röltgen K., Powell A.E., Wirz O.F., Stevens B.A., Hogan C.A., Najeeb J., et al., Defining the features and duration of antibody responses to SARS-CoV-2 infection associated with disease severity and outcome. ScienceImmunology, 2020, p. 1–19. https://doi.org/10.1126/sciimmunol.abe0240 PMID: 33288645

41. Piccoli L., Park Y.J., Tortorici M.A., Czudnochowski N., Walls A.C., Beltramello M., et al., Mapping Neutralizing and Immunodominant Sites on the SARS-CoV-2 Spike Receptor-Binding Domain by Structure-Guided High-Resolution Serology. Cell, 2020. 183(4): p. 1024–+. https://doi.org/10.1016/j.cell.2020.09.037 PMID: 32991844

42. Burton D.R., Williamson R.A., and Parren P.W., Antibody and virus: binding and neutralization. Virology, 2000. 270(1): p. 1–3. https://doi.org/10.1006/viro.2000.0239 PMID: 10772973

43. Yao T., Gao Y., Cui Q., Peng B., Chen Y., Li J.,et al., Clinical characteristics of a group of deaths with COVID-19 pneumonia in Wuhan, China: a retrospective case series. BMC Infect Dis, 2020. 20(1): p. 695. https://doi.org/10.1186/s12879-020-05423-7 PMID: 32962639

44. Iwasaki A., What reinfections mean for COVID-19. Lancet, 2020. 21: p. 3–5. https://doi.org/10.1016/S1473-3099(20)30783-0 PMID: 33058796

45. Tillett R.L., Sevinsky J.R., Hartley P.D., Kerwin H., Crawford N., Gorzalski A., et al., Genomic evidence for reinfection with SARS-CoV-2: a case study. Lancet Infect Dis, 2021. 21(1): p. 52–58. https://doi.org/10.1016/S1473-3099(20)30764-7 PMID: 33058797

46. Hansen C.H., Michlmayr D., and et al., Assessment of protection against reinfection with SARS-CoV-2 among 4 million PCR-tested individuals in Denmark in 2020: a population-level observational study. Lancet, 2021. 397: p. 1204–12. https://doi.org/10.1016/S0140-6736(21)00575-4 PMID: 33743221

47. Abu-Raddad L.J. and Chemaitelly H., SARS-CoV-2 reinfection in a cohort of 43,000 antibody-positive individuals followed for up to 35 weeks. MedRxiv, 2021.

Since January 2020 Elsevier has created a COVID-19 resource centre with free information in English and Mandarin on the novel coronavirus COVID-19. The COVID-19 resource centre is hosted on Elsevier Connect, the company's public news and information website.

Elsevier hereby grants permission to make all its COVID-19-related research that is available on the COVID-19 resource centre - including this research content - immediately available in PubMed Central and other publicly funded repositories, such as the WHO COVID database with rights for unrestricted research re-use and analyses in any form or by any means with acknowledgement of the original source. These permissions are granted for free by Elsevier for as long as the COVID-19 resource centre remains active.

Cell

Extremely potent human monoclonal antibodies from COVID-19 convalescent patients

Graphical abstract

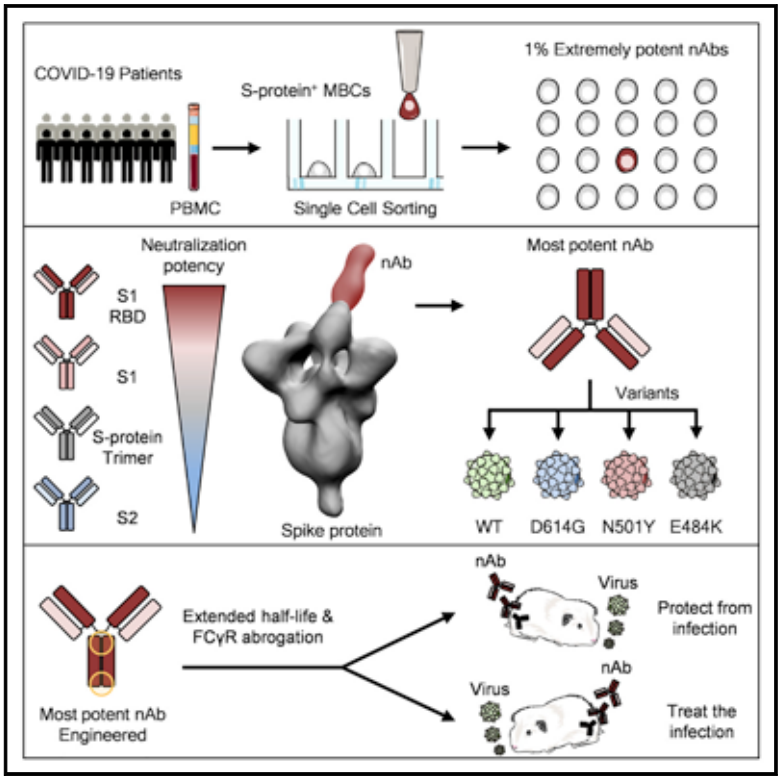

Highlights

- Human memory B cells encoding extremely potent neutralizing antibodies are rare
- Most potent antibodies recognize the tip of the spike receptor-binding domain
- Selected neutralizing antibody neutralizes SARS-CoV-2 emerging variants
- Potent antibody prevents and treats hamster infection without Fc-functions

Authors

Emanuele Andreano, Emanuele Nicastri, Ida Paciello, ..., Claudia Sala, Giuseppe Ippolito, Rino Rappuoli

Correspondence

rino.r.rappuoli@gsk.com

In brief

Extremely potent neutralizing human monoclonal antibodies, though rare, are isolated from COVID-19 convalescent patients and suitable for prophylactic and therapeutic interventions of wild-type SARS-CoV-2 as well as emerging variants.

Andreano et al., 2021, Cell *184*, 1–15
April 1, 2021
https://doi.org/10.1016/j.cell.2021.02.035

Please cite this article in press as: Andreano et al., Extremely potent human monoclonal antibodies from COVID-19 convalescent patients, Cell (2021), https://doi.org/10.1016/j.cell.2021.02.035

Cell

CellPress

Article

Extremely potent human monoclonal antibodies from COVID-19 convalescent patients

Emanuele Andreano,[1,17] Emanuele Nicastri,[4,17] Ida Paciello,[1] Piero Pileri,[1] Noemi Manganaro,[1] Giulia Piccini,[2] Alessandro Manenti,[2,3] Elisa Pantano,[1] Anna Kabanova,[1,11] Marco Troisi,[1,9] Fabiola Vacca,[1,9] Dario Cardamone,[1,10] Concetta De Santi,[1] Jonathan L. Torres,[16] Gabriel Ozorowski,[16] Linda Benincasa,[3] Hyesun Jang,[13] Cecilia Di Genova,[15] Lorenzo Depau,[12] Jlenia Brunetti,[12] Chiara Agrati,[4] Maria Rosaria Capobianchi,[4] Concetta Castilletti,[4] Arianna Emiliozzi,[5,6] Massimiliano Fabbiani,[6] Francesca Montagnani,[5,6] Luisa Bracci,[12] Giuseppe Sautto,[13] Ted M. Ross,[13,14] Emanuele Montomoli,[2,3,7] Nigel Temperton,[15] Andrew B. Ward,[16] Claudia Sala,[1] Giuseppe Ippolito,[4] and Rino Rappuoli[1,8,18,*]

[1]Monoclonal Antibody Discovery (MAD) Lab, Fondazione Toscana Life Sciences, Siena, Italy
[2]VisMederi S.r.l, Siena, Italy
[3]VisMederi Research S.r.l., Siena, Italy
[4]National Institute for Infectious Diseases Lazzaro Spallanzani, IRCCS, Rome, Italy
[5]Department of Medical Biotechnologies, University of Siena, Siena, Italy
[6]Department of Medical Sciences, Infectious and Tropical Diseases Unit, University Hospital of Siena, Siena, Italy
[7]Department of Molecular and Developmental Medicine, University of Siena, Siena, Italy
[8]Faculty of Medicine, Imperial College, London, UK
[9]Department of Biotechnology, Chemistry and Pharmacy, University of Siena, Siena, Italy
[10]University of Turin, Turin, Italy
[11]Tumour Immunology Unit, Fondazione Toscana Life Sciences, Siena, Italy
[12]MedBiotech Hub and Competence Center, Department of Medical Biotechnologies, University of Siena, Siena, Italy
[13]Center for Vaccines and Immunology, University of Georgia, Athens, GA 30602, USA
[14]Department of Infectious Diseases, University of Georgia, Athens, GA 30602, USA
[15]Viral Pseudotype Unit, Medway School of Pharmacy, University of Kent, Chatham, UK
[16]Department of Integrative Structural and Computational Biology, The Scripps Research Institute, La Jolla, CA 92037, USA
[17]These authors contributed equally
[18]Lead contact
*Correspondence: rino.r.rappuoli@gsk.com
https://doi.org/10.1016/j.cell.2021.02.035

SUMMARY

Human monoclonal antibodies are safe, preventive, and therapeutic tools that can be rapidly developed to help restore the massive health and economic disruption caused by the coronavirus disease 2019 (COVID-19) pandemic. By single-cell sorting 4,277 SARS-CoV-2 spike protein-specific memory B cells from 14 COVID-19 survivors, 453 neutralizing antibodies were identified. The most potent neutralizing antibodies recognized the spike protein receptor-binding domain, followed in potency by antibodies that recognize the S1 domain, the spike protein trimer, and the S2 subunit. Only 1.4% of them neutralized the authentic virus with a potency of 1–10 ng/mL. The most potent monoclonal antibody, engineered to reduce the risk of antibody-dependent enhancement and prolong half-life, neutralized the authentic wild-type virus and emerging variants containing D614G, E484K, and N501Y substitutions. Prophylactic and therapeutic efficacy in the hamster model was observed at 0.25 and 4 mg/kg respectively in absence of Fc functions.

INTRODUCTION

The impact of the severe acute respiratory syndrome coronavirus 2 (SARS-CoV-2) pandemic, with more than 100 million cases, over 2 million deaths, an estimated cost of 16 trillion US dollars to the USA economy (Cutler and Summers, 2020), and 45 million people filing unemployment in the United States alone, is unprecedented (Aratani, 2020).

Vaccines and drugs against SARS-CoV-2 have recently received emergency use authorization (EUA) by the Food and Drug Administration (FDA) for prevention and treatment of coronavirus disease 2019 (COVID-19) (FDA, 2021, 2020).

In spite of this, it is predictable that waves of infection will continue to spread globally, and it is likely to be followed by additional waves over the next few years. This is supported by the emergence of new SARS-CoV-2 variants in the United Kingdom, South Africa, Brazil, and Japan (CDC, 2021).

It is therefore imperative to quickly develop, in parallel to vaccines, therapeutic tools against SARS-CoV-2 and its variants. Among the many therapeutic options available, human

Please cite this article in press as: Andreano et al., Extremely potent human monoclonal antibodies from COVID-19 convalescent patients, Cell (2021), https://doi.org/10.1016/j.cell.2021.02.035

monoclonal antibodies (mAbs) can be developed in the shortest time frame. In fact, the extensive clinical experience with the safety of more than 50 commercially available mAbs approved to treat cancer, inflammatory, and autoimmune disorders provides high confidence of their safety (Wellcome and IAVI, 2020). These advantages, combined with the urgency of the SARS-CoV-2 pandemic, support and justify an accelerated regulatory pathway. In addition, the long industrial experience in developing and manufacturing mAbs decreases risks usually associated with technical development of investigational products. Finally, the incredible technical progress in this field allows shortening of conventional timelines and enables a path from discovery to proof-of-concept trials within 5–6 months (Kelley, 2020). A key example is the Ebola case, where mAbs were developed faster than vaccines or other drugs (Kupferschmidt, 2019), becoming the first therapeutic intervention recommended by the World Health Organization (WHO) and approved by the FDA (Mullard, 2020).

During the first months of this pandemic, many groups have been active in isolating and characterizing human monoclonal antibodies from COVID-19 convalescent patients or from humanized mice, and some of them have been progressing quickly to clinical trials for the prevention and cure of SARS-CoV-2 infection (Shi et al., 2020; Hansen et al., 2020; Hsieh et al., 2020; Pinto et al., 2020; Zost et al., 2020a, 2020b; Rogers et al., 2020, Alsoussi et al., 2020). Few of them are already in phase III clinical trials and reported promising preliminary results. Two of them received the EUA from the FDA (Lilly, 2020; Regeneron, 2020).

All these antibodies neutralize SARS-CoV-2 infection by binding to the spike glycoprotein (S protein), a trimeric class I viral fusion protein that mediates virus entry into host cells by engaging with the human angiotensin-converting enzyme 2 (hACE2) and cellular heparan sulfate as receptors (Clausen et al., 2020). The S protein exists in a metastable pre-fusion conformation and in a stable post-fusion form (Wang et al., 2020; Walls et al., 2020; Schäfer et al., 2020). Each S protein monomer is composed of two distinct regions, the S1 and S2 subunits. The S1 subunit contains the receptor-binding domain (RBD), which is responsible for the interaction with hACE2 and heparan sulfate on host cell membranes triggering the destabilization of the prefusion state of the S protein and consequent transition into the post-fusion conformation. This event results in the entry of the virus particle into the host cell and the onset of infection (Wrapp et al., 2020; Walls et al., 2020; Tay et al., 2020; Zou et al., 2020).

As for other mAbs in the field of infectious diseases (Hooft van Huijsduijnen et al., 2020; Sparrow et al., 2017), the dose of mAbs so far used in clinical trials against SARS-CoV-2 is high, ranging from 500 to 8,000 mgs (NCT04411628; NCT04427501; NCT04441918; NCT04425629; NCT04426695; NCT04452318). The high dose poses two important limits to the application of mAbs in the infectious diseases field. First, the high dosage has cost-associated implications, and it only allows for intravenous delivery, making this therapeutic intervention extremely costly and therefore available almost exclusively in high-income countries. Indeed, the high price of this intervention has been a barrier to the global access of mAbs and their use to other fields such as infectious diseases. A solution would be the development of extremely potent mAbs that can be used at lower dosages leading to cost reductions and that can be delivered via intramuscular or subcutaneous injections. A first example is the respiratory syncytial virus (RSV) case, where a potent mAb has recently shown its therapeutic effect in premature infants after only one intramuscular injection of 50 mg (Griffin et al., 2020).

The second limit of mAbs in the field of infectious diseases is the risk of antibody-dependent enhancement (ADE) of disease, which is usually mediated by the binding of the fragment crystallizable (Fc) region portion of the antibody to Fc gamma receptors (FcγRs) expressed by immune cells (Lee et al., 2020). ADE has been clearly demonstrated in the case of SARS-CoV, RSV, and dengue viruses, and the theoretical risk has been raised in the case of SARS-CoV-2 (Lee et al., 2020; Katzelnick et al., 2017; Arvin et al., 2020).

In this work, we pushed the limits of mAb application to fight infectious diseases by selecting extremely potent antibodies with the aim of using them at low dosage to make them affordable and conveniently delivered by intramuscular injection. In addition, we mitigated the risk of ADE by engineering their Fc region. Despite complete lack of Fc-receptor-binding and Fc-mediated cellular activities, engineered mAbs were able to prevent and treat SARS-CoV-2 infection in golden Syrian hamster at a concentration of 0.25 and 4 mg/kg respectively. These antibodies have the potential to globally extend the access and affordability of this important medical tool.

RESULTS

Isolation and characterization of S protein-specific antibodies from SARS-CoV-2 convalescent patients

To retrieve mAbs specific for SARS-CoV-2 S protein, peripheral blood mononuclear cells (PBMCs) from fourteen COVID-19 convalescent patients enrolled in this study were collected and stained with fluorescently labeled S protein trimer to identify antigen-specific memory B cells (MBCs). Figure 1 summarizes the overall experimental strategy. The gating strategy described in Figure S1A was used to single-cell sort, into 384-well plates, IgG^+ and IgA^+ MBCs binding to the SARS-CoV-2 S protein trimer in its prefusion conformation. The sorting strategy aimed to specifically identify class-switched MBCs ($CD19^+CD27^+IgD^-IgM^-$) to identify only memory B lymphocytes that underwent maturation processes. A total of 4,277 S protein-binding MBCs were successfully retrieved with frequencies ranging from 0.17% to 1.41% (Table S1). Following the sorting procedure, S $protein^+$ MBCs were incubated over a layer of 3T3-CD40L feeder cells in the presence of IL-2 and IL-21 stimuli for 2 weeks to allow natural production of immunoglobulins (Huang et al., 2013). Subsequently, MBC supernatants containing IgG or IgA were tested for their ability to bind either the SARS-CoV-2 S protein trimer in its prefusion conformation or the S protein S1 + S2 subunits (Figure 2A; Figure S2B) by enzyme linked immunosorbent assay (ELISA). A panel of 1,731 mAbs specific for the SARS-CoV-2 S protein were identified showing a broad range of signal intensities (Figure 2A; Table S1).

Please cite this article in press as: Andreano et al., Extremely potent human monoclonal antibodies from COVID-19 convalescent patients, Cell (2021), https://doi.org/10.1016/j.cell.2021.02.035

CellPress

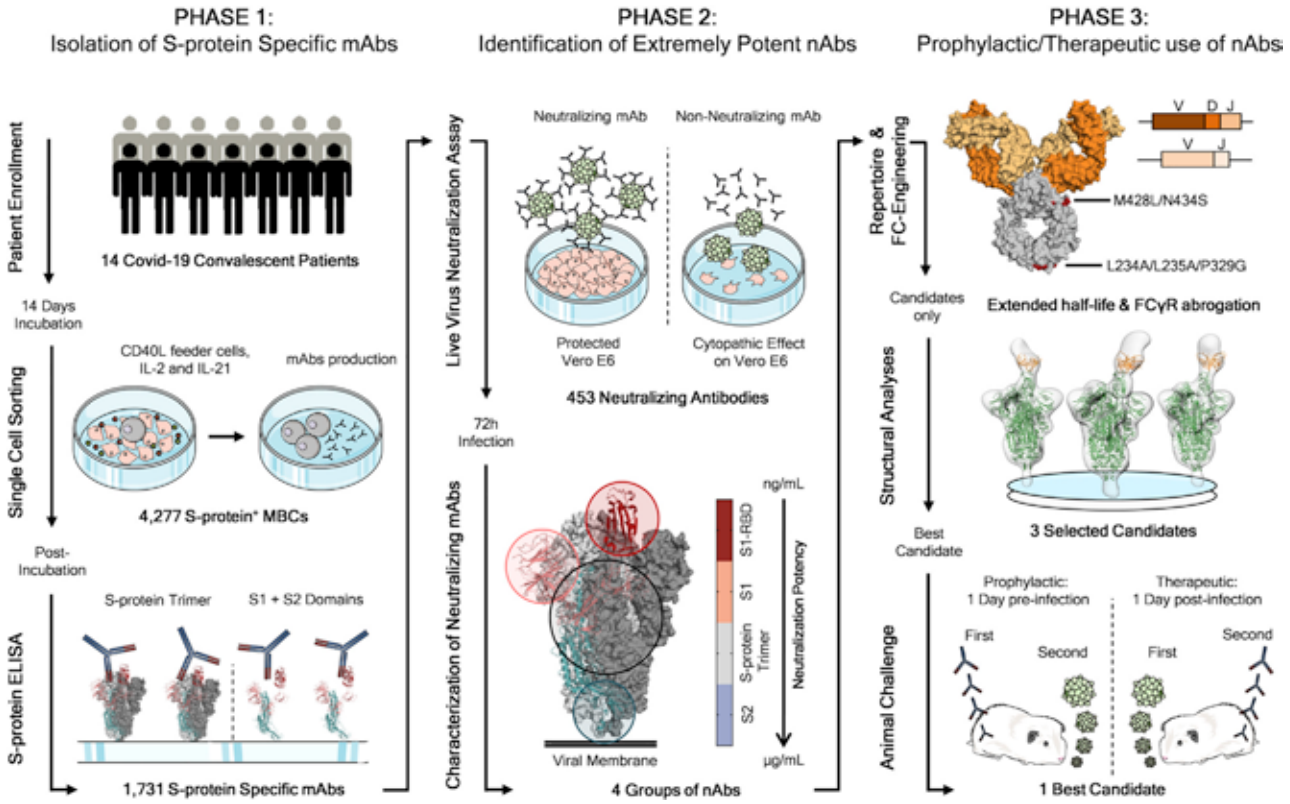

Figure 1. Workflow and timeline for SARS-CoV-2 neutralizing antibodies identification

The overall scheme shows three different phases for the identification of SARS-CoV-2 neutralizing antibodies (nAbs). Phase 1 consisted in the enrolment of COVID-19 patients (n = 14) from which PBMCs were isolated. Memory B cells were single-cell sorted (n = 4,277), and after 2 weeks of incubation, antibodies were screened for their binding specificity against the S protein trimer and S1/S2 domains. Once S protein-specific monoclonal antibodies (mAbs) were identified (n = 1,731) phase 2 started. All specific mAbs were tested *in vitro* to evaluate their neutralization activity against the authentic SARS-CoV-2 virus, and 453 nAbs were identified. nAbs showing different binding profiles on the S protein surface were selected for further functional characterization and to identify different neutralizing regions on the antigen. Phase 3 starts with the characterization of the heavy and light chain sequences of selected mAbs (n = 14) and the engineering of the Fc portion of three most promising candidates. The latter were also selected for structural analyses that allowed the identification of the neutralizing epitopes on the S protein. Finally, the most potent antibody was tested for its prophylactic and therapeutic effect in a golden Syrian hamster model of SARS-CoV-2 infection.

Identification of S protein-specific mAbs able to neutralize SARS-CoV-2

The 1,731 supernatants containing S protein-specific mAbs, were screened *in vitro* for their ability to block the binding of the streptavidin-labeled S protein to Vero E6 cell receptors and for their ability to neutralize authentic SARS-CoV-2 virus by *in vitro* microneutralization assay. In the neutralization of binding (NoB) assay, 339 of the 1,731 tested (19.6%) S protein-specific mAbs were able to neutralize the antigen/receptor binding, showing a broad array of neutralization potency ranging from 50% to 100% (Figure S2C; Table S1).

As for the authentic virus neutralization assay, supernatants containing naturally produced IgG or IgA were tested for their ability to protect the layer of Vero E6 cells from the cytopathic effect triggered by SARS-CoV-2 infection. To increase the throughput of our approach, supernatants were tested at a single-point dilution, and to increase the sensitivity of our first screening, a viral titer of 25 50% tissue culture infectious dose ($TCID_{50}$) was used. For this screening, mAbs were classified as neutralizing, partially neutralizing, and non-neutralizing based on their complete, partial, or absent ability to prevent the infection of Vero E6 cells, respectively. Out of 1,731 mAbs tested in this study, a panel of 453 (26.2%) mAbs neutralized the authentic virus and prevented infection of Vero E6 cells (Table S1). The percentage of partially neutralizing antibodies and neutralizing antibodies (nAbs) identified in each donor was extremely variable ranging from 2.6%–29.7% and 2.8%–26.4% respectively (Figure 2B; Table S2). The majority of nAbs were able to specifically recognize the S protein S1 domain (57.5%; n = 244), while 7.3% (n = 53) of nAbs were specific for the S2 domain, and 35.2% (n = 156) did not recognize single domains but only the S protein in its trimeric conformation (Figure S2A; Table S3). From the panel of 453 nAbs, we recovered the heavy chain (HC) and light chain (LC) variable regions of 220 nAbs, which were expressed as full-length immunoglobulin G1 (IgG1) using the transcriptionally active PCR (TAP) approach to characterize their neutralization potency against the live virus at 100 $TCID_{50}$. The vast majority of nAbs identified (65.9%; n = 145) had a low neutralizing potency and required more than 500 ng/mL to achieve 100% inhibitory concentration (IC_{100}). A smaller fraction of the antibodies had an intermediate neutralizing potency (23.6%; n = 52)

Please cite this article in press as: Andreano et al., Extremely potent human monoclonal antibodies from COVID-19 convalescent patients, Cell (2021), https://doi.org/10.1016/j.cell.2021.02.035

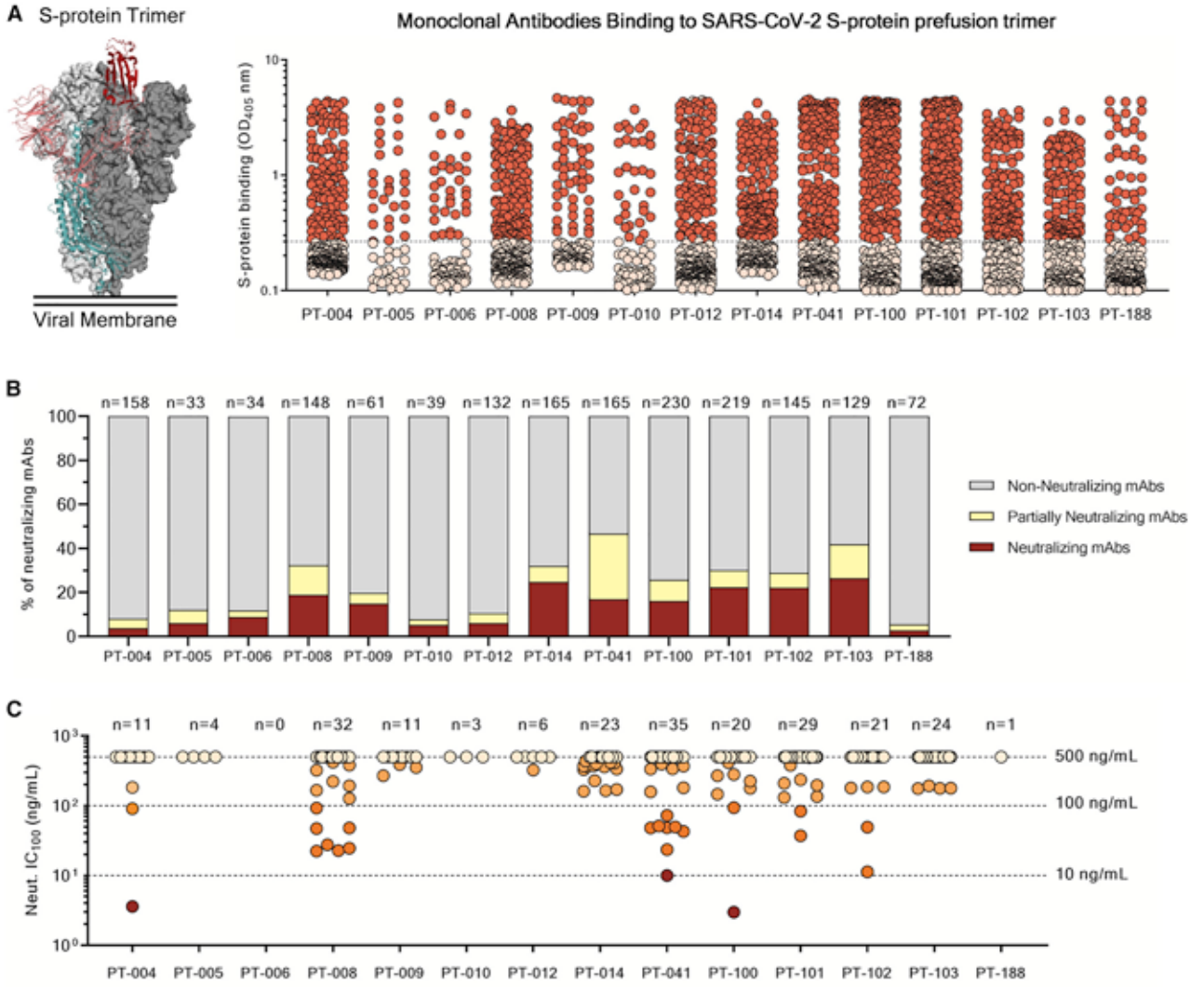

Figure 2. Identification of SARS-CoV-2 S protein-specific nAbs

(A) The graph shows supernatants tested for binding to the SARS-CoV-2 S-protein stabilized in its prefusion conformation. Threshold of positivity has been set as two times the value of the blank (dotted line). Red dots represent mAbs that bind to the S protein, while pink dots represent mAbs that do not bind.

(B) The bar graph shows the percentage of non-neutralizing (gray), partially neutralizing (pale yellow), and neutralizing antibodies (dark red) identified per each donor. The total number (n) of antibodies tested per individual is shown on top of each bar.

(C) The graph shows the neutralization potency of each nAb tested once expressed as recombinant full-length IgG1. Dashed lines show different ranges of neutralization potency (500, 100, and 10 ng/mL). Dots were colored based on their neutralization potency and were classified as weakly neutralizing (>500 ng/mL; pale orange), medium neutralizing (100–500 ng/mL; orange), highly neutralizing (10–100 ng/mL; dark orange), and extremely neutralizing (1–10 ng/mL; dark red). The total number (n) of antibodies tested per individual is shown on top of each graph. A COVID-19 convalescent plasma and an unrelated plasma were used as positive and negative control, respectively, in all the assays.

requiring between 100 and 500 ng/mL to achieve the IC_{100}, while 9.1% (n = 20) required between 10 and 100 ng/mL. Finally, only 1.4% (n = 3) of the expressed nAbs were classified as extremely potent nAbs, showing an IC_{100} lower than 10 ng/mL (Figure 2C; Figure S2B; Table S4).

SARS-CoV-2 neutralizing antibodies can be classified into four groups

Based on the first round of screening, 14 nAbs were selected for further characterization. All nAbs were able to bind the SARS-CoV-2 S protein in its trimeric conformation (Figure 3A). The mAbs named J08, I14, F05, G12, C14, B07, I21, J13, and D14 were also able to specifically bind the S1 domain (Figure 3B). The nAbs named H20, I15, F10, and F20 were not able to bind single S1 or S2 domains but only the Sprotein in its trimeric state, while the nAb L19 bound only the S2 subunit (Figures 3B and 3C). Among the group of S1-specific nAbs, only J08, I14, F05, G12, C14, and B07 were able to bind the S1 RBD and to strongly inhibit the interaction between the S protein and Vero E6 receptors, showing a half maximal effective concentration (EC_{50}) at the

Please cite this article in press as: Andreano et al., Extremely potent human monoclonal antibodies from COVID-19 convalescent patients, Cell (2021), https://doi.org/10.1016/j.cell.2021.02.035

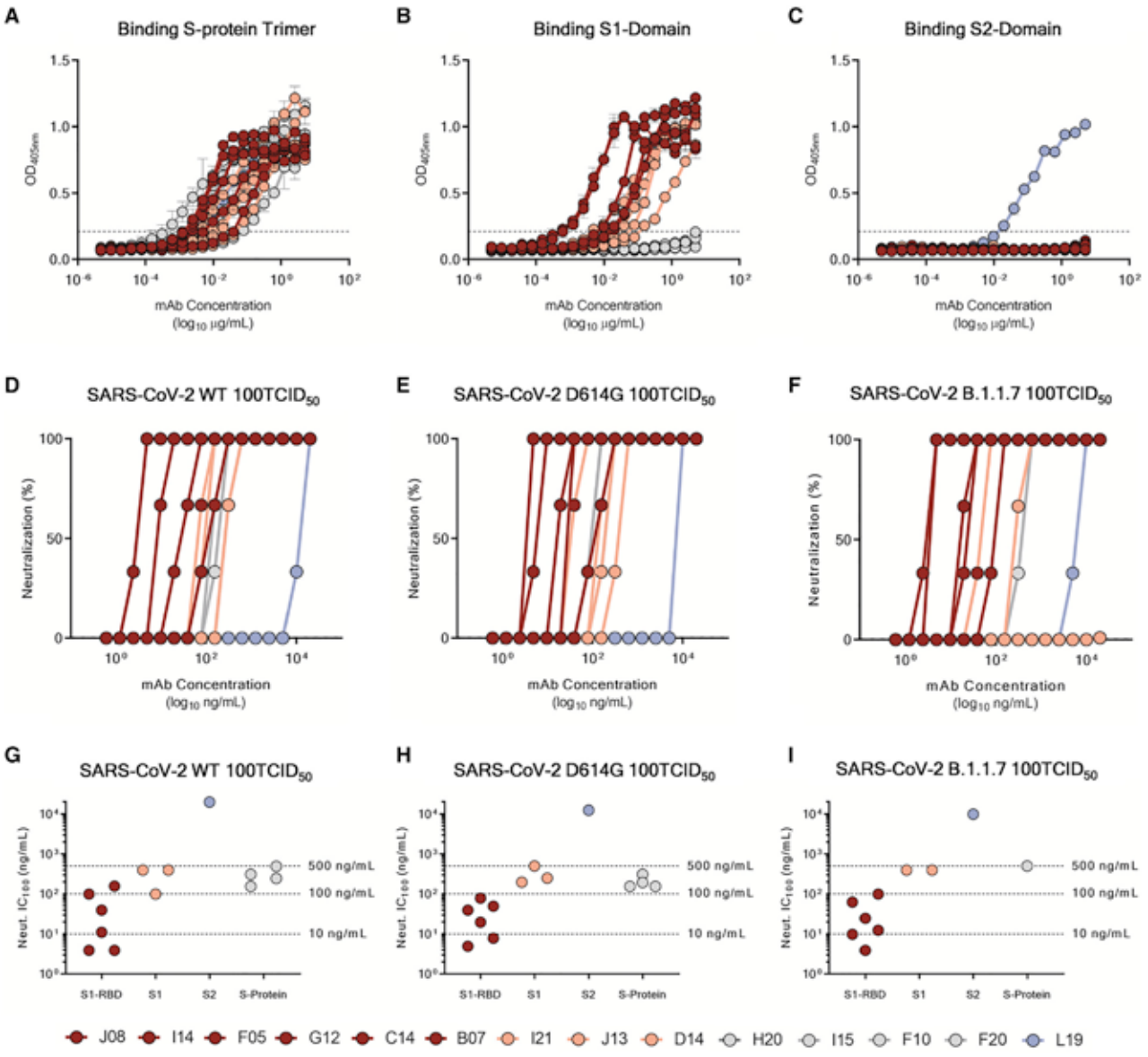

Figure 3. Functional characterization of potent SARS-CoV-2 S protein-specific nAbs

(A–C) Graphs show binding curves to the S protein in its trimeric conformation, S1 domain, and S2 domain. Mean ± SD of technical triplicates are shown. Dashed lines represent the threshold of positivity.

(D–F) Neutralization curves for selected antibodies were shown as percentage of viral neutralization against the authentic SARS-CoV-2 wild type (D), D614G variant (E), and the emerging variant B.1.1.7 (F). Data are representative of technical triplicates. A neutralizing COVID-19 convalescent plasma and an unrelated plasma were used as positive and negative control, respectively.

(G–I) Neutralization potency of 14 selected antibodies against the authentic SARS-CoV-2 wild type (G), D614G variant (H), and the emerging variant B.1.1.7 (I). Dashed lines show different ranges of neutralization potency (500, 100, and 10 ng/mL). In all graphs, selected antibodies are shown in dark red, pink, gray, and light blue based on their ability to recognize the SARS-CoV-2 S1 RBD, S1 domain, S protein trimer only, and S2 domain, respectively.

NoB assay of 78.6, 15.6, and 68.5 ng/mL for J08-MUT, I14-MUT, and F05-MUT, respectively (Figures S3A and S3B). On the other hand, I21, J13, and D14, despite showing S1 binding specificity, did not show any binding to the RBD and NoB activity (Figure S3A). Based on this description, four different groups of nAbs against SARS-CoV-2 were identified. The first group (Group I) is composed of S1 RBD-specific nAbs (J08, I14, F05, G12, C14, and B07), which showed neutralization potency against the authentic wild type (WT), the D614G variant, and the emerging variant recently isolated in the UK B.1.1.7. S1 RBD-specific nAbs showing a neutralizing potency ranging from 3.9 to 157.5 ng/mL (Figures 3D–3I; Table S5) and picomolar affinity to the S protein with an equilibrium dissociation constant (KD) ranging from 0.2 to 4.6 E^{-10}M (Figure S4). In addition to the

Please cite this article in press as: Andreano et al., Extremely potent human monoclonal antibodies from COVID-19 convalescent patients, Cell (2021), https://doi.org/10.1016/j.cell.2021.02.035

D614G and the B.1.1.7 variants, the S1 RBD-specific nAb J08 showed also to neutralize SARS-CoV-2 variants containing the E484K mutation (Andreano et al., 2020). The second group (Group II) included S1-specific nAbs that did not bind the RBD (I21, J13, and D14). These antibodies also showed good neutralization potency ranging from 99.2 to 500.0 ng/mL (Figures 3D–3I; Table S5) but inferior to that of S1 RBD-directed nAbs. One antibody from this group was not able to neutralize the B.1.1.7 variant (I21). The third group (Group III) is composed of antibodies able to bind the S-protein only in its whole trimeric conformation (H20, I15, F10, and F20). Antibodies belonging to this group showed lower affinity to the S protein trimer (KD 64.0 E^{-10}M–757.0 E^{-10}M) compared to Group I nAbs and medium neutralization potencies ranging from 155.0 to 492.2 ng/mL against the authentic WT and D614G (Figures 3D–3I; Figure S4; Table S5). On the other hand, only one S protein-specific nAb (D21) showed moderate neutralization activity against the B.1.1.7 with an IC_{100} of 500.0 ng/mL. Three S protein-specific nAbs (I15, F10, and F20) did not show any functional activity against this latter variant (Figures 3D–3I; Table S5). The fourth and final group (Group IV) is composed of antibodies that exclusively recognized the S2 domain. Different antibodies with similar properties were identified for Group IV, but only the nAb L19 is shown. The Group IV nAb L19 shows the lowest neutralization potency with 19.8 μg/mL for the authentic WT, 12.5 μg/mL against the D614G, and 9.9 μg/mL against the B.1.1.7 variant (Figures 3D–3I; Table S5).

All the antibodies described above were also tested for their ability to cross-neutralize other human coronavirus strains. nAbs were tested against lentiviral pseudotypes expressing the SARS-CoV-2, SARS-CoV-2 D614G, SARS-CoV, and Middle East respiratory syndrome (MERS)-CoV S protein on their viral membrane surface. Neutralization activity was shown against SARS-CoV-2 and D614G pseudotypes, therefore confirming previous data. None of the antibodies reported here were able to cross-neutralize other coronavirus species (Figure S5).

Different pathogen vulnerability regions identified on the S protein

The fourteen selected nAbs were further characterized by a competition assay that allowed speculation on the S protein regions recognized by these antibodies. Briefly, beads were coated with SARS-CoV-2 trimeric S protein and incubated with a primary unlabeled antibody in order to saturate the binding site on the antigen surface. Following the first incubation step, a secondary Alexa-647-labeled antibody was incubated with the antigen/unlabeled-mAb complex. If the secondary labeled antibody did not recognize the same epitope as the primary unlabeled mAb, a fluorescent signal would be detected when tested by flow cytometry. Through this assay, we observed that all Group I nAbs competed among themselves for binding to the S protein RBD, indicating that these antibodies possibly clash against each other and recognize a similar epitope region. All Group II nAbs showed different competition profiles and competed with Group II and Group III nAbs. These results confirmed that Group III antibodies can recognize various regions on the S protein surface as they compete with themselves as well as with antibodies belonging to Group II. Interestingly, nAbs belonging to Group II also competed with the B07 RBD-directed antibody, thereby suggesting that this latter nAb may have a different binding orientation compared to other nAbs included in the Group I. Finally, the Group IV nAb L19 did not compete with any of the other groups identified in this study, suggesting that this class of nAbs recognizes a distant epitope region as compared to Group I, II, and III nAbs (Figures 4A and 4B)

Genetic characterization of SARS-CoV-2 nAbs

The genes encoding the HCs and LCs of the 14 selected nAbs were sequenced, and their IGHV and IGKV genes were compared with publicly available SARS-CoV-2 neutralizing antibody sequences (Figures 5A and 5B). Four nAbs used one of the most predominant HC V genes for SARS-CoV-2 nAbs (IGHV1-69), while three nAbs used one of the least representative HCV genes (IGHV1-24). Two other nAbs employed the most common germline observed for SARS-CoV-2 nAbs, which is IGHV3-53 (Figure 5A) (Yuan et al., 2020). Interestingly, while IGHV1-69 and IGHV1-24 accommodate IGHJ diversity, nAbs belonging to the IGHV3-53 gene family only showed recombination with the IGHJ6 gene (Table S6). The HC V genes somatic hypermutation level and complementary determining region 3 (H-CDR3) length were also evaluated. Our selected nAbs displayed a low level of somatic mutations when compared to the inferred germlines with sequence identities ranging from 95.6% to 99.3% (Figure 5C left panel; Table S6), confirming what was observed in previous publications (Pinto et al., 2020; Zost et al., 2020b; Rogers et al., 2020; Griffin et al., 2020). The H-CDR3 length spanned from 7 to 21 amino acids (aa) with the majority of the antibodies (n = 6; 42.0%) having a length of 14 to 16 aa that is slightly bigger than previously observed (Figure 5C right panel; Table S6). All of our nAbs used the κ chain, and the majority of them used the common genes IGKV1-9 and IGKV3-11 (n = 6; 42.0%) (Figure 5B; Table S6). The level of IGKV somatic hypermutation was extremely low for LCs showing a percentage of sequence identities ranging from 94.3% to 98.9% (Figure 5D left panel; Table S6). The LC CDR3 (L-CDR3) lengths were ranging from 5 to 10 aa, which is in line with what was previously observed for SARS-CoV-2 nAbs (Figure 5D right panel; Table S6). When paired HC and LC gene analysis was performed, IGHV1-69-derived nAbs were found to rearrange exclusively with IGKV3 gene family, whereas IGHV1-24-derived nAbs accommodate LC diversity (Table S6). Of note, some of our candidates showed unique HC and LC pairing when compared to the public SARS-CoV-2 nAb repertoire. Particularly, five different HC and LC rearrangements not previously described for nAbs against SARS-CoV-2 were identified. These included the IGHV1-24;IGKV1-9, IGHV1-24;IGKV3-15, IGHV1-46;IGKV1-16, IGHV3-30;IGKV1-9, and IGHV3-53;IGKV1-17 (Figure 5E).

Fc engineering of candidate nAbs to abrogate Fc receptor binding and extend half-life

ADE of disease is a potential clinical risk following coronavirus infection (Lee et al., 2020). Therefore, to optimize the suitability for clinical development and reduce the risk of ADE, five different point mutations were introduced in the constant region (Fc) of the three most potent nAbs (J08, I14, and F05), which were renamed

Please cite this article in press as: Andreano et al., Extremely potent human monoclonal antibodies from COVID-19 convalescent patients, Cell (2021), https://doi.org/10.1016/j.cell.2021.02.035

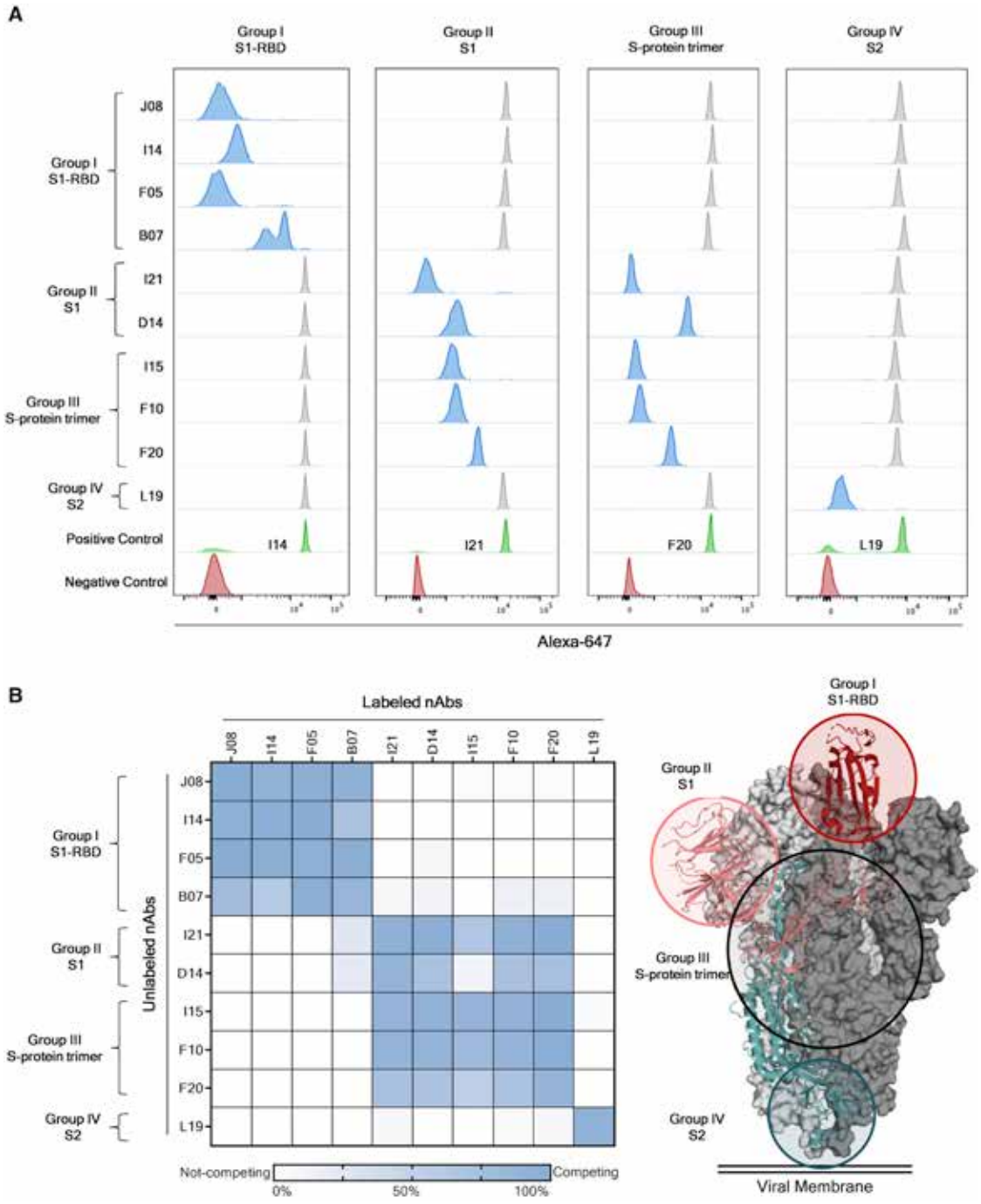

Figure 4. Identification of four different sites of pathogen vulnerability on the S protein surface

(A) Representative cytometer peaks per each of the four antibody groups are shown. Positive (beads conjugated with only primary labeled antibody) and negative (un-conjugated beads) controls are shown as green and red peaks, respectively. Competing and not-competing nAbs are shown in blue and gray peaks, respectively.

(B) The heatmap shows the competition matrix observed among the 14 nAbs tested. Threshold of competition was set at 50% of fluorescent signal reduction. A speculative representation of the vulnerability sites is shown on the S protein surface.

J08-MUT, I14-MUT, and F05-MUT. The first two point mutations (M428L and N434S) were introduced to enhance antibody half-life and to increase tissue distribution and persistence (Zalevsky et al., 2010; Gaudinski et al., 2018; Pegu et al., 2017). The remaining three point mutations (L234A, L235A, and P329G) were introduced to reduce antibody dependent

Please cite this article in press as: Andreano et al., Extremely potent human monoclonal antibodies from COVID-19 convalescent patients, Cell (2021), https://doi.org/10.1016/j.cell.2021.02.035

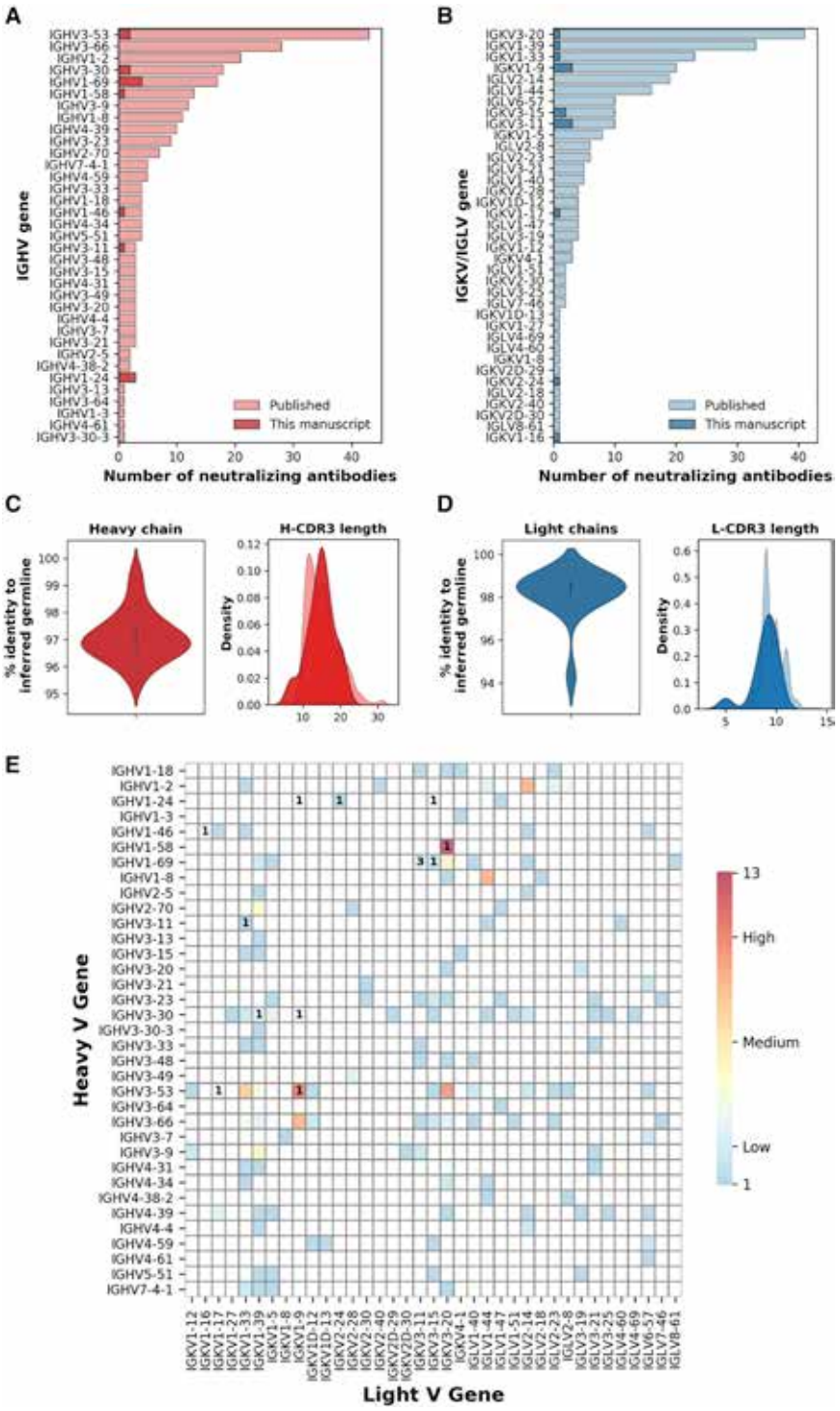

Figure 5. Heavy and light chain analyses of selected nAbs

(A and B) Bar graphs show the heavy and light chains usage for neutralizing antibodies against SARS-CoV-2 in the public repertoire compared to the antibodies identified in this study. Our and public antibodies are shown in dark and light colors, respectively.

(C and D) The heavy and light chain percentage of identity to the inferred germline and amino acidic CDR3 length are shown as violin and distribution plot, respectively.

(E) The heatmap shows the frequency of heavy and light chain pairing for SARS-CoV-2 neutralizing human mAbs already published. The number within the heatmap cells represent the amount of nAbs described in this manuscript showing already published (colored cells) or novel heavy and light chain rearrangements (blank cells).

functions such as binding to FcγRs and cell-based activities (Schlothauer et al., 2016).

To confirm the lack of FcγR binding as well as the extended half-life, a beads-based Luminex assay was performed. Briefly the beads were coated with SARS-CoV-2 S protein RBD. Antibodies were tested at eight-point dilutions, and the binding was detected with FcγR2A and neonatal Fc receptor (FcRn) at pH6.2 and 7.4. The FcγR2A was selected as it is predominantly expressed on the surface of phagocytic cells (such as monocytes, macrophages, and neutrophils) and is associated with phagocytosis of immune complexes and antibody-opsonized targets (Ackerman et al., 2013). On the other hand, FcRn, which is highly expressed on endothelial cells and circulating monocytes, was selected as it is responsible for the recycling and serum half-life of IgG in the circulation (Mackness et al., 2019). This latter receptor was shown to possess a tighter binding at lower pH (e.g., pH 6.2) compared to a physiological pH (e.g., pH 7.4) (Booth et al., 2018). Results shown in Figure S6 demonstrate that binding to the FcγR2A was completely abrogated for the mutated version of candidate nAbs (J08-MUT, I14-MUT, and F05-MUT) compared to their respective WT versions (J08, I14, and F05) and controls (CR3022 and unrelated protein) (Figure S6A). Furthermore, Fc-engineered antibodies showed increased binding activity to the FcRn at both pH 6.2 and 7.4 compared to their WT counterpart (Figures S6B and S6C). Finally, to evaluate the lack of Fc-mediated cellular activities by our three candidate nAbs, the antibody-dependent neutrophil phagocytosis (ADNP) and antibody-dependent natural killer (ADNK) cell activations were evaluated (Butler et al., 2019; Ackerman et al., 2016; Karsten et al., 2019; Boudreau et al., 2020). For the ADNP assay, primary human neutrophils were used to detect antibody binding to SARS-CoV-2 S protein RBD-coated beads, while ADNK

Please cite this article in press as: Andreano et al., Extremely potent human monoclonal antibodies from COVID-19 convalescent patients, Cell (2021), https://doi.org/10.1016/j.cell.2021.02.035

activity was evaluated by using primary human NK cells and detecting the release of the proinflammatory cytokine interferon gamma (IFN-γ). Complete abrogation of both ADNP and ADNK was observed for all three Fc-engineered candidate nAbs compared to their WT versions and control antibody (CR3022), thus confirming the lack of Fc-mediated cellular activities (Figures S6D and S6E).

Potency and autoreactivity evaluation of Fc-engineered candidates

The three engineered antibodies were tested to confirm their binding specificity and neutralization potency against both the WT, the widespread SARS-CoV-2 D614G mutant and the emerging variant B.1.1.7 (Korber et al., 2020, CDC, 2021) to evaluate their cross-neutralization ability. The three engineered nAbs maintained their S1 domain binding specificity and extremely high neutralization potency with J08-MUT and F05-MUT being able to neutralize both the WT and the D614G variant with an IC_{100} lower than 10 ng/mL (both at 3.9 ng/mL for the WT and the D614G strains) (Figure S6F – K; Table S5). The antibody J08-MUT also showed extreme neutralization potency against emerging variants as it was able to neutralize the B.1.1.7 with an identical IC_{100} compared to the WT virus (Figure S6K; Table S5) and has also showed to neutralize variants that include the E484K mutation (Andreano et al., 2020).

Since it has been reported that SARS-CoV-2 elicited antibodies that can cross-react with human tissues, cytokines, phospholipids, and phospholipid-binding proteins (Zuo et al., 2020; Bastard et al., 2020; Kreer et al., 2020), the three candidate mAbs in both their WT and MUT versions were tested through an indirect immunofluorescent assay against human epithelial type 2 (HEp-2) cells, which expose clinically relevant proteins to detect autoantibody activities (Figure S7A). As reported in Figure S7B, the positive control presents a different range of detectable signals based on the initial dilution steps (from bright green at 1:1 to very dim green at 1:100). Among all samples tested, only F05 showed moderate level of autoreactivity to human cells, while no signal could be measured for the other antibodies (Figure S7B).

Structural analyses of candidate nAbs

Single-particle negative-stain electron microscopy (nsEM) was used to visualize a stabilized SARS-2-CoV-6P-Mut7 S protein in complex with three separate Fabs: J08, I14, and F05. This recombinant, soluble S protein primarily exhibits 3 RBD's "down" but can switch to RBD "up" conformation with antibody bound. Inspection of the 2D class averages revealed a mixed stoichiometry of unbound S protein, one Fab bound, and two Fab bound classes, which allowed for 3D refinements of each (Figure 6A). The three different Fabs bind to the RBD in the "up" conformation, although at different angles and rotations, likely due to the flexibility of the RBD. Model docking of PDB 7BYR (one RBD "up" bound to antibody) shows that the fabs overlap with the receptor-binding motif (RBM) and therefore are positioned to sterically block receptor hACE2 engagement (Figure 6B). To determine the epitope, HC and LC sequences of Fabs J08, I14, and F05 were used to create synthetic models for docking into the nsEM maps. Based on the docking, we predicted that a loop containing residues 477 to 489 (STPCNGVEGFNCY) appeared to be involved in the binding specifically with residue F486 extending into a cavity that is in the middle of the HC and LC of each antibody.

J08-MUT prevents SARS-CoV-2 infection in the golden Syrian hamster

The golden Syrian hamster model has been widely used to assess monoclonal antibody prophylactic and therapeutic activities against SARS-CoV-2 infection. This model has shown to manifest severe forms of SARS-CoV-2 infection mimicking more closely the clinical disease observed in humans (Baum et al., 2020; Imai et al., 2020; Rogers et al., 2020; Sia et al., 2020). We designed a prophylactic study in golden Syrian hamster to evaluate the efficacy of J08-MUT in preventing SARS-CoV-2 infection. For this study, 30 hamsters were divided into five arms (six animals each), which received, J08-MUT at 4, 1, and 0.25 mg/kg via intraperitoneal injection. Placebo and IgG1 isotype control groups were included in the study, which received a saline solution and an anti-influenza antibody at the concentration of 4 mg/kg, respectively. The J08-MUT at 4 mg/kg group and the 1 and 0.25 mg/kg groups were tested in two independent experiments. The IgG1 isotype control group was tested in parallel with the J08-MUT 4 mg/kg group, whereas the placebo is an average of the two experiments. Animals were challenged with 100 μL of SARS-CoV-2 solution (5×10^5 plaque-forming units [PFU]) via intranasal distillation 24 h post-administration of the antibody. Three hamsters per group were sacrificed at 3 days post infection, while the remaining animals were culled at day 8 (Figure 7A). Body weight change was evaluated daily and considered as a proxy for disease severity. Animals in the control group and those that received the IgG1 isotype antibody lost more than 5% of their original body weight from day 1 to day 6 and then stabilized. These data are in line with previously published data of SARS-CoV-2 infection in a golden Syrian hamster model (Kreye et al., 2020; Liu et al., 2020). In marked contrast, in the prophylactic study, all animals that received J08-MUT were significantly protected from weight loss. Protection was present at all J08-MUT concentrations and was dose dependent (Figure 7B). When J08-MUT was administered at 4 mg/kg, we observed protection from SARS-CoV-2 infection and only a minimal weight loss (average −1.8% of body weight) was noticed 1 day post viral challenge. A higher body weight loss was observed 1 day post infection in hamsters that received J08-MUT at 1 mg/kg (from −1.8% to −3.3%) and 0.25 mg/kg (from −1.8% to −4.7%). In the J08-MUT 4 mg/kg group, all animals quickly recovered and reached their initial weight by day 3. From day 4 on all hamsters gained weight increasing up to 5% from their initial body weight. Hamsters that received the 1 and 0.25 mg/kg dosages completely recovered their initial body weight at day 6 and 8, respectively. Hamsters in the control groups did not recover their initial body weight and at day 8, still showed around 5% of weight loss (Figure 7B). The prophylactic activity of J08-MUT was also reflected in the complete absence of viral titer in the lung tissue at 3 days post infection in all hamsters that received J08-MUT at 4 and 1 mg/kg and also in two out of three hamsters that received J08-MUT at 0.25 mg/kg. On the other hand, hamsters that

Please cite this article in press as: Andreano et al., Extremely potent human monoclonal antibodies from COVID-19 convalescent patients, Cell (2021), https://doi.org/10.1016/j.cell.2021.02.035

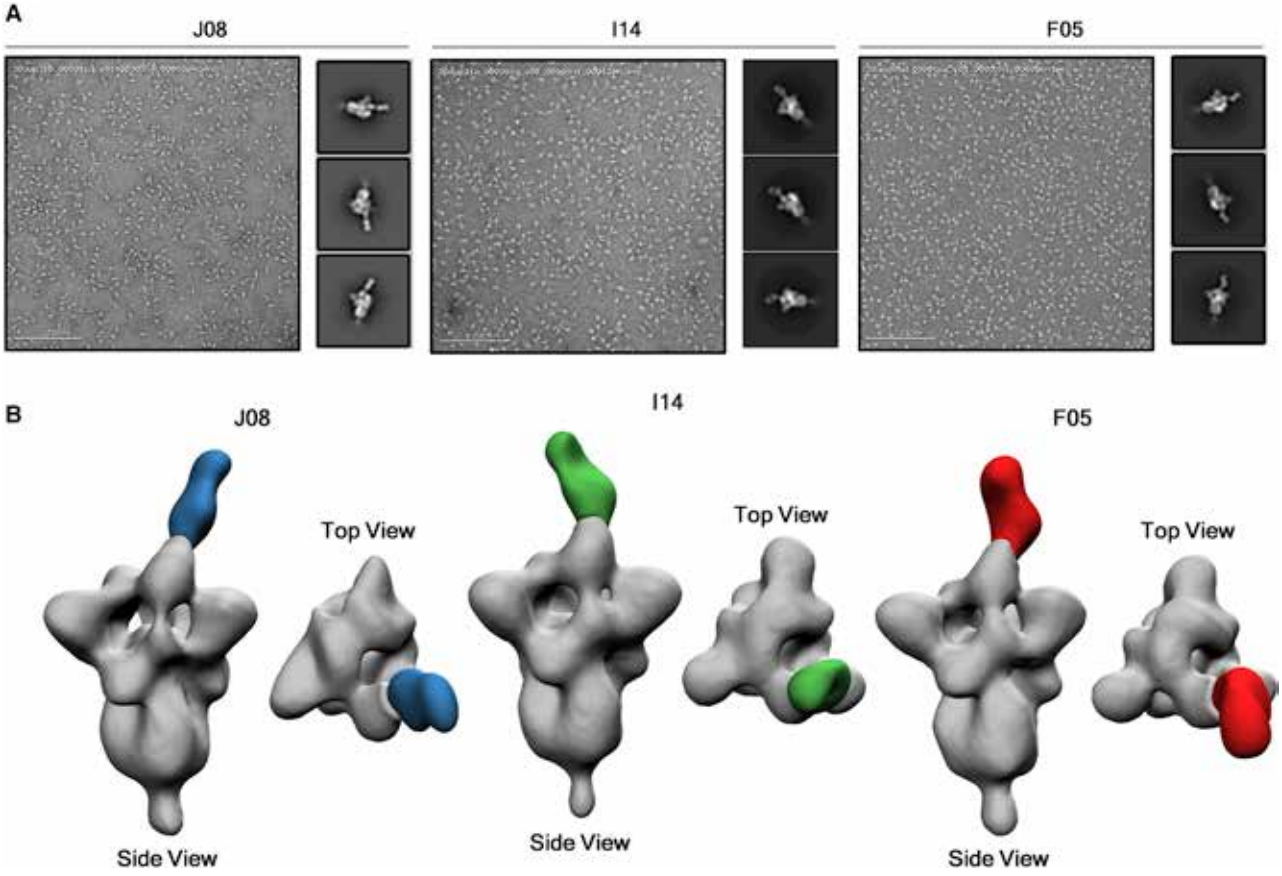

Figure 6. EM epitope mapping of RBD mAbs

(A) Negative stain for J08, I14, and F05 in complex with the S protein. 200 nm scale bar is shown.

(B) Figures show the binding of J08 (blue), I14 (green), and F05 (red) to the SARS-CoV-2 S protein RBD.

received the IgG1 isotype control or in the placebo group showed a significantly higher viral titer (Figure 7D).

Finally, we performed an ELISA assay to detect the presence of human IgG in hamster sera. All samples that received J08-MUT or the IgG1 isotype control showed detectable human IgGs in the sera in a dose-dependent fashion, while no human IgGs were detected in the placebo group (Figures 7E and 7F). Human IgGs were detected at 3 and up to 7 days post infection (Figures 7E and 7F).

J08-MUT therapy of SARS-CoV-2 infection in the golden Syrian hamster

For the therapeutic study, three groups of six animals each were used to evaluate the ability of J08-MUT to treat SARS-CoV-2 infection in the golden Syrian hamster model. One group received J08-MUT via intraperitoneal injection at 4 mg/kg, and the other two groups received placebo and 4mg/kg IgG1 isotype control, respectively. The experiment was performed in parallel with the initial prophylactic study where J08-MUT was administered at 4 mg/kg and the two control groups. Animals were challenged with 100 μL of SARS-CoV-2 solution (5×10^5 PFU) via intranasal distillation 24 h prior to the administration of the antibody. Three hamsters per group were sacrificed at 3 days post infection while the remaining animals were culled at day 12 (Figure 7A). Despite J08-MUT and control groups showed a similar trend in weight loss in the first 4 days post infection, the treatment group showed a significantly quicker weight recovery (Figure 7C). At day 12, only hamsters that received J08-MUT recovered the initial body weight (Figure 7C). When we analyzed the viral titer in lung tissues, we observed complete absence of the virus at day 3 in all the hamsters treated with J08-MUT at 4 mg/kg, while animals that received the IgG1 isotype control or in the placebo group showed a significantly higher viral titer (Figure 7G). To evaluate the presence of human antibodies in hamster sera, we performed an ELISA assay. All samples that received J08-MUT or the IgG1 isotype control showed detectable human IgGs in the sera in a dose-dependent fashion, while no human IgGs were detected in the placebo group (Figures 7H and 7I). Human IgGs were detected at 3 and up to 11 days post infection (Figures 7H and 7I).

DISCUSSION

This work describes a systematic screening of memory B cells from SARS-CoV-2 convalescent patients to identify extremely potent mAbs against SARS-CoV-2 and their engineering to

Please cite this article in press as: Andreano et al., Extremely potent human monoclonal antibodies from COVID-19 convalescent patients, Cell (2021), https://doi.org/10.1016/j.cell.2021.02.035

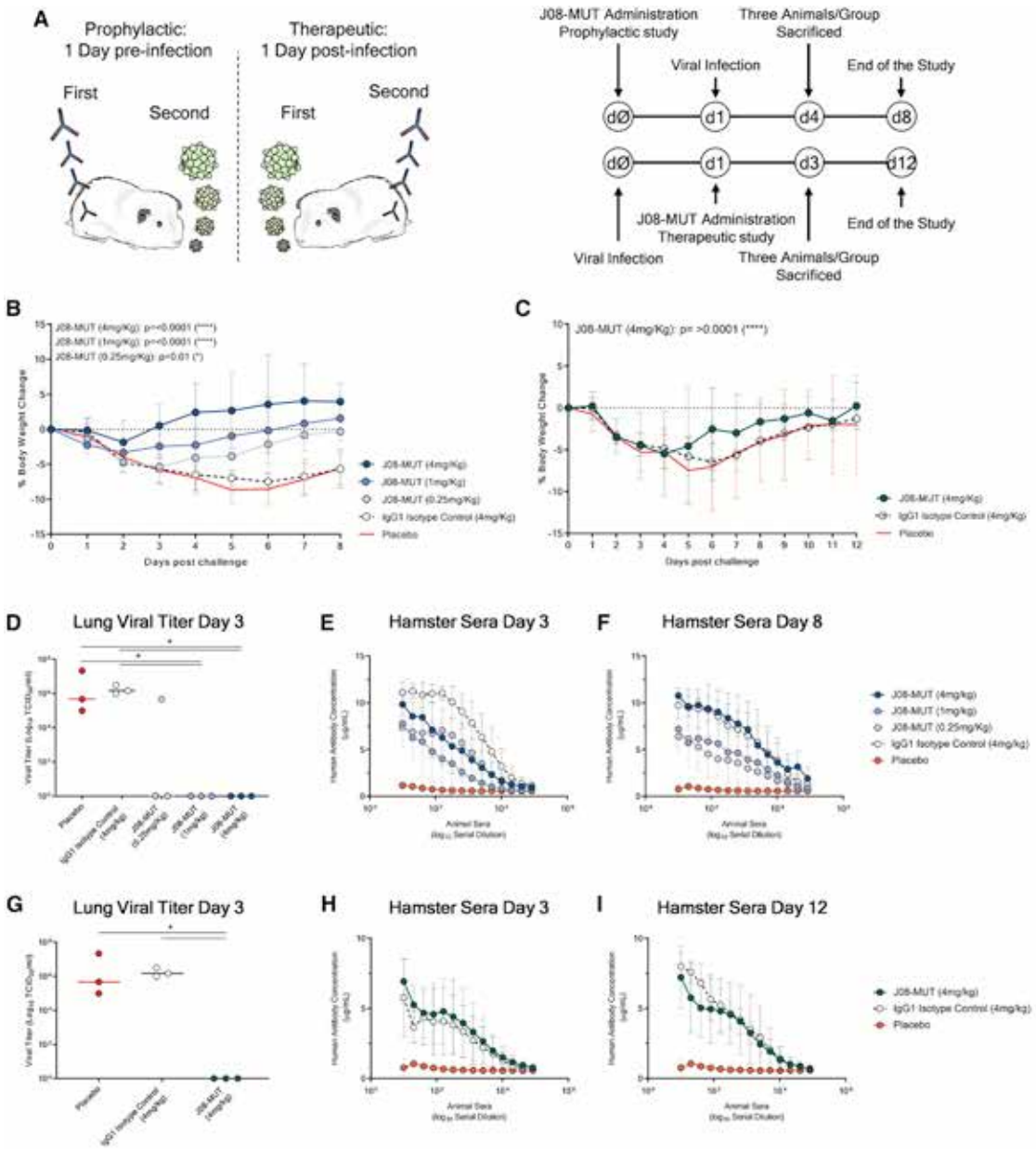

Figure 7. Prophylactic and therapeutic efficacy of J08-MUT in the golden Syrian hamster model of SARS-CoV-2 infection

(A) Schematic representation and timelines of prophylactic and therapeutic studies performed in golden Syrian hamster.

(B and C) The figure shows the prophylactic impact of J08-MUT at three different concentrations (4, 1, and 0.25 mg/kg) (B) on body weight loss change (C). The figure shows the therapeutic impact of J08-MUT at 4 mg/kg on body weight loss change. Mean ± SD are denoted in the graphs.

(D–F) The figures show the lung viral titer at day 3 (D) and the detection of human antibodies in hamster sera at day 3 (E) and day 8 (F) in the prophylactic study. Mean ± SD of technical triplicates are shown.

(G–I) The figures show the lung viral titer at day 3 (G) and the detection of human antibodies in hamster sera at day 3 (H) and day 12 (I) in the therapeutic study. Mean ± SD of technical triplicates are shown. Statistical differences were calculated with two-way analysis of variance (ANOVA) for body weight change and with a nonparametric Mann–Whitney t test for the lung viral titer. Significances are shown as *p < 0.05, **p < 0.01, ***p < 0.001, and ****p < 0.0001.

extend half-life and eliminate the potential risk of ADE. The best antibody neutralized the authentic WT virus and emerging variants at pico molar concentration *in vitro* and showed prophylactic and therapeutic efficacy in a SARS-CoV-2 hamsters model of infection when used at 0.25 and 4 mg/kg, respectively. The antibody described is a promising candidate for the development of a broadly affordable tool for prevention and therapy of COVID-19.

In the search for potent antibodies, we found that approximately 10% of the total B cells against the S protein isolated

Please cite this article in press as: Andreano et al., Extremely potent human monoclonal antibodies from COVID-19 convalescent patients, Cell (2021), https://doi.org/10.1016/j.cell.2021.02.035

produce neutralizing antibodies, and these can be divided into four different groups recognizing the S1 RBD, S1 domain, S2 domain, and the S protein trimer. Most potently neutralizing antibodies are extremely rare and recognize the RBD, followed in potency by antibodies recognizing the S1 domain, the trimeric structure and the S2 subunit. From these data we can conclude that in COVID-19 convalescent patients, most of the observed neutralization titers are likely mediated by antibodies with medium-high neutralizing potency. Indeed, the extremely potent antibodies and the antibodies against the S2 subunit are unlikely to contribute to the overall neutralizing titers because they are respectively too rare and too poor neutralizers to be able to make a difference. We and others found that the antibody repertoire of convalescent patients is mostly germline-like. This may be a consequence of the loss of Bcl-6-expressing follicular helper T cells and the loss of germinal centers in COVID-19 patients, which may limit and constrain the B cell affinity maturation (Kaneko et al., 2020). It will be therefore important to perform similar studies following vaccination as it is likely that the repertoire of neutralizing antibodies induced by vaccination may be different from the one described here.

Out of the 453 neutralizing antibodies that were tested and characterized, one antibody (J08) showed extremely high neutralization potency against both the WT SARS-CoV-2 virus isolated in Wuhan and emerging variants containing the D614G, E484K, and N501Y variants. During the last few months, several groups reported the identification, 3D structure and passive protection in animal models of neutralizing antibodies against SARS-CoV-2. Most of these studies, with few exceptions, reported antibodies that require from 20 to several hundred ng/mL to neutralize 50% of the virus *in vitro*. While these antibodies are potentially good for therapy, they will require a high dosage, which is associated with elevated cost of goods, low production capacity, and delivery by intravenous infusion.

The extremely potent mAb described in our study is likely to allow the use of lower quantities of antibodies to reach prophylactic and therapeutic efficacy and as a consequence, decrease the cost of goods and enable sustainable development and manufacturability. This solution may increase the number of doses produced annually and therefore increase antibodies availability in high-income countries as well as low-and middle-income countries. Therefore, our antibodies have the potential to meet the expectations of the call to action to expand access to mAb-based products, recently published by the Wellcome Trust and supported by the WHO and the Coalition for Epidemic Preparedness Innovations (Wellcome and IAVI, 2020).

A potential issue associated with the use of human mAbs against viral pathogens is the potential selection of escape mutants. This is usually addressed by using a combination of antibodies directed against non-overlapping epitopes. While this is an ultimate clear solution, it increases the complexity of development, costs of production, drug availability, and affordability. In our case, we believe that selection of escape mutants upon treatment with a single mAb may be quite difficult as the SARS-CoV-2 RNA-dependent polymerase possesses a proofreading machinery (Romano et al., 2020), and the epitope recognized by the antibodies herein described overlaps with the region necessary to bind the hACE2 receptor. In this regard, it took more than 70 days of continuous co-culture of the virus in presence of the antibodies before we were able to detect the first emergence of escape mutants of the WT SARS-CoV-2 (data not shown).

Finally, a peculiar part of our approach consisted in depleting possible antibody Fc-mediated functions of the antibodies to avoid the risk of ADE. While there is no evidence of ADE in SARS-CoV-2, and most vaccines and mAbs tested so far seem to be safe, it is too early to make definitive conclusions. In addition, two recently published reports suggested that we need to continue to monitor the potential risk of ADE. The first report showed that severe SARS-CoV-2 patients are characterized by an increased proinflammatory signature mediated by the Fcγ receptors triggered by afucosylated IgG1 antibodies (Chakraborty et al., 2020). The second report described that one antibody was associated with worse clinical outcomes when administered to hospitalized patients requiring high-flow oxygen or mechanical ventilation (Lilly, 2020). Therefore, we believe it is important to develop and test antibodies where Fc-mediated functions have been eliminated in the clinical practice. Since the Fc portion contributes significantly to the *in vivo* potency of the antibodies (Schäfer et al., 2020), removing Fc functions may be a problem for mAbs with low neutralization potency because they may no longer be effective when tested in clinical settings, as already described in other contexts (DiLillo et al., 2014). The extremely high potency shown by our antibodies allowed us to remove Fc functions while maintaining *in vivo* potency at minimal dosage.

Limitations of the study

While we believe that our antibodies are extremely potent when compared to most of those described in literature, we acknowledge that in most cases, direct comparison was not performed, and we rely on published data.

The second limitation of the study is that *in vitro* neutralization and *in vivo* protection in the SARS-CoV-2 hamster model of infection cannot be fully predictive of the behavior of the same antibody in humans, and therefore the real benefit of described antibodies can only be assessed in clinical studies.

STAR★METHODS

Detailed methods are provided in the online version of this paper and include the following:

- KEY RESOURCES TABLE
- RESOURCE AVAILABILITY
  - Lead contact
  - Materials availability
  - Data and code availability
- EXPERIMENTAL MODEL AND SUBJECT DETAILS
  - Enrollment of SARS-COV-2 convalescent donors and human sample collection
- METHOD DETAILS
  - Single cell sorting of SARS-CoV-2 S-protein$^+$ memory B cells from COVID-19 convalescent donors
  - Expression and purification of SARS-CoV-2 S-protein prefusion trimer and receptor binding domain

Please cite this article in press as: Andreano et al., Extremely potent human monoclonal antibodies from COVID-19 convalescent patients, Cell (2021), https://doi.org/10.1016/j.cell.2021.02.035

- ELISA assay with S1 and S2 subunits of SARS-CoV-2 S-protein
- ELISA assay with SARS-CoV-2 S-protein prefusion trimer and S1 – S2 subunits
- SARS-CoV-2 virus and cell infection
- Neutralization of Binding (NoB) Assay
- Single cell RT-PCR and Ig gene amplification
- Cloning of variable region genes and recombinant antibody expression in transcriptionally active PCR
- Flask expression and purification of human monoclonal antibodies
- Viral propagation and titration
- SARS-CoV-2 authentic virus neutralization assay
- Production and titration of SARS-CoV-2 pseudotyped lentiviral reporter particles
- SARS-CoV-2 pseudotyped lentivirus neutralization assay
- Characterization of SARS-CoV-2 RBD-Antibodies binding by Flow cytometry
- Flow Cytometry-Based S-protein Competition assay
- Antigen-specific FcγR binding
- Antibody-dependent neutrophil phagocytosis
- Antibody-dependent NK cell activation
- Affinity evaluation of SARS-CoV-2 neutralizing antibodies
- Autoreactivity screening test on HEp-2 Cells
- Genetic Analyses of SARS-CoV-2 S-protein specific nAbs
- Negative-stain electron microscopy
- Prophylactic and therapeutic passive transfer studies in golden Syrian hamsters
- Determination of viral load by $TCID_{50}$ assay
- Human IgG detection in hamster sera

SUPPLEMENTAL INFORMATION

Supplemental Information can be found online at https://doi.org/10.1016/j.cell.2021.02.035.

ACKNOWLEDGMENTS

We wish to thank Fondazione Toscana Life Sciences in the persons of Dr. Fabrizio Landi and Dr. Andrea Paolini and the whole Administration for their help and support. In particular, we would like to thank Mr. Francesco Senatore, Mrs. Laura Canavacci, and Mrs. Cinzia Giordano for their support in preparing all the documents needed for the ethical approval of the clinical studies carried out within this project. We wish to thank the National Institute for Infectious Diseases, IRCCS, Lazzaro Spallanzani Rome (IT), and the Azienda Ospedaliera Universitaria Senese, Siena (IT) for providing blood samples from COVID-19 convalescent donors under studies approved by local ethic committees. We also wish to thank all the nursing staff who chose to cooperate for blood withdrawal and all the donors who decided to participate in this study. We would like to thank the whole GSK Vaccines Pre-clinical Evidence Generation and Assay – Immunolgy function led by Dr. Oretta Finco for their availability and support as well as Mrs. Simona Tavarini, Mrs. Chiara Sammicheli, Dr. Monia Bardelli, Dr. Michela Brazzoli, Dr. Elisabetta Frigimelica, Dr. Erica Borgogni, and Dr. Elisa Faenzi for sharing their expertise, extreme availability, and technical support. We would also like to thank Dr. Mariagrazia Pizza and Dr. Simone Pecetta for initial insightful advice and discussions on this project. We would like to thank Dr. Jason McLellan and his team for generously providing the SARS-CoV-2 S protein stabilized in its prefusion conformation used in this study. Furthermore, we would like to thank Dr. Daniel Wrapp and Dr. Nianshuang Wang for the precious information and suggestions. The authors wish to thank Seromyx for their support in assessing the functionality of the antibodies Fc portion. The authors would like to thank the University of Georgia Animal Resource staff, technicians, and veterinarians for animal care as well as the staff of the University of Georgia AHRC BSL-3 facility for providing biosafety and animal care. The following reagent was deposited by the Centers for Disease Control and Prevention and obtained through BEI Resources, NIAID, NIH: SARS-Related Coronavirus 2 Isolate USA-WA1/2020, NR-52281. This work was funded by the European Research Council (ERC) advanced grant agreement no. 787552 (vAMRes). The Laboratory is also supported by the Wellcome Trust. This publication was supported by funds from the "Centro Regionale Medicina di Precisione" and by all the people who answered the call to fight with us the battle against SARS-CoV-2 with their kind donations on the platform ForFunding (https://www.forfunding.intesasanpaolo.com/DonationPlatform-ISP/nav/progetto/id/3380). This publication was supported by the European Virus Archive goes Global (EVAg) project, which has received funding from the European Union's Horizon 2020 research and innovation program under grant agreement no. 653316. This publication was supported by the COVID-2020-12371817 project, which has received funding from the Italian Ministry of Health. This work was funded, in part, by the University of Georgia (UGA) (UGA-001) and a contract by Fondazione Toscana Life Sciences. In addition, T.M.R. is supported by the Georgia Research Alliance as an Eminent Scholar. We wish to thank AchilleS Vaccines and the EU Malaria Fund for funding and managing the development of the human monoclonal antibody for clinical studies.

AUTHOR CONTRIBUTIONS

E.A., I.P., P.P., N.M., E.P., G.P., A.M., L. Benincasa, M.T., F.V., A.K., J.B., L.D., C.D.G., H.J., G.S., J.L.T., G.O., C.D.S., and D.C. conceived, performed experiments, and analyzed data. E.N., C.A., C.C., F.M., A.E., and M.F. enrolled patients and isolated PBMCs. R.R. and E.A. wrote the manuscript. A.B.W., E.M., N.T., T.M.R., M.R.C., G.I., L. Bracci, C.S., and R.R. coordinated the project.

DECLARATION OF INTERESTS

R.R. is an employee of GSK group of companies. E.A., A.K., D.C., C.D.S, I.P., N.M., E.P., P.P., C.S., M.T., F.V., and R.R. are listed as inventors of full-length human monoclonal antibodies described in Italian patent applications no. 102020000015754 filed on June 30, 2020 and no. 102020000018955 filed on August 3, 2020.

Received: November 24, 2020
Revised: January 25, 2021
Accepted: February 16, 2021
Published: February 23, 2021

REFERENCES

Ackerman, M.E., Dugast, A.-S., McAndrew, E.G., Tsoukas, S., Licht, A.F., Irvine, D.J., and Alter, G. (2013). Enhanced phagocytic activity of HIV-specific antibodies correlates with natural production of immunoglobulins with skewed affinity for FcγR2a and FcγR2b. J. Virol. *87*, 5468–5476.

Ackerman, M.E., Mikhailova, A., Brown, E.P., Dowell, K.G., Walker, B.D., Bailey-Kellogg, C., Suscovich, T.J., and Alter, G. (2016). Polyfunctional HIV-Specific Antibody Responses Are Associated with Spontaneous HIV Control. PLoS Pathog. *12*, e1005315.

Alsoussi, W.B., Turner, J.S., Case, J.B., Zhao, H., Schmitz, A.J., Zhou, J.Q., Chen, R.E., Lei, T., Rizk, A.A., McIntire, K.M., et al. (2020). A Potently Neutralizing Antibody Protects Mice against SARS-CoV-2 Infection. J. Immunol. *205*, 915–922.

Andreano, E., Piccini, G., Licastro, D., Casalino, L., Johnson, N.V., Paciello, I., Monego, S.D., Pantano, E., Manganaro, N., Manenti, A., et al. (2020). SARS-CoV-2 escape in vitrofrom a highly neutralizing COVID-19 convalescent plasma. bioRxiv. https://doi.org/10.1101/2020.12.28.424451.

Please cite this article in press as: Andreano et al., Extremely potent human monoclonal antibodies from COVID-19 convalescent patients, Cell (2021), https://doi.org/10.1016/j.cell.2021.02.035

Aratani, L. (2020). Jobless America: the coronavirus unemployment crisis in figures. The Guardian, May 28, 2020. https://www.theguardian.com/business/2020/may/28/jobless-america-unemployment-coronavirus-in-figures.

Arvin, A.M., Fink, K., Schmid, M.A., Cathcart, A., Spreafico, R., Havenar-Daughton, C., Lanzavecchia, A., Corti, D., and Virgin, H.W. (2020). A perspective on potential antibody-dependent enhancement of SARS-CoV-2. Nature *584*, 353–363.

Bastard, P., Rosen, L.B., Zhang, Q., Michailidis, E., Hoffmann, H.H., Zhang, Y., Dorgham, K., Philippot, Q., Rosain, J., Béziat, V., et al. (2020). Autoantibodies against type I IFNs in patients with life-threatening COVID-19. Science *370*, eabd4585.

Baum, A., Ajithdoss, D., Copin, R., Zhou, A., Lanza, K., Negron, N., Ni, M., Wei, Y., Mohammadi, K., Musser, B., et al. (2020). REGN-COV2 antibodies prevent and treat SARS-CoV-2 infection in rhesus macaques and hamsters. Science *370*, 1110–1115.

Booth, B.J., Ramakrishnan, B., Narayan, K., Wollacott, A.M., Babcock, G.J., Shriver, Z., and Viswanathan, K. (2018). Extending human IgG half-life using structure-guided design. MAbs *10*, 1098–1110.

Boudreau, C.M., Yu, W.-H., Suscovich, T.J., Talbot, H.K., Edwards, K.M., and Alter, G. (2020). Selective induction of antibody effector functional responses using MF59-adjuvanted vaccination. J. Clin. Invest. *130*, 662–672.

Butler, A.L., Fallon, J.K., and Alter, G. (2019). A Sample-Sparing Multiplexed ADCP Assay. Front. Immunol. *10*, 1851.

Carnell, G.W., Ferrara, F., Grehan, K., Thompson, C.P., and Temperton, N.J. (2015). Pseudotype-based neutralization assays for influenza: a systematic analysis. Front. Immunol. *6*, 161.

Carnell, G.W., Grehan, K., Ferrara, F., Molesti, E., and Temperton, N. (2017). An Optimized Method for the Production Using PEI, Titration and Neutralization of SARS-CoV Spike Luciferase Pseudotypes. Bio Protoc. *7*, e2514.

CDC (2021). Emerging SARS-CoV-2 Variants. https://www.cdc.gov/coronavirus/2019-ncov/more/science-and-research/scientific-brief-emerging-variants.html.

Chakraborty, S., Gonzalez, J., Edwards, K., Mallajosyula, V., Buzzanco, A.S., Sherwood, R., Buffone, C., Kathale, N., Providenza, S., Xie, M.M., et al. (2020). Proinflammatory IgG Fc structures in patients with severe COVID-19. Nat. Immunol. *22*, 67–73.

Clausen, T.M., Sandoval, D.R., Spliid, C.B., Pihl, J., Perrett, H.R., Painter, C.D., Narayanan, A., Majowicz, S.A., Kwong, E.A., McVicar, R.N., et al. (2020). SARS-CoV-2 Infection Depends on Cellular Heparan Sulfate and ACE2. Cell *183*, 1043–1057.e15.

Cutler, D.M., and Summers, L.H. (2020). The COVID-19 Pandemic and the $16 Trillion Virus. JAMA *324*, 1495–1496.

DiLillo, D.J., Tan, G.S., Palese, P., and Ravetch, J.V. (2014). Broadly neutralizing hemagglutinin stalk-specific antibodies require FcγR interactions for protection against influenza virus in vivo. Nat. Med. *20*, 143–151.

FDA (2020). Coronavirus (COVID-19) Update: FDA Authorizes Monoclonal Antibodies for Treatment of COVID-19. https://www.fda.gov/news-events/press-announcements/coronavirus-covid-19-update-fda-authorizes-monoclonal-antibodies-treatment-covid-19.

FDA (2021). COVID-19 Vaccines. https://www.fda.gov/emergency-preparedness-and-response/coronavirus-disease-2019-covid-19/covid-19-vaccines.

Gaudinski, M.R., Coates, E.E., Houser, K.V., Chen, G.L., Yamshchikov, G., Saunders, J.G., Holman, L.A., Gordon, I., Plummer, S., Hendel, C.S., et al.; VRC 606 Study Team (2018). Safety and pharmacokinetics of the Fc-modified HIV-1 human monoclonal antibody VRC01LS: A Phase 1 open-label clinical trial in healthy adults. PLoS Med. *15*, e1002493.

Grehan, K., Ferrara, F., and Temperton, N. (2015). An optimised method for the production of MERS-CoV spike expressing viral pseudotypes. MethodsX *2*, 379–384.

Griffin, M.P., Yuan, Y., Takas, T., Domachowske, J.B., Madhi, S.A., Manzoni, P., Simões, E.A.F., Esser, M.T., Khan, A.A., Dubovsky, F., et al.; Nirsevimab Study Group (2020). Single-Dose Nirsevimab for Prevention of RSV in Preterm Infants. N. Engl. J. Med. *383*, 415–425.

Hansen, J., Baum, A., Pascal, K.E., Russo, V., Giordano, S., Wloga, E., Fulton, B.O., Yan, Y., Koon, K., Patel, K., et al. (2020). Studies in humanized mice and convalescent humans yield a SARS-CoV-2 antibody cocktail. Science *369*, 1010–1014.

Hooft van Huijsduijnen, R., Kojima, S., Carter, D., Okabe, H., Sato, A., Akahata, W., Wells, T.N.C., and Katsuno, K. (2020). Reassessing therapeutic antibodies for neglected and tropical diseases. PLoS Negl. Trop. Dis. *14*, e0007860.

Hsieh, C.L., Goldsmith, J.A., Schaub, J.M., DiVenere, A.M., Kuo, H.C., Javanmardi, K., Le, K.C., Wrapp, D., Lee, A.G., Liu, Y., et al. (2020). Structure-based design of prefusion-stabilized SARS-CoV-2 spikes. Science *369*, 1501–1505.

Huang, J., Doria-Rose, N.A., Longo, N.S., Laub, L., Lin, C.L., Turk, E., Kang, B.H., Migueles, S.A., Bailer, R.T., Mascola, J.R., and Connors, M. (2013). Isolation of human monoclonal antibodies from peripheral blood B cells. Nat. Protoc. *8*, 1907–1915.

Imai, M., Iwatsuki-Horimoto, K., Hatta, M., Loeber, S., Halfmann, P.J., Nakajima, N., Watanabe, T., Ujie, M., Takahashi, K., Ito, M., et al. (2020). Syrian hamsters as a small animal model for SARS-CoV-2 infection and countermeasure development. Proc Natl Acad Sci U S A *117*, 16587–16595.

Jang, H., and Ross, T.M. (2020). Dried SARS-CoV-2 virus maintains infectivity to Vero E6 cells for up to 48 h. Vet. Microbiol. *251*, 108907.

Kaneko, N., Kuo, H.-H., Boucau, J., Farmer, J.R., Allard-Chamard, H., Mahajan, V.S., Piechocka-Trocha, A., Lefteri, K., Osborn, M., Bals, J., et al.; Massachusetts Consortium on Pathogen Readiness Specimen Working Group (2020). Loss of Bcl-6-Expressing T Follicular Helper Cells and Germinal Centers in COVID-19. Cell *183*, 143–157.e13.

Karsten, C.B., Mehta, N., Shin, S.A., Diefenbach, T.J., Slein, M.D., Karpinski, W., Irvine, E.B., Broge, T., Suscovich, T.J., and Alter, G. (2019). A versatile high-throughput assay to characterize antibody-mediated neutrophil phagocytosis. J. Immunol. Methods *471*, 46–56.

Katzelnick, L.C., Gresh, L., Halloran, M.E., Mercado, J.C., Kuan, G., Gordon, A., Balmaseda, A., and Harris, E. (2017). Antibody-dependent enhancement of severe dengue disease in humans. Science *358*, 929–932.

Kelley, B. (2020). Developing therapeutic monoclonal antibodies at pandemic pace. Nat. Biotechnol. *38*, 540–545.

Korber, B., Fischer, W.M., Gnanakaran, S., Yoon, H., Theiler, J., Abfalterer, W., Hengartner, N., Giorgi, E.E., Bhattacharya, T., Foley, B., et al. (2020). Tracking Changes in SARS-CoV-2 Spike: Evidence that D614G Increases Infectivity of the COVID-19 Virus. Cell *182*, 812–827.e19.

Kreer, C., Zehner, M., Weber, T., Ercanoglu, M.S., Gieselmann, L., Rohde, C., Halwe, S., Korenkov, M., Schommers, P., Vanshylla, K., et al. (2020). Longitudinal Isolation of Potent Near-Germline SARS-CoV-2-Neutralizing Antibodies from COVID-19 Patients. Cell *182*, 843–854.e12.

Kreye, J., Reincke, S.M., Kornau, H.-C., Sánchez-Sendin, E., Corman, V.M., Liu, H., Yuan, M., Wu, N.C., Zhu, X., Lee, C.D., et al. (2020). A Therapeutic Non-self-reactive SARS-CoV-2 Antibody Protects from Lung Pathology in a COVID-19 Hamster Model. Cell *183*, 1058–1069.e19.

Kundi, M. (1999). One-hit models for virus inactivation studies. Antiviral Res. *41*, 145–152.

Kupferschmidt, K. (2019). Successful Ebola treatments promise to tame outbreak. Science *365*, 628–629.

Lander, G.C., Stagg, S.M., Voss, N.R., Cheng, A., Fellmann, D., Pulokas, J., Yoshioka, C., Irving, C., Mulder, A., Lau, P.-W., et al. (2009). Appion: an integrated, database-driven pipeline to facilitate EM image processing. J. Struct. Biol. *166*, 95–102.

Lee, W.S., Wheatley, A.K., Kent, S.J., and DeKosky, B.J. (2020). Antibody-dependent enhancement and SARS-CoV-2 vaccines and therapies. Nat. Microbiol. *5*, 1185–1191.

Lilly (2020). Lilly's neutralizing antibody bamlanivimab (LY-CoV555) receives FDA emergency use authorization for the treatment of recently diagnosed COVID-19. https://investor.lilly.com/news-releases/news-release-details/lillys-neutralizing-antibody-bamlanivimab-ly-cov555-receives-fda.

Please cite this article in press as: Andreano et al., Extremely potent human monoclonal antibodies from COVID-19 convalescent patients, Cell (2021), https://doi.org/10.1016/j.cell.2021.02.035

Liu, L., Wang, P., Nair, M.S., Yu, J., Rapp, M., Wang, Q., Luo, Y., Chan, J.F.W., Sahi, V., Figueroa, A., et al. (2020). Potent neutralizing antibodies against multiple epitopes on SARS-CoV-2 spike. Nature *584*, 450–456.

Mackness, B.C., Jaworski, J.A., Boudanova, E., Park, A., Valente, D., Mauriac, C., Pasquier, O., Schmidt, T., Kabiri, M., Kandira, A., et al. (2019). Antibody Fc engineering for enhanced neonatal Fc receptor binding and prolonged circulation half-life. MAbs *11*, 1276–1288.

Manenti, A., Maggetti, M., Casa, E., Martinuzzi, D., Torelli, A., Trombetta, C.M., Marchi, S., and Montomoli, E. (2020). Evaluation of SARS-CoV-2 neutralizing antibodies using a CPE-based colorimetric live virus micro-neutralization assay in human serum samples. J. Med. Virol. *92*, 2096–2104.

Mullard, A. (2020). FDA approves antibody cocktail for Ebola virus. Nat. Rev. Drug Discov. *19*, 827.

Pegu, A., Hessell, A.J., Mascola, J.R., and Haigwood, N.L. (2017). Use of broadly neutralizing antibodies for HIV-1 prevention. Immunol. Rev. *275*, 296–312.

Pettersen, E.F., Goddard, T.D., Huang, C.C., Couch, G.S., Greenblatt, D.M., Meng, E.C., and Ferrin, T.E. (2004). UCSF Chimera–a visualization system for exploratory research and analysis. J. Comput. Chem. *25*, 1605–1612.

Pinto, D., Park, Y.J., Beltramello, M., Walls, A.C., Tortorici, M.A., Bianchi, S., Jaconi, S., Culap, K., Zatta, F., De Marco, A., et al. (2020). Cross-neutralization of SARS-CoV-2 by a human monoclonal SARS-CoV antibody. Nature *583*, 290–295.

Regeneron (2020). Regeneron's casirivimab and imdevimab antibody cocktail for COVID-19 is first combination therapy to receive FDA emergency use authorization. https://investor.regeneron.com/news-releases/news-release-details/regenerons-regen-cov2-first-antibody-cocktail-covid-19-receive.

Rogers, T.F., Zhao, F., Huang, D., Beutler, N., Burns, A., He, W.-T., Limbo, O., Smith, C., Song, G., Woehl, J., et al. (2020). Isolation of potent SARS-CoV-2 neutralizing antibodies and protection from disease in a small animal model. Science *369*, 956–963.

Romano, M., Ruggiero, A., Squeglia, F., Maga, G., and Berisio, R. (2020). A Structural View of SARS-CoV-2 RNA Replication Machinery: RNA Synthesis, Proofreading and Final Capping. Cells *9*, 1267.

Schäfer, A., Muecksch, F., Lorenzi, J.C.C., Leist, S.R., Cipolla, M., Bournazos, S., Schmidt, F., Maison, R.M., Gazumyan, A., Martinez, D.R., et al. (2020). Antibody potency, effector function, and combinations in protection and therapy for SARS-CoV-2 infection *in vivo*. J. Exp. Med. *218*, e20201993.

Scheres, S.H. (2012). RELION: implementation of a Bayesian approach to cryo-EM structure determination. J. Struct. Biol. *180*, 519–530.

Schlothauer, T., Herter, S., Koller, C.F., Grau-Richards, S., Steinhart, V., Spick, C., Kubbies, M., Klein, C., Umaña, P., and Mössner, E. (2016). Novel human IgG1 and IgG4 Fc-engineered antibodies with completely abolished immune effector functions. Protein Eng. Des. Sel. *29*, 457–466.

Shi, R., Shan, C., Duan, X., Chen, Z., Liu, P., Song, J., Song, T., Bi, X., Han, C., Wu, L., et al. (2020). A human neutralizing antibody targets the receptor-binding site of SARS-CoV-2. Nature *584*, 120–124.

Sia, S.F., Yan, L.M., Chin, A.W.H., Fung, K., Choy, K.T., Wong, A.Y.L., Kaewpreedee, P., Perera, R.A.P.M., Poon, L.L.M., Nicholls, J.M., et al. (2020). Pathogenesis and transmission of SARS-CoV-2 in golden hamsters. Nature *583*, 834–838.

Sparrow, E., Friede, M., Sheikh, M., and Torvaldsen, S. (2017). Therapeutic antibodies for infectious diseases. Bull. World Health Organ. *95*, 235–237.

Suloway, C., Pulokas, J., Fellmann, D., Cheng, A., Guerra, F., Quispe, J., Stagg, S., Potter, C.S., and Carragher, B. (2005). Automated molecular microscopy: the new Leginon system. J. Struct. Biol. *151*, 41–60.

Tay, M.Z., Poh, C.M., Renia, L., Macary, P.A., and Ng, L.F.P. (2020). The trinity of COVID-19: immunity, inflammation and intervention. Nat. Rev. Immunol. *20*, 363–374.

Tiller, T., Meffre, E., Yurasov, S., Tsuiji, M., Nussenzweig, M.C., and Wardemann, H. (2008). Efficient generation of monoclonal antibodies from single human B cells by single cell RT-PCR and expression vector cloning. J. Immunol. Methods *329*, 112–124.

Voss, N.R., Yoshioka, C.K., Radermacher, M., Potter, C.S., and Carragher, B. (2009). DoG Picker and TiltPicker: software tools to facilitate particle selection in single particle electron microscopy. J. Struct. Biol. *166*, 205–213.

Walls, A.C., Park, Y.J., Tortorici, M.A., Wall, A., McGuire, A.T., and Veesler, D. (2020). Structure, Function, and Antigenicity of the SARS-CoV-2 Spike Glycoprotein. Cell *181*, 281–292.e6.

Wang, Q., Zhang, Y., Wu, L., Niu, S., Song, C., Zhang, Z., Lu, G., Qiao, C., Hu, Y., Yuen, K.Y., et al. (2020). Structural and Functional Basis of SARS-CoV-2 Entry by Using Human ACE2. Cell *181*, 894–904.e9.

Wardemann, H., and Busse, C.E. (2019). Expression Cloning of Antibodies from Single Human B Cells. Methods Mol. Biol. *1956*, 105–125.

Wellcome and IAVI (2020). Expanding access to monoclonal antibody-based products: a global call to action. https://www.iavi.org/news-resources/expanding-access-to-monoclonal-antibody-based-products-a-global-call-to-action.

Wrapp, D., Wang, N., Corbett, K.S., Goldsmith, J.A., Hsieh, C.L., Abiona, O., Graham, B.S., and McLellan, J.S. (2020). Cryo-EM structure of the 2019-nCoV spike in the prefusion conformation. Science *367*, 1260–1263.

Yuan, M., Liu, H., Wu, N.C., Lee, C.-C.D., Zhu, X., Zhao, F., Huang, D., Yu, W., Hua, Y., Tien, H., et al. (2020). Structural basis of a shared antibody response to SARS-CoV-2. Science *369*, 1119–1123.

Zalevsky, J., Chamberlain, A.K., Horton, H.M., Karki, S., Leung, I.W.L., Sproule, T.J., Lazar, G.A., Roopenian, D.C., and Desjarlais, J.R. (2010). Enhanced antibody half-life improves in vivo activity. Nat. Biotechnol. *28*, 157–159.

Zost, S.J., Gilchuk, P., Case, J.B., Binshtein, E., Chen, R.E., Nkolola, J.P., Schäfer, A., Reidy, J.X., Trivette, A., Nargi, R.S., et al. (2020a). Potently neutralizing and protective human antibodies against SARS-CoV-2. Nature *584*, 443–449.

Zost, S.J., Gilchuk, P., Chen, R.E., Case, J.B., Reidy, J.X., Trivette, A., Nargi, R.S., Sutton, R.E., Suryadevara, N., Chen, E.C., et al. (2020b). Rapid isolation and profiling of a diverse panel of human monoclonal antibodies targeting the SARS-CoV-2 spike protein. Nat. Med. *26*, 1422–1427.

Zou, X., Chen, K., Zou, J., Han, P., Hao, J., and Han, Z. (2020). Single-cell RNA-seq data analysis on the receptor ACE2 expression reveals the potential risk of different human organs vulnerable to 2019-nCoV infection. Front. Med. *14*, 185–192.

Zuo, Y., Estes, S.K., Ali, R.A., Gandhi, A.A., Yalavarthi, S., Shi, H., Sule, G., Gockman, K., Madison, J.A., Zuo, M., et al. (2020). Prothrombotic autoantibodies in serum from patients hospitalized with COVID-19. Sci. Transl. Med. *12*, eabd3876.

Please cite this article in press as: Andreano et al., Extremely potent human monoclonal antibodies from COVID-19 convalescent patients, Cell (2021), https://doi.org/10.1016/j.cell.2021.02.035

STAR★METHODS

KEY RESOURCES TABLE

REAGENT or RESOURCE	SOURCE	IDENTIFIER
Antibodies and fluorophores		
CD19 V421	BD Biosciences	Cat# 562440; RRID:AB_11153299
IgM PerCP-Cy5.5	BD Biosciences	Cat# 561285; RRID:AB_10611998
CD27 PE	BD Biosciences	Cat# 340425; RRID:AB_400032
IgD-A700	BD Biosciences	Cat# 561302; RRID:AB_10646035
CD3 PE-Cy7	BioLegend	Cat# 300420; RRID:AB_439781
CD14 PE-Cy7	BioLegend	Cat# 301814; RRID:AB_389353
Streptavidin-PE	Thermo Fisher	Cat#12-4317-87
Goat Anti-Human IgA-UNLB	Southern Biotech	Cat# 2050-01; RRID:AB_2795701
Goat Anti-Human IgA-Alkaline Phosphatase	Southern Biotech	Cat# 2050-04; RRID:AB_2795704
Goat Anti-Human IgG-UNLB	Southern Biotech	Cat# 2040-01; RRID:AB_2795640
Bacterial and virus strains		
SARS-CoV-2 wild type	EVAg	GenBank: MT066156.1
SARS-CoV-2 D614G	EVAg	GenBank: MT527178.1
SARS-CoV-2 B.1.1.7	INMI	GISAID accession number: EPI_ISL_736997
Biological samples		
PBMCs and IgGs of donor PT-004	This paper	N/A
PBMCs and IgGs of donor PT-005	This paper	N/A
PBMCs and IgGs of donor PT-006	This paper	N/A
PBMCs and IgGs of donor PT-008	This paper	N/A
PBMCs and IgGs of donor PT-009	This paper	N/A
PBMCs and IgGs of donor PT-010	This paper	N/A
PBMCs and IgGs of donor PT-012	This paper	N/A
PBMCs and IgGs of donor PT-014	This paper	N/A
PBMCs and IgGs of donor PT-041	This paper	N/A
PBMCs and IgGs of donor PT-100	This paper	N/A
PBMCs and IgGs of donor PT-101	This paper	N/A
PBMCs and IgGs of donor PT-102	This paper	N/A
PBMCs and IgGs of donor PT-103	This paper	N/A
PBMCs and IgGs of donor PT-188	This paper	N/A
Chemicals, peptides, and recombinant proteins		
Fetal Bovine Serum (FBS) Hyclone	Sigma-Aldrich	Cat#D2650
DMSO	Sigma-Aldrich	Cat#D2650
RNaseOUT Recombinant Ribonuclease Inhibitor	Thermo Fisher	Cat#10777-019
SuperScript IV Reverse Transcriptase	Thermo Fisher	Cat#18091200
DEPC-Treated water	Thermo Fisher	Cat#AM9916
dNTP Set (100 mM)	Thermo Fisher	Cat#10297018
MgCl2 Magnesium Chloride 25mM	Thermo Fisher	Cat#AB0359
Kapa Long Range Polymerase	Sigma-Aldrich	Cat#KK3005
NEBuilder® HiFi DNA Assembly Master Mix	New England BioLabs	Cat#E2621X
Q5® High-Fidelity DNA Polymerases	New England BioLabs	Cat#M0491L
Expi293™ Expression Medium	Thermo Fisher	Cat#A1435101

(*Continued on next page*)

Please cite this article in press as: Andreano et al., Extremely potent human monoclonal antibodies from COVID-19 convalescent patients, Cell (2021), https://doi.org/10.1016/j.cell.2021.02.035

Continued

REAGENT or RESOURCE	SOURCE	IDENTIFIER
ExpiFectamine™ 293 Transfection Kit	Thermo Fisher	Cat#A14524
Ultra Pure Bovine serum albumin (BSA)	Thermo Fisher	Cat#AM2618
DMEM high Glucose	Thermo Fisher	Cat#11965092
Ficoll-Paque™ PREMIUM	Sigma-Aldrich	Cat#GE17-5442-03
MycoZap Plus-PR	Lonza	Cat#VZA2022
IMDM with GlutaMAX	Thermo Fisher	Cat# 31980048
Benzonase Nuclease	Sigma-Aldrich	Cat#70664-3
IL-2 Recombinant Human Protein	Thermo Fisher	Cat#PHC0023
IL-21 Recombinant Human Protein	Thermo Fisher	Cat#PHC0211
Strep-Tactin DY488	IBA lifesciences	Cat#2-1562-050
Slide-A-Lyzer™ Dialysis Cassettes	Thermo Fisher	Cat#66003
HiTrap Protein G HP column	Cytiva	Cat#17040503
HisTrap FF Crude column	Cytiva	Cat#17528601
SARS Coronavirus Spike Glycoprotein (S1)	The Native Antigen Company	Cat#REC31809
SARS Coronavirus Spike Glycoprotein (S2)	The Native Antigen Company	Cat#REC31807
Tween-20	VWR	Cat#A4974.0250
SARS Coronavirus Spike Glycoprotein (S1)	The Native Antigen Company	Cat#REC31806-500
SARS Coronavirus Spike Glycoprotein (S2)	The Native Antigen Company	Cat#REC31807-500
Alkaline Phosphatase Yellow (pNPP) Liquid Substrate System	Sigma-Aldrich	Cat#P7998
Goat Anti-Human IgG-UNLB	SouthernBiotech	Cat#2040-01
Critical commercial assays		
NOVA Lite Hep-2 ANA Kit	Inova Diagnostics / Werfen	Cat#066708100
ELISA Starter Accessory Kit	Bethyl Laboratories	Cat#E101
APEX Alexa Fluor 647 Antibody Labeling Kit	Thermo Fisher	Cat#A10475
Pierce BCA Protein Assay Kit	Thermo Fisher	Cat#23227
Deposited data		
Cloned and tested SARS-CoV-2-neutralizing antibodies	This paper	Patent Application
Experimental models: cell lines		
VERO E6 cell line	ATCC	Cat#CRL-1586
Expi293F™ cells	Thermo Fisher	Cat#A14527
3T3-msCD40L Cells	NIH AIDS Reagent Program	Cat#12535
Oligonucleotides		
Single cell PCR Primer	This paper	N/A
Random Hexamer Primer	Thermo Fisher	Cat#SO142
TAP forward primer (TTAGGCACCCCAGGCTTTAC)	This paper	N/A
TAP forward primer (AGATGGTTCTTTCCGCCTCA)	This paper	N/A
Recombinant DNA		
Human antibody expression vectors (IgG1, Igl, Igk)	(Tiller et al., 2008)	N/A
Plasmid encoding SARS-CoV-2 S ectodomain (amino acids 1-1208 of SARS-CoV-2 S; GenBank: MN908947)	(Wrapp et al., 2020)	N/A
Plasmid encoding SARS-CoV-2 RBD (amino acids 319 - 591 of SARS-CoV-2 S; GenBank: MN908947)	Jason McLellan Lab	N/A
pCDNA3.1+-SARS-CoV-2 Spike from Wuhan-Hu-1 isolate (GenBank MN908947.3) codon optimized	This paper	pCDNA-S2

(*Continued on next page*)

Please cite this article in press as: Andreano et al., Extremely potent human monoclonal antibodies from COVID-19 convalescent patients, Cell (2021), https://doi.org/10.1016/j.cell.2021.02.035

Continued

REAGENT or RESOURCE	SOURCE	IDENTIFIER
pCAGGS-SARS-CoV-2 Spike from Wuhan-Hu-1 isolate (GenBank MN908947.3) encoding D614G mutation and codon optimized	This paper	pCAGGS-S2 D614G
pCAGGS-SARS1 Spike protein codon optimized	(Carnell et al., 2017)	pCAGGS-S1
pCAGGS-MERS Spike protein codon optimized	(Grehan et al., 2015)	pCAGGS-MERS
pCSFLW Firefly luciferase encoding plasmid	(Carnell et al., 2015)	pCSFLW
p8.91 HIV Gag/Pol-encoding plasmid	(Carnell et al., 2015)	p8.91
Software and algorithms		
Prism 8	GraphPad	https://www.graphpad.com/
FlowJo 10.5.3	FlowJo, LLC	https://www.flowjo.com
FastQC	Babraham Institute	https://www.bioinformatics.babraham.ac.uk/projects/fastqc/
MultiQC 1.9	MultiQC	https://multiqc.info/
Trimmomatic 0.39	USADELLAB	http://www.usadellab.org/cms/?page=trimmomatic
MiXCR	MI Lanoratory	https://mixcr.readthedocs.io/en/master/index.html
NumPy	NumPy	https://numpy.org/
Python 3.7.4	Python Software Foundation	https://www.python.org/
Other		
BD FACS Aria III Cell Sorter	BD Biosciences	https://www.bdbiosciences.com
BD FACS Canto II	BD Biosciences	https://www.bdbiosciences.com
Leica DMI-microscope	Leica Biosystem	https://www.leica-microsystems.com
LUNA-II Automated Cell Counter	Logo Biosystems	https://logosbio.com
Qubit Fluorometric Quantification	Thermo Fisher	https://www.thermofisher.com
ÄKTA go	Cytiva Lifesciences	https://www.cytivalifesciences.com
GloMax Luminometer	Promega	https://ita.promega.com
Varioskan LUX multimode microplate reader	Thermo Fisher	https://www.thermofisher.com

RESOURCE AVAILABILITY

Lead contact

Further information and requests for resources and reagents should be directed to and will be fulfilled by the Lead Contact, Rino Rappuoli (rino.r.rappuoli@gsk.com).

Materials availability

Reasonable amounts of antibodies will be made available by the Lead Contact upon request under a Material Transfer Agreement (MTA) for non-commercial usage.

Data and code availability

Nucleotide and amino acidic sequences of all SARS-CoV-2-neutralizing antibodies were deposited in the Italian patent applications n. 102020000015754 filed on June 30th 2020 and 102020000018955 filed on August 3rd 2020. The accession number for the nucleotide sequences of all SARS-CoV-2-neutralizing antibodies reported in this paper is GenBank: MW_598287 - MW_598314.

EXPERIMENTAL MODEL AND SUBJECT DETAILS

Enrollment of SARS-COV-2 convalescent donors and human sample collection

This work results from a collaboration with the National Institute for Infectious Diseases, IRCCS – Lazzaro Spallanzani Rome (IT) and Azienda Ospedaliera Universitaria Senese, Siena (IT) that provided samples from SARS-CoV-2 convalescent donors, of both sexes, who gave their written consent. The study was approved by local ethics committees (Parere 18_2020 in Rome and Parere 17065 in Siena) and conducted according to good clinical practice in accordance with the declaration of Helsinki (European Council 2001, US Code of Federal Regulations, ICH 1997). This study was unblinded and not randomized.

Please cite this article in press as: Andreano et al., Extremely potent human monoclonal antibodies from COVID-19 convalescent patients, Cell (2021), https://doi.org/10.1016/j.cell.2021.02.035

CellPress

METHOD DETAILS

Single cell sorting of SARS-CoV-2 S-protein$^+$ memory B cells from COVID-19 convalescent donors

Blood samples were screened for SARS-CoV-2 RNA and for antibodies against HIV, HBV and HCV. Peripheral blood mononuclear cells (PBMCs) were isolated from heparin-treated whole blood by density gradient centrifugation (Ficoll-Paque PREMIUM, Sigma-Aldrich). After separation, PBMC were stained with Live/Dead Fixable Aqua (Invitrogen; Thermo Scientific) in 100 μL final volume diluted 1:500 at room temperature RT. After 20 min incubation cells were washed with PBS and unspecific bindings were saturated with 50 μL of 20% normal rabbit serum (Life technologies) in PBS . Following 20 min incubation at 4°C cells were washed with PBS and stained with SARS-CoV-2 S-protein labeled with Strep-Tactin®XT DY-488 (iba-lifesciences cat# 2-1562-050) for 30 min at 4°C. After incubation the following staining mix was used CD19 V421 (BD cat# 562440), IgM PerCP-Cy5.5 (BD cat# 561285), CD27 PE (BD cat# 340425), IgD-A700 (BD cat# 561302), CD3 PE-Cy7 (BioLegend cat# 300420), CD14 PE-Cy7 (BioLegend cat# 301814), CD56 PE-Cy7 (BioLegend cat# 318318) and cells were incubated at 4°C for additional 30 min. Stained MBCs were single cell-sorted with a BD FACS Aria III (BD Biosciences) into 384-well plates containing 3T3-CD40L feeder cells and were incubated with IL-2 and IL-21 for 14 days as previously described (Huang et al., 2013).

Expression and purification of SARS-CoV-2 S-protein prefusion trimer and receptor binding domain

Plasmid encoding SARS-CoV-2 S-2P construct (Wrapp et al., 2020) and S-protein RBD (generously provided by Jason S. McLellan) were transiently transfected at 1 μg/mL culture into Expi293F cells (Thermo Fisher) using ExpiFectamine 293 Reagent. Cells were grown for six days at 37°C with 8% CO_2 shaking 125 rpm according to the manufacturer's protocol (Thermo Fisher); ExpiFectamine 293 Transfection Enhancers 1 and 2 were added 16 to 18 h post-transfection to boost transfection, cell viability, and protein expression. Cell cultures were harvested three and six days after transfection. Cells were separated from the medium by centrifugation (1,100 g for 10 min at 24°C). Collected supernatants were then pooled and clarified by centrifugation (3,000 g for 15 min at 4°C) followed by filtration through a 0.45 μm filter. Chromatography was conducted at room temperature using the ÄKTA go purification system from GE Healthcare Life Sciences. Expressed proteins were purified by using an immobilized metal affinity chromatography (FF Crude) followed by dialysis into final buffer. Specifically, the filtrated culture supernatant was purified with a 5 mL HisTrap FF Crude column (GE Healthcare Life Sciences) previously equilibrated in Buffer A (20 mM NaH_2PO_4, 500 mM NaCl + 30 mM imidazol pH 7.4).

The flow rate for all steps of the HisTrap FF Crude column was 5 mL/min. The culture supernatant of spike and RBD cell culture was applied to a single 5 mL HisTrap FF Crude column. The column was washed in Buffer A for 4 column volumes (CV) with the all 4 CV collected as the column wash. Recombinant proteins were eluted from the column applying a first step elution of 4 CV of 50% Buffer B (20 mM NaH2PO4, 500 mM NaCl + 500 mM imidazol pH 7.4) and a second step elution of 2 CV of 100% Buffer B. Elution steps were collected in 1 fractions of 1 mL each. Eluted fractions were analyzed by SDS-PAGE and appropriate fractions containing recombinant proteins were pooled. Final pools were dialyzed against phosphate buffered saline (PBS) pH 7.4 using Slide-A-Lyzer G2 Dialysis Cassette 3.5K (Thermo Scientific) overnight at 4°C. The dialysis buffer used was at least 200 times the volume of the sample.

The final protein concentration was determined by measuring the A520 using the Pierce BCA protein assay kit (Thermo Scientific). Final protein was dispensed in aliquots of 0.5 mL each and stored at −80°C.

ELISA assay with S1 and S2 subunits of SARS-CoV-2 S-protein

The presence of S1- and S2-binding antibodies in culture supernatants of monoclonal S-protein-specific memory B cells was assessed by means of an ELISA implemented with the use of a commercial kit (ELISA Starter Accessory Kit, Catalogue No. E101; Bethyl Laboratories). Briefly, 384-well flat-bottom microtiter plates (384 well plates, Microplate Clear, Greiner Bio-one) were coated with 25 μL/well of antigen (1:1 mix of S1 and S2 subunits, 1 μg/mL each; The Native Antigen Company, Oxford, United Kingdom) diluted in coating buffer (0.05 M carbonate-bicarbonate solution, pH 9.6), and incubated overnight at 4°C. The plates were then washed three times with 100 μL/well washing buffer (50 mM Tris Buffered Saline (TBS) pH 8.0, 0.05% Tween-20) and saturated with 50 μL/well blocking buffer containing Bovine Serum Albumin (BSA) (50 mM TBS pH 8.0, 1% BSA, 0.05% Tween-20) for 1 h (h) at 37°C. After further washing, samples diluted 1:5 in blocking buffer were added to the plate. Blocking buffer was used as a blank. After an incubation of 1 h at 37°C, plates were washed and incubated with 25 μL/well secondary antibody (horseradish peroxidase (HRP)-conjugated goat anti-human IgG-Fc Fragment polyclonal antibody, diluted 1:10,000 in blocking buffer, Catalogue No. A80-104P; (Bethyl Laboratories) for 1 h at 37°C. After three washes, 25 μL/well TMB One Component HRP Microwell Substrate (Bethyl Laboratories) was added and incubated 10–15 min at RT in the dark. Color development was terminated by addition of 25 μL/well 0.2 M H_2SO_4. Absorbance was measured at 450 nm in a Varioskan Lux microplate reader (Thermo Fisher Scientific). Plasma from COVID-19 convalescent donors (Andreano et al., 2020) and unrelated plasma were used as positive and negative control respectively. The threshold for sample positivity was set at twice the optical density (OD) of the blank.

ELISA assay with SARS-CoV-2 S-protein prefusion trimer and S1 – S2 subunits

ELISA assay was used to detect SARS-CoV-2 S-protein specific mAbs and to screen plasma from SARS-CoV-2 convalescent donors. 384-well plates (384 well plates, microplate clear; Greiner Bio-one) were coated with 3 μg/mL of streptavidin (Thermo Fisher) diluted in coating buffer (0.05 M carbonate-bicarbonate solution, pH 9.6) and incubated at RT overnight. Plates were then coated with SARS-CoV-2 S-protein, S1 or S2 domains at 3 μg/mL and incubated for 1 h at RT. 50 μL/well of saturation buffer (PBS/BSA 1%) was

Please cite this article in press as: Andreano et al., Extremely potent human monoclonal antibodies from COVID-19 convalescent patients, Cell (2021), https://doi.org/10.1016/j.cell.2021.02.035

used to saturate unspecific binding and plates were incubated at 37°C for 1 h without CO_2. For the first round of screening, supernatants were diluted 1:5 in PBS/BSA 1%/Tween20 0.05% in 25 μL/well final volume and incubated for 1 h at 37°C without CO_2. For purified antibodies, and to assess EC_{50}, mAbs were tested at a starting concentration of 5 μg/mL and diluted step 1:2 in PBS/BSA 1%/Tween20 0.05% in 25 μL/well final volume for 1 h at 37°C without CO_2. 25 μL/well of alkaline phosphatase-conjugated goat anti-human IgG (Sigma-Aldrich) and IgA (Southern Biotech) were used as secondary antibodies. Wells were washed three times between each step with PBS/BSA 1%/Tween20 0.05%. pNPP (p-nitrophenyl phosphate) (Sigma-Aldrich) was used as soluble substrate to detect SARS-CoV-2 S-protein, S1 or S2 specific mAbs and the final reaction was measured by using the Varioskan Lux Reader (Thermo Fisher Scientific) at a wavelength of 405 nm. Plasma from COVID-19 convalescent donors (Andreano et al., 2020) and unrelated plasma were used as positive and negative control respectively. Samples were considered as positive if OD at 405 nm (OD_{405}) was twice the blank.

SARS-CoV-2 virus and cell infection

African green monkey kidney cell line Vero E6 cells (American Type Culture Collection [ATCC] #CRL-1586) were cultured in Dulbecco's Modified Eagle's Medium (DMEM) - high glucose (Euroclone, Pero, Italy) supplemented with 2 mM L- Glutamine (Lonza, Milano, Italy), penicillin (100 U/mL) - streptomycin (100 μg/mL) mixture (Lonza, Milano, Italy) and 10% Foetal Bovine Serum (FBS) (Euroclone, Pero, Italy). Cells were maintained at 37°C, in a 5% CO_2 humidified environment and passaged every 3-4 days.

Wild type SARS-CoV-2 (SARS-CoV-2/INMI1-Isolate/2020/Italy: MT066156), D614G (SARS-CoV-2/human/ITA/INMI4/2020, clade GR, D614G (S): MT527178) and B.1.1.7 (INMI-118 GISAID accession number EPI_ISL_736997) viruses were purchased from the European Virus Archive goes Global (EVAg, Spallanzani Institute, Rome)or received from the Spallanzani Institute, Rome. For virus propagation, sub-confluent Vero E6 cell monolayers were prepared in T175 flasks (Sarstedt) containing supplemented D-MEM high glucose medium. For titration and neutralization tests of SARS-CoV-2, Vero E6 were seeded in 96-well plates (Sarstedt) at a density of 1.5×10^4 cells/well the day before the assay.

Neutralization of Binding (NoB) Assay

To study the binding of the SARS-CoV-2 S-protein to cell-surface receptor(s) we developed an assay to assess recombinant S-protein specific binding to target cells and neutralization thereof. To this aim the stabilized S-protein was coupled to Streptavidin-PE (eBioscience # 12-4317-87, Thermo Fisher) for 1 h at RT and then incubated with Vero E6 cells. Binding was assessed by flow cytometry. The stabilized S-protein bound Vero E6 cells with high affinity (data not shown). To assess the content of neutralizing antibodies in sera or in B cell culture supernatants, two microliters of SARS-CoV-2 Spike-Streptavidin-PE at 5 - 10 μg/mL in PBS-5%FCS were mixed with two microliters of various dilutions of sera or B cell culture supernatants in U bottom 96-well plates. After incubation at 37°C for 1 h, 30×10^3 Vero E6 cells suspended in two microliters of PBS 5% FCS were added and incubated for additional 45 min at 4°C. Non-bound protein and antibodies were removed and cell-bound PE-fluorescence was analyzed with a FACS Canto II flow cytometer (Becton Dickinson). Data were analyzed using the FlowJo data analysis software package (TreeStar, USA). The specific neutralization was calculated as follows: NoB (%) = 1 – (Sample MFI value – background MFI value) / (Negative Control MFI value – background MFI value). Plasma from COVID-19 convalescent donors (Andreano et al., 2020) and unrelated plasma were used as positive and negative control respectively.

Single cell RT-PCR and Ig gene amplification

From the original 384-well sorting plate, 5 μL of cell lysate was used to perform RT-PCR. Total RNA from single cells was reverse transcribed in 25 μL of reaction volume composed by 1 μL of random hexamer primers (50 ng/μL), 1 μL of dNTP-Mix (10 mM), 2 μL 0.1 M DTT, 40 U/μL RNase OUT, $MgCl_2$ (25 mM), 5x FS buffer and Superscript IV reverse transcriptase (Invitrogen). Final volume was reached by adding nuclease-free water (DEPC). Reverse transcription (RT) reaction was performed at 42°C/10', 25°C/10', 50°C/60' and 94°/5¿. Heavy (VH) and light (VL) chain amplicons were obtained via two rounds of PCR. All PCR reactions were performed in a nuclease-free water (DEPC) in a total volume of 25 μL/well. Briefly, 4 μL of cDNA were used for the first round of PCR (PCRI). PCRI-master mix contained 10 μM of VH and 10 μM VL primer-mix, 10mM dNTP mix, 0.125 μL of Kapa Long Range Polymerase (Sigma), 1.5 μL MgCl2 and 5 μL of 5x Kapa Long Range Buffer. PCRI reaction was performed at 95°/3¿, 5 cycles at 95°C/30'', 57°C/30'', 72°C/30'' and 30 cycles at 95°C/30'', 60°C/30'', 72°C/30'' and a final extension of 72°/2'. All nested PCR reactions (PCRII) were performed using 3.5 μL of unpurified PCRI product using the same cycle conditions. PCRII products were then purified by Millipore MultiScreen® PCRμ96 plate according to manufacture instructions. Samples were eluted with 30 μL nuclease-free water (DEPC) into 96-well plates and quantify by.

Cloning of variable region genes and recombinant antibody expression in transcriptionally active PCR

Vector digestions were carried out with the respective restriction enzymes AgeI, SalI and XhoI as previously described (Tiller et al., 2008, Wardemann and Busse, 2019). Briefly, 75 ng of IgH, Igλ and Igκ purified PCRII products were ligated by using the Gibson Assembly NEB into 25 ng of respective human Igγ1, Igκ and Igλ expression vectors. The reaction was performed into 5 μL of total volume. Ligation product was 10-fold diluted in nuclease-free water (DEPC) and used as template for transcriptionally active PCR (TAP) reaction which allowed the direct use of linear DNA fragments for *in vitro* expression. The entire process consists of one PCR amplification step, using primers to attach functional promoter (human CMV) and terminator sequences (SV40) onto the

Please cite this article in press as: Andreano et al., Extremely potent human monoclonal antibodies from COVID-19 convalescent patients, Cell (2021), https://doi.org/10.1016/j.cell.2021.02.035

fragment PCRII products. TAP reaction was performed in a total volume of 25 μL using 5 μL of Q5 polymerase (NEB), 5 μL of GC Enhancer (NEB), 5 μL of 5X buffer,10 mM dNTPs, 0.125 μL of forward/reverse primers and 3 μL of ligation product. TAP reaction was performed by using the following cycles: 98°/2', 35 cycles 98°/10'', 61°/20'', 72°/1' and 72°/5¿ as final extention step. TAP products were purified under the same PCRII conditions, quantified by Qubit Fluorometric Quantitation assay (Invitrogen) and used for transient transfection in Expi293F cell line using manufacturing instructions.

Flask expression and purification of human monoclonal antibodies

Expi293F cells (Thermo Fisher) were transiently transfected with plasmids carrying the antibody heavy chain and the light chains with a 1:2 ratio. Cells were grown for six days at 37°C with 8% CO_2 shaking at 125 rpm according to the manufacturer's protocol (Thermo Fisher); ExpiFectamine 293 transfection enhancers 1 and 2 were added 16 to 18 h post-transfection to boost cell viability and protein expression. Cell cultures were harvested three and six days after transfection. Cells were separated from the medium by centrifugation (1,100 g for 10 min at 24°C). Supernatants collected were then pooled and clarified by centrifugation (3000 g for 15 min, 4°C) followed by filtration through a 0.45 μm filter. Chromatography was conducted at room temperature using the ÄKTA go purification system from GE Healthcare Life Sciences. Affinity chromatography was used to purify expressed monoclonal antibodies using an immobilized protein G column able to bind to Fc region. Specifically, filtrated culture supernatants were purified with a 1 mL HiTrap Protein G HP column (GE Healthcare Life Sciences) previously equilibrated in Buffer A (0.02 M NaH_2PO_4 pH 7). The flow rate for all steps of the HiTrap Protein G HP column was 1 mL/min. The culture supernatant for every monoclonal antibody cell culture was applied to a single 1 mL HiTrap Protein G HP column. The column was equilibrated in Buffer A for at least 6 column volumes (CV) which was collected as column wash. Each monoclonal antibody was eluted from the column applying a step elution of 6 CV of Buffer B (0.1 M glycine-HCl, pH 2.7). Elution steps were collected in 1 fractions of 1 mL each. Eluted fractions were analyzed by non-reducing SDS-PAGE and fractions showing the presence of IgG were pooled together. Final pools was dialyzed in PBS buffer pH 7.4 using Slide-A-Lyzer G2 Dialysis Cassette 3.5K (Thermo Scientific) overnight at 4°C. The dialysis buffer used was at least 200 times the volume of the sample. For each antibody purified the concentration was determined by measuring the A520 using Pierce BCA Protein Assay Kit (Thermo Scientific). All the purified antibodies were aliquoted and stored at −80°C.

Viral propagation and titration

The SARS-CoV-2 virus was propagated in Vero E6 cells cultured in DMEM high Glucose supplemented with 2% FBS, 100 U/mL penicillin, 100 μg/mL streptomycin. Cells were seeded at a density of $1x10^6$ cells/mL in T175 flasks and incubated at 37°C, 5% CO_2 for 18 - 20 h. The sub-confluent cell monolayer was then washed twice with sterile Dulbecco's PBS (DPBS). Cells were inoculated with 3,5 mL of the virus properly diluted in DMEM 2% FBS at a multiplicity of infection (MOI) of 0.001, and incubated for 1 h at 37°C in a humidified environment with 5% CO_2. At the end of the incubation, 50 mL of DMEM 2% FBS were added to the flasks. The infected cultures were incubated at 37°C, 5% CO_2 and monitored daily until approximately 80%–90% of the cells exhibited cytopathic effect (CPE). Culture supernatants were then collected, centrifuged at 4°C at 1,600 rpm for 8 min to allow removal of cell debris, aliquoted and stored at −80°C as the harvested viral stock. Viral titers were determined in confluent monolayers of Vero E6 cells seeded in 96-well plates using a 50% tissue culture infectious dose assay ($TCID_{50}$). Cells were infected with serial 1:10 dilutions (from 10^{-1} to 10^{-11}) of the virus and incubated at 37°C, in a humidified atmosphere with 5% CO_2. Plates were monitored daily for the presence of SARS-CoV-2 induced CPE for 4 days using an inverted optical microscope. The virus titer was estimated according to Spearman-Karber formula (Kundi, 1999) and defined as the reciprocal of the highest viral dilution leading to at least 50% CPE in inoculated wells.

SARS-CoV-2 authentic virus neutralization assay

All SARS-CoV-2 authentic virus neutralization assays were performed in the biosafety level 3 (BSL3) laboratories at Toscana Life Sciences in Siena (Italy) and Vismederi Srl, Siena (Italy). BSL3 laboratories are approved by a Certified Biosafety Professional and are inspected every year by local authorities. The neutralization activity of culture supernatants from monoclonal was evaluated using a CPE-based assay as previously described (Manenti et al., 2020). S-protein-specific memory B cells produced antibodies were initially evaluated by means of a qualitative live-virus based neutralization assay against a one-point dilution of the samples. Supernatants were mixed in a 1:3 ratio with a SARS-CoV-2 viral solution containing 25 $TCID_{50}$ of virus (final volume: 30 μL). After 1 h incubation at 37°C, 5% CO_2, 25 μL of each virus-supernatant mixture was added to the wells of a 96-well plate containing a sub-confluent Vero E6 cell monolayer. Following a 2 h incubation at 37°C, the virus-serum mixture was removed and 100 μl of DMEM 2% FBS were added to each well. Plates were incubated for 3 days at 37°C in a humidified environment with 5% CO_2, then examined for CPE by means of an inverted optical microscope. Absence or presence of CPE was defined by comparison of each well with the positive control (plasma sample showing high neutralizing activity of SARS-CoV-2 in infected Vero E6 cells (Andreano et al., 2020) and negative control (human serum sample negative for SARS-CoV-2 in ELISA and neutralization assays). Following expression as full-length IgG1 recombinant antibodies were quantitatively tested for their neutralization potency against both the wild type, D614G variant and the B.1.1.7 emerging variants. The assay was performed as previously described but using a viral titer of 100 $TCID_{50}$. Antibodies were prepared at a starting concentration of 20 μg/mL and diluted step 1:2. Technical triplicates were performed for each experiment.

Please cite this article in press as: Andreano et al., Extremely potent human monoclonal antibodies from COVID-19 convalescent patients, Cell (2021), https://doi.org/10.1016/j.cell.2021.02.035

Production and titration of SARS-CoV-2 pseudotyped lentiviral reporter particles

Pseudotype stocks were prepared by FuGENE-HD (Promega) co-transfection of HEK293T/17 with SARS-CoV-2 spike pcDNA3.1 + expression plasmid, HIV gag-pol p8.91 plasmid and firefly luciferase expressing plasmid pCSFLW in a 1:0.8:1.2 ratio. 2×10^6 cells/cm^2 were plated 24 h prior to transfection in 10cm cell culture dishes. 48 and 72 h post transfection, pseudotype-containing culture medium was harvested and filtered thought a 0.45um syringe filter to clear cell debris. Aliquots were stored at −80°C. Titration assays were performed by transduction of HEK293T/17 cells pre-transfected with ACE2 and TMPRRS2 plasmids to calculate the viral titer and infectious dose (PV input) for neutralization assays. SARS-CoV-2 D614G pseudotype was produced using the same procedure as described above. SARS-1 pseudotype was produced in a 1:0.5:0.8 ratio. MERS-pseudotype was produced as previously described (Grehan et al., 2015).

SARS-CoV-2 pseudotyped lentivirus neutralization assay

The potency of the neutralizing mAbs was assessed using lentiviral particles expressing SARS-CoV-2 spike protein on their surface and containing firefly luciferase as marker gene for detection of infection. Briefly, 2×10^6 HEK293T cells were pre-transfected in a 10 cm dish the day before the neutralization assay with ACE2 and TMPRSS2 plasmids in order to be used as optimal target cells for SARS-CoV-2 PV entry. In a 96-well plate mAbs were 2-fold serially diluted in duplicate in culture medium (DMEM supplemented with 10% fetal bovine serum and 1% penicillin/streptomycin) starting at 20 μg/mL in a total volume of 100 μL. $1x10^6$ RLU of SARS-CoV-2 pseudotyped lentiviral particles were added to each well and incubated at 37°C for 1 h. Each plate included PV plus cell only (virus control) and cells only (background control). 1×10^4 pre-transfected HEK293T cells suspended in 50 μL complete media were added per well and incubated for 48 h at 37°C and 5% CO2. Firefly luciferase activity (luminescence) was measured using the Bright-Glo assay system with a GloMax luminometer (Promega, UK). The raw Relative Luminescence Unit (RLU) data points were converted to a percentage neutralization value, whereby 100% neutralization equals the mean cell only RLU value control and 0% neutralization equals the mean PV only RLU value control. The normalized data was then plotted using Prism 8 (GraphPad) on a neutralization percentage scale and a NT50 value calculated, using the non-linear regression analysis. Plasma from COVID-19 convalescent donors showing neutralization activity against SARS-CoV-2 (Andreano et al., 2020) were also assessed in this assay.

Characterization of SARS-CoV-2 RBD-Antibodies binding by Flow cytometry

Flow cytometry analysis was performed to define antibodies interaction with S-protein-receptor-binding domain (RBD). Briefly, APEX Antibody Labeling Kits (Invitrogen) was used to conjugate 20 μg of selected antibodies to Alexa fluor 647, according to the manufacturer instructions. To assess the ability of each antibody to bind the RBD domain, 1 mg of magnetic beads (Dynabeads His-Tag, Invitrogen) were coated with 70 μg of histidine tagged RBD, and then 20 μg/mL of each labeled antibody were incubated with 40 μg/mL of beads-bound RBD for 1 h on ice. Then, samples were washed with 200 μL of Phosphate-buffered saline (PBS), resuspended in 150 μL of PBS and assessed with a FACS Canto II flow cytometer (Becton Dickinson). Results were analyzed by FlowJo (version 10).

Flow Cytometry-Based S-protein Competition assay

Antibodies specificity to bind SARS-CoV-2 S-protein and their possible competition was analyzed performing a Flow cytometer-based assay. To this aim, 200 μg of stabilized histidine tagged S-protein were coated with 1 mg of magnetic beads (Dynabeads His-Tag, Invitrogen). 20 μg of each antibody were labeled with Alexa fluor 647 working with the APEX Antibody Labeling Kits (Invitrogen). To test competitive binding profiles of the antibody panel selected, beads-bound S-protein (40 μg/mL) were pre-incubated with unlabeled antibodies (40 μg/mL) for 1 h on ice. Then, each set of the beads-antibody complexes were washed with PBS and separately incubated with each labeled antibody (20 μg/mL) for 1 h on ice. After incubation, the mix Beads-antibodies was washed, resuspended in 150 μL of PBS and analyzed using FACS Canto II flow cytometer (Becton Dickinson). Beads-bound and non-bound S-protein incubated with labeled antibodies were used as positive and negative control, respectively. Population gating and analysis was carried out using FlowJo (version 10).

Antigen-specific FcγR binding

Fluorescently coded microspheres were used to profile the ability of selected antibodies to interact with Fc receptors (Boudreau et al., 2020). The antigen of interest (SARS –CoV-2 S-protein RBD) was covalently coupled to different bead sets via primary amine conjugation. The beads were incubated with diluted antibody (diluted in PBS), allowing ''on bead'' affinity purification of antigen-specific antibodies. The bound antibodies were subsequently probed with tetramerized recombinant human FcγR2A and FcRN and analyzed using Luminex. The data is reported as the median fluorescence intensity of PE for a specific bead channel.

Antibody-dependent neutrophil phagocytosis

Antibody-dependent neutrophil phagocytosis (ADNP) assesses the ability of antibodies to induce the phagocytosis of antigen-coated targets by primary neutrophils. The assay was performed as previously described (Karsten et al., 2019, Boudreau et al., 2020). Briefly, fluorescent streptavidin-conjugated polystyrene beads were coupled to biotinylated SARS-CoV-2 Spike trimer. Diluted antibody (diluted in PBS) was added, and unbound antibodies were washed away. The antibody:bead complexes are added to primary neutrophils isolated from healthy blood donors using negative selection (StemCell EasySep Direct Human Neutrophil

Please cite this article in press as: Andreano et al., Extremely potent human monoclonal antibodies from COVID-19 convalescent patients, Cell (2021), https://doi.org/10.1016/j.cell.2021.02.035

Isolation Kit), and phagocytosis was allowed to proceed for 1 h. The cells were then washed and fixed, and the extent of phagocytosis was measured by flow cytometry. The data is reported as a phagocytic score, which considers the proportion of effector cells that phagocytosed and the degree of phagocytosis. Each sample is run in biological duplicate using neutrophils isolated from two distinct donors. The mAb were tested for ADNP activity at a range of 30 μg/mL to 137.17 ng/mL.

Antibody-dependent NK cell activation

Antibody-dependent NK cell activation (ADNKA) assesses antigen-specific antibody-mediated NK cell activation against protein-coated plates. This assay was performed as previously described (Boudreau et al., 2020). Stabilized SARS-CoV-2 Spike trimer was used to coat ELISA plates, which were then washed and blocked. Diluted antibody (diluted in PBS) was added to the antigen coated plates, and unbound antibodies were washed away. NK cells, purified from healthy blood donor leukopaks using commercially available negative selection kits (StemCell EasySep Human NK Cell Isolation Kit) were added, and the levels of IFN-γ was measured after 5 h using flow cytometry. The data is reported as the percent of cells positive for IFN-γ. Each sample is tested with at least two different NK cell donors, with all samples tested with each donor. The monoclonal antibodies were tested for ADNKA activity at a range of 20 μg/mL to 9.1449 ng/mL.

Affinity evaluation of SARS-CoV-2 neutralizing antibodies

Anti-Human IgG Polyclonal Antibody (Southern Biotech 2040-01) was immobilized via amine group on two flow cells of a CM5 sensor chip. For the immobilization, anti-human IgG Ab diluted in 10mM Na acetate pH 5.0 at the concentration of 25 μg/mL was injected for 360 s over the dextran matrix, which had been previously activated with a mixture of 0.1M 1-ethyl-3(3-dimethylaminopropyl)-carbodiimide (EDC) and 0.4 M N-hydroxyl succinimide (NHS) for 420 s. After injection of the antibody, Ethanolamine 1M was injected to neutralize activated group. 10 μL/min flow rate was used during the whole procedure. Anti-SPIKE protein human mAbs were diluted in HBS-EP+ (HEPES 10 mM, NaCl 150 mM, EDTA 3.4 mM, 0.05% p20, pH 7.4) and injected for 120 s at 10 μL/min flow rate over one of the two flow cells containing the immobilized Anti-Human IgG Antibody, while running buffer (HBS-EP+) was injected over the other flow cell to be taken as blank. Dilution of each mAb was adjusted in order to have comparable levels of RU for each capture mAb. Following the capture of each mAb by the immobilized anti-human IgG antibody, different concentrations of SPIKE protein (20 μg/mL, 10 μg/mL, 5 μg/mL, 2.5 μg/mL and 1 μg/mL in HBS-EP+) were injected over both the blank flow cell and the flow cell containing the captured mAb for 180 s at a flow rate of 80 μL/min. Dissociation was followed for 800 s, regeneration was achieved with a pulse (60 s) of Glycine pH 1.5. Kinetic rates and affinity constant of SPIKE protein binding to each mAb were calculated applying a 1:1 binding as fitting model using the Bia T200 evaluation software 3.1.

Autoreactivity screening test on HEp-2 Cells

The NOVA Lite HEp-2 ANA Kit (Inova Diagnostics) was used in accordance to the manufacturer's instructions to test antibodies the autoreactivity of selected antibodies which were tested at a concentration of 100 μg/mL. Kit positive and negative controls were used at three different dilutions (1:1, 1:10 and 1:100). Images were acquired using a DMI3000 B microscope (Leica) and an exposure time of 300 ms, channel intensity of 2000 and a gamma of 2.

Genetic Analyses of SARS-CoV-2 S-protein specific nAbs

A custom pipeline was developed for the analyses of antibody sequences and the characterization of the immunoglobulin genes. Raw sequences were stored as ab1 file and transformed into fastaq using Biopython. The reads were then quality checked using FastQC (https://www.bioinformatics.babraham.ac.uk/projects/fastqc/) and a report was generated using MultiQC (https://multiqc.info/). The antibody leader sequence and the terminal part of the constant region were removed by trimming using Trimmomatic (http://www.usadellab.org/cms/?page=trimmomatic). This latter program was also used to scan and remove low-quality reads using a sliding-window parameter. Once sequences were recovered, germline gene assignment and annotation were perfromed with MiXCR (https://mixcr.readthedocs.io/en/master/index.html), using the single-read alignment parameters, and a CSV-formatted output was generated. Finally, the sequences retrieved from the antibodies described in this manuscript were compared to published neutralizing antibodies against SARS-CoV-2. For this purpose, the Coronavirus Antibody Database, CoV-AbDab (http://opig.stats.ox.ac.uk/webapps/covabdab/) was downloaded and the antibodies with reported neutralization activity against SARS-CoV-2 were extracted. Comparison analysis were performed in Python using NumPy (https://numpy.org/) and, Pandas (https://pandas.pydata.org/) while figures were produced using the Matplotlib tool (https://matplotlib.org/) and Seaborn (https://seaborn.pydata.org/).

Negative-stain electron microscopy

Complexes were formed by incubating SARS-2 CoV-GSAS-6P-Mut7 and respective fabs at a 1:3 (trimer to fab) molar ratio for 30 min at room temperature. After diluting to 0.03 mg/mL in 1X TBS pH 7.4, the samples were deposited on plasma-cleaned copper mesh grids and stained with 2% uranyl formate for 55 s. Automated data collection was made possible through the Leginon software (Suloway et al., 2005) and a FEI Tecnai Spirit (120keV, 56,000x mag) paired with a FEI Eagle (4k by 4k) CCD camera. Other details include a defocus value of −1.5 μm, a pixel size of 2.06 Å per pixel, and a dose of 25 $e^{-}/Å^{2}$. Raw micrographs were stored in the Appion

Please cite this article in press as: Andreano et al., Extremely potent human monoclonal antibodies from COVID-19 convalescent patients, Cell (2021), https://doi.org/10.1016/j.cell.2021.02.035

database (Lander et al., 2009), particles were picked with DoGPicker (Voss et al., 2009), and 2D and 3D classification and refinements were performed in RELION 3.0 (Scheres, 2012). Map segmentation and model docking was done in UCSF Chimera (Pettersen et al., 2004).

Prophylactic and therapeutic passive transfer studies in golden Syrian hamsters

Six- to eight-month-old female Syrian hamsters were purchased from Charles River Laboratories and housed in microisolator units, allowed free access to food and water and cared for under U.S. Department of Agriculture (USDA) guidelines for laboratory animals. For the passive transfer prophylactic experiments, the day prior to SARS-CoV-2 infection six hamsters per group were intraperitoneally administered with 500 μL of a 4, 1 or 0.25 mg/kg dose of J08-MUT mAb. For the passive transfer therapeutic experiments, the day after SARS-CoV-2 infection six hamsters per group were intraperitoneally administered with 500 μL of a 4 mg/kg dose of J08-MUT mAb. Another two groups (n = 6/each) were administered with 500 μL of 4 mg/kg of the anti-influenza virus #1664 human mAb (manuscript in preparation) or PBS only to serve as human IgG1 isotype and mock control groups, respectively. The day after, hamsters were anesthetized using 5% isoflurane, and inoculated with 5×10^5 PFU of SARS-CoV-2 (2019-nCoV/USA-WA1/2020) via the intranasal route, in a final volume of 100 μL. Baseline body weights were measured before infection as well as monitored daily for 7 and 11 days post infection in the prophylactic and therapeutic studies respectively. All experiments with the hamsters were performed in accordance with the NRC Guide for Care and Use of Laboratory Animals, the Animal Welfare act, and the CDC/NIH Biosafety and Microbiological and Biomedical Laboratories as well as the guidelines set by the Institutional Animal Care and Use Committee (IACUC) of the University of Georgia who also approved the animal experimental protocol. All animal studies infection with SARS-CoV-2 were conducted in the Animal Health Research Center (AHRC) Biosafety Level 3 (BSL-3) laboratories of the University of Georgia.

Determination of viral load by $TCID_{50}$ assay

Lung tissues were homogenized in 1 mL of DMEM containing 1% fetal bovine serum (FBS) and 1% penicillin/streptomycin. The lung homogenate supernatant was diluted 10-fold (10° to 10^6) and used to determine median tissue culture infection dose ($TCID_{50}$) in Vero E6 cells as previously described (Jang and Ross, 2020).

Human IgG detection in hamster sera

ELISA assay was used to detect the human IgG J08-MUT in hamster sera. 384-well plates (384 well plates, Microplate Clear; Greiner Bio-one) were coated with 2 μg/mL of unlabled goat anti-human IgG (SouthernBiotech) diluted in sterile PBS and incubated at 4°C overnight. 50 μL/well of saturation buffer (PBS/BSA 1%) was used to saturate unspecific binding and plates were incubated at 37°C for 1 h without CO_2. Hamster sera were diluted in PBS/BSA 1%/Tween20 0.05% at a starting dilution of 1:10. Fourteen reciprocal dilutions were performed. Alkaline phosphatase-conjugated goat anti-human IgG (Sigma-Aldrich) was used as secondary antibody and pNPP (p-nitrophenyl phosphate) (Sigma-Aldrich) was used as soluble substrate. Wells were washed three times between each step with PBS/BSA 1%/Tween20 0.05%. The final reaction was measured by using the Varioskan Lux Reader (Thermo Fisher Scientific) at a wavelength of 405 nm. Samples were considered as positive if OD at 405 nm (OD_{405}) was twice the blank.

Cell
Article

CellPress

Supplemental figures

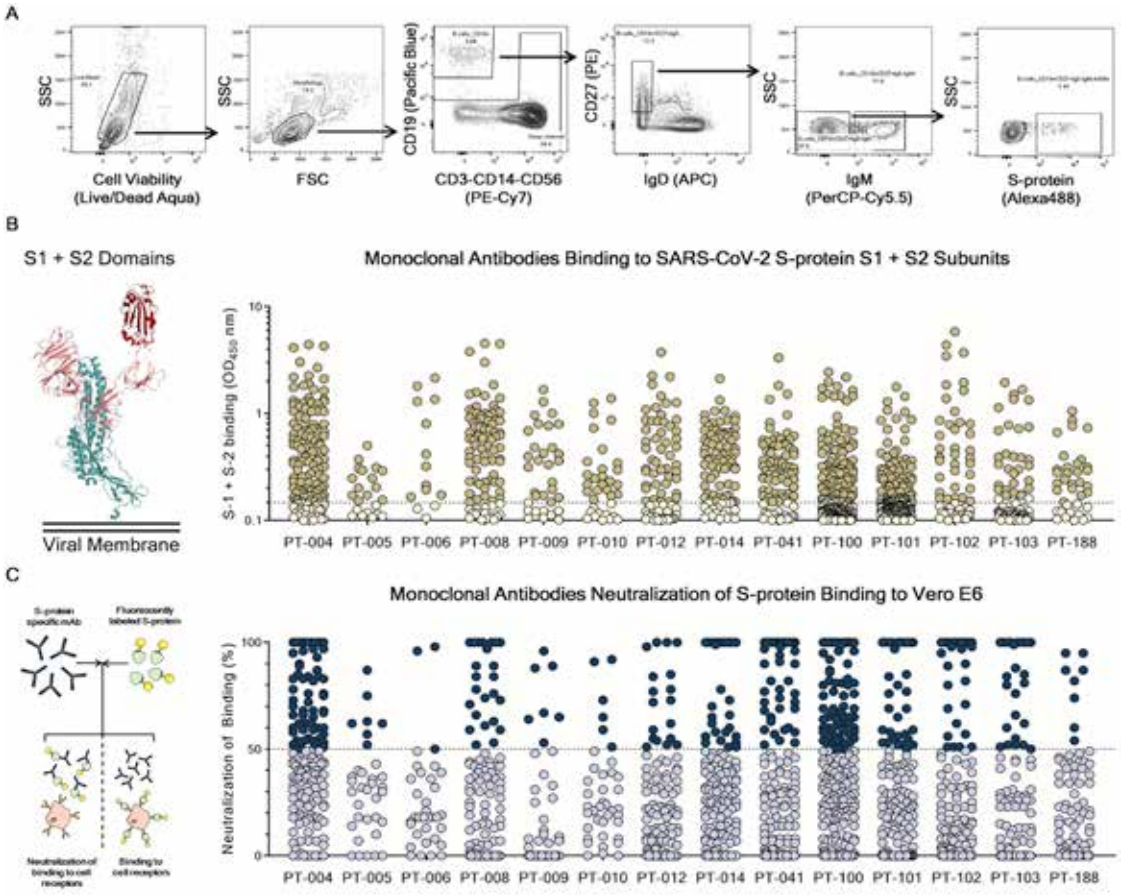

Figure S1. Gating strategy for single-cell sorting and monoclonal antibodies screening for S protein S1 + S2 subunits binding and neutralization of binding (NoB) activity, related to Figure 2

(A) Starting from top left to the right panel, the gating strategy shows: Live/Dead; Morphology; $CD19^+$ B cells; $CD19^+CD27^+IgD^-$; $CD19^+CD27^+IgD^-IgM^-$; $CD19^+CD27^+IgD^-IgM^-$S-protein$^+$ B cells.

(B) The graph shows supernatants tested for binding to the SARS-CoV-2 S-protein S1 + S2 subunits. Threshold of positivity has been set as two times the value of the blank (dotted line). Darker dots represent mAbs which bind to the S1 + S2 while light yellow dots represent mAbs which do not bind. (B) The graph shows supernatants tested by NoB assay. Threshold of positivity has been set as 50% of binding neutralization (dotted line). Dark blue dots represent mAbs able to neutralize the binding between SARS-CoV-2 and receptors on Vero E6 cells, while light blue dots represent non-neutralizing mAbs.

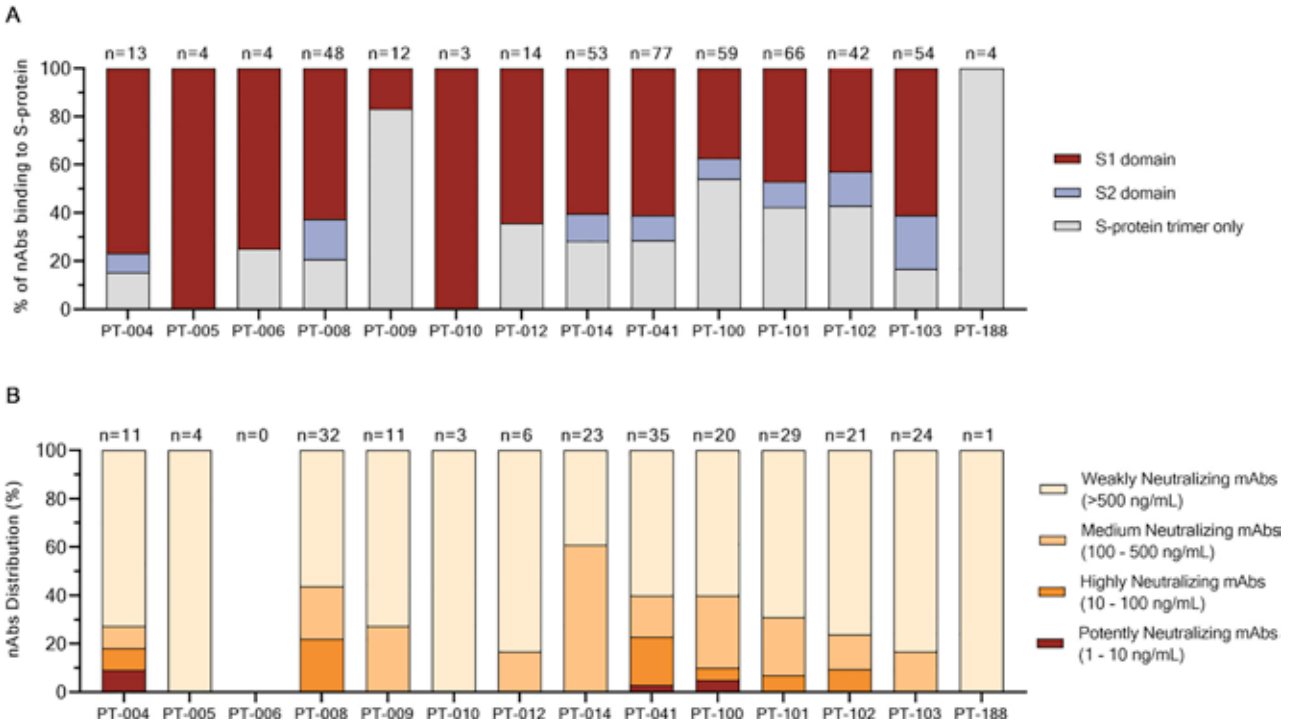

Figure S2. Characterization and distribution of SARS-CoV-2 S protein-specific nAbs, related to Figure 2

(A) The bar graph shows the distribution of nAbs binding to different S-protein domains. In dark red, light blue and gray are shown antibodies binding to the S1-domain, S2-domain and S-protein trimer respectively. The total number (n) of antibodies tested per individual is shown on top of each bar.

(B) The bar graph shows the distribution of nAbs with different neutralization potencies. nAbs were classified as weakly neutralizing (> 500 ng/mL; pale orange), medium neutralizing (100 – 500 ng/mL; orange), highly neutralizing (10 – 100 ng/mL; dark orange) and extremely neutralizing (1 – 10 ng/mL; dark red). The total number (n) of antibodies tested per individual is shown on top of each bar.

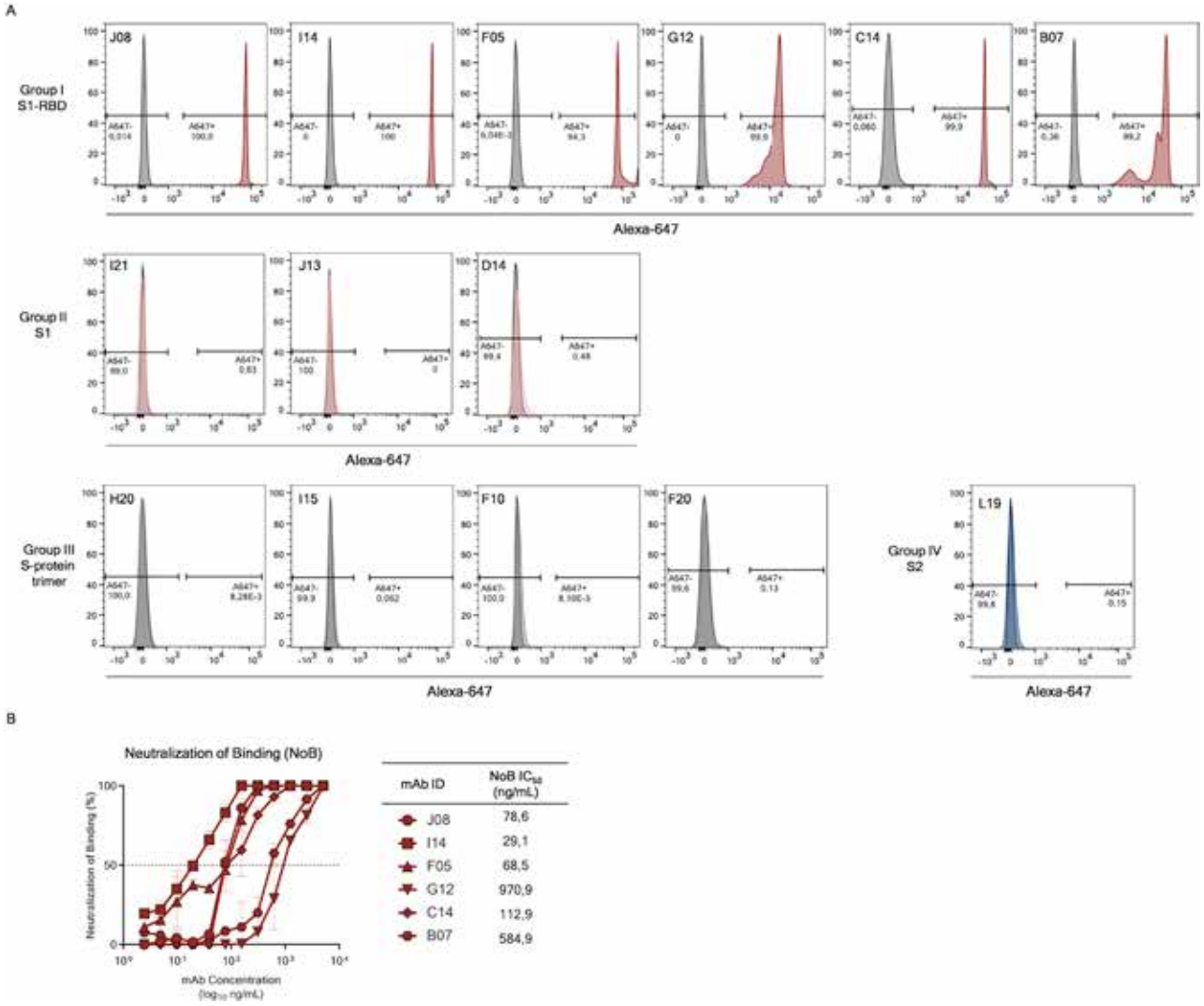

Figure S3. Binding to S protein receptor binding domain (RBD) and NoB activity of S1-RBD antibodies, related to Figure 3

(A) Histograms show the ability of selected antibodies to bind the S-protein RBD. Gray histograms represent the negative control while colored histograms show tested antibodies. Percentage of positive and negative populations are denoted on each graph.

(B) Neutralization of binding (NoB) curves for S1-RBD specific antibodies are shown as percentage of reduction of signal emitted by a fluorescently labled S-protein incubated with Vero E6 cells. Mean ± SD of technical duplicates are shown. Dashed lines represent the threshold of positivity; A neutralizing COVID-19 convalescent plasma and an unrelated plasma were used as positive and negative control, respectively.

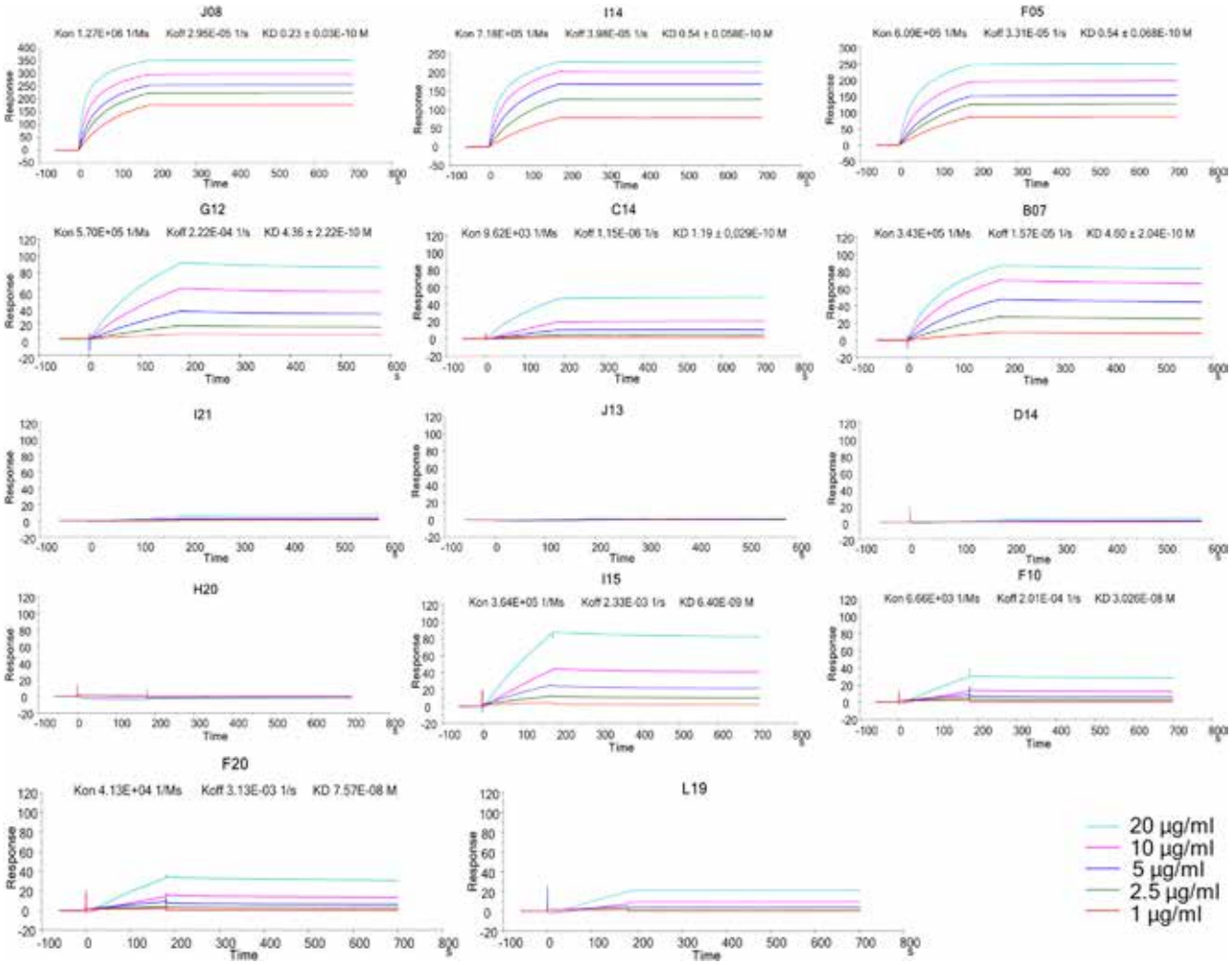

Figure S4. Binding kinetics of SARS-CoV-2 nAbs to the S protein antigen, related to Figure 3

Representative binding curves of selected antibodies to SARS-CoV-2 S-protein trimer. Different curve colors define the spike concentration used in the experiment. Kon, Koff and KD are denoted on each graph.

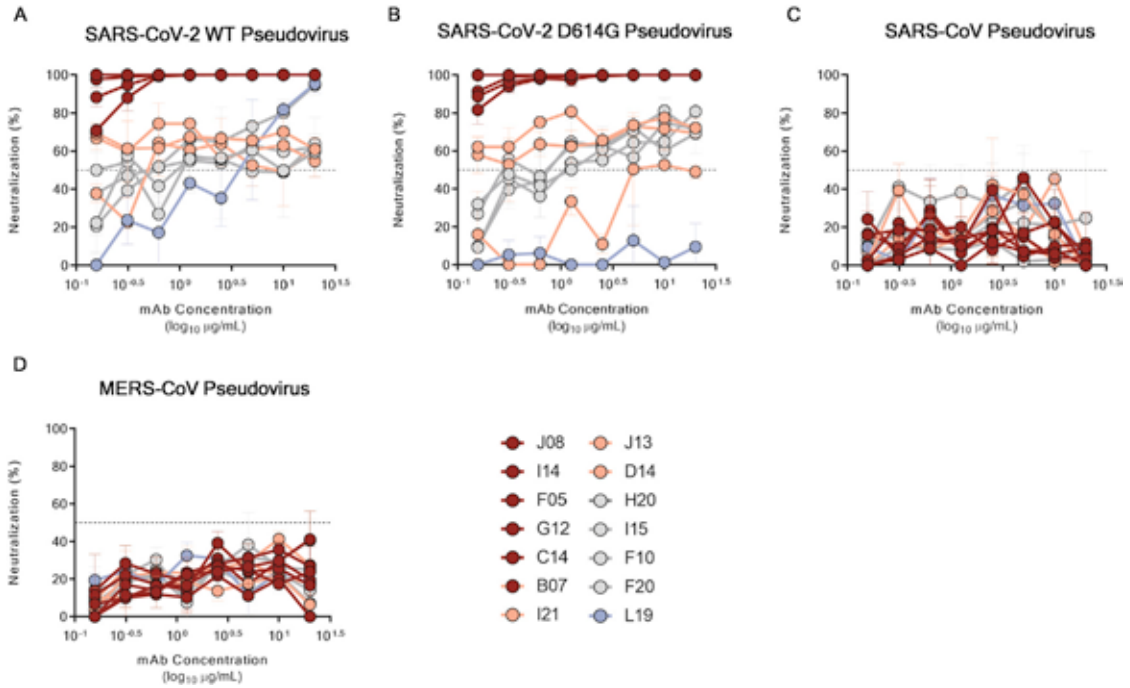

Figure S5. Neutralization activity of selected nAbs against SARS-CoV-2, SARS-CoV, and MERS-CoV pseudotypes, related to Figure 3

(A–D) Graphs show the neutralizing activities of 14 selected nAbs with different SARS-CoV-2 S-protein binding profiles against SARS-CoV-2, SARS-CoV-2 D614G, SARS-CoV and MERS-CoV pseudotypes respectively. Dashed lines represent the threshold of positivity. Mean ± SD of technical duplicates are shown. In all graphs selected antibodies are shown in dark red, pink, gray and light blue based on their ability to recognize the SARS-CoV-2 S1-RBD, S1-domain, S-protein trimer only and S2-domain respectively.

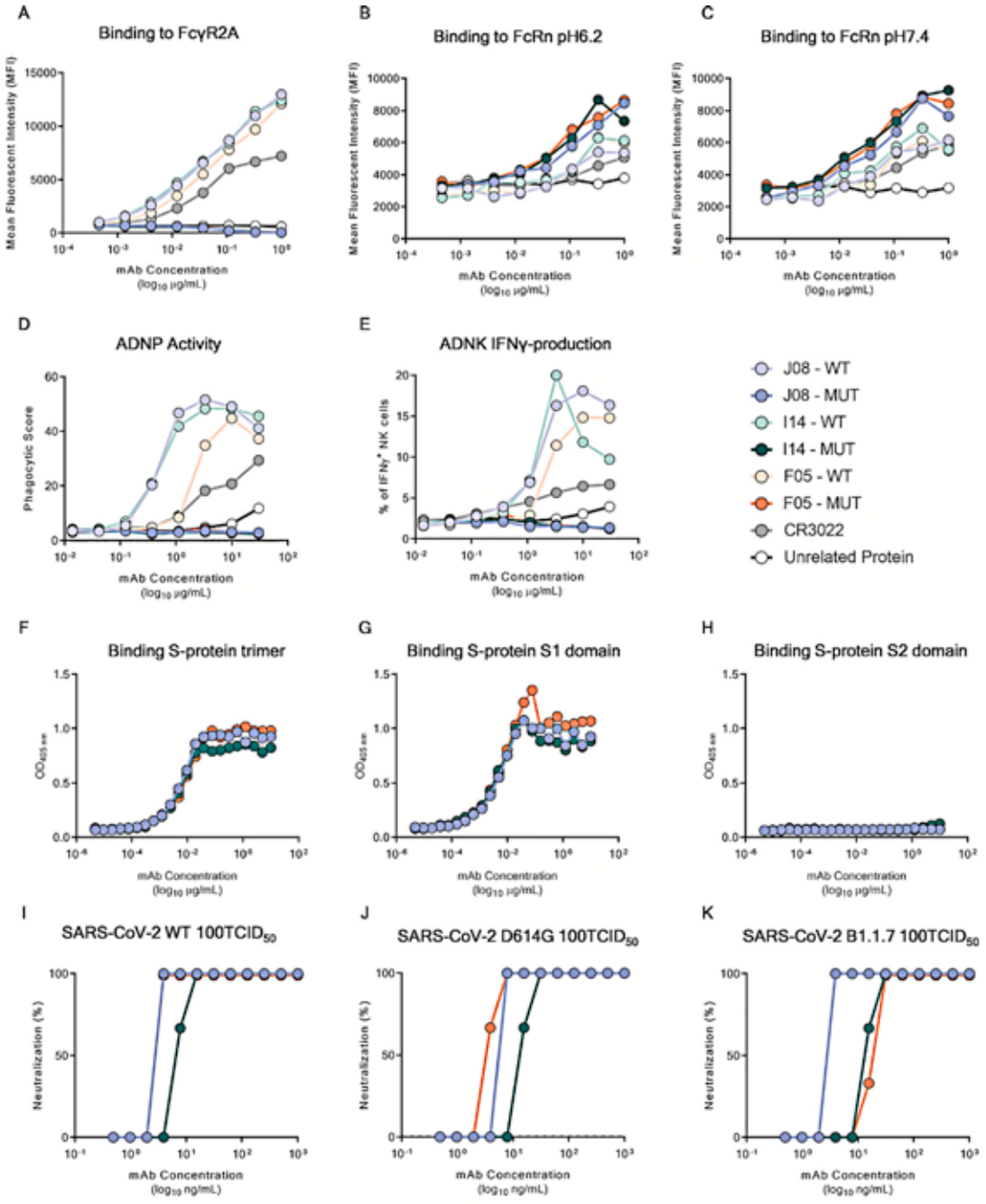

Figure S6. Characterization of Fc-engineered candidate nAbs, related to Figure 7

(A) the graph shows binding curves of J08, I14 and F05 MUT and WT to the FcγR2A.

(B and C) graphs show binding curves of J08, I14 and F05 MUT and WT to the FcRn at pH 6.2 (B) and 7.4 (C).

(D and E) Graphs show the ADNP and ADNK induced by J08, I14 and F05 MUT and WT versions; all the experiments were run as technical duplicates. In every experiment a control antibody (CR3022) and an unrelated protein were used as positive and negative control respectively.

(F–H) Graphs show binding curves to the S-protein in its trimeric conformation, S1-domain and S2-domain. Mean of technical triplicates are shown.

(I–K) Neutralization curves against the authentic SARS-CoV-2 wild type, the D614G variant and the B.1.1.7 emerging variant for J08-MUT, I14-MUT and F05-MUT shown in blue, green and red respectively. Data are representative of technical triplicates.

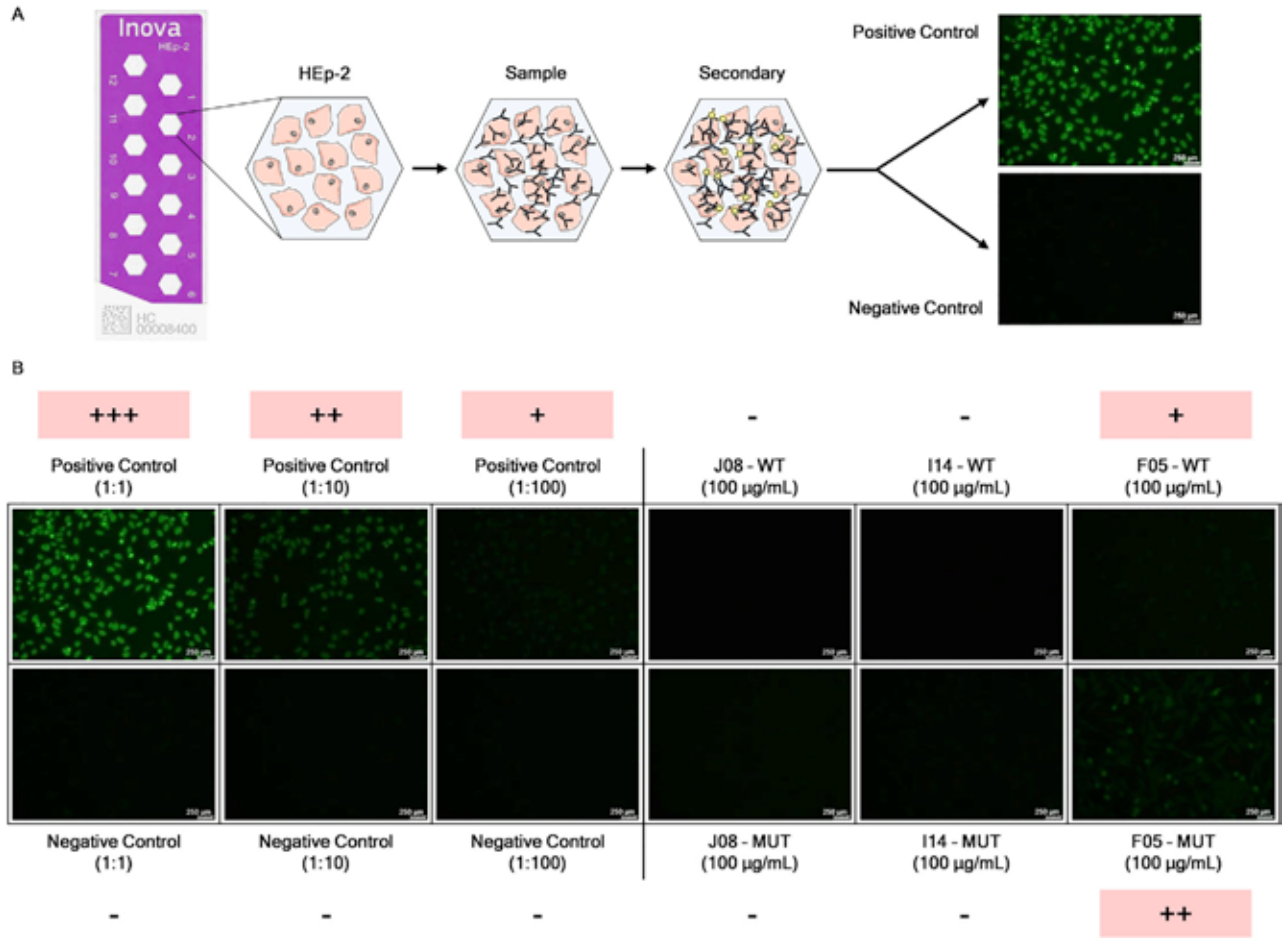

Figure S7. Autoreactivity assessment of selected SARS-CoV-2 candidate nAbs, related to Figure 7

(A) Schematic representation of the indirect immunofluorescent assay for the screening of autoreactive nAb.

(B) Single figures show the fluorescent signal detected per each sample tested in this assay. Positive and negative controls were used at three different dilutions (1:1, 1:10 and 1:100). Three candidate nAbs were incubated on HEp-2 cells at a concentration of 100 µg/mL. Representative pictures of the scoring system are shown. Autoreactive samples are highlighted in pink. 250 nm scale bar is shown.

ARTICLE IN PRESS

Journal of Immunological Methods xxx (xxxx) xxx

Contents lists available at ScienceDirect

Journal of Immunological Methods

journal homepage: www.elsevier.com/locate/jim

Research paper

Comparative analyses of SARS-CoV-2 binding (IgG, IgM, IgA) and neutralizing antibodies from human serum samples

Livia Mazzini [a], Donata Martinuzzi [b], Inesa Hyseni [b], Linda Benincasa [b], Eleonora Molesti [b,*], Elisa Casa [b], Giulia Lapini [a], Pietro Piu [a], Claudia Maria Trombetta [c], Serena Marchi [c], Ilaria Razzano [b], Alessandro Manenti [a,b], Emanuele Montomoli [a,b,c]

[a] VisMederi S.r.l., Siena, Italy
[b] VisMederi Research S.r.l., Siena, Italy
[c] Department of Molecular and Developmental Medicine, University of Siena, Siena, Italy

ARTICLE INFO

Keywords:
ELISA
SARS-CoV-2
Human samples
Micro-neutralization
Receptor-binding domain

ABSTRACT

A newly identified coronavirus, named SARS-CoV-2, emerged in December 2019 in Hubei Province, China, and quickly spread throughout the world; so far, it has caused more than 49.7 million cases of disease and 1,2 million deaths. The diagnosis of SARS-CoV-2 infection is currently based on the detection of viral RNA in nasopharyngeal swabs by means of molecular-based assays, such as real-time RT-PCR. Furthermore, serological assays detecting different classes of antibodies constitute an excellent surveillance strategy for gathering information on the humoral immune response to infection and the spread of the virus through the population. In addition, it can contribute to evaluate the immunogenicity of novel future vaccines and medicines for the treatment and prevention of COVID-19 disease.

The aim of this study was to determine SARS-CoV-2-specific antibodies in human serum samples by means of different commercial and in-house ELISA kits, in order to evaluate and compare their results first with one another and then with those yielded by functional assays using wild-type virus. It is important to identify the level of SARS-CoV-2-specific IgM, IgG and IgA antibodies in order to predict human population immunity, possible cross-reactivity with other coronaviruses and to identify potentially infectious subjects.

In addition, in a small sub-group of samples, a subtyping IgG ELISA has been performed. Our findings showed a notable statistical correlation between the neutralization titers and the IgG, IgM and IgA ELISA responses against the receptor-binding domain of the spike protein. Thus confirming that antibodies against this portion of the virus spike protein are highly neutralizing and that the ELISA Receptor-Binding Domain-based assay can be used as a valid surrogate for the neutralization assay in laboratories that do not have biosecurity level-3 facilities.

1. Introduction

Coronaviruses (CoVs) are enveloped, positive single-stranded RNA viruses belonging to the *Coronaviridae* subfamily. The Coronavirus subfamily comprises 4 Genera: Alpha-coronavirus which contains the human coronavirus (HCoV)-229E and HCoV-NL63; Beta-coronavirus which includes HCoV-OC43, Severe Acute Respiratory Syndrome human coronavirus (SARS-CoV-1), Middle Eastern respiratory syndrome coronavirus (MERS-CoV) and the newly emerged Severe Acute Respiratory Syndrome Coronavirus 2 (SARS-CoV-2).

Several members of this family, such as HCoV OC43, NL63 and 229E, cause mild common colds every year in the human population (Corman et al., 2019). Three highly pathogenic novel CoVs have appeared in the last 18 years; SARS-CoV-1 virus emerged in November 2002 in Guangdong province, causing more than 8,000 confirmed cases and 774 deaths (de Wit et al., 2016; Gorbalenya et al., 2020), MERS-CoV virus was discovered in June 2012 (Zaki et al., 2012) causing 2494 laboratory confirmed cases including 858 associated deaths, and SARS-CoV-2 virus emerged in Wuhan, Hubei province, China, in December 2019; this last was declared a pandemic on March 11th 2020 by the World Health Organization (WHO). The global impact of the SARS-CoV-2 outbreak, with over 49,7 million COVID-19 cases and 1,2 million deaths reported to WHO (as of 10th November 2020) (WHO, n.d.-a), is unprecedented.

Several data have confirmed that the infection initially arose from

* Corresponding author at: VisMederi Research S.r.l., 53100 Siena, Italy.
E-mail address: eleonora.molesti@vismederiresearch.com (E. Molesti).

https://doi.org/10.1016/j.jim.2020.112937
Received 24 September 2020; Received in revised form 17 November 2020; Accepted 23 November 2020
Available online 28 November 2020

contact with animals in the Wuhan seafood market. Subsequently, human-to-human transmission occurred, leading to a very high rate of laboratory-confirmed infections in China (Chan et al., 2020; WHO, 2020). Precise diagnosis of Coronavirus disease (COVID-19) is essential in order to promptly identify infected individuals, to limit the spread of the virus and to allow those who have been infected to be treated in the early phases of the infection. To date, real-time polymerase chain reaction (RT-PCR) is the most widely employed method of diagnosing COVID-19. However, rapid, large-scale testing has been prevented by the high volume of demand and the shortage of the materials needed for mucosal sampling (Zou et al., 2020). Standardized serological assays able to measure antibody responses may help to overcome these issues and may support a significant number of relevant applications. Indeed, serological assays are the basis on which to establish the rate of infection (severe, mild and asymptomatic) in a given area, to calculate the percentage of the population susceptible to the virus and to determine the fatality rate of the disease. It has been demonstrated in a non-human primate model (Bao et al., 2020) that, once the antibody response has been established, re-infection and, consequently, viral shedding, is unlikely. Furthermore, serological assays can help to identify subjects with strong antibody responses, who could serve as donors for the generation of monoclonal antibody therapeutics (Andreano et al., 2020).

The spike glycoprotein (S-protein), a large transmembrane homotrimer of approximately 140 kDa, has a pivotal role in viral pathogenesis, mediating binding to target cells through the interaction between its receptor-binding domain (RBD) (Wrapp et al., 2020) and the human angiotensin converting enzyme 2 (ACE2) receptor. The S-protein has been found to be highly immunogenic, and the RBD is possibly considered the main target in the effort to elicit potent neutralizing antibodies (Tay et al., 2020; Berry et al., 2010). Two subunits constitutes the S-protein: S1, which mediates attachment, and the S2, which mediates membrane fusion. The CoV S-protein is a class I fusion protein, and protease cleavage is required for activation of the fusion process (Ou et al., 2016).

To date, the complexity of the systemic immunoglobulin G (IgG) together with IgG subclasses and IgM and IgA, in terms of responses against SARS-CoV-2, have not been elucidated yet. Moreover, data comparing the differences between these responses and the neutralizing responses detected by functional assays such as Micro-Neutralization test (MN), are still not well defined.

Undoubtedly, it is well recognized that the IgG levels have a crucial role for protection from viral disease (Murin et al., 2019). In humans, the four IgG subclasses (IgG1, IgG2, IgG3, IgG4) differ in function (Schroeder and Cavacini, 2010) and IgG1 and IgG3 play a key role in many fundamental immunological functions, including virus neutralization, opsonization and complement fixation (Frasca et al., 2013). Therefore, we conducted a comparative study for two purposes: the first aim was to investigate the sensitivity and specificity, in terms of detection, of different ELISA kits compared with MN results; the second objective was to investigate the difference relatively to the spike-RBD-specific IgG, IgM and IgA antibody responses in human serum samples.

2. Materials and methods

2.1. Serum samples

In March/April 2020, 181 human serum samples were collected by the laboratory of Molecular Epidemiology of the University of Siena, Italy. The samples were anonymously collected in compliance with Italian ethics law.

Three human serum samples from confirmed cases of COVID-19 were kindly provided by Prof. Valentina Bollati from the University of Milan, Italy. Human IgG1 anti-SARS-CoV-2 Spike (S1) antibody CR3022 (Native Antigen,21 Drydock Avenue, 7th Floor Boston, MA 02210, USA), Human IgM anti-SARS-CoV-2 Spike (S1) Antibody CR3022 (Native Antigen, Oxford, UK) and anti-Spike RBD (SARS-CoV-2/COVID 19) human monoclonal antibody (eEnzyme, Gaithersburg, USA) were used as positive controls in ELISA. Human serum minus (IgA/IgM/IgG) (Cod. S5393, Sigma, St. Louis, USA) was also used as a negative control in MN assay and ELISA.

Three human serum samples containing heterologous neutralizing antibodies, provided by NIBSC (WHO 1st International Standard for Pertussis antiserum (lot. 06/140); WHO 2nd International Standard for antibody to influenza H1N1pdm virus (lot. 10/202); WHO 1st International Standard for Diphtheria Antitoxin (lot: 10/262)), plus a panel of commercial human serum samples ($n = 26$, provided by BioIVT company (West Sussex, United Kingdom), with confirmed non SARS-CoV-2 virus cross reactivity (positive towards different HCoVs), were used to verify the specificity of the ELISA test.

2.2. Cell culture

Vero E6 cells, acquired from the American Type Culture Collection (ATCC - CRL 1586), were cultured in Dulbecco's Modified Eagle's Medium (DMEM) - High Glucose (Euroclone, Pero, Italy) supplemented with 2 mM L-Glutamine (Lonza, Milan, Italy), 100 units/mL penicillin-streptomycin mixture (Lonza, Milan, Italy) and 10% of Fetal Bovine Serum (FBS), at 37 °C, in a 5% CO_2 humidified incubator.

VERO E6 cells were seeded in a 96-well plate using D-MEM high glucose 2% FBS at a density of 1.5×10^6 cells per well, in order to obtain a 70–80% sub-confluent cell monolayer after 24 h.

2.3. SARS-CoV-2 purified antigen, live virus and titration

Five different purified recombinant S proteins (S1 and RBD domain) were tested for their ability to detect specific human antibodies: S1-SARS-CoV-2 (HEK293) Cod. REC31806-500, (Native Antigen, Oxford, UK); S1-SARS-CoV-2 (HEK293) Cod. SCV2-S1-150P (eEnzyme, Gaithersburg, MD, USA); S1-SARS-CoV-2 (HEK293) Cod. S1N-C52H3 (ACROBiosystems, Newark, DE, USA); Spike RBD-SARS-CoV-2 (Baculovirus-Insect cells) Cod. 40592-V08B and (HEK293) Cod. 40592-V08H (Sino Biological, Beijing, China).

SARS CoV-2 - strain *2019-nCov/Italy-INMI1* – wild-type virus was purchased from the European Virus Archive Global (EVAg, Spallanzani Institute, Via Portuense, 292, 00148-00153, Rome). The virus was titrated in Biosecurity Level 3 laboratories (BSL) in serial 1-log dilutions to obtain a 50% tissue culture infective dose ($TCID_{50}$) on 96-well culture plates of VERO E6 cells. The plates have been observed daily for the presence of cytopathic effect (CPE) by means of an inverted optical microscope for a total of 4 days. The end-point titers were calculated according to the Spearman-Karber formula (Kundi, 1999).

2.4. Micro-neutralization assay

The MN assay was performed as previously reported by Manenti et al. (Manenti et al., 2020). Briefly, 2-fold serial dilutions of heat-inactivated serum samples were mixed with an equal volume of viral solution containing 100 $TCID_{50}$ of SARS-CoV-2. The serum-virus mixture was incubated for 1 h at 37 °C in a humidified atmosphere with 5% CO_2. After incubation, 100 µL of the mixture at each dilution was passed to a 96-well cell plate containing a 70–80% confluent VERO E6 monolayer. The plates were incubated for 3 days at 37 °C in a humidified atmosphere with 5% CO_2. After the incubation time, each well was inspected by means of an inverted optical microscope to evaluate the percentage of CPE. The highest serum dilution that protected more than 50% of cells from CPE was taken as the neutralization titer.

2.5. Commercial Enzyme-Linked Immunosorbent Assay (ELISA)

Specific anti-SARS-CoV-2 IgG antibodies were detected by means of the Euroimmun commercial ELISA kit.

Euroimmun-ELISA plates were coated with recombinant structural

protein (S1 domain) of SARS-CoV-2. The assay provides semi-quantitative results by calculating the ratio of the optical density (OD) of the serum sample over the OD of the calibrator. According to the manufacturer's instructions, positive samples have a ratio $\geq$ 1.1, borderline samples a ratio between 0.8 and 1.1 and negative samples a ratio $<$ 0.8.

2.5.1. In-House S1 and RBD Enzyme-Linked Immunosorbent Assay (ELISA) IgG, IgM and IgA

ELISA plates were coated with 1 μg/mL of purified recombinant Spike S1 Protein (aa 18–676) (eEnzyme, Gaithersburg, MD, USA) or with 1 μg/mL Spike-RBD (Arg319-Phe541) (Sino Biological, China), both expressed and purified from HEK 293 cells. After overnight incubation at +4 °C, coated plates were washed three times with 300 μL/well of ELISA washing solution containing Tris Buffered Saline (TBS)-0.05% Tween 20, then blocked for 1 h at 37 °C with a solution of TBS containing 5% of Non-Fat Dry Milk (NFDM; Euroclone, Pero, Italy). Serum samples were heat-inactivated at 56 °C for 1 h in order to reduce the risk of the presence of live virus in the sample. Subsequently, 3-fold serial dilutions, starting from 1:100 in TBS-0.05% Tween 20 5% NFDM, were performed up to 1:2700. Plates were washed three times, as previously; then 100 μL of each serial dilution was added to the coated plates by means of a multichannel pipette and incubated for 1 h at 37 °C. Next, after the washing step, 100 μL/well of Goat anti-Human IgG-Fc Horse Radish Peroxidase (HRP)-conjugated antibody or IgM (μ-chain) and IgA (α- chain) diluted 1:100,000 or 1:100,000 and 1:75,000, respectively, (Bethyl Laboratories, Montgomery USA) were added. Plates were incubated at 37 °C for 30 min. Following incubation, plates were washed and 100 μL/well of 3,3′,5,5′-Tetramethylbenzidine (TMB) substrate (Bethyl Laboratories, Montgomery, USA) was added and incubated in the dark at room temperature for 20 min. The reaction was stopped by adding 100 μL of ELISA stop solution (Bethyl Laboratories, Montgomery, USA) and read within 20 min at 450 nm. To evaluate the OD a SpectraMax ELISA plate (Medical Device) reader was used.

A cut-off value was defined as 3 times the average of OD values from blank wells (background: no addition of analyte). Samples with the ODs under the cut off value at the first 1:100 dilution were assigned as negative, samples where the ODs at 1:100 dilution were above the cut-off value were assigned as positive. Borderline samples were defined where one replicate was under the cut-off and the other was above.

2.5.2. In-house RBD Enzyme-Linked Immunosorbent Assay (ELISA) IgG1, IgG2, IgG3 and IgG4

An indirect ELISA was performed in order to determine the RBD-specific IgG1, IgG2, IgG3 and IgG4 antibody concentration in serum samples (Manenti et al., 2017). 96-well plates were coated with 1 μg/mL of purified Spike-RBD (Sino Biologicals). Serum samples were diluted from 1:50 to 1:400. Mouse anti-human IgG1, IgG2, IgG3 and IgG4 Fc-HRP (Southern Biotech, USA) secondary antibodies were used at 1:8000 dilution. The cut-off values were established as reported above (paragraph 1.5.1).

2.6. Generation of depleted-IgA serum

ELISA plates were coated with 10 μg/mL of high affinity purified goat anti-human IgA antibodies (Bethyl Laboratories) than blocked for 1 h at 37 °C. 10 μL of each heat inactivated serum sample (positive for MN and IgA ELISA) were then seeded in an ELISA coated plate and incubated for 2 h at 37 °C. After the incubation time the serum samples were harvested and stored at +4 °C until the MN assay.

2.7. Statistical analysis

Spearman's rank correlation analysis enabled us to determine whether, and to what extent, the MN assay was associated with the ELISAs. A classification analysis gave further insight into the relationship between the MN and the in-house ELISAs. We defined the MN as the target variable and recoded its results by assigning the label "0" to values of 5, and the label "1" otherwise. We implemented an elastic net (EN) to classify the Micro-neutralization titers (MNT). The EN is a rather sophisticated generalized linear model (GLM), which addresses the issues caused by multi-collinearity among predictors. We set the binomial family for the GLM after dichotomizing the variable MNT; therefore, we followed a logistic-like model approach in the implementation of the EN. The EN produces a selection of the variables based on a convex penalty function, which is a combination of the ridge regression and the LASSO (Least Absolute Shrinkage and Selection Operator) penalties, say l1 and l2 respectively, controlled by the hyper-parameter alpha = l2/(l1 + l2). The hyper-parameter, lambda, by contrast, regulates the level of penalization in the model (Zou and Hastie, 2005). To improve the generalization capability of the EN, we trained the model over a randomly selected subset of data (121/181) and verified its robustness over an independent subset of the residual data (60/181), which did not enter the model during the training stage. The cross-validation technique prevented the occurrence of over-fitting problems in the estimates. On the base of the values of the predictors of the test set, X, and their estimated EN coefficients, b, we built a score function, S, as follows:

$$S(X, b) = e^{X \cdot b}$$

The probability of a positive MNT assignment for the predicted results was then expressed as:

$$P(MNT = \text{Positive}) = \frac{S(X, b)}{(1 + S(X, b))}$$

We calculated the performance of the EN in terms of sensitivity, i.e., the percentage of positive MNT correctly predicted, and specificity, i.e., the percentage of negative MNT correctly predicted, and represented their related Receiver Operating Characteristic (ROC) curve. The optimal combination of sensitivity and specificity enabled us to detect the cut-off in the score function; test samples were classified as positive if their score was above this cut-off value and as negative if the score was below it, with the minimum error probability.

3. Results

3.1. Set-up and standardization of in-house ELISAs

Several purified recombinant S-proteins (S1 and RBD domain) were tested for their ability to detect specific human antibodies: S1-SARS-CoV-2 (HEK293) (from Native Antigen); S1-SARS-CoV-2 (HEK293) (from eEnzyme); S1-SARS-CoV-2 (HEK293) (from ACROBiosystems); Spike RBD-SARS-CoV-2 (Baculovirus-Insect cells) and (HEK293) (from Sino Biological). Each protein was evaluated using three coating concentrations (1, 2 and 3 μg/mL) and four different dilutions of the secondary HRP conjugate anti-human IgG, IgM and IgA antibodies. The optimal concentration chosen for antigen coating was 1 microgram/mL while the optimal dilution for the secondary HRP conjugate anti-human IgG, IgM was 1:100,000 and 1: 75,000 for anti-Human IgA. We also evaluated the impact of the incubation time of the HRP by incubating the plates for 1 h or 30 min, and concluded that the best and clearest signal was always seen after the shortest incubation. To set the assays, three human serum samples derived from convalescent donors, along with a pool of MN and ELISA (commercial Kit)-negative human serum samples, were used as positive and negative controls, respectively. As a test control, human IgG1 monoclonal antibody (mAb) anti-SARS-CoV-2 spike (S1) (CR3022 Native antigen), human IgM mAb anti-SARS-CoV-2 spike (S1) (CR3022 Absolute antibody) and human IgG1 anti-Spike RBD (SCV2-RBD eEnzyme) were used. Additionally, several human sera hyper-immune to various infectious diseases (influenza, diphtheria and pertussis) were used to assess the specificity of the assay in detecting

Table 1
Comparative table showing the results obtained when human sera were tested by different ELISA kits and by micro neutralization test (MN).

ID Sample	Elisa Euroimmun	MNT titer	ELISA_VM_IgG_S1	ELISA_VM_IgG_RBD	ELISA_VM_IgM_S1	ELISA_VM_IgM_RBD	ELISA_VM_IgA_RBD
From 1 to 8	Negative	5	Negative	Negative	Negative	Negative	Negative
9	Negative	5	Negative	Negative	Negative	Positive	Negative
10–11	Negative	5	Negative	Negative	Negative	Negative	Negative
12	Negative	5	Negative	Negative	Negative	Positive	Negative
13	Negative	5	Negative	Negative	Negative	Negative	Negative
14	Borderline	5	Negative	Negative	Negative	Negative	Negative
15	Negative	5	Negative	Negative	Negative	Negative	Negative
16	Negative	5	Negative	Negative	Positive	Negative	Negative
From 17 to 21	Negative	5	Negative	Negative	Negative	Negative	Negative
22	Borderline	5	Positive	Negative	Negative	Negative	Negative
From 23 to 31	Negative	5	Negative	Negative	Negative	Negative	Negative
32	Negative	5	Negative	Positive	Negative	Negative	Negative
From 33 to 36	Negative	5	Negative	Negative	Negative	Negative	Negative
37	Positive	5	Negative	Negative	Negative	Positive	Negative
38–39	Negative	5	Negative	Negative	Negative	Negative	Negative
40	Positive	5	Negative	Negative	Negative	Negative	Negative
41	Negative	5	Negative	Negative	Negative	Negative	Negative
42	Borderline	5	Negative	Negative	Negative	Negative	Negative
43	Positive	5	Positive	Positive	Negative	Negative	Negative
44–45	Negative	5	Negative	Negative	Negative	Negative	Negative
46	Positive	5	Positive	Negative	Negative	Negative	Negative
From 47 TO 49	Negative	5	Negative	Negative	Negative	Negative	Negative
50	Negative	5	Negative	Negative	Negative	Positive	Negative
51–52	Negative	5	Negative	Negative	Negative	Negative	Negative
53	Negative	5	Negative	Negative	Negative	Positive	Negative
From 54 to 60	Negative	5	Negative	Negative	Negative	Negative	Negative
61	Positive	5	Negative	Negative	Negative	Negative	Negative
62	Negative	5	Positive	Negative	Negative	Negative	Negative
63–64	Negative	5	Negative	Negative	Negative	Negative	Negative
65	Borderline	5	Negative	Negative	Negative	Negative	Negative
66–67	Negative	5	Negative	Negative	Negative	Negative	Negative
68	Positive	5	Positive	Negative	Negative	Positive	Negative
69	Positive	5	Positive	Negative	Negative	Negative	Negative
From 70 to 72	Negative	5	Negative	Negative	Negative	Negative	Negative
73	Borderline	5	Negative	Negative	Negative	Negative	Negative
From**74 to 76**	Negative	5	Negative	Negative	Negative	Negative	Negative
77	Positive	5	Positive	Negative	Negative	Negative	Negative
78	Borderline	5	Negative	Negative	Positive	Negative	Negative
79	Borderline	5	Negative	Negative	Negative	Negative	Negative
80	Positive	5	Negative	Negative	Negative	Negative	Negative
81	Borderline	5	Negative	Negative	Negative	Negative	Negative
From 82 to 91	Negative	5	Negative	Negative	Negative	Negative	Negative
92	Positive	5	Positive	Negative	Negative	Positive	Negative
93	Borderline	5	Positive	Negative	Positive	Negative	Negative
94–95	Negative	5	Negative	Negative	Negative	Negative	Negative
96	Negative	5	Negative	Negative	Negative	Positive	Negative
97–98	Negative	5	Negative	Negative	Negative	Negative	Negative
99	Positive	5	Positive	Negative	Negative	Negative	Negative
From 100 to 107	Negative	5	Negative	Negative	Negative	Negative	Negative
108	Negative	5	Negative	Negative	Negative	Positive	Positive
109	Negative	5	Negative	Negative	Positive	Negative	Negative
110	Negative	5	Negative	Negative	Positive	Positive	Negative
111	Negative	5	Negative	Negative	Positive	Positive	Negative
112	Negative	5	Negative	Negative	Negative	Negative	Negative
113	Positive	5	Positive	Positive	Positive	Positive	Negative
From 114 to 117	Negative	5	Negative	Negative	Negative	Negative	Negative
118	Negative	5	Negative	Negative	Positive	Negative	Negative
119–120	Negative	5	Negative	Negative	Negative	Negative	Negative
121	Positive	5	Positive	Negative	Positive	Negative	Negative
From 122 to 127	Negative	5	Negative	Negative	Negative	Negative	Negative
128	Positive	5	Positive	Positive	Negative	Negative	Positive
129	Negative	5	Negative	Negative	Negative	Negative	Negative
130	Negative	5	Negative	Negative	Negative	Positive	Negative
131–132	Negative	5	Negative	Negative	Negative	Negative	Negative
133	Positive	5	Positive	Negative	Negative	Negative	Negative
From 134 to 142	Negative	5	Negative	Negative	Negative	Negative	Negative
143	Negative	5	Negative	Negative	Negative	Positive	Negative
from 144 to 146	Negative	5	Negative	Negative	Negative	Negative	Negative
147	Negative	5	Negative	Negative	Positive	Positive	Negative
148	Negative	5	Negative	Negative	Negative	Negative	Negative
149	Negative	5	Negative	Negative	Negative	Positive	Negative
150	Positive	5	Positive	Positive	Negative	Negative	Negative
151	Negative	5	Negative	Negative	Negative	Negative	Negative

(*continued on next page*)

Table 1 (*continued*)

ID Sample	Elisa Euroimmun	MNT titer	ELISA_VM_IgG_S1	ELISA_VM_IgG_RBD	ELISA_VM_IgM_S1	ELISA_VM_IgM_RBD	ELISA_VM_IgA_RBD
152	Positive	5	Positive	Negative	Negative	Negative	Negative
153	Negative	5	Negative	Negative	Negative	Negative	Negative
154	Negative	10	Negative	Negative	Negative	Positive	Negative
155	Positive	1280	Positive	Positive	Positive	Positive	Positive
156	Negative	10	Negative	Positive	Negative	Negative	Negative
157	Negative	10	Negative	Negative	Positive	Negative	Negative
158	Positive	20	Positive	Positive	Negative	Positive	Positive
159	Negative	20	Negative	Positive	Negative	Positive	Positive
160	Negative	20	Negative	Negative	Negative	Negative	Positive
161	Negative	20	Negative	Negative	Positive	Negative	Negative
162	Negative	20	Negative	Positive	Positive	Positive	Positive
163	Positive	40	Positive	Positive	Positive	Positive	Positive
164	Negative	40	Negative	Positive	Negative	Positive	Negative
165	Negative	40	Negative	Positive	Negative	Positive	Positive
166	Negative	80	Negative	Positive	Negative	Positive	Positive
167	Borderline	80	Negative	Positive	Positive	Positive	Negative
168	Negative	80	Positive	Positive	Negative	Positive	Positive
169	Negative	80	Negative	Positive	Negative	Positive	Positive
170	Positive	80	Positive	Positive	Positive	Positive	Positive
171	Negative	160	Negative	Positive	Negative	Positive	Positive
172	Positive	160	Positive	Positive	Negative	Positive	Positive
173	Positive	160	Positive	Positive	Positive	Positive	Negative
174	Positive	320	Negative	Positive	Positive	Positive	Positive
175–176	Positive	640	Positive	Positive	Positive	Positive	Positive
177	Positive	640	Positive	Positive	Negative	Positive	Positive
178–179	Positive	640	Positive	Positive	Positive	Positive	Positive
180–181	Positive	1280	Positive	Positive	Positive	Positive	Positive

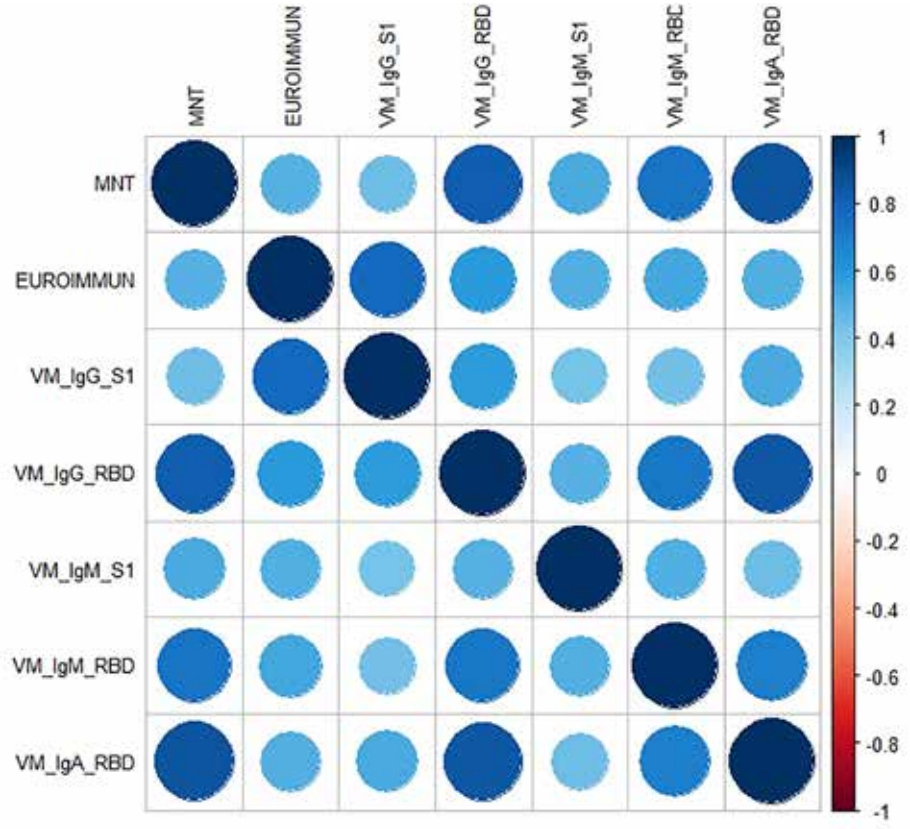

Fig. 1. The correlation plot associated to the measured coefficients of Spearman's rank correlation. The magnitude of the coefficient is represented by circles and a color gradient: the larger the area of the circle and the more intense the tone of the color, the greater the correlation. The direction of the correlation is indicated by the color scale: blue tones for positive correlations and red tones for negative correlations. (For interpretation of the references to color in this figure legend, the reader is referred to the web version of this article.)

only antibodies against SARS-CoV-2 S1 or the RBD protein. Alternative blocking/diluent solutions containing 1% Bovine Serum Albumin (BSA), 2.5% milk and 5% milk were tested. The specificity of the test increased significantly on using the 5% milk blocking solution in comparison with BSA, which occasionally yielded non-specific results and displayed a generally higher background. Finally, the two proteins that yielded the best results in terms of sensitivity and specificity were chosen as candidates for the tests: the purified S1-protein (HEK derived) from eEnzyme and the Purified RBD protein (HEK derived) from Sino Biological.

Table 2
Specificity of in House ELISA test for IgG and IgM responses against SARS-CoV-2 RBD.

Sample ID	ELISA In house RBD - IgG	ELISA In house RBD - IgM
368424 SR1 COVID-19 IgG/IgM	POS	POS
368424 SR1 COVID-19+ IgG/IgM	POS	POS
368424 SR1 COVID-19+ IgG/IgM	POS	POS
368424 SR1 COVID-19+ IgG/IgM	POS	POS
373,647-SR1 COVID-19+ IgG	POS	POS
373647-SR1 COVID-19+ IgG	POS	NEG
373647-SR1 COVID-19+ IgG	POS	NEG
373647-SR1 COVID-19+ IgG	POS	NEG
HMN406906 **229E**+	NEG	NEG
HMN406954 **OC43/229E**+	NEG	NEG
HMN406901 **OC43/229E**+	NEG	NEG
HMN406939 **229E**+	NEG	NEG
HMN406903 **HKU/OC43/229E**+	NEG	NEG
HMN406909 **HKU/OC43/229E**+	NEG	NEG
HMN406913 **HKU/OC43/229E**+	NEG	NEG
HMN406910 **HKU/OC43/229E/NL63**+	NEG	NEG
HMN406927 **HKU/OC43/229E**+	NEG	NEG
HMN406944 **OC43/229E**+	NEG	NEG
HMN406945 **OC43/229E**+	NEG	NEG
HMN406919 **OC43/229E/NL63**+	NEG	NEG
HMN406924 **229E/NL63**+	NEG	NEG
HMN406929 **HKU/OC43/229E**+	NEG	NEG
HMN406920 **HKU/OC43/229E/NL63**+	NEG	NEG
HMN406922 **HKU/OC43/229E**+	NEG	NEG
HMN406933 **HKU/OC43/229E/NL63**+	NEG	NEG
HMN406938 **HKU/OC43/229E**+	NEG	NEG

3.2. Correlation between ELISAs and Neutralization

Each serum sample was tested by means of *in-house* ELISA S1 and RBD-specific IgG, IgM and IgA (VM_IgG_S1, VM_IgG_RBD, VM_IgM_S1, VM_IgM_RBD, VM_IgA_RBD) and by means of the Euroimmun S1 Commercial ELISA kit, along with the functional MN assay (Table 1). The distribution of the micro-neutralization titers (MNTs) was strongly asymmetric, with most of the values (153/181) being equal to 5 (i.e. negative). The other values observed (from 10 to 1280 in a 2-fold dilution series) were uniformly distributed. Concerning the ELISA S1, we performed two different tests: one by means of a commercial (Euroimmun) kit and the other an in-house ELISA. According to Spearman's rank correlation coefficients and statistical significance (Tables 3 and 4), we registered the highest agreement between the ELISA VM_IgG_RBD and MNT, and between the VM_IgA_RBD and MNT, with coefficients of 0.83 and 0.85, respectively. The lowest correlations were found for ELISA Euroimmun vs MNT, and for VM_IgG_S1 vs MNT, with coefficients of 0.49 and 0.45, respectively. As can be seen from the correlation plot (Fig. 1), the IgA response was closely linked with a positive MN response. Moreover, on dissecting all the results for each serum sample (data not shown), we noted that, in those subjects in whom we registered a high neutralization titer, we always observed a positive IgA signal.

Interestingly, in 9 MNT-positive samples, we found a complete absence of S1 signal on using Euroimmun, VM_IgG_S1 and VM_IgM_S1 ELISA kits but, on the other hand, high and detectable IgG and IgM RBD-specific signals.

To confirm the analytical specificity of the in-house RBD of the in-house RBD-ELISA test, commercial human serum samples with confirmed non-SARS-COV-2 Coronavirus cross-reactivity (positives towards different HCoVs) were tested and the selectivity of this test to discriminate between IgG/IgM and IgG only responses in COVID-19 positive samples was evaluated. Among these samples 5 were confirmed positives for IgG and IgM, while 3 samples were confirmed IgG positives and IgM negatives. For all the remaining 18 samples, positives towards different HCoV strains, (from n.9 to n.26) no cross-reactivity was confirmed and these panel of sera were tested by In-house RBD ELISA (Table 2).

3.3. Classification analysis: elastic net

Over a training set of data, the optimal hyper-parameters estimated for the Elastic Net (EN) model were lambda = 0.0136 and alpha = 0.76, which minimized the error of cross-validation (=0.3809). The EN model selected three significant predictors of the MN results, namely VM-IgG-RBD, VM-IgM-RBD, and VM-IgA-RBD; the estimates of their coefficients were 0.0035, 0.0060 and 0.0013, respectively, while the intercept of the model was −2.9741. These results were entered into the score function, whereby we predicted the MNTs. From the ROC curve (Fig. 2A), we evaluated the performance of the predictions in terms of sensitivity and specificity. On balancing sensitivity and specificity, we obtained the optimal cut-off of 0.092, with sensitivity = 85.7% (95% CI = [42.1%–99.6%]) and specificity = 98.1% (95% CI = [89.9%–99.6%]) (Fig. 2B). Overall, these findings indicated that the in-house RBD-based ELISA methods were highly accurate and, particularly, presented the features of a highly specific diagnostic test when jointly considered.

The samples, which yielded a score below the identified cut-off, were classified as "negative", and the remaining samples as "positive". We then compared these predictions with the known results of the test-set (Fig. 2C).

Analysis of the error matrix indicated an overall Accuracy (ACC) of 96.7% (95% CI = [88.5%–99.6%]), and a No Information Rate (NIR) of 88.3% (95% CI = [77.4%–95.2%]). Since the ACC was significantly higher than the NIR ($p = 0.02$), we may claim that the model built with the In-house (VM) RBD-based ELISAs conveyed effective information. The extremely high value of the odds ratio (OR) = 312.0, (95% CI = [17.2–5657.7]) revealed the strong association between the MN results and the model predictions. Specifically, the positive predictions were 312 times more likely to occur in association with positive MNT than the negative predictions.

3.4. IgG subtyping of serum samples

We also evaluated the ELISA IgG subtyping response (IgG1, IgG2, IgG3, and IgG4) in a small subgroup (14) of MN-positive samples. ELISA plates were coated with RBD purified antigen. Our results, although derived from a small group of subjects, are in line with previous findings by Amanat and colleagues (Amanat et al., 2020). Strong reactivity for

Table 3
Spearman's rank correlation coefficients.

	MNT	EUROIMMUN	VM_IgG_S1	VM_IgG_RBD	VM_IgM_S1	VM_IgM_RBD	VM_IgA_RBD
MNT	1.00	0.49	0.45	0.83	0.52	0.73	0.85
EUROIMMUN	0.49	1.00	0.77	0.59	0.50	0.54	0.51
VM_IgG_S1	0.45	0.77	1.00	0.59	0.43	0.44	0.53
VM_IgG_RBD	0.83	0.59	0.59	1.00	0.49	0.73	0.84
VM_IgM_S1	0.52	0.50	0.43	0.49	1.00	0.50	0.45
VM_IgM_RBD	0.73	0.54	0.44	0.73	0.50	1.00	0.69
VM_IgA_RBD	0.85	0.51	0.53	0.84	0.45	0.69	1.00

Table 4
Statistical significance of Spearman's rank correlation coefficients.

	MNT	EUROIMMUN	VM_IgG_S1	VM_IgG_RBD	VM_IgM_S1	VM_IgM_RBD	VM_IgA_RBD
MNT	0.0E+00	3.8E-07	3.3E-10	8.1E-47	3.5E-14	1.5E-31	7.0E-53
EUROIMMUN	3.8E-07	0.0E+00	2.8E-20	1.9E-10	1.8E-07	1.5E-08	1.3E-07
VM_IgG_S1	3.3E-10	2.8E-20	0.0E+00	3.4E-18	2.1E-09	5.8E-10	2.1E-14
VM_IgG_RBD	8.1E-47	1.9E-10	3.4E-18	0.0E+00	1.5E-12	3.1E-31	2.5E-50
VM_IgM_S1	3.5E-14	1.8E-07	2.1E-09	1.5E-12	0.0E+00	5.5E-13	3.1E-10
VM_IgM_RBD	1.5E-31	1.5E-08	5.8E-10	3.1E-31	5.5E-13	0.0E+00	2.9E-27
VM_IgA_RBD	7.0E-53	1.3E-07	2.1E-14	2.5E-50	3.1E-10	2.9E-27	0.0E+00

Table 5
Comparative table showing the results obtained when human sera were tested by IgA ELISA kits and by micro neutralization test to assess the contribution of the IgA antibodies on the neutralizing potency of the serum samples.

ID sample	Elisa Euroimmun	ELISA_VM_ IgG_S1	ELISA_VM_ IgG_RBD	ELISA_VM_ IgM_S1	ELISA_VM_ IgM_RBD	ELISA_VM_ IgA_RBD	MN Titres before IgA treatment	MN Titres after IgA treatment
158	Positive	Positive	Positive	Negative	Positive	Positive	20	20
159	Negative	Negative	Positive	Negative	Positive	Positive	20	20
160	Negative	Negative	Negative	Negative	Negative	Positive	20	20
161	Negative	Negative	Negative	Positive	Negative	Negative	n.a.	n.a.
162	Negative	Negative	Positive	Positive	Positive	Positive	n.a.	n.a.
163	Positive	Positive	Positive	Positive	Positive	Positive	40	40
164	Negative	Negative	Positive	Negative	Positive	Negative	n.a.	n.a.
165	Negative	Negative	Positive	Negative	Positive	Positive	80	40
166	Negative	Negative	Positive	Negative	Positive	Positive	80	40
167	Borderline	Negative	Positive	Positive	Positive	Negative	80	80
168	Negative	Positive	Positive	Negative	Positive	Positive	80	80
169	Negative	Negative	Positive	Negative	Positive	Positive	80	40
170	Positive	Positive	Positive	Positive	Positive	Positive	80	80
171	Negative	Negative	Positive	Negative	Positive	Positive	160	160
172	Positive	Positive	Positive	Negative	Positive	Positive	160	80
173	Positive	Positive	Positive	Positive	Positive	Negative	160	160
174	Positive	Negative	Positive	Positive	Positive	Positive	320	80
175–176	Positive	Positive	Positive	Positive	Positive	Positive	640	640
177	Positive	Positive	Positive	Negative	Positive	Positive	640	640
178–179	Positive	Positive	Positive	Positive	Positive	Positive	640	320
180–181	Positive	Positive	Positive	Positive	Positive	Positive	1280	640

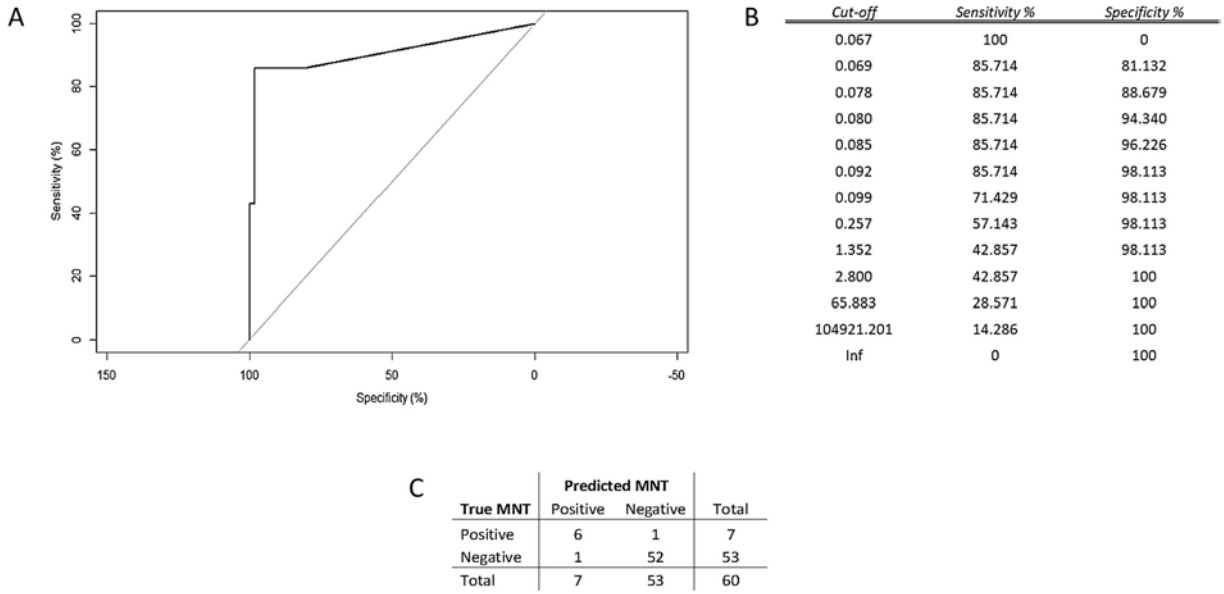

Fig. 2. A) Analysis of the ROC curve referred to the test set proved that the results of the EN model attained high accuracy in predicting the MNT values. Measurement of the area under the curve, AUC = 90.7%, supported this conclusion; B) Summary table of ROC analysis; C) Error matrix.

IgG1 and IgG3 was found in almost all samples, with the IgG3 subclass showing the highest percentage of detection. Low and very low reactivity was found for IgG4 and IgG3, respectively (Fig. 3).

3.5. IgA antibodies increase the neutralization potency of the serum

Due to the high correlation observed between the IgA ELISA and MN results we tried to assess the real contribution of the IgA antibodies on

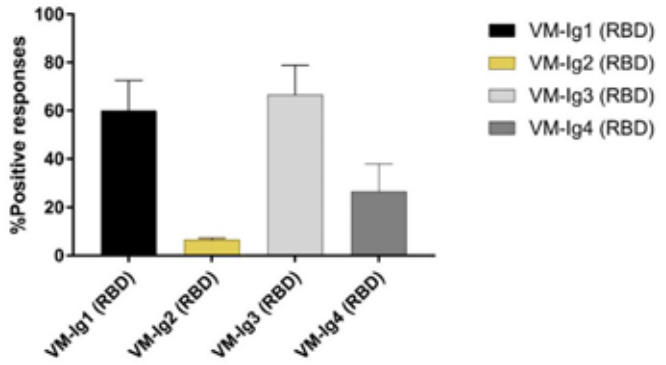

Fig. 3. Percentage of detection of IgG1, IgG2, IgG3 and IgG4 in all 14 human samples positive on MN assay. Each column represents the contribution, in terms of percentage, each IgG subclasses versus SARS- CoV- 2 RBD. Error bars showing the variance of sample proportion.

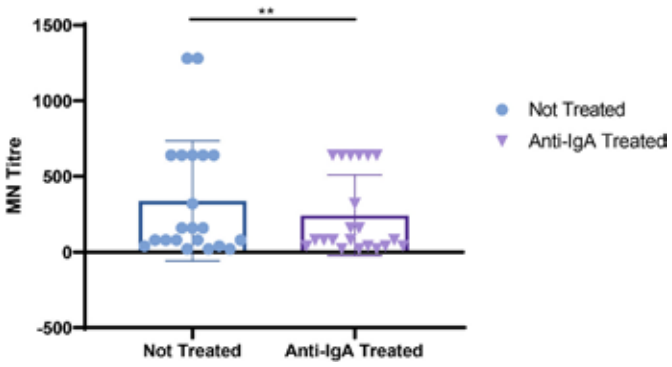

Fig. 4. Log transformed MNTs before and after the treatment with the goat anti-human IgA antibodies; *t*-Test shows a significant decrease in the MN titers for those samples with high neutralizing titers.

the neutralizing potency of the serum samples. As is possible to observe in Fig. 4 and Table 5, after the sample treatment we registered an evident decrease in the neutralizing titers. Interesting is the fact that the decrease is showed only in those sera that showed high starting neutralizing titers. Samples with medium/low MNTs did not show any decrease.

4. Discussion

Like most of the emerging infectious diseases that affect humans, this new HCoV also originated from animals (WHO, n.d.-b; Andersen et al., 2020). Owing to the rapid increase in some human practices, such as deforestation, urbanization and the husbandry of wild animal species, over the years the emergence of new pathogens has become an extremely serious problem. The rapid global spread of the novel SARS-CoV-2 is posing a serious health threat to the entire world. There is now an urgent need for well-standardized serological assays that can detect different classes of antibodies against the novel coronavirus, and which can be used alongside the classical diagnostic molecular methods such as RT-PCR. Indeed, due to the huge demand in the recent months, the availability of the reagents and equipment needed to promptly carry out analyses is still inadequate.

Moreover, if sample collection and storage are improperly conducted,molecular tests may yield false-negative results in subjects who carry the virus (Liu et al., 2020). Previous studies on SARS-CoV-1 have shown that virus-specific IgG and IgM levels can be valid surrogate for serological diagnosis (Guan et al., 2004; Hsueh et al., 2004). Indeed, the present study had two major goals: a) to standardize and make as reliable as possible ELISA tests in order to detect different classes of immunoglobulins, and b) to broaden the data-set of information on comparisons between the results of different serological tests, which could be precious for future evaluation of serological diagnoses and vaccine assessments (Madore et al., 2010). Specifically, in this study, ELISA results were always compared with those obtained by the functional assay (MN), which is commonly assumed as a benchmark and the gold standard.

Since its first isolation and characterization, this new HCoV strain has been classified, according to the WHO guidelines, as BSL3 pathogen. This has placed some limits on the implementation of neutralization tests, as relatively few laboratories have level-3 biocontainment facilities. The ELISAs are a good surrogate for the MN assay in terms of sensitivity, safety and throughput (Dessy et al., 2008; Gonda et al., 2012; Ivanov et al., 2019). However, it is very important to evaluate and estimate the best antigen/s to use in these platforms in order to obtain a reliable and similar response to that of the neutralization test, which indicates the functional response. This is why we compared all our results with those of the MNT. As in the case of influenza hemagglutinin (Clements et al., 1986), antibodies specific to the RBD domain of the S-protein seem to strongly contribute to viral neutralization. In this study, together with the IgG, IgM and IgA analyses, we also evaluated the responses of IgG subclasses in those subjects who showed both a high RBD ELISA signal and proven neutralization activity. Our results are in line with previous findings (Amanat et al., 2020) and confirm IgG1 and IgG3 as the subtypes with the strongest reactivity in all samples (Seow et al., 2020). Only in a small number of subjects did we find IgG2 and IgG4 responses. IgG1 and IgG3 are involved in critical immunologic functions, such as neutralization, opsonization, complement fixation and antibody-dependent cellular cytotoxicity (ADCC). On the other hand, IgG2 plays an important role in protecting against infection by encapsulated microorganisms (Ferrante et al., 1990); IgG4 is generally a minor component of the total immunoglobulin response and is induced in response to continuous antigenic stimulation (Aalberse et al., 1983).

Regarding the ELISA IgG, IgM and IgA, the main results can be summarized as follows: a) all the proposed statistical analyses indicated a close relationship between the results of MN and in-house RBD-based ELISAs, namely VM-IgG-RBD, VM-IgM-RBD and VM-IgA-RBD (results are in line with previous reports by Amanat and colleagues (Amanat et al., 2020; Okba et al., 2020)); b) the cross-validation technique applied to the EN model allowed us to obtain robust results.

In the out-of-sample data (i.e., the randomly chosen test-data) highly accurate, and, particularly, highly specific performance was observed; c) in large-scale screening operations, it is very important to have a highly specific test, as this guards against the risk of misclassification of true-negative samples with a wide margin of certainty. A highly specific test is particularly useful in order to confirm a diagnosis already made by means of other methods, and when a false-positive result would have a great impact. Indeed, a highly specific test is of most help to the clinician when it provides a positive result.

An overview of all the results yielded by ELISA and MN (data not shown), along with those obtained by treating the sample with anti-human IgA, reveals that the highest neutralization activity against SARS-CoV-2 is achieved when all three immunoglobulins, IgG, IgM and IgA are detected, as if to indicate the presence of a synergistic or additive effect between different classes of antibodies. This observation can be explained by the fact that the human population is completely naïve for SARS-CoV-2 and that IgG or IgM alone is not able to mount an ideal neutralizing immune response. Indeed, one of the most important features of adaptive immunity is the generation of immunological memory and the ability of the immune system to learn from its experiences of encounters with the same pathogen, thereby becoming more effective over time (Bonilla and Oettgen, 2010).

Interestingly, in nine samples, neither in-house nor commercial kits detected any IgG and IgM signal for the S1 protein, while a noticeable signal for RBD-specific IgG, IgM and IgA was detected.

As all nine samples displayed exactly same trend, it seems that these results could be due to the folding of the three-dimensional S1 protein structure after the production in HEK293 cells, which could have masked some epitopes recognized by the antibodies expressed in these nine subjects. By contrast, these epitopes may be well exposed in the RBD protein and can be bound by antibodies, which would explain the differences in signals.

To conclude, these results confirm what has already been reported (Robbiani et al., 2020), i.e. that the immune response to SARS-CoV-2 is very variable, but that antibodies targeting the RBD domain of Spike protein have an important role relatively to their neutralization activity. However, it is unclear whether neutralizing antibodies to S protein are the major contributor to a protective immune response as evidenced by a recent study (Hachim et al., 2020). So, the present study constitutes preliminary research into the development of an ELISA that can semi-quantify anti-SARS-CoV-2 human antibodies in a specific and repeatable way. The next step will be to completely validate these ELISAs according to the criteria established by the International Council for Harmonization of Technical Requirements for Pharmaceuticals for Human Use (Q 2 (R1), 2006), and to analyze the performance and specificity of these tests with a panel human serum samples that are highly positive towards different HCoVs.

Authors' contributions

LM performed the set-up experiments and standardized *in-house* ELISAs; LM, DM and IH performed all the ELISA experiments; PP evaluated the results and performed the statistical analyses; LB and IR handled the Vero E6 cells and prepared the plates for neutralization experiments; AM and EC performed the Micro-neutralization experiments; CMT and SM performed the Euroimmun ELISA assays at the University site and provided the human serum samples; AM and GL designed the experiments; AM, LM, EM (Eleonora Molesti) prepared the draft of the manuscript; EM supervised the study. All authors have approved the final version of the manuscript.

Acknowledgments

We thank the Laboratory of Molecular and Developmental Medicine of the University of Siena for providing the human serum samples. Furthermore, we thank Dr. Valentina Bollati from the University of Milan for providing the serum samples from COVID-19-positive patients. This publication was supported by the European Virus Archive Global (EVAg) project, which has received funding from the European Union's Horizon 2020 research and innovation program under grant agreement No 653316.

Declaration of Competing Interest

The authors declare that they have no conflict of interest.

References

Aalberse, R.C., Dieges, P.H., Knul-Bretlova, V., Vooren, P., Aalbers, M., van Leeuwen, J., Jun. 1983. IgG4 as a blocking antibody. Clin. Rev. Allergy 1 (2), 289–302. https://doi.org/10.1007/BF02991163.

Amanat, F., et al., May 2020. A serological assay to detect SARS-CoV-2 seroconversion in humans. Nat. Med. 1–4. https://doi.org/10.1038/s41591-020-0913-5.

Andersen, K.G., Rambaut, A., Lipkin, W.I., Holmes, E.C., Garry, R.F., Apr. 2020. The proximal origin of SARS-CoV-2. Nat. Med. 26 (4) https://doi.org/10.1038/s41591-020-0820-9. Art. no. 4.

Andreano, E., et al., May 2020. Identification of neutralizing human monoclonal antibodies from Italian Covid-19 convalescent patients. Immunology. https://doi.org/10.1101/2020.05.05.078154 preprint.

Bao, L., et al., Mar. 2020. Lack of Reinfection in Rhesus Macaques Infected with SARS-CoV-2. Microbiology. https://doi.org/10.1101/2020.03.13.990226 preprint.

Berry, J.D., et al., 2010. Neutralizing epitopes of the SARS-CoV S-protein cluster independent of repertoire, antigen structure or mAb technology. mAbs 2 (1), 53–66.

Bonilla, F.A., Oettgen, H.C., Feb. 2010. Adaptive immunity. J. Allergy Clin. Immunol. 125 (2), S33–S40. https://doi.org/10.1016/j.jaci.2009.09.017.

Chan, J.F.-W., et al., 2020. A familial cluster of pneumonia associated with the 2019 novel coronavirus indicating person-to-person transmission: a study of a family cluster. Lancet Lond. Engl. 395 (10223), 514–523. https://doi.org/10.1016/S0140-6736(20)30154-9.

Clements, M.L., Betts, R.F., Tierney, E.L., Murphy, B.R., Jul. 1986. Serum and nasal wash antibodies associated with resistance to experimental challenge with influenza A wild-type virus. J. Clin. Microbiol. 24 (1), 157–160.

Corman, V.M., Lienau, J., Witzenrath, M., 2019. Coronaviren als Ursache respiratorischer Infektionen. Internist 60 (11), 1136–1145. https://doi.org/10.1007/s00108-019-00671-5.

Dessy, F.J., et al., Nov. 2008. Correlation between direct ELISA, single epitope-based inhibition ELISA and Pseudovirion-based neutralization assay for measuring anti-HPV-16 and anti-HPV-18 antibody response after vaccination with the AS04-adjuvanted HPV-16/18 cervical cancer vaccine. Hum. Vaccine 4 (6), 425–434. https://doi.org/10.4161/hv.4.6.6912.

Ferrante, A., Beard, L.J., Feldman, R.G., Aug. 1990. IgG subclass distribution of antibodies to bacterial and viral antigens. Pediatr. Infect. Dis. J. 9 (8 Suppl), S16–S24.

Frasca, D., Diaz, A., Romero, M., Mendez, N.V., Landin, A.M., Blomberg, B.B., Apr. 2013. Effects of age on H1N1-specific serum IgG1 and IgG3 levels evaluated during the 2011–2012 influenza vaccine season. Immun. Ageing A 10 (1), 14. https://doi.org/10.1186/1742-4933-10-14.

Gonda, M.G., Fang, X., Perry, G.A., Maltecca, C., Oct. 2012. Measuring bovine viral diarrhea virus vaccine response: using a commercially available ELISA as a surrogate for serum neutralization assays. Vaccine 30 (46), 6559–6563. https://doi.org/10.1016/j.vaccine.2012.08.047.

Gorbalenya, A.E., et al., Apr. 2020. The species Severe acute respiratory syndrome-related coronavirus : classifying 2019-nCoV and naming it SARS-CoV-2. Nat. Microbiol. 5 (4) https://doi.org/10.1038/s41564-020-0695-z (Art. no. 4).

Guan, M., Chen, H.Y., Foo, S.Y., Tan, Y.-J., Goh, P.-Y., Wee, S.H., Mar. 2004. Recombinant protein-based enzyme-linked immunosorbent assay and Immunochromatographic tests for detection of immunoglobulin G antibodies to Severe Acute Respiratory Syndrome (SARS) coronavirus in SARS patients. Clin. Diagn. Lab. Immunol. 11 (2), 287–291. https://doi.org/10.1128/CDLI.11.2.287-291.2004.

Hachim, A., et al., Oct. 2020. ORF8 and ORF3b antibodies are accurate serological markers of early and late SARS-CoV-2 infection. Nat. Immunol. 21 (10), 1293–1301. https://doi.org/10.1038/s41590-020-0773-7.

Hsueh, P.-R., et al., Sep. 2004. SARS antibody test for serosurveillance. Emerg. Infect. Dis. 10 (9), 1558–1562. https://doi.org/10.3201/eid1009.040101.

Ivanov, A.P., Klebleyeva, T.D., Malyshkina, L.P., Ivanova, O.E., 2019. Poliovirus-binding inhibition ELISA based on specific chicken egg yolk antibodies as an alternative to the neutralization test. J. Virol. Methods 266, 7–10. https://doi.org/10.1016/j.jviromet.2019.01.007.

Kundi, M., Apr. 1999. One-hit models for virus inactivation studies. Antivir. Res. 41 (3), 145–152. https://doi.org/10.1016/s0166-3542(99)00008-x.

Liu, W., et al., 2020. Evaluation of nucleocapsid and spike protein-based enzyme-linked immunosorbent assays for Detecting antibodies against SARS-CoV-2. J. Clin. Microbiol. 58 (6) https://doi.org/10.1128/JCM.00461-20.

Madore, D.V., Meade, B.D., Rubin, F., Deal, C., Lynn, F., Jun. 2010. Utilization of serologic assays to support efficacy of vaccines in nonclinical and clinical trials: meeting at the crossroads. Vaccine 28 (29), 4539–4547. https://doi.org/10.1016/j.vaccine.2010.04.094.

Manenti, A., et al., 2017. Comparative analysis of influenza A(H3N2) virus hemagglutinin specific IgG subclass and IgA responses in children and adults after influenza vaccination. Vaccine 35 (1), 191–198. https://doi.org/10.1016/j.vaccine.2016.10.024.

Manenti, A., et al., May 2020. Evaluation of SARS-CoV-2 neutralizing antibodies using a CPE-based colorimetric live virus micro-neutralization assay in human serum samples. J. Med. Virol. https://doi.org/10.1002/jmv.25986.

Murin, C.D., Wilson, I.A., Ward, A.B., 2019. Antibody responses to viral infections: a structural perspective across three different enveloped viruses. Nat. Microbiol. 4 (5), 734–747. https://doi.org/10.1038/s41564-019-0392-y.

Okba, N.M.A., et al., Jul. 2020. Severe acute respiratory syndrome coronavirus 2-specific antibody responses in coronavirus disease patients. Emerg. Infect. Dis. 26 (7), 1478–1488. https://doi.org/10.3201/eid2607.200841.

Ou, X., et al., 2016. Identification of the Fusion Peptide-Containing Region in Betacoronavirus Spike Glycoproteins. J. Virol. 90 (12), 5586–5600. https://doi.org/10.1128/JVI.00015-16.

Q 2 (R1), 2006. Validation of Analytical Procedures: Text and Methodology, p. 15.

Robbiani, D.F., et al., Jun. 2020. Convergent antibody responses to SARS-CoV-2 in convalescent individuals. Nature. https://doi.org/10.1038/s41586-020-2456-9.

Schroeder, H.W., Cavacini, L., Feb. 2010. Structure and function of immunoglobulins. J. Allergy Clin. Immunol. 125 (2 Suppl 2), S41–S52. https://doi.org/10.1016/j.jaci.2009.09.046.

Seow, J., et al., Jul. 2020. Longitudinal evaluation and decline of antibody responses in SARS-CoV-2 infection. Infectious Diseases (except HIV/AIDS). https://doi.org/10.1101/2020.07.09.20148429 preprint.

Tay, M.Z., Poh, C.M., Rénia, L., MacAry, P.A., Ng, L.F.P., Jun. 2020. The trinity of COVID-19: immunity, inflammation and intervention. Nat. Rev. Immunol. 20 (6) https://doi.org/10.1038/s41577-020-0311-8. Art. no. 6.

WHO, 2020. Coronavirus disease 2019 (COVID19) Situation Report 23. In: Coronavirus disease 2019 (COVID-19) Situation Report - 23. https://www.who.int/docs/default-source/coronaviruse/situation-reports/20200212-sitrep-23-ncov.pdf?sfvrsn=41e9fb78_4 (accessed 10.07.20).

WHO. Coronavirus disease COVID-19 Situation Reports - Weekly Updates. https://www.who.int/emergencies/diseases/novel-coronavirus-2019/situation-reports (accessed 23.09.20).

WHO, Manual for the laboratory diagnosis and virological surveillance of influenza', WHO. https://www.who.int/influenza/gisrs_laboratory/manual_diagnosis_surveillance_influenza/en/ (accessed 10.07.20).

de Wit, E., van Doremalen, N., Falzarano, D., Munster, V.J., 2016. SARS and MERS: recent insights into emerging coronaviruses. Nat. Rev. Microbiol. 14 (8), 523–534. https://doi.org/10.1038/nrmicro.2016.81.

Wrapp, D., et al., Mar. 2020. Cryo-EM structure of the 2019-nCoV spike in the prefusion conformation. Science 367 (6483), 1260–1263. https://doi.org/10.1126/science.abb2507.

Zaki, A.M., van Boheemen, S., Bestebroer, T.M., Osterhaus, A.D.M.E., Fouchier, R.A.M., Nov. 2012. Isolation of a novel coronavirus from a man with pneumonia in Saudi Arabia. N. Engl. J. Med. 367 (19), 1814–1820. https://doi.org/10.1056/NEJMoa1211721.

Zou, H., Hastie, T., Apr. 2005. Regularization and variable selection via the elastic net. J. R. Stat. Soc. Ser. B Stat Methodol. 67 (2), 301–320. https://doi.org/10.1111/j.1467-9868.2005.00503.x.

Zou, L., et al., Mar. 2020. SARS-CoV-2 viral load in upper respiratory specimens of infected patients. N. Engl. J. Med. 382 (12), 1177–1179. https://doi.org/10.1056/NEJMc2001737.

Received: 26 April 2020 | Accepted: 4 May 2020

DOI: 10.1002/jmv.25986

RESEARCH ARTICLE

JOURNAL OF MEDICAL VIROLOGY WILEY

Evaluation of SARS-CoV-2 neutralizing antibodies using a CPE-based colorimetric live virus micro-neutralization assay in human serum samples

Alessandro Manenti[1,2] | Marta Maggetti[2] | Elisa Casa[1,2] | Donata Martinuzzi[1] | Alessandro Torelli[1] | Claudia M. Trombetta[3] | Serena Marchi[3] | Emanuele Montomoli[1,2,3]

[1]VisMederi Research s.r.l., Siena, Italy

[2]VisMederi s.r.l., Siena, Italy

[3]Department of Molecular and Developmental Medicine, University of Siena, Siena, Italy

Correspondence
Alessandro Manenti, Strada del Petriccio e Belriguardo, 35, 53100 Siena, Italy.
Email: alessandro.manenti@vismederiresearch.com

Abstract

The micro-neutralization assay is a fundamental test in virology, immunology, vaccine assessment, and epidemiology studies. Since the SARS-CoV-2 outbreak at the end of December 2019 in China, it has become extremely important to have well-established and validated diagnostic and serological assays for this new emerging virus. Here, we present a micro-neutralization assay with the use of SARS-CoV-2 wild type virus with two different methods of read-out. We evaluated the performance of this assay using human serum samples taken from an Italian sero-epidemiological study being performed at the University of Siena, along with the human monoclonal antibody CR3022 and some iper-immune animal serum samples against Influenza and Adenovirus strains. The same panel of human samples have been previously tested in enzyme-linked immunosorbent assay (ELISA) as a pre-screening. Positive, borderline, and negative ELISA samples were evaluated in neutralization assay using two different methods of read-out: subjective (by means of an inverted optical microscope) and objective (by means of a spectrophotometer). Our findings suggest that at least 50% of positive ELISA samples are positive in neutralization as well, and that method is able to quantify different antibody concentrations in a specific manner. Taken together, our results confirm that the colorimetric cytopathic effect-based microneutralization assay could be used as a valid clinical test method for epidemiological and vaccine studies.

KEYWORDS

epidemiology, humoral immunity, neutralization, pandemic, SARS coronavirus

1 | INTRODUCTION

Coronavirus (CoV), along with Influenza virus, is a major public health concern. CoVs are enveloped, positive single-stranded RNA viruses belonging to the *Coronaviridae* family; they contain a single genome of 30 Kbp, and consist of four groups: *Alphacoronavirus*, *Betacoronavirus*, *Gammacoronavirus*, and *Deltacoronavirus*.[1,2] To date, seven CoV strains are known to infect humans, affecting the lower respiratory tract, gastrointestinal system, heart, liver, kidney, and central nervous system.[3,4] Over the past 23 years, outbreaks in humans, including Severe Acute Respiratory Syndrome (SARS) and Middle-East Respiratory Syndrome (MERS),[5] have heightened the daunting possibility

that a future pandemic may be caused by one of these agents, underlining the urgent need to prepare for such an eventuality, since no vaccines or approved therapies, are as yet available.[6] At the end of December 2019 in Wuhan, Hubei Province, China, a novel CoV strain, called SARS-CoV-2 by the International Committee on Taxonomy of Viruses (ICTV), caused 27 cases of pneumonia of unidentified etiology.[7] Due to the rapid and uncontrollable spread of the virus in almost every country in the world, the World Health Organization (WHO) officially declared the pandemic status in March 2020. The disease caused by SARS-CoV-2, named COVID-19, is considered a self-limiting infectious disease with five different possible outcomes: asymptomatic cases (1.2%), mild cases (80.9%), severe cases (13.8%), critical cases (4.7%), and deaths (2.3%).[7,8] However, some authors reported a higher percentage of asymptomatic infections in children under the age of 10 (15.8%).[9] Because of the lack of specific antiviral drugs or vaccines, several thousands of serious cases and deaths occur every day all over the world, and strict quarantine measures have been imposed either nationally or internationally. Since the antibody response of the serum, after a natural CoV infection remains detectable for a long time,[10] medical authorities in many countries are trying to calculate the percentage of the population that may be protected against the new circulating strain through the assessment of anti-SARS-CoV-2 Immunoglobulin G (IgG) and M (IgM) levels in serum samples. Principal serological tests used in these studies are ELISA-based assays. Most of these tests focus on different combinations of coatings on the viral spike (S) protein (*S1; S1+S2; S1-S2 extracellular domain-ECD, receptor binding domain*-RBD), due to the fact that the CoV's ability to attach and consequently enter the cell is mainly mediated by this protein.[11] Enzyme-linked immunosorbent assays (ELISAs) certainly have advantages, such as high throughput, speed of testing, and the possibility of avoiding the requirement for a high containment laboratory, as BSL 3. However, most of these assays present some limitations, such as low specificity and sensitivity, and use of alternative purified proteins that can be produced in different hosts (human-derived cells vs insect cells). In addition, the mismatch between results obtained from the same samples, using different ELISA reagents and coatings (eg, source of antigen), may lead to confusion.[12] To date, the Micro-Neutralization assay (MN), currently considered the gold-standard is the most specific and sensitive serological assay capable of evaluating and detecting, functional neutralizing antibodies (nAbs). In this paper, a live virus-based MN assay is presented for the quantification of SARS-CoV-2-specific nAbs in human serum samples by two different methods of detection: a classical read-out by checking the percentage of cytopathic effect (CPE) in the cell monolayer, and a colorimetric read-out by a spectrophotometer.

2 | MATERIALS AND METHODS

2.1 | Serum samples and human monoclonal antibody IgG1

A total of 83 human serum samples were collected as part of a seroepidemiological study that is being performed in the laboratory of Molecular Epidemiology of the University of Siena, Italy. Serum samples were anonymously collected in compliance with Italian ethics law. The human monoclonal antibody IgG1-*CR3022* (absolute antibody) was tested along with the serum samples in the MN assay and ELISA. Hyperimmune sheep antisera against Influenza A/H1N1/California/7/2009 (10/218), B/Brisbane/60/2008 (13/312), and A/Anhui/1/2013 (15/248) strains were purchased from the National Institute for Biological Standard and Controls (NIBSC, UK). Hyperimmune rabbit serum samples against Adenovirus Type 4 (V204-502-565) were provided by the National Institute of Allergy and Infectious Diseases (NIH, Bethesda). Human serum minus IgA/IgM/IgG (S5393-1VL) (Sigma, St. Louis, MO) was used as a negative control.

2.2 | Cell culture

VERO cells, an African Green monkey kidney cell line, were purchased from the European Collection of Authenticated Cell Cultures (ECACC - Code 84121903). VERO cells were cultured in Eagle's minimum essential medium (EMEM) (Lonza, Milano, Italy) supplemented with 2 mM L- Glutamine (Lonza, Milano, Italy), 100 units/mL penicillin-streptomycin mixture (Lonza, Milano, Italy) and fetal bovine serum (FBS) (Euroclone, Pero, Italy) to a final concentration of 5%, at 37°C, in a 5% CO_2 humidified incubator.

VEROE6 cells, an epithelial cell line from the kidney of a normal monkey (*Cercopithecus aethiops*), were acquired from the American Type Culture Collection (ATCC - CRL 1586).

Huh-7 cells, an epithelial cell line from Human hepatocellular carcinoma, were kindly provided by the University of Siena (ECACC-Code 01042712). Both VEROE6 and Huh-7 cells were cultured in Dulbecco's Modified Eagle's Medium (DMEM)-high glucose (Euroclone, Pero, Italy) supplemented with 2 mM L-Glutamine (Lonza, Milano, Italy), 100 units/mL penicillin-streptomycin mixture (Lonza, Milano, Italy) and 10% of FBS, at 37°C, in a 5% CO_2 humidified incubator.

Adherent sub-confluent cell monolayers of VERO, VERO E6, and Huh-7 were prepared in growth medium, E-MEM or D-MEM high glucose containing 2% FBS in T175 flasks or 96-well plates for propagation or titration and neutralization tests of SARS-CoV-2, respectively.

2.3 | Virus and titration

SARS CoV-2 2019-*2019-nCoV strain 2019-nCov/Italy-INMI1*-wild type virus was purchased from the European Virus Archive goes Global (EVAg, Spallanzani Institute, Rome). The virus was titrated in serial 1 log dilutions (from 1 log to 11 log) to obtain a 50% tissue culture infective dose (TCID50) on 96-well culture plates of VERO and VERO E6 cells. The plates were observed daily for a total of 4 days for the presence of CPE by means of an inverted optical microscope. The end-point titres were calculated according to the Reed & Muench method[13] based on eight replicates for titration.

2.4 | Viral growth in cell culture

The SARS-CoV-2 virus was seeded and propagated in VERO, VERO E6, and Huh-7 cells by using EMEM (for VERO and Huh-7) and DMEM high glucose (for VERO E6) both supplemented with 2% FBS and 100 IU/mL penicillin-streptomycin.

Cells were seeded in T175 flasks at a density of 1×10^6 cells/mL. After 18 to 20 hours, the sub-confluent cell monolayer was washed twice with sterile Dulbeccos's phosphate buffered saline (DPBS). After removal of the DPBS, the cells were infected with 3.5 mL of EMEM/DMEM 2% FBS containing the virus at a multiplicity of infection of 0.001 and 0.01. After 1 hour of incubation at 37°C in a humidified atmosphere with 5% CO_2, 50 mL of EMEM/DMEM containing 2% FBS was added for VERO-Huh7/VERO E6. The flasks were daily observed and the virus was harvested when 80%-90% of the cells manifested CPE. The culture medium was centrifuged at +4°C 1600 rpm for 8 minutes, to remove the cell debris, then they aliquoted and stored at −80°C.

2.5 | Micro-neutralization assay

Serum samples were heat-inactivated for 30 minutes at 56°C; two-fold serial dilutions, starting from 1:10, were then mixed with an equal volume of viral solution containing 100 TCID50 of SARS-CoV-2. The serum-virus mixture was incubated for 1 hour at 37°C in a humidified atmosphere with 5% CO_2. After incubation, 100 µL of the mixture at each dilution was added in duplicate to a cell plate containing a semi-confluent VERO E6 monolayer. The plates were incubated for 4 days at 37°C in a humidified atmosphere with 5% CO_2.

2.5.1 | CPE-read out

After 4 days of incubation, the plates were inspected by an inverted optical microscope. The highest serum dilution that protected more than the 50% of cells from CPE was taken as the neutralization titre.

2.5.2 | Colorimetric read-out

After 3 days of incubation, the supernatant of each plate was carefully discarded and 100 µl of a sterile DPBS solution containing 0.02% neutral red (Sigma, St. Louis, MO) was added to each well of the MN plates. After 1 hour of incubation at room temperature, the neutral red solution was discarded and the cell monolayer was washed twice with sterile DPBS containing 0.05% Tween 20. After the second incubation, the DPBS was carefully removed from each well; then, 100 µL of a lysis solution made up of 50 parts of absolute ethanol (Sigma, St. Louis, MO), 49 parts of MilliQ and 1 part of glacial acetic acid (Sigma) was added to each well. Plates were incubated for 15 minutes at room temperature and then read by a spectrophotometer at 540 nm. The highest serum dilution, showing an optical density (OD) value greater than the cut-off value, was considered as the neutralization titre. The cut-off value is calculated as the average of the OD values of the cell control wells divided by two.

2.6 | Enzyme-linked immunosorbent assay

Specific anti-SARS-CoV-2 IgG antibodies were detected through a commercial ELISA kit (Euroimmun, Lübeck, Germany). ELISA plates are coated with recombinant structural protein (S1 domain) of SARS-CoV-2. According to the manufacturer, cross-reactions may occur with anti-SARS-CoV(-1) IgG antibodies, due to the close relationship between SARS-CoV(-1) and SARS-CoV-2, while cross-reactions with other human pathogenic CoVs (MERS-CoV, HCoV-229E, HCoV-NL63, HCoV-HKU1, and HCoV-OC43) are excluded. The assay provides semi-quantitative results by calculating the ratio of the OD of the serum sample over the OD of the calibrator. According to the manufacturer's instructions, positive samples have a ratio ≥1.1, borderline samples a ratio between 0.8 and 1.1 and negative samples a ratio <0.8.

2.7 | Statistics analysis

Data analysis was performed using GraphPad Prism Version 5 and Microsoft Excel 2019. Friedman test was used to compare viral titres obtained at different time points during viral growth in cell culture. A P value <.05 was considered statistically significant.

3 | RESULTS

3.1 | High viral load for VERO and VERO E6, no propagation for Huh-7

SARS-CoV-2 has been propagated for three times in three independent experiments in VERO, VERO E6, and Huh-7 cells. We decided to investigate the viral growth in these specific cell lines because of, as reported in literature, they are the preferred lines for SARS-CoV isolation and replication.[14,15] Different harvest timepoints were evaluated to obtain the infection curve for each cell line: 36, 48 to 52 and 72 to 76 hours postinfection. A high viral titre was obtained for VERO and VERO E6 cells. In both cell lines we tried two different multiplicity of infection (MOI) (0.001 and 0.01), starting from a viral stock containing $10^{7.25}$ TCID50/mL (only results for MOI = 0.001 are reported in this study). After 24 hours postinfection, no CPE or infection plaques were observed in the cell monolayer in any of the three cell lines. After 36 hours, VERO E6 and VERO T-Flasks proved to have detectable CPE of 30%-40% ($10^{3.63}$ TCID50/mL ± 0.14 SD) and 15%-20% ($10^{3.78}$ TCID50/mL ± 0.2 SD), respectively. Between 48 and 52 hours after infection, both cell lines reached 80% of CPE (Figure 1) recording a significant increase of the viral titre according to Friedman test with a mean equal to $10^{7,63}$ TCID50/mL ± 0.38 SD for VERO E6 cells, and $10^{7.17}$

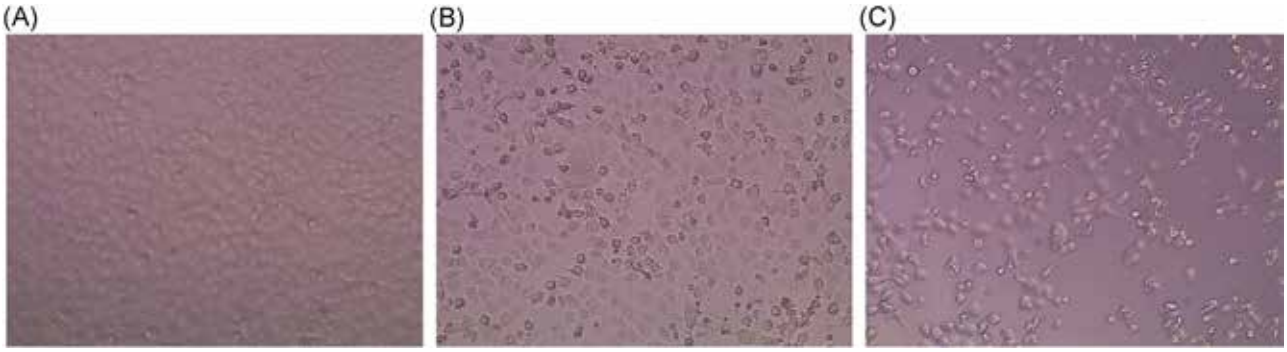

FIGURE 1 Vero E6 cells at different stage of infection. A, Not infected VERO E6 cell monolayer after 72 hours, complete absence of CPE. B, SARS-CoV-2 infected VERO E6 cell monolayer after 36 hours postinfection, 20%-30% of CPE recovered. C, SARS-CoV-2 infected VERO E6 after 52 hours postinfection, 80% of CPE recovered. CPE, cytopathic effect; SARS-CoV-2, Severe Acute Respiratory Syndrome-Coronavirus-2

TCID50/mL ± 0.1 SD for VERO cells. Lower titres were registered in flasks 72 to 76 hours postinfection for VERO ($10^{6.5}$ TCID50/mL ± 0.2 SD) and VERO E6 ($10^{6.4}$ TCID50/mL ± 0.13 SD), with flasks showing 100% of CPE (Figure 2). No detectable CPE was observed for Huh-7 cells up to the 7th day after infection.

To check the viral production in Huh-7 cells, we passed the supernatant in VERO E6 cells but no CPE was detected in this cell line. This confirms that Huh-7 cells are not able to support the viral replication of this CoV strain, as already showed by Harcourt et al.[16] The supernatants derived from VERO, VERO E6 and Huh-7 were titrated in 96-well plates, which were read after 72 hours; titres reached ranged from $10^{6.2}$ to $10^{7.8}$ TCID50/mL either for VERO and VERO E6-derived virus; no titre has been detected for Huh-7-derived virus (data not shown).

3.2 | Comparison between ELISA and MN assays

A total of 83 serum samples were tested for the presence of anti-SARS-CoV-2 antibodies by ELISA and MN assay. On ELISA, 42 samples proved positive, 20 borderline and the remaining 21 negative. Along with the human serum samples, to evaluate the specificity of the MN assay, we tested several animal sera that were highly immunized against different viral diseases, such as Influenza (seasonal and pandemic) and Adenovirus type 4. These sera proved to have high nAb titres against the homologous strain in the MN assay (data not shown). In the MN assay, we assessed the serum response by using two different viral infective doses: a standard dose of 100 TCID50/well and a lower dose of 25 TCID50/well. Neutralization test results confirmed the complete absence (100%) of nAbs in samples already negative on ELISA. Of the 42 samples positive on ELISA, 22 (52.3%) confirmed the presence of CPE-inhibiting nAbs in the cell monolayer, with titres ranging between 10 and 1280/2560. Of 20 borderline ELISA samples, only 3 (15%) confirmed the capability of neutralizing the virus on MN assay. Each sample was tested in duplicate by two different operators, to confirm and validate the results obtained. Each sample was also evaluated by the colorimetric read-out. The results yielded by MN on using the lower infective dose (25 TCID50) were in line with those obtained with the standard infective dose; in some cases, however, we detected a titre that was one dilution step higher, which maintained all negative sample negative (Table 1). All animal samples tested against Influenza and Adenovirus type 4 proved completely negative, confirming the specificity of the MN assay in the detection of anti-SARS-CoV-2 nAbs.

3.3 | Absence of neutralizing activity for human IgG1 monoclonal antibody CR3022

As reported[17] that the *CR3022* monoclonal antibody (mAb) has a high capability of neutralizing the SARS-CoV strain, we included this mAb (IgG1) within the human serum samples in our neutralization assay. The CR3022 antibody targets a highly conserved epitope on the RBD of SARS-CoV. The concentrations tested in MN ranged from 10 μg down to 0.009 μg. The monoclonal antibody was pre-incubated for 1 hour with 100 TCID50 of live SARS-CoV-2 virus before being passed on the VERO E6 monolayer. After 72 hours of incubation, no neutralizing activity was obtained at any of the concentrations tested. By contrast, very high ELISA titres were detected (data not shown). As reported by Tian et al,[18] CR3022, unlike other SARS-CoV monoclonal antibodies, recognizes a different epitope from that one recognized on the RBD by the ACE2 receptor. Moreover, the C-terminal RBD residue of SARS-CoV-2 virus has been found to be quite different from that of SARS-CoV, which may have a critical impact on the cross-reactivity of neutralizing antibodies. Also, as already reported by Tian et al,[19] some antibodies with a high capability of neutralizing SARS-CoV, were found to be unable to bind the S protein of the new SARS-CoV-2 strain; this requires new dedicated monoclonal antibodies.

3.4 | Neutralization assay read-out: subjective vs objective methods

The results obtained in the MN assay in all serum samples were evaluated through two methods of read-out: by inspecting the

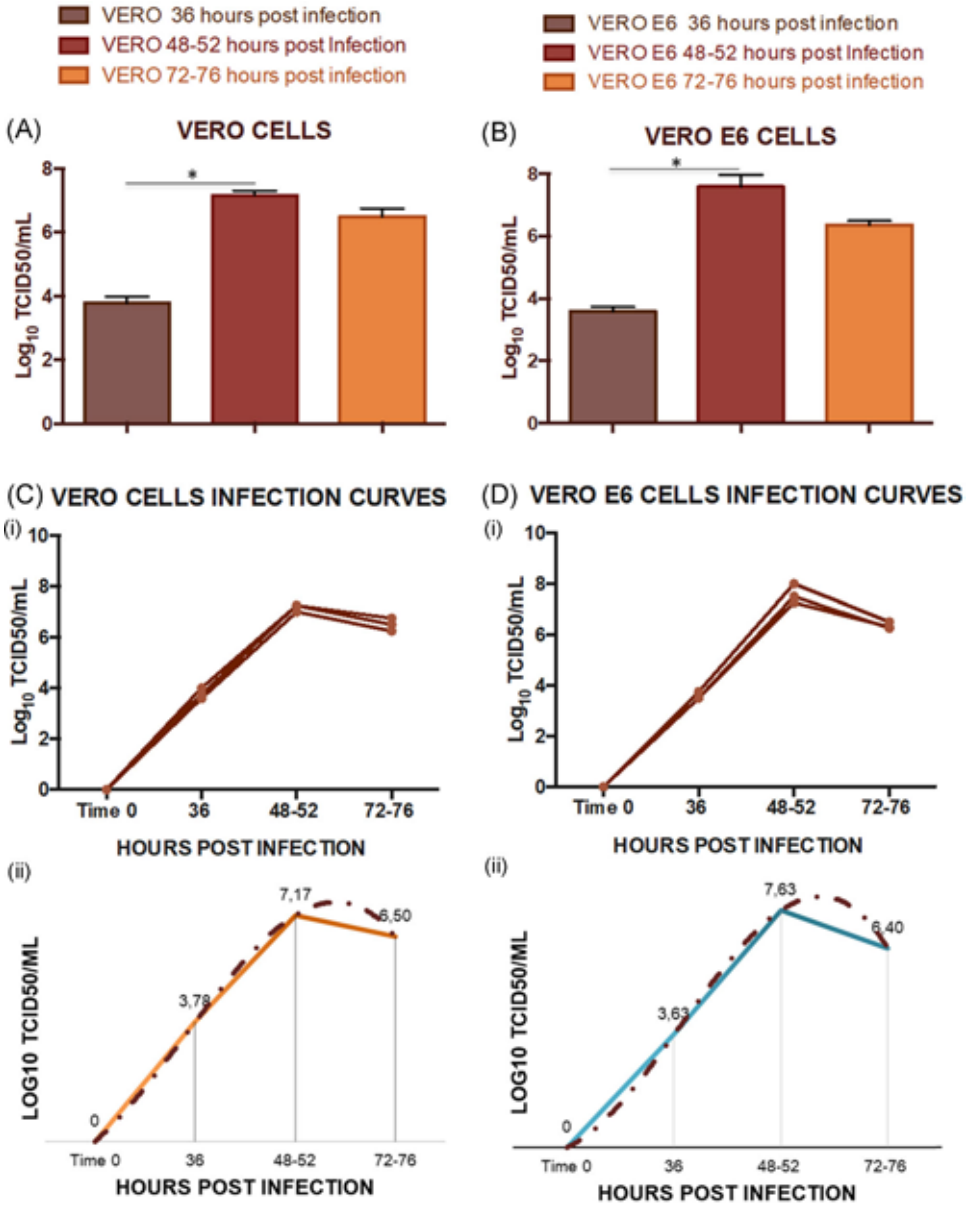

FIGURE 2 Viral titres reached for VERO and VERO E6 in three different viral infection experiments in T-175 flasks. A, Titres registered in triplicate (n = 3) for VERO cells after 36, 48 to 52 and 72 to 76 hours post infection. A significant increase in the viral titre has been registered after 48 to 52 hours according to Friedman test ($P < .05$), error bars indicate the standard deviation among the three independent measures. B, Titres registered (n = 3) for VERO E6 cells after 36, 48 to 52 and 72 to 76 hours post infection. A significant increase in the viral titre has been registered after 48 to 52 hours according to Friedman test ($P < .05$), error bars indicate the standard deviation among the three independent measures. C.1, Infection curves for VERO cells for three independent experiments of viral growth. C.2, Polynomial infection curve derived from the average of the three experimental curves for VERO cells. D.1, Infection curves for VERO E6 for three independent experiments of viral growth. D.2, Polynomial infection curve derived from the average of the three experimental curves for VERO E6 cells

inhibition of the CPE at each serum dilution (subjective method) by an inverted optical microscope, and by applying a colorimetric method in which the healthy cell monolayer is stained with a neutral red solution. As can be seen in Figure 3, the 12th and the 11th columns of each plate were set up as a virus control (CV) and a cell control (CC), respectively. Serum samples were progressively diluted from column 1 to column 10. The cut-off value, calculated mathematically as the average of all cell control ODs divided by two, indicates the titre of each sample tested. Results of the comparison between ELISA and MN (Table 1) suggest that a well-trained operator is able to read the CPE, thereby providing the same results as the spectrophotometer in terms of titre with no differences between the results provided by the two different operators and the spectrophotometric evaluation of the ODs.

One of the advantages of the colorimetric read-out is that, being a completely automated method, it offers a higher throughput, while

TABLE 1 ELISA and neutralization results for all 83 human serum samples

Sample ID	ELISA	MN CPE titre analyst 1 100 $TCID_{50}$	MN CPE titre analyst 2 100 $TCID_{50}$	Colorimetric MN 100 $TCID_{50}$	MN CPE titre 25 $TCID_{50}$
From 1 to 21	Negative	5	5	5	5
22	Borderline	5	5	5	5
23	Borderline	5	5	5	5
24	Borderline	5	5	5	5
25	Borderline	5	5	5	5
26	Borderline	5	5	5	5
27	Borderline	5	5	5	5
28	Borderline	5	5	5	5
29	Borderline	5	5	5	5
30	Borderline	5	5	5	5
31	Borderline	5	5	5	5
32	Borderline	5	5	5	5
33	Borderline	5	5	5	5
34	Borderline	5	5	5	5
35	Borderline	5	5	5	5
36	Borderline	5	5	5	5
37	Borderline	5	5	5	5
38	Borderline	5	5	5	5
22	Borderline	20	20	20	40
23	Borderline	80	40	80	80
24	Borderline	20	20	20	20
42	Positive	640	640	640	640
43	Positive	20	20	20	40
44	Positive	320	320	320	320
45	Positive	640	320	320	640
46	Positive	40	40	40	40
47	Positive	640	640	640	640
48	Positive	20	20	20	20
49	Positive	10	20	10	20
50	Positive	160	320	320	320
51	Positive	40	40	40	40
52	Positive	160	160	160	320
53	Positive	640	640	640	640
54	Positive	80	80	80	80
55	Positive	1280	2560	1280	1280
56	Positive	160	160	160	320
57	Positive	80	80	80	80
58	Positive	10	10	10	20
59	Positive	80	80	80	80
60	Positive	640	640	640	640
61	Positive	10	10	10	10
62	Positive	40	40	40	40
63	Positive	40	40	40	40
64	Positive	5	5	5	5
65	Positive	5	5	5	5
66	Positive	5	5	5	5
67	Positive	5	5	5	5
68	Positive	5	5	5	5
69	Positive	5	5	5	5
70	Positive	5	5	5	5
71	Positive	5	5	5	5
72	Positive	5	5	5	5
73	Positive	5	5	5	5
74	Positive	5	5	5	5
75	Positive	5	5	5	5
76	Positive	5	5	5	5
77	Positive	5	5	5	5
78	Positive	5	5	5	5
79	Positive	5	5	5	5
80	Positive	5	5	5	5
81	Positive	5	5	5	5
82	Positive	5	5	5	5
83	Positive	5	5	5	5

Note: Negative samples are indicated in the first row of the table. Neutralizing titres, obtained with CPE (100 and 25 TCID50 infective dose) and colorimetric read-out methods, are indicated for each sample.

inspection of each dilution well by means of the optical microscope slows down the process.

4 | DISCUSSION

The availability of a specific serological assay capable of providing the most reliable and accurate antibody response in a given sample is a crucial factor in all epidemiological studies. This is particularly important in an emergency situation, such as during a sudden epidemic or, even worse, a pandemic. Indeed, knowing which percentage of the

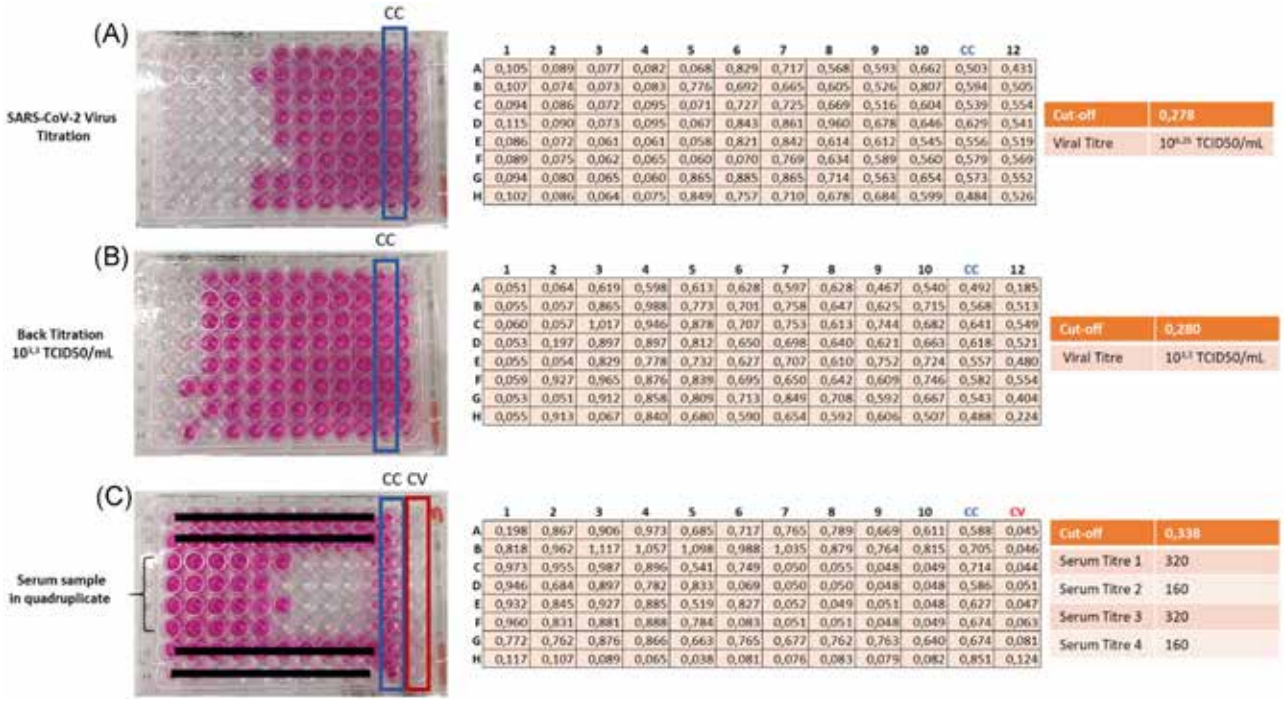

FIGURE 3 Schematic overview of the colorimetric MN read-out. A, SARS-CoV-2 virus titration. B, Titration of the working viral solution. C, Neutralization plate with a serum sample tested in quadruplicate. In each plate, the column highlighted in blue is the cell control (highest OD value), while the column highlighted in red is the virus control (no OD values). The cut-off value is evaluated for each plate, and is equal to the average of the cell control ODs divided by two. Wells that show OD values lower than the cut-off are considered virus-positive, and hence infected. The viral titres in both the stock solution (A) and the working viral solution (B) are calculated by means of the Reed and Muench method. The titre of the serum sample (C) was calculated as the reciprocal of the highest dilution at which the OD value was higher than or equal to the cut-off value. OD, optical density; ARS-CoV-2, Severe Acute Respiratory Syndrome-Coronavirus-2

population has already come in contact with the virus, and consequently developed a specific immune response, can drive the type and timing of prevention and containment measures. Virus nAbs can be induced by natural infection or vaccination, and they have a crucial role in controlling and limiting viral infection and transmission among people. In this paper, we present a possible approach to evaluate anti-SARS-CoV-2 neutralizing antibodies in human and animal samples using the wild-type virus. We evaluated the performance of the MN assay on a subset of samples that are being tested by ELISA in a seroepidemiological study currently underway at the University of Siena. We also tested four animal antisera against Influenza and Adenovirus and human CR3022 mAb. Since SARS-CoV-2 and SARS-CoV display a high sequence identity of the S protein,[18] it is possible that SARS-CoV nAbs may elicit cross-neutralization activity against SARS-CoV-2. Unfortunately, our preliminary neutralization results showed no ability of the CR3022 mAb to prevent viral attachment and entry into cell monolayer, which developed CPE in less than 48 hours postinfection. On the other hand, the high signal registered on ELISA confirmed the potential of the CR3022 mAb to bind with high affinity an epitope on the RBD of the SARS-CoV-2 S protein.[19] For human serum samples, the MN assay confirmed that at least 50% of the samples, tested positive on ELISA assay, presented antibodies with neutralizing ability. This finding is broadly in line with previous Influenza studies, in which that assay was able to detect all binding antibodies without a prediction of their functionality.[20,21] It is interesting to note that the ELISA kit used in the present study has been validated for sensitivity and specificity for SARS-CoV-2 by Okba et al in a previous work,[22] and it has been found to have 96% of specificity and 65% of sensitivity compared to other 8 commercial ELISA kits for SARS-CoV-2.[23] The fact that we detected fairly low neutralizing titres in samples and that only half of those assessed positive on ELISA may be due to different factors: (a) at this stage the human population is completely naïve about this CoV strain, and several waves of exposure to the pathogen may be necessary to stimulate a strong neutralizing response; (b) as it has already proved for other viruses, such as Lassa,[24] neutralizing antibodies are not always elicited after vaccination or natural infection; in fact, other mechanisms of the immune system may be involved in the protection, such as the complement-fixation reaction mediated by IgG_1 and IgG_3, antigen-dependent cellular cytotoxicity and T-cell responses. Samples that are not able to show a high signal on ELISA (borderline samples) may, instead, have neutralizing capabilities, as it was confirmed by three of our samples. In this study, we show a possible and objective method of read-out using spectrophotometry and a solution containing 0.02% of neutral red able to stain lysosomes and other cell organelles.[25] Moreover, the aforementioned method increases throughput by enabling more samples to be processed per run. The difference between the titres registered by the two analysts

in evaluation of CPE may be attributed to those wells where the ratio between the percentage of infected and uninfected cells is quite difficult to estimate under the microscope. The colorimetric method, on the other hand, based on a numerical value of optical density, obviates this problem. However, the present study has limitations. At this stage, the major difficulty lies in the lack of a standardized positive control that would enable the proper standardization of the assays. Furthermore, the number of samples analyzed in this preliminary assessment was small. The next step in this study will be to fully validate the colorimetric MN assay according to the criteria established by the International Council for Harmonization of Technical Requirements for Pharmaceuticals for Human Use.[26] This will involve the inclusion of samples from individuals with confirmed SARS-CoV-2 diagnosis and the use of additional positive sera from other alpha or beta CoVs to investigate possible serological cross-reactions. Finally, another aspect to examine is the optimal infective dose to be use in the MN assay (100 TCID50 or lower) for this viral strain, to have a more reliable and accurate response based on the actual immunological status.

5 | CONCLUSIONS

To conclude, the method of viral growth, titration and neutralization of SARS-CoV-2 presented in this study results suitable for the quantification of the neutralizing antibody titre in serum samples. Together with ELISA assay, this test should always be included in seroepidemiological and immunogenicity studies of vaccines. The necessity for a BSL 3 laboratory could certainly be a limiting factor for neutralizing antibodies studies using wild type viruses, but it is currently the most reliable method in terms of results provided.

ACKNOWLEDGMENTS

This publication was supported by the European Virus Archive goes Global (EVAg) project, which has received funding from the European Union's Horizon 2020 research and innovation programme under grant agreement No 653316. We thank the University of Siena for providing the human serum samples from the Epidemiological study on SARS-CoV-2. The authors would like to thank Inesa Hyseni, Virginia Cianchi, Ilaria Razzano and Linda Benincasa for the lab support in VisMederi Research.

CONFLICT OF INTERESTS

The authors declare that there are no conflict of interests.

AUTHOR CONTRIBUTIONS

AM designed and performed the neutralization set-up experiments, conducted the viral growth procedures in BSL 3, and prepared the manuscript; MM and EC performed the neutralization tests in BSL 3 and elaborated the results; DM prepared and cultured the VERO E6 cell line. AT purchased the virus, the monoclonal antibody and cell lines; CMT and SM performed the ELISA assay at the University of Siena; EM supervised the study. All authors have approved the final version of the manuscript.

ORCID

Alessandro Manenti http://orcid.org/0000-0002-4027-7296

REFERENCES

1. Park WB, Kwon NJ, Choi SJ, et al. Virus isolation from the first patient with SARS-CoV-2 in Korea. *J Korean Med Sci*. 2020;35(7):e84. https://doi.org/10.3346/jkms.2020.35.e84
2. Wang J, Deng F, Ye G, et al. Comparison of lentiviruses pseudotyped with S proteins from coronaviruses and cell tropisms of porcine coronaviruses. *Virol Sin*. 2016;31(1):49-56. https://doi.org/10.1007/s12250-015-3690-4
3. Zhu N, Zhang D, Wang W, et al. A novel coronavirus from patients with pneumonia in China, 2019. *N Engl J Med*. 2020;382(8):727-733. https://doi.org/10.1056/NEJMoa2001017
4. Prompetchara E, Ketloy C, Palaga T. Immune responses in COVID-19 and potential vaccines: lessons learned from SARS and MERS epidemic. *Asian Pac J Allergy Immunol*. 2020;38(1):1-9. https://doi.org/10.12932/AP-200220-0772
5. Zaki AM, van Boheemen S, Bestebroer TM, Osterhaus AD, Fouchier RA. Isolation of a novel coronavirus from a man with pneumonia in Saudi Arabia. *N Engl J Med*. 2012;367(19):1814-1820.
6. Cheng VC, Lau SK, Woo PC, Yuen KY. Severe acute respiratory syndrome coronavirus as an agent of emerging and reemerging infection. *Clin Microbiol Rev*. 2007;20(4):660-694. https://doi.org/10.1128/CMR.00023-07
7. Jin Y, Yang H, Ji W, et al. Virology, epidemiology, pathogenesis, and control of COVID-19. *Viruses*. 2020;12(4):E372. https://doi.org/10.3390/v12040372
8. Novel Coronavirus Pneumonia Emergency Response Epidemiology Team. The epidemiological characteristics of an outbreak of 2019 novel coronavirus diseases (COVID-19) in China. *Zhonghua Liu Xing Bing Xue Za Zhi*. 2020;41(2):145-151. https://doi.org/10.3760/cma.j.issn.0254-6450.2020.02.003
9. Lu X, Zhang L, Du H, et al. SARS-CoV-2 infection in children [published online ahead of print, 2020 Mar 18]. *N Engl J Med*. 2020. https://doi.org/10.1056/NEJMc2005073
10. Perera R, Wang P, Gomaa M, et al. Seroepidemiology for MERS coronavirus using microneutralisation and pseudoparticle virus neutralisation assays reveal a high prevalence of antibody in dromedary camels in Egypt. *Euro Surveill*. 2013;18(36):20574. https://doi.org/10.2807/1560-7917.es2013.18.36.20574
11. Heald-Sargent T, Gallagher T. Ready, set, fuse! The coronavirus spike protein and acquisition of fusion competence. *Viruses*. 2012;4(4):557-580. https://doi.org/10.3390/v4040557
12. Algaissi A, Hashem AM. Evaluation of MERS-CoV neutralizing antibodies in sera using live virus microneutralization assay. *Methods Mol Biol*. 2020;2099:107-116. https://doi.org/10.1007/978-1-0716-0211-9_9
13. Reed LJ, Muench H. A simple method of estimating fifty percent endpoints. *Am J Epidemiol*. 1938;27:493-497.
14. Kaye M. SARS-associated coronavirus replication in cell lines. *Emerg Infect Dis*. 2006;12(1):128-133. https://doi.org/10.3201/eid1201.050496
15. Lu Y, Liu DX, Tam JP. Lipid rafts are involved in SARS-CoV entry into Vero E6 cells. *Biochem Biophys Res Commun*. 2008;369(2):344-349. https://doi.org/10.1016/j.bbrc.2008.02.023
16. Harcourt J, Tamin A, Lu X, et al. Severe Acute Respiratory Syndrome Coronavirus 2 from patient with 2019 Novel Coronavirus Disease, United States. *Emerg Infect Dis*. 2020;26(6), https://doi.org/10.3201/eid2606.200516
17. ter Meulen J, van den Brink EN, Poon LLM, et al. Human monoclonal antibody combination against SARS coronavirus: synergy and

coverage of escape mutants. *PLoS Med*. 2006;3(7):e237. https://doi.org/10.1371/journal.pmed.0030237

18. Zhou P, Yang XL, Wang XG, et al. A pneumonia outbreak associated with a new coronavirus of probable bat origin. *Nature*. 2020;579(7798):270-273. https://doi.org/10.1038/s41586-020-2012-7
19. Tian X, Li C, Huang A, et al. Potent binding of 2019 novel coronavirus spike protein by a SARS coronavirus-specific human monoclonal antibody. *Emerg Microbes Infect*. 2020;9(1):382-385. https://doi.org/10.1080/22221751.2020.1729069
20. Trombetta CM, Remarque EJ, Mortier D, Montomoli E. Comparison of hemagglutination inhibition, single radial hemolysis, virus neutralization assays, and ELISA to detect antibody levels against seasonal influenza viruses. *Influenza Other Respir Viruses*. 2018;12(6):675-686. https://doi.org/10.1111/irv.12591
21. Manenti A, Maciola AK, Trombetta CM, et al. Influenza anti-stalk antibodies: development of a new method for the evaluation of the immune responses to universal vaccine. *Vaccines*. 2020;8(1):E43. https://doi.org/10.3390/vaccines8010043
22. Okba NMA, Müller MA, Li W, et al. Severe Acute Respiratory Syndrome Coronavirus 2-specific antibody responses in Coronavirus disease 2019 patients. *Emerg Infect Dis*. 2020;26(5):1024–1027. https://doi.org/10.3201/eid2607.200841
23. Lassaunière Ria, Frische Anders, Harboe Zitta B, et al. Evaluation of nine commercial SARS-CoV-2 immunoassays. https://www.medrxiv.org/content/10.1101/2020.04.09.20056325v1.full.pdf
24. Abreu-Mota T, Hagen KR, Cooper K, et al. Non-neutralizing antibodies elicited by recombinant Lassa-Rabies vaccine are critical for protection against Lassa fever. *Nat Commun*. 2018;9(1):4223. https://doi.org/10.1038/s41467-018-06741-w
25. Winckler J. Vital staining of lysosomes and other cell organelles of the rat with neutral Red. *Prog Histochem Cytochem*. 1974;6:1-89.
26. EMA, 1995. Q2(R1) Validation of Analytical Procedures: Text and Methodology (CPMP/ICH/381/95).

How to cite this article: Manenti A, Maggetti M, Casa E, et al. Evaluation of SARS-CoV-2 neutralizing antibodies using of a CPE-based colorimetric live virus micro-neutralization assay in human serum samples. *J Med Virol*. 2020;1–9. https://doi.org/10.1002/jmv.25986

viruses

MDPI

Article

Characterisation of SARS-CoV-2 Lentiviral Pseudotypes and Correlation between Pseudotype-Based Neutralisation Assays and Live Virus-Based Micro Neutralisation Assays

Inesa Hyseni [1], Eleonora Molesti [1,*], Linda Benincasa [1], Pietro Piu [2], Elisa Casa [1,2], Nigel J Temperton [3], Alessandro Manenti [1,2] and Emanuele Montomoli [1,2,4]

1 VisMederi Research s.r.l., 53100 Siena, Italy; hyseni@vismederiresearch.com (I.H.); linda.benincasa@vismederiresearch.com (L.B.); casa@vismederiresearch.com (E.C.); alessandro.manenti@vismederiresearch.com (A.M.); montomoli@unisi.it (E.M.)
2 VisMederi s.r.l., 53100 Siena, Italy; pietro.piu@vismederi.com
3 Viral Pseudotype Unit, Medway School of Pharmacy, The Universities of Kent and Greenwich at Medway, Chatham ME7 4TB, UK; n.temperton@kent.ac.uk
4 Department of Molecular and Developmental Medicine, University of Siena, 53100 Siena, Italy
* Correspondence: eleonora.molesti@vismederiresearch.com

Received: 23 July 2020; Accepted: 6 September 2020; Published: 10 September 2020

Abstract: The recent outbreak of a novel Coronavirus (SARS-CoV-2) and its rapid spread across the continents has generated an urgent need for assays to detect the neutralising activity of human sera or human monoclonal antibodies against SARS-CoV-2 spike protein and to evaluate the serological immunity in humans. Since the accessibility of live virus microneutralisation (MN) assays with SARS-CoV-2 is limited and requires enhanced bio-containment, the approach based on "pseudotyping" can be considered a useful complement to other serological assays. After fully characterising lentiviral pseudotypes bearing the SARS-CoV-2 spike protein, we employed them in pseudotype-based neutralisation assays in order to profile the neutralising activity of human serum samples from an Italian sero-epidemiological study. The results obtained with pseudotype-based neutralisation assays mirrored those obtained when the same panel of sera was tested against the wild type virus, showing an evident convergence of the pseudotype-based neutralisation and MN results. The overall results lead to the conclusion that the pseudotype-based neutralisation assay is a valid alternative to using the wild-type strain, and although this system needs to be optimised and standardised, it can not only complement the classical serological methods, but also allows serological assessments to be made when other methods cannot be employed, especially in a human pandemic context.

Keywords: SARS-CoV-2; wild type virus; lentiviral pseudotypes; biosafety; microneutralisation; serological assays

1. Introduction

In early December 2019, cases of severe pneumonia of unknown aetiology were reported by the China Health Authority. In January 2020, a novel coronavirus was identified as 2019-nCoV (subsequently renamed as SARS-CoV-2).

An initial site of infections was the Huanan seafood market, where live animals are sold. Progressively, human-to-human transmission occurred [1], causing a disease named coronavirus disease 2019 (COVID-19). On 20th July 2020, the World Health Organization (WHO) estimated the global incidence of COVID-19 as 14,348,858 cases and the number of the deaths as 603,691 [2].

SARS-CoV-2 is a member of the *Coronaviridae* family, which comprises two subfamilies of enveloped, positive-stranded RNA viruses. The subfamilies of *Coronavirinae* are classified in four genera: alpha-CoV, beta-CoV, gamma-CoV and delta-CoV [3].

Genome sequence analysis has shown that SARS-CoV-2 belongs to the Betacoronavirus genus, which includes Bat SARS-like coronavirus, Severe Acute Respiratory Syndrome coronavirus (SARS-CoV) and Middle Eastern Respiratory Syndrome coronavirus (MERS-CoV) [4].

The SARS-CoV-2 genome contains four main structural proteins: the spike (S), membrane (M), envelope (E) and nucleocapsid (N) protein [5,6].

The spike (S) protein of coronaviruses, a type I membrane glycoprotein expressed on the viral surface, mediates the attachment of SARS-CoV-2 to the target cells and its subsequently entry. As previously shown in the case of SARS-CoV [7,8], the SARS-CoV-2 S protein engages angiotensin-converting enzyme 2 (ACE2) as its host target receptor. ACE2 is the main host cell receptor of SARS-CoV-2 and plays a crucial role in the entry of the virus into the cells [9].

In addition, viral entry requires S protein priming by cellular proteases, such as the serine protease TMPRSS2, which allows the fusion of viral and cellular membranes to fuse [10,11]. As a result, the spike is cleaved into two subunits: the N-terminal domain, called S1, which is responsible for receptor binding [12–15], and a C-terminal S2 domain, which is responsible for fusion [14,15].

As the coronavirus S glycoprotein is surface-exposed and mediates entry into host cells, it is the main target of neutralising antibodies (Abs) [16] upon infection, and therefore, the focus of therapeutic strategies and vaccine design.

However, since SARS-CoV-2 displays marked pathogenicity (COVID-19) [17], working with the live virus (LV) implies the need for high biosafety levels laboratories (BSL3). By contrast, the lentiviral pseudotypes system, which has already been successfully adopted in the fight against emerging and re-emerging viruses, constitutes a useful, safe and versatile tool for studies on potential vaccines and therapies. Indeed, the lentiviral pseudotype platform can be efficiently used in conventional biosafety conditions to study cell type susceptibility on the bases of the cell's expression of ACE2 and protease priming [18–20]. Moreover, pseudotypes bearing the spike S-protein of the novel SARS-CoV-2 could prove essential for antibody detection and for the evaluation of neutralisation activity in association with the well-characterised serological methods, such as the Enzyme-linked immunoassay (ELISA) and Micro-Neutralisation assay (MN) [21–23].

In the present study, we described the production and characterisation of lentiviral pseudotype particles bearing the SARS-CoV-2 S protein and used these to study S-protein-mediated cell entry. Subsequently, SARS-CoV-2 pseudotypes were also used to measure neutralising antibody responses in serum samples derived from a subset of subjects involved in a sero-epidemiological study in the Tuscany region of Italy during the 2019 outbreak and a panel of negative confirmed sera.

The results were compared with the data obtained when the SARS-CoV-2 live virus was tested in the MN assay.

2. Materials and Methods

2.1. Cell Line Cultures

HEK 293 T/17 cells (Human embryonic kidney 293 cells) (ATCC–CRL 1573), MDCK cells (Madin-Darby Canine Kidney cells) (ATCC® CCL-34), Vero E6 cells (Epithelial cell line from the kidney of a normal monkey Cercopithecus aethiops) (ATCC–CRL 1586) and Caco2 cells (epithelial cell line from Human Colorectal Adenocarcinoma) (ATCC HTB37) were acquired from the American Type Culture Collection.

Huh-7 cells (Epithelial cell line from Human hepatocellular carcinoma) (ECACC—Code 01042712) and Hep G2 cells (Human Caucasian hepatocyte carcinoma) were provided by the University of Siena, Italy.

Hep G2 cells were cultured in RPMI 1640 (Gibco) supplemented with 2 mM L-Glutamine (Lonza, Milan, Italy), 100 units/mL penicillin-streptomycin (Lonza, Milano, Italy) and 10% foetal bovine serum (FBS) (Euroclone, Pero, Italy).

HEK293 T/17, MDCK and Huh-7 cell lines were cultured in Dulbecco's Modified Eagle's Medium (DMEM) High Glucose (Euroclone, Pero, Italy) supplemented with 2 mM L-Glutamine (Lonza, Milan, Italy), 100 units/mL penicillin-streptomycin (Lonza, Milan, Italy) and 10% of FBS (FBS Euroclone, Pero, Italy).

Vero E6 and Caco2 cells were cultured in Eagle's Minimum Essential Medium (EMEM) (Lonza, Milan, Italy) supplemented with 2 mM L-Glutamine (Lonza, Milan, Italy), 100 units/mL penicillin-streptomycin (Lonza, Milan, Italy) and FBS (Euroclone, Pero, Italy) to a final concentration of 10% for Vero E6 and 20% for Caco2.

All the cell lines used were incubated at 37 °C, 5% CO_2 in humidified atmosphere and were sub-cultured twice a week until passage 20.

2.2. Serum Samples

A total of 65 samples from an Italian sero-epidemiological study, anonymously collected in compliance with Italian ethics law, were provided by the laboratory of Molecular Epidemiology of the University of Siena, Italy. The human sera, derived from a sero-epidemiological study, had previously been tested in an ELISA assay as pre-screening, and positive, borderline and negative ELISA samples were tested in a micro-neutralisation assay, as previously described [24]. This panel of sera was subsequently tested with SARS-CoV-2 pseudotypes in order to compare the neutralisation profiles when they were tested against the live virus and the surrogate virus. As an internal positive control, a panel of samples collected from health care workers (confirmed positive for SARS-CoV-2 by Reverse Real-Time PCR) were kindly provided by Prof. Valentina Bollati, University of Milan.

In addition, three monoclonal antibodies (mAbs) were included in the serological assay: Human IgG1 anti-S1 CR3022 (Native Antigen, Oxford, UK), Human IgG1 Anti-RBD (eEnzyme, Gaithersburg, MD, USA) and Human Anti-IgM SARS-CoV-2 spike S1 CR3022 (Absolute Antibody, 21 Drydock Avenue, 7th Floor Boston, MA 02210, USA (1:100 starting dilutions).

2.3. Production, Quantification and Characterisation of Lentiviral Pseudotypes with S Protein from SARS-CoV-2

2.3.1. Plasmids

The full-length S protein (GenBank accession number: YP_009724390.1) was codon-optimised and synthesised (GenScript, Cina), and the S fragment was cloned into the expression vector as described previously [25]. The HIV *gag-pol* plasmid (p8.91) [26], the firefly luciferase-expressing plasmid (PCSFLW) [27], the pCAGGS-TMPRSS2 plasmid and the plasmid encoding for the spike's human ACE2 receptor were kindly provided by Dr. Nigel Temperton and have previously been described [28–30].

As a control, a vesicular stomatitis virus (VSV-G) plasmid was used (pCMV-VSV-G) (Addgene plasmid 8454; http://n2t.net/addgene:8454) [31]. The day before transfection, confluent plates of HEK 293T/17 cells were split 1:4 and seeded into 10 cm^2 plates in DMEM 10% FBS.

Cells (at the 60% of confluence) were co-transfected with the S plasmid from SARS-CoV-2 (2 ug/uL), HIV *gag-pol* (1 ug/uL) and the pCSFLW (1.5 ug/uL) using EndoFectin™ Lenti transfection reagent (Tebu Bio—217EF002, Via Pretorio 4—C.P. 70. I-20013 Magenta, Milano) in accordance with the manufacturer's instructions.

The following day, the supernatants were replaced with DMEM without phenol red (Thermo Fisher Scientific, 168 3rd Ave, Waltham, MA 02451, United States containing 10% FBS, and the plates were incubated for 48 h at 37 °C in an atmosphere of 5% CO_2. After 48 h, the supernatants of transfected cells were harvested and filtered by Millex-HA 0.45 um filter.

Concurrently, HEK 293T/17 cells were also transfected with VSV-G plasmid (1 μg/μL), and a no-spike control (Δ envelope) was generated by co-transfection with HIV *gag-pol* and pCSFLW plasmids only.

2.3.2. SARS-CoV-2 Pseudotypes Titration

For SARS-CoV-2 titration, a further transfection is required in order to allow pseudotypes to enter target cells.

The day before titration, HEK 293T/17 cells were co-transfected with two plasmids encoding for the ACE2 receptor gene and TMPRSS2, by means of EndoFectin™ Lenti transfection reagent; after overnight incubation at 37 °C, the supernatant was replaced by DMEM containing 10% FBS.

The following day, supernatants were serially two-fold diluted in a fresh cell culture medium in 96-well, flat-bottomed culture plates, and 1×10^4 HEK 293T/17 target cells were added to each well. As controls, VSV-G and Δ-envelope pseudotypes were also included. After 72 h, the luminescence of cell cultures (in Relative Luminescence Units or RLUs) was evaluated by luminometry (Tecan Infinite M1000 Pro Multi-Detection Plate Reader) using the Bright-Glo assay system (Bright-Glo™ Luciferase Assay System, Promega, Viale Piero e Alberto Pirelli, 6, 20126 Milano MI).

2.4. p24 Capsid ELISA

Serial dilutions of SARS-CoV-2 pseudotype-containing media were tested by means of the Lenti-X p24 Rapid titre kit (Cat. No. 632200) (Takara, Japan) in accordance with the manufacturer's instructions.

2.5. Western Blotting

In order to verify the incorporation of the S glycoprotein of SARS-CoV-2, the S protein expressed on the lentiviral pseudotypes was detected by Western blot analysis.

Western blot analysis of spike protein was performed on the supernatant from sub-confluent HEK 293T/17 cells co-transfected with HIV *gag-pol* plasmid, CSFLW plasmid and the S plasmid from SARS-CoV-2. Western blot analysis was also performed on LV in a BSL3 facility.

Δ-envelope (no-spike control) pseudotypes prepared with the same procedure were run as a negative control. SARS-CoV-2 pseudotypes, SARS-CoV-2 live virus and Δ-envelope pseudotypes were mixed with SDS sample buffer. The mixture was heated for 10 min at 75 °C and electrophoresis (50 μg of protein/sample) was carried out in 4–12% Bis-Tris Gels (Life Technologies, Carlsbad, CA, USA). Proteins were then blotted onto nitrocellulose membranes and incubated overnight with 500-fold diluted sera from convalescent SARS-CoV-2 patients. A Goat Anti-human IgG (Bethyl, 25043 FM 1097, Montgomery, TX 77356, United States) was used as a secondary antibody (1:5000 dilution). The chemiluminescent signals from the nitrocellulose membranes were captured by a camera system (ImageQuant LAS 400 instrument).

2.6. SARS-CoV-2 Pseudotypes Tropism Study

In this study, different cell lines have been tested in order to study their susceptibility to SARS-CoV-2 S protein driven entry, the role of the ACE2 receptor and TMPSSRS2 for S protein priming.

One day before pseudotypes titration, MDCK, Vero E6, Caco2, Hep G2 and Huh7 cells were transfected with the pCAGGS-TMPRSS2 plasmid, while HEK 293T/17 cells were co-transfected with ACE2 and pCAGGS-TMPRSS2 plasmids. After 24 h, the cells were removed by trypsinisation, counted and used for the subsequent titration.

In parallel with SARS-CoV-2 pseudotypes, VSV-G and Δ-envelope pseudotypes were titrated as controls. Plates were incubated for 48–72 h with the pseudotypes, at 37 °C in an atmosphere of 5% CO2, and the efficiency of pseudotypes entry was characterised on the basis of luciferase activity (Relative Luminescence Units or RLUs).

2.7. Pseudotype-Based Neutralisation Assays

To measure the neutralisation activity of this panel of sera, neutralising antibody titres were defined as endpoint two-fold seral dilutions of test samples, and the 50% inhibitory concentration (IC_{50}) was determined as the serum dilution resulting in a 50% reduction of a single round of infection (reporter gene-mediated signal). Values were expressed as a percentage in comparison with the signal from the cell-only control (equivalent to 100% neutralisation and/or no infection) and the signal from a pseudotype-only control (equivalent to 0% neutralisation or 100% infection).

In brief, two-fold serial dilution of serum samples, starting from 1:10, was performed in a culture medium (DMEM, 5% FBS, 1% PEN-STREP, 1% L-Glutamine). The serum was mixed with SARS-CoV-2 pseudotypes in a 1:1 vol/vol ratio in a 96-well culture plate. The virus input used was 1×10^6 RLU/well (based on the previous titration).

The serum-pseudotypes mixture was then incubated for 1 h at 37 °C in a humidified atmosphere with 5% CO2. After 1 h, HEK 293/ACE2 transfected cell suspensions (1.5×10^4 cell/mL) were seeded into each well of flat-bottomed tissue culture plates. The plates were incubated at 37 °C for 48–72 h, and the neutralising antibodies were characterised on the basis of luciferase activity.

2.8. Live Virus, Titration and Microneutralisation Assay

The SARS-CoV-2 strain 2019-nCov/Italy-INMI1-wild-type virus was purchased from the European Virus Archive Goes Global (EVAg, Spallanzani Institute, Via Portuense, 292, 00148–00153, Rome) and propagated in Vero E6 cells. The virus was titrated in a Tissue Culture Infective Dose 50% assay (TCID50) on 96-well culture plates with 1-log serial dilution. The plates were observed daily for a total of four days for the presence of cytopathic effect (CPE). The end-point titre was calculated according to the Spearman–Karber formula [32].

The MN assay was performed as previously reported by Manenti et al. [24]. Briefly, two-fold serial dilutions of serum samples were mixed with an equal volume of viral solution containing 100 TCID50 of SARS-CoV-2. The serum-virus mixture was incubated for 1 h at 37 °C in a humidified atmosphere with 5% CO_2, then passed to a VERO E6 culture plate. The plates were incubated for four days at 37 °C in a humidified atmosphere with 5% CO_2. After the incubation time, each well of a 96-well plate was inspected by means of an inverted optical microscope to evaluate the percentage of CPE.

2.9. Statistical Analyses

2.9.1. Calculation of SARS-CoV-2 Pseudotype Titres

Pseudotype transduction titres were estimated by means of Excel™ software; the pseudotype titres obtained at each point in a range of dilution points were expressed as RLU/mL, and the arithmetic mean was calculated. For the analyses of pseudotype-based neutralisation assays, titres were firstly normalised, and IC_{50} values were calculated by a non-linear regression model (log (inhibitor) vs. normalised response-variable slope) analysis. Titres were subsequently expressed as the range of dilution in which the IC_{50} value lay. In order to evaluate cell infectivity, two-way analysis of variance (ANOVA) with Dunnett posttest was used to test for statistical significance ($p > 0.05$ (ns, not significant), $p \leq 0.05$ (*), $p \leq 0.01$ (**), $p \leq 0.001$ (***), and $p \leq 0.0001$ (****)). For all statistical analyses, the GraphPad Prism version 8.4 package was used (GraphPad Software, GraphPad, 2365 Northside Dr., Suite 560, San Diego, CA 92108, USA).

2.9.2. Comparison between Live Virus Microneutralisation Titres (MNT) and Pseudotype Neutralising Titres (PNT)

The statistical analyses have been undertaken with the R software (version 3.6.2). Different approaches drove our statistical analyses, as shown in Figure 1.

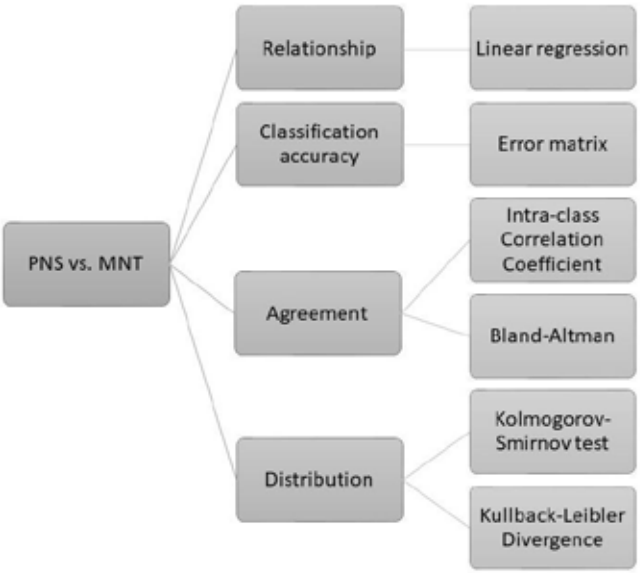

Figure 1. Flowchart of the statistical methods. Comparison between pseudotype neutralising titres (PNT) and live virus micro-neutralisation titres (MNT) was conducted via different approaches, which enabled us to elucidate the overall convergence of the PNT and MNT results.

All the titres underwent preliminary base-2 logarithmic transformation. In accordance with the classification approach, the titres greater than log2 (5) were labelled as "Positive," and otherwise as "Negative." With MNT taken as the reference ("true") results, the misclassifications were counted and displayed in an error matrix table.

A linear regression model provided a measure of the strength of the relationship between PNT and MNT. As the dependent variable, we considered the log2 of PNT, and as the independent variable, the log2 of MNT.

For the evaluation of the agreement between PNT and MNT, we used the intra-class correlation coefficient (ICC). In addition, the Bland–Altman method (BA) enabled us to search for possible systematic difference (bias) between the PNT and MNT, as well as to identify the presence of outliers. The BA evaluation mainly consists in a scatter plot of the differences between the measurements vs. their means. The 95% limits of agreement (LOAs) were calculated around the mean of the differences. We set a maximum acceptable difference (MAD) of 0.5 times the MNT, below which the observed PNT-MNT differences were considered as not having a significant biological effect. We interpreted the differences below the MAD and within the 95% limits of agreement as interchangeable. By comparing the distributions of PNT and MNT, we got further insight into their similarity degree. Thus, we applied the Kolmogorov–Smirnov test and measured the Kullbac–Leibler divergence (KLD). The former considers the largest difference between the empirical distribution functions of the PNT and MNT tests, and the latter is an information theoretic-based value, which indicates how much information is lost when taking PNT as an approximation of MNT. The KLD was calculated as the "true" reference the MNT distribution, and normalised as follows:

$$nKLD(p_{MNT} \| p_{PNT}) = \frac{1}{1 + e^{KLD}} - \frac{1}{2} \quad (1)$$

where *nKLD* is the normalised divergence, and *pMNT* and *pPNT* are the distributions of *MNT* and *PNT*, respectively. This normalisation restricts the divergence values in the range [−0.5, + 0.5], such that *nKLD* = 0 if the *PNT* distribution perfectly reproduces the *MNT* distribution, while the extremes *nKLD* = −0.5 or *nKLD* = 0.5 are attained if *KLD* tends towards infinite, (positive or negative infinite, respectively). Lastly, we conducted a bootstrap test (100,000 resamples with replacement from the *MNT* and *PNT* data) on the *KLD* statistic under the null hypothesis of *nKLD* = 0.

3. Results

3.1. SARS-CoV-2 Spike Protein Expression Evaluated by Western Blotting and p24 Quantification

SARS-CoV-2 S glycoprotein and gag-p24 in pseudotypes were characterised by immunoblot analysis and p24 ELISA, respectively.

To verify the expression of the spike protein in the SARS-CoV-2 pseudotypes, the spike was detected by Western blot; sera from convalescent SARS-CoV-2 patients, which have been shown to have a high neutralising titre in microneutralisation with a live virus, were used as the primary antibody, and goat anti-Human IgG as the secondary antibody.

SARS CoV-2 strain 2019-nCov/Italy wild-type virus (LV), which was handled in a level 3 bio-containment facility (BSL 3), was used as positive control in order to evaluate the spike glycoprotein expression, while a Δ-envelope pseudotype, prepared with the same procedure, was used as a negative control.

Three different batches of pseudotypes were tested; specific bands were found for SARS-CoV-2 pseudotypes and for SARS-CoV-2 live virus, but not for the Δ-envelope control (Figure 2).

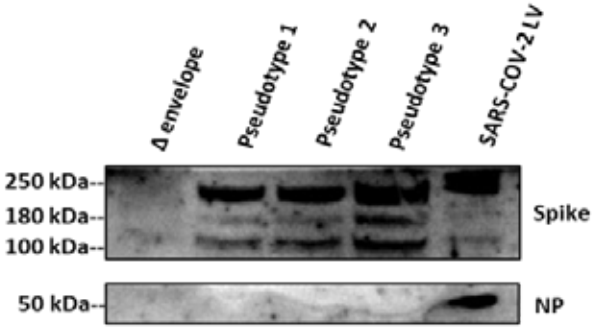

Figure 2. Incorporation of SARS-CoV-2 protein into pseudotypes. The spike protein of the particles was investigated by Western blotting. From left to right: lanes showing Δ-envelope pseudotype; SARS-CoV-2 Pseudotype batch 1, batch 2, batch 3; and SARS-CoV-2 live virus (LV). The LV was used as a positive control and the Δ-envelope (particles bearing no envelope protein), prepared with the same procedure, was used as a negative control. Uncleaved S protein, about 180 kDa; cleaved S protein, about 100 kDa; dimeric-trimeric S protein, above 250 kDa; Nucleocapsid protein, about 50 kDa. Experiments were done twice and one is shown.

Regarding the pseudotypes, we observed three main bands: one just below 250 kDa, and the remaining two bands at 180 kDa and 100 kDa, corresponding to the full-length and cleaved S protein, as shown in previous studies [33].

These two bands (180 kDa and 100 kDa) were barely detectable in the live virus, in which was observed one just above 250 kDa, possibly reflecting the dimeric-trimeric S protein (detected in the pseudotypes below 250 kDa), and the other band was around 50 kDa, possibly corresponding to the Nucleocapsid Protein (NP). The high glycosylation potential to which the spike is subjected during the infection differs from the spike expressed on the pseudotyped particles that do not undergo the same post-translational modifications [34]. This would explain the presence of a protein with a weight greater than 250 kDa in the wild type virus, compared to the three isoforms with detectable molecular weight between 100 KDa and below 250 kDa related to the pseudotypes [33].

Moreover, the quantitative data can slightly differ when a convalescence serum sample is used instead of an antibody (e.g., monoclonal antibody), specifically directed against a defined protein's portion.

Although, in this study, the evaluation of SARS-CoV-2 pseudotype titres is based on the reporter gene expression (RLUs/mL), a number of eight different batches of SARS-CoV-2 lentiviral pseudotypes

were also compared for the HIV-1 viral core protein p24 amount (directly correlating to the number of particles) by ELISA (values reported as pg of p24 for mL).

The results showed that all batches tested consistently contained around 13–15 pg/mL of p24 gag capsid protein, corresponding approximately to a titre of 1.30e + 05 RLUs/mL. Similar vector infectivity was also identified for VSV-G pseudotyped vectors, around 15–16 pg/mL of p24 gag capsid protein corresponding to an approximate titre of 1.56e + 05 RLUs/mL, while a value of 9–10 pg/mL, corresponding to a titre of 9.94e + 0 4, was obtained for Δ-envelope pseudotypes, as shown in Figure 3. The values obtained for the Delta envelope are slightly higher for the p24 amount compared to the RLUs. A possible explanation, as showed by Geraerts [35], is that p24 quantification by ELISA will detect cores lacking envelope glycoproteins (non-functional) as well as cores belonging to transduction competent (functional) pseudotypes, and this technique usually overestimates the functional vector titre. In fact, it also been shown that omission of the envelope plasmid during the vector production resulted in p24 being comparable with those of a normal production although with a non-detectable functional titre.

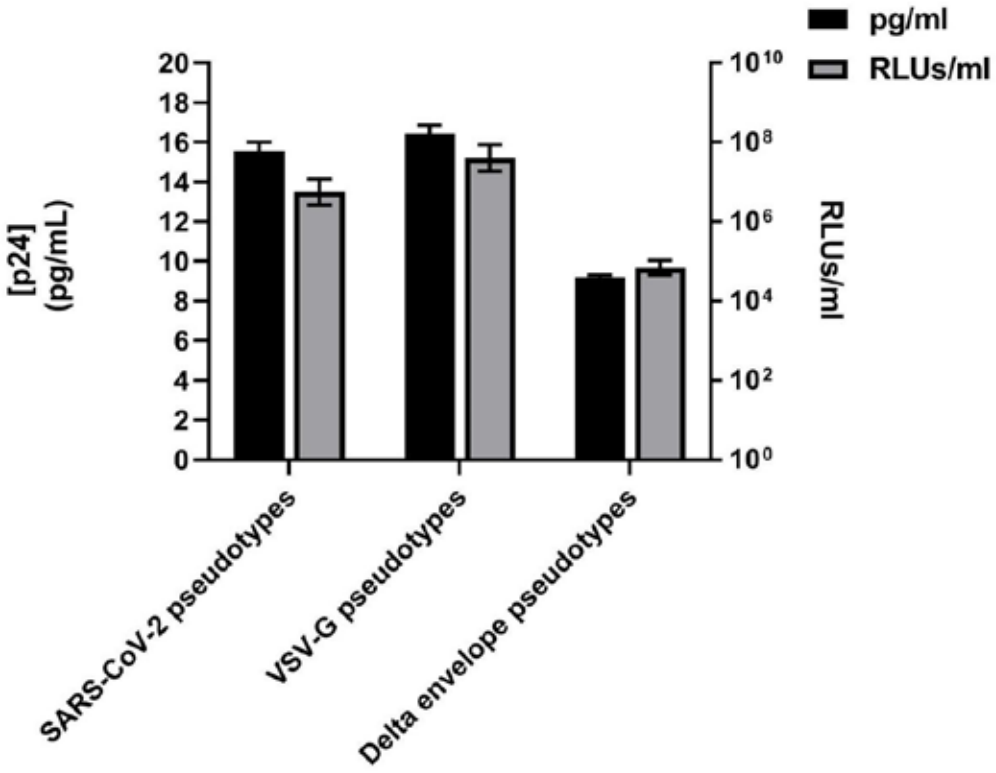

Figure 3. p24 quantification. Vector particle concentration (pg p24 protein per mL) determined by p24 ELISA and corresponding lentiviral vector infectivity (RLUs/mL). Values expressed as the means ± SD of independent measurements (n = 8).

3.2. Susceptibility of Cell Lines Panel to SARS-CoV-2 for Pseudotype-Based Neutralisation Assays

After the production of the SARS-CoV-2 pseudotypes, we asked which cell lines were susceptible to pseudotype-driven entry in order to have a panel of cell lines that can be used in downstream pseudotype-neutralisation assays. For this purpose, we used a panel of cell lines of human and animal origin.

Since SARS-CoV-2 live virus has been successfully isolated in Vero (African Green monkey kidney cell line), Vero E6 and Huh7 cell lines at high titres (as shown previously [24]), these were chosen for the cell tropism study. The Hep G2, MDCK and Caco cells were also included in this panel because a previous study evidenced ACE2 receptor expression, except for HEK 293T/17 [36]. However, HEK 293/17 cells have also been included as control cell line due to their high transfectability,

and they were firstly optimised using different ACE2-expressing plasmid concentrations. Based on these preliminary results, this panel of cell lines was tested against SARS-CoV-2, VSV-G and Delta envelope pseudotypes.

As also seen in previous studies [10,20], all the cell lines tested were highly susceptible to entry driven by VSV-G pseudotypes as demonstrated by titres of 10^7–10^8 RLUs/mL (Figure 4). All the cell lines tested were also susceptible to entry by SARS-CoV-2 pseudotypes, in particular, HEK 293 ACE2/TMPRSS2-transfected cells, as demonstrated by titres of 10^8–10^9 RLUs/mL. However, no statistical differences have been observed when SARS-CoV-2 pseudotypes have been tested against different cell lines. This comparable susceptibility can be due to the similar ACE2 expression (except for MDCK cell line as also showed by Nie et al. [20]). Moreover, co-transfection with TMPRSS2 protease can potentially level the titres obtained with different cell lines except for HEK 293/17.

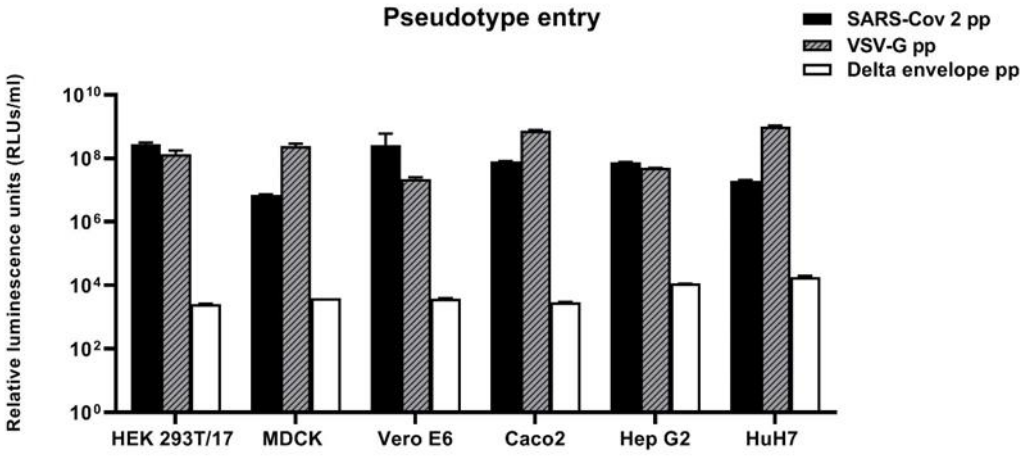

Figure 4. Susceptibility of cell lines to SARS-COV-2 driven entry. Cell lines of human and animal origin infected with Δ-envelope pseudotypes, SARS-COV-2 pseudotypes and VSV-G pseudotypes. At 72 h post-infection, pseudotype entry was analysed by determining luciferase activity in cell lysates. Cell background without pseudotypes infection was used for normalisation. Values are expressed as the means of independent results ± SD (n = 3). Two-way analysis of variance (ANOVA) test was used for statistical analysis.

As expected, when cell lines were tested with Δ-envelope control (particles without envelope proteins) the transduction activity dropped drastically (4-log), corresponding to 10^3–10^4 RLUs/mL (Figure 4).

3.3. Correlation between Live Virus MN and Pseudotype-Based Neutralisation Assays

As shown in Table 1, of 65 human serum samples tested, 24 proved positive for PNT, with titres ranging between 10–20 and >1280, and 28 positives for MNT, with titres ranging between 10 and 1280 (Table 2). Forty-one human samples were found negative for PNT and 37 negative for MNT. Therefore, only titres obtained for 4 sera were found to be discordant.

Table 1. Error matrix. Reliability of PNT compared to MNT in serum samples from 65 subjects. Titres greater than log2(5) were labelled as "Positive", and otherwise as "Negative". With MNT taken as the reference (true) results, the table shows the misclassifications.

	MNT		
PNT	**Negative**	**Positive**	**Total**
Negative	37	4	41
Positive	0	24	24
Total	37	28	65

Table 2. Panel of human sera tested by live virus MN and pseudotype-based neutralisation assays. Responses against SARS-CoV-2 are expressed as antibody titres for both assays (end-point dilution).

ID Samples	Live Virus Micro Neutralisation Titres (MNT)	Pseudotype Neutralisation Titres (PNT)
1	5	<10
2	5	<10
3	5	<10
4	5	<10
5	5	<10
6	5	<10
7	5	<10
8	5	<10
9	5	<10
10	5	<10
11	10	10–20
12	10	<10
13	10	<10
14	20	40–80
15	20	40–80
16	20	<10
17	20	<10
18	20	160–320
19	40	160–320
20	40	160–320
21	40	80–160
22	80	160–320
23	80	160–320
24	80	320–640
25	80	160–320
26	80	160–320
27	160	160–320
28	160	160–320
29	160	>1280
30	320	640–1280
31	640	>1280
32	640	20–40
33	640	320–640
34	640	>1280
35	640	>1280
36	1280	>1280
37	1280	>1280
38	1280	640–1280
39	5	<10
40	5	<10
41	5	<10
42	5	<10
43	5	<10
44	5	<10
45	5	<10
46	5	<10
47	5	<10
48	5	<10
49	5	<10
50	5	<10
51	5	<10
52	5	<10
53	5	<10

Table 2. *Cont.*

ID Samples	Live Virus Micro Neutralisation Titres (MNT)	Pseudotype Neutralisation Titres (PNT)
54	5	<10
55	5	<10
56	5	<10
57	5	<10
58	5	<10
59	5	<10
60	5	<10
61	5	<10
62	5	<10
63	5	<10
64	5	<10
65	5	<10

When mABs have been tested against pseudotypes and the live virus, no neutralisation activity was observed on MN, while an evident neutralisation profile was seen for PNT against Human Anti-IgM [37] SARS-CoV-2 spike S1 (IC_{50} > 1280).

In addition, we defined the parameters of sensitivity, specificity and accuracy. From the error matrix (Table 1), we obtained the following results: accuracy = 93.8% (95% CI (85.0%–98.3%)), which was significantly higher ($p < 0.0001$) than the no-information rate (56.9%), sensitivity = 85.7% (95% CI (67.3%–96.0%)) and specificity = 100% (95% CI (90.5%–100%)).

A simple linear regression was conducted to predict the log2 PNT based on the log2 MNT data (Figure 5). The linear regression was found to be significant, F (1, 63) = 344.6, $p < 0.0001$, with an $R^2 = 0.84$. The PNT increased 1.09 for each log2 of the MNT.

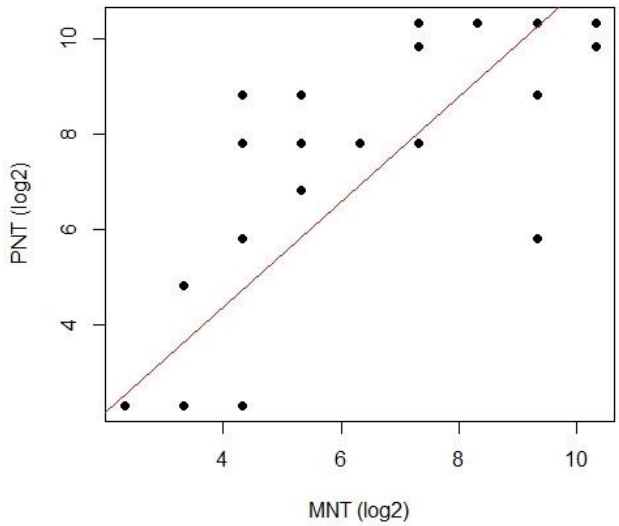

Figure 5. PNT vs. MNT relationship. The scatterplot of the MNT (*x*-axis) and PNT (*y*-axis) presented a linear pattern.

To evaluate the agreement between PNT and MNT, we used the intra-class correlation coefficient (ICC). The one-way random single score ICC (Table 3) calculated between the neutralisation titres PNT and MNT was 0.872 (95% CI (0.799–0.92)), $p < 0.0001$. This indicated excellent agreement [38].

Table 3. Summary of the intra-class correlation analysis. The one-way random single score ICC calculated between the neutralisation titres PNT and MNT was 0.872 (95% CI (0.799–0.92)), $p < 0.0001$.

Model	one-way
Type	agreement
Subjects	65
Raters	2
ICC(1)	0.872
CI 95%	[0.799–0.92]
F-test	14.7
p	<0.0001

The Bland–Altman (BA) analysis (Figure 6) revealed the presence of a significant relationship between differences and means, which made applying a regression approach consistent [39].

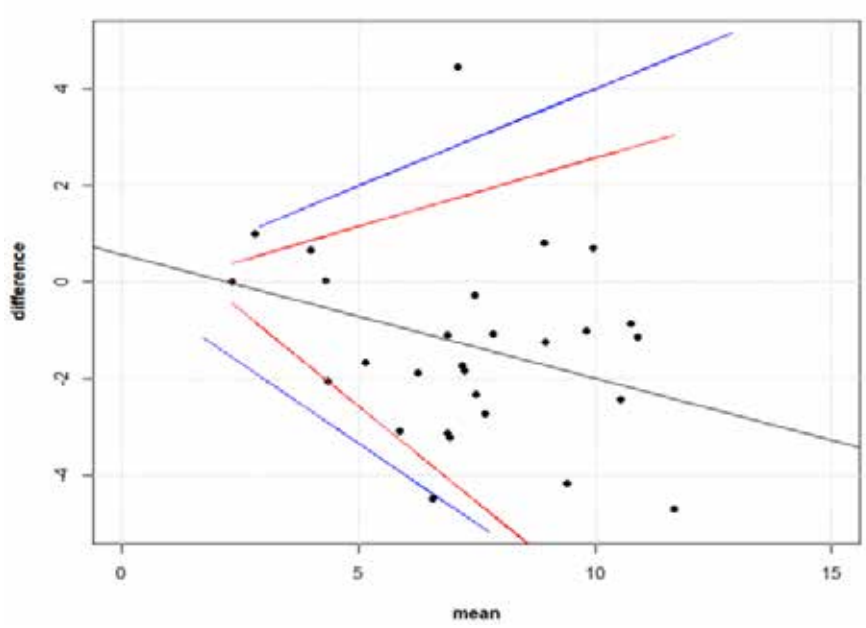

Figure 6. Bland–Altman plot. The Bland–Altman plot evaluating PNT-MNT agreement. The maximum acceptable differences (blue lines) embrace the LOAs (red lines), which makes the interpretation of the statistical results biologically plausible. We found a significant linear relationship between the differences and the means of the titres. Moreover, except for one outlier, all the differences were both biologically and statistically acceptable. In other words, there was substantial agreement between PNT and MNT.

We found that most of the data-points were within the 95% Limit of Agreements (LOAs), while one outlier, corresponding to a means of titres equal to 6.56 (log2-units), was detected. These findings suggested that there was substantial agreement and interchangeability between PNT and MNT.

In addition, the BA method enabled us to search for possible systematic difference (bias) between the PNT and MNT, and to identify the presence of outliers.

We also concluded, on the basis of the Kolmogorov–Smirnov test, that there was not enough evidence to reject the null hypothesis of equal distributions of PNT and MNT, (KS test = 0.17, $p = 0.31$). The normalised Kullback–Leibler divergences (nKLD) between the original PNT and MNT data was equal to −0.0098. The result of the bootstrap testing evidenced that the hypothesis of a zero nKLD between PNT and MNT was consistent with the data, $p = 0.44$ (Figure 7).

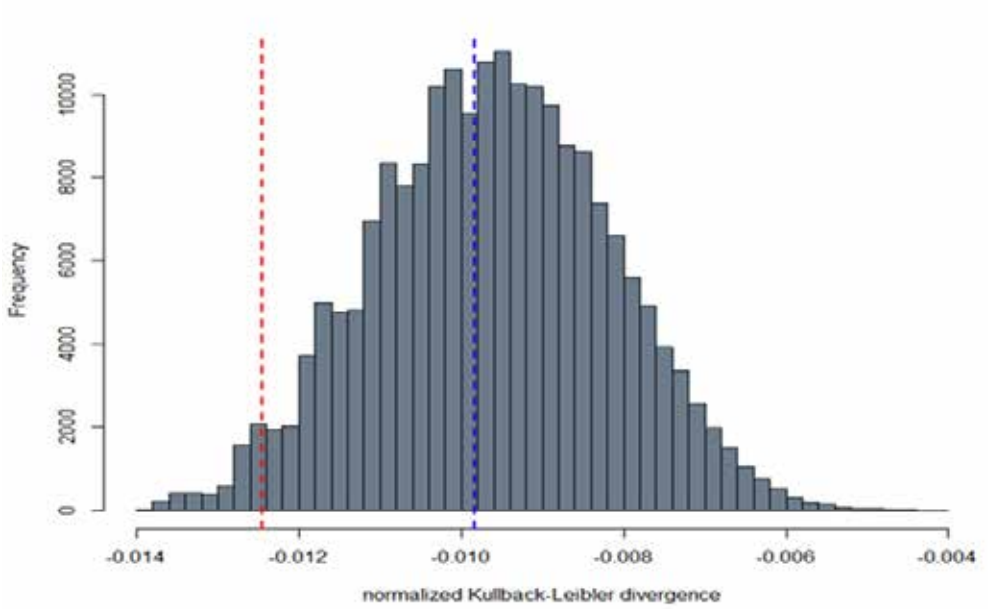

Figure 7. Bootstrap distribution of the Kullback–Leibler divergence. The histogram shows the distribution of the normalised Kullback–Leibler divergences evaluated via the bootstrap method. The nKLD between the original MNT and PNT was −0.0098 (blue dotted line). The MNT and PNT data were re-sampled with replacement 100,000 times. The red dotted line shows the 5% lower-tail quantile (−0.0125) of the bootstrap distribution. Since the observed nKLD was lower (in absolute value) than the 5% lower-tail quantile, we concluded that the divergence was not significantly different from zero (p-value = 0.44).

4. Discussions

The recent emergence of the novel pathogenic SARS-Coronavirus-2 constitutes a global health emergency. As previously shown [16,21], infection with SARS-CoV-2 elicits antibodies that bind to the virus. Although several studies are still ongoing regarding the virus and the complexity of the human immune responses, neutralising antibodies are known to be strongly correlated with protection [40]. Currently, polyclonal antibodies from recovered SARS-CoV-2-infected patients have been used to treat the SARS-CoV-2 infection, but identification of SARS-CoV-2-specific neutralising mAbs is still ongoing. Once such antibodies are selected and produced, the subsequent steps will involve testing for neutralising and/or cross-neutralising activity [41], which should simplify the analysis of functional humoral immune responses.

The demand for serological testing for SARS-CoV-2 is high, as there is a need to better quantify the number of cases of COVID-19, including asymptomatic carriers [42] and patients who have recovered.

As we know, SARS-CoV-2 have a strong pathogenicity and working with the wild-type virus implies the need for level 3 bio-containment facility, according to the WHO guidelines. However, serological assays for the evaluation of neutralising activity against the SARS-CoV-2 currently require the use of isolated-live virus.

Indeed, high-throughput methods (such as ELISA) that do not require the live virus are limited by the fact that they detect total antibody binding to SARS-CoV-2 or to some of its key constituent proteins [43,44]. For this reason, we produced and characterised a lentiviral pseudotype system that expresses the S protein of SARS-CoV-2 with the same approach used by for other pathogenic coronaviruses including SARS-CoV and MERS [29,30].

This pseudotype system can be a useful tool because of its safety and versatility. Its versatility lies in the fact that the virus can be pseudotyped with different envelope proteins [30,45,46]. Moreover, this approach does not necessitate handling the live virus, and does not require high-level

bio-containment facilities, as the pseudotype is devoid of virulent viral components and it is involved in a single round of replication [46].

The production of pseudotypes harbouring novel glycoproteins could permit elucidation of viral biological characteristics and a better understanding if they have potential to cause pandemics by the generation of mutants (via mutation of glycoprotein) without the risk of creating potentially dangerous viruses. It can also reflect key aspects of host cell entry and receptor binding specificity [10,33].

However, the need of additional reagents seems a requirement due to cellular receptor specificity and TMPRSS2 priming for SARS-CoV-2 pseudotypes; thus, necessitating us to optimise the batch-to-batch variations in order to reduce the variability in terms of pseudotype titres and stability.

Since previous studies have evidenced that most amino acid residues for ACE2 binding by SARS-CoV were also conserved in SARS-CoV-2 [47], we have studied different cell susceptibility to SARS-CoV-2 pseudotype entry. Understanding the entry mechanisms determined by the S glycoprotein and the susceptibility of different cells (based on specific cellular receptor expression) can also provide important information to study critical process in which the S spike protein of SARS- CoV-2 is involved. Moreover, the use of multiple target cell lines is particularly valid since one of the advantages of the pseudotype-based assays is that they are deployable across different stakeholder laboratories who have access to different cell lines.

It also represents a determinant for the development and optimisation of cell-based assays and for the screening of potential entry inhibitors.

Once the SARS-CoV-2 pseudotypes have been efficiently produced, we have also developed a lentiviral pseudotype-based assay that facilitates the accurate determination of neutralising antibody responses to SARS-CoV-2 that can be paired to the more intensive and laborious MN.

Although it is unclear as to how the display of S protein on heterologous virus impacts viral entry, antibody recognition and antibody neutralisation [48], our results suggest that pseudotype-based neutralisation assays correlate well with the MN assays when testing human sera, and our findings show significant accuracy, sensitivity and specificity when both assays are compared.

When employed in the screening of vaccinated human sera and other influenza serological studies [49–52], pseudotype-based neutralisation assays have been described to be more sensitive than classical MN. The sensitivity of pseudotypes can also detect particularly low antibody responses or facilitate the antibody's recognition that cannot always be determined by conventional assays, possibly due to lower density/quantity of glycoprotein expressed on the pseudotypes [53,54]. This could explain the ability of human mAB IgM to recognise certain epitopes of S1 protein, as it has been seen for pseudotype-based neutralisation but not for live virus MN.

Although the model (PNT instead of MNT) returned a relatively high percentage of false-negatives, in large-scale serological testing, having a highly specific test is advantageous when a false-positive result has a great clinical impact. Indeed, it guarantees against the risk of misclassification of the true-negative samples.

Undoubtedly, for a wider use of pseudotypes, it will be necessary to take into consideration additional aspects required for standardisation such as comparison between viral vectors/expression plasmids used, optimisation of particle titres and establishment of adequate positive, negative controls and reference standards (making it more difficult to evaluate the reproducibility of different serological assays).

Moreover, as in all the cell-based assays, cell input [55,56] is an important aspect in standardisation: the use of an automatic cell counter, cell viability and requirement of different proteases should be taken into account and it could be important for the consistency of the assay during different analytical sessions. Undoubtedly, a permanent cell line could be a valid alternative [18] (it would require only TMPRSS2 priming), and the generation of a cell line expressing proteases as a pseudotype producer could be investigated.

5. Conclusions

Our findings suggest that SARS-CoV-2 pseudotype-based assays and the live-virus microneutralisation correlate well when employed in testing antibody responses against the novel SARS-CoV-2 virus. Undoubtedly, they would help to dissect out these diversities of immunological responses, and they can, additionally, have an important role in evaluating the neutralising antibody potency (but not necessarily predicting protection), and in testing the efficacy of potential SARS-CoV-2 vaccines.

Author Contributions: Conceptualization, I.H., E.M. (Eleonora Molesti) and A.M.; methodology, I.H., E.M. (Eleonora Molesti), E.C., L.B., A.M.; validation, I.H, and E.M. (Eleonora Molesti); formal analysis, I.H., E.M. (Eleonora Molesti) and P.P.; resources, E.M., N.JT.; data curation, P.P., I.H., E.M. (Eleonora Molesti); writing—original draft preparation, I.H. and E.M. (Eleonora Molesti); writing—review, I.H., E.M. (Eleonora Molesti), L.B., N.JT., A.M. and E.M.; visualization, I.H., E.M. (Eleonora Molesti) and P.P.; supervision and project administration, E.M. All authors have read and agreed to the published version of the manuscript.

Funding: This publication was supported by the European Virus Archive goes Global (EVAg) project, which has received funding from the European Union's Horizon 2020 research and innovation programme under grant agreement No 653316.

Acknowledgments: Thanks to Claudia Trombetta and Serena Marchi from the Department of Molecular and Developmental Medicine, University of Siena, Italy, for providing us the human serum samples from the sero-epidemiological study on SARS-CoV-2. Thanks to Prof. Valentina Bollati, from the University of Milan, for providing the sera sample from Covid-19-positive healthcare workers. Thanks to Nigel Temperton, and the Pseudotypes Unit, University of Kent, for providing the panel of plasmids used for SARS-CoV-2 pseudotype production. We thank also: Virginia Cianchi and Donata Martinuzzi for their lab support in Vismederi Research.

Conflicts of Interest: The authors declare no conflict of interest.

References

1. Chan, J.F.-W.; Yuan, S.; Kok, K.-H.; To, K.K.-W.; Chu, H.; Yang, J.; Xing, F.; Liu, J.; Yip, C.C.-Y.; Poon, R.W.-S.; et al. A familial cluster of pneumonia associated with the 2019 novel coronavirus indicating person-to-person transmission: A study of a family cluster. *Lancet* **2020**, *395*, 514–523. [CrossRef]
2. WHO 2020, Coronavirus Disease 2019 (COVID19) Situation Report 23. Coronavirus Disease 2019 (COVID-19) Situation Report—23. Available online: https://www.who.int/docs/default-source/coronaviruse/situation-reports/20200212-sitrep-23-ncov.pdf?sfvrsn=41e9fb78_4 (accessed on 10 July 2020).
3. Fehr, A.R.; Perlman, S. Coronaviruses: An Overview of Their Replication and Pathogenesis. *Methods Mol. Biol.* **2015**, *1282*, 1–23. [CrossRef] [PubMed]
4. Zhou, P.; Yang, X.-L.; Wang, X.-G.; Hu, B.; Zhang, L.; Zhang, W.; Si, H.-R.; Zhu, Y.; Li, B.; Huang, C.-L.; et al. A pneumonia outbreak associated with a new coronavirus of probable bat origin. *Nature* **2020**, *579*, 270–273. [CrossRef] [PubMed]
5. Wormser, G.P.; Aitken, C. *Clinical Virology*, 3rd ed.; Richman, D.D., Whitley, R.J., Hayden, F.G., Eds.; ASM Press: Washington, DC, USA, 2009; 1408p.
6. Wu, A.; Peng, Y.; Huang, B.; Ding, X.; Wang, X.; Niu, P.; Meng, J.; Zhu, Z.; Zhang, Z.; Wang, J.; et al. Genome Composition and Divergence of the Novel Coronavirus (2019-nCoV) Originating in China. *Cell Host Microbe* **2020**, *27*, 325–328. [CrossRef]
7. Li, W.; Zhang, C.; Sui, J.; Kuhn, J.H.; Moore, M.J.; Luo, S.; Wong, S.K.; Huang, I.C.; Xu, K.; Vasilieva, N.; et al. Receptor and viral determinants of SARS-coronavirus adaptation to human ACE2. *EMBO J.* **2005**, *24*, 1634–1643. [CrossRef]
8. Li, F.; Li, W.; Farzan, M.; Harrison, S.C. Structure of SARS coronavirus spike receptor-binding domain complexed with receptor. *Science* **2005**, *309*, 1864–1868. [CrossRef]
9. Zhang, H.; Penninger, J.M.; Li, Y.; Zhong, N.; Slutsky, A.S. Angiotensin-converting enzyme 2 (ACE2) as a SARS-CoV-2 receptor: Molecular mechanisms and potential therapeutic target. *Intensive Care Med.* **2020**, *46*, 586–590. [CrossRef]
10. Hoffmann, M.; Kleine-Weber, H.; Schroeder, S.; Krüger, N.; Herrler, T.; Erichsen, S.; Schiergens, T.S.; Herrler, G.; Wu, N.-H.; Nitsche, A.; et al. SARS-CoV-2 Cell Entry Depends on ACE2 and TMPRSS2 and Is Blocked by a Clinically Proven Protease Inhibitor. *Cell* **2020**, *181*, 271–280. [CrossRef]

11. Glowacka, I.; Bertram, S.; Müller, M.A.; Allen, P.; Soilleux, E.; Pfefferle, S.; Steffen, I.; Tsegaye, T.S.; He, Y.; Gnirss, K.; et al. Evidence that TMPRSS2 activates the severe acute respiratory syndrome coronavirus spike protein for membrane fusion and reduces viral control by the humoral immune response. *J. Virol.* **2011**, *85*, 4122–4134. [CrossRef]
12. Wong, S.K.; Li, W.; Moore, M.J.; Choe, H.; Farzan, M. A 193-amino acid fragment of the SARS coronavirus S protein efficiently binds angiotensin-converting enzyme 2. *J. Biol. Chem.* **2004**, *279*, 3197–3201. [CrossRef]
13. Liu, S.; Xiao, G.; Chen, Y.; He, Y.; Niu, J.; Escalante, C.R.; Xiong, H.; Farmar, J.; Debnath, A.K.; Tien, P.; et al. Interaction between heptad repeat 1 and 2 regions in spike protein of SARS-associated coronavirus: Implications for virus fusogenic mechanism and identification of fusion inhibitors. *Lancet* **2004**, *363*, 938–947. [CrossRef]
14. Simmons, G.; Gosalia, D.N.; Rennekamp, A.J.; Reeves, J.D.; Diamond, S.L.; Bates, P. Inhibitors of cathepsin L prevent severe acute respiratory syndrome coronavirus entry. *Proc. Natl. Acad. Sci. USA* **2005**, *102*, 11876–11881. [CrossRef] [PubMed]
15. Bosch, B.J.; Martina, B.E.E.; Van Der Zee, R.; Lepault, J.; Haijema, B.J.; Versluis, C.; Heck, A.J.R.; De Groot, R.; Osterhaus, A.D.M.E.; Rottier, P.J.M. Severe acute respiratory syndrome coronavirus (SARS-CoV) infection inhibition using spike protein heptad repeat-derived peptides. *Proc. Natl. Acad. Sci. USA* **2004**, *101*, 8455–8460. [CrossRef] [PubMed]
16. Wu, F.; Wang, A.; Liu, M.; Wang, Q.; Chen, J.; Xia, S.; Ling, Y.; Zhang, Y.; Xun, J.; Lu, L.; et al. Neutralizing Antibody Responses to SARS-CoV-2 in a COVID-19 Recovered Patient Cohort and Their Implications. *medRxiv* **2020**. [CrossRef]
17. Cheng, H.Y.; Jian, S.W.; Liu, D.P.; Ng, T.C.; Huang, W.T.; Lin, H.H. High transmissibility of COVID-19 near symptom onset. *medRxiv* **2020**. [CrossRef]
18. Crawford, K.H.D.; Eguia, R.; Dingens, A.S.; Loes, A.N.; Malone, K.D.; Wolf, C.R.; Chu, H.Y.; Tortorici, M.A.; Veesler, D.; Murphy, M.; et al. Protocol and Reagents for Pseudotyping Lentiviral Particles with SARS-CoV-2 Spike Protein for Neutralization Assays. *Viruses* **2020**, *12*, 513. [CrossRef]
19. Millet, J.K.; Tang, T.; Nathan, L.; Jaimes, J.A.; Hsu, H.-L.; Daniel, S.; Whittaker, G.R. Production of Pseudotyped Particles to Study Highly Pathogenic Coronaviruses in a Biosafety Level 2 Setting. *J. Vis. Exp.* **2019**, *145*, e59010. [CrossRef]
20. Nie, J.; Li, Q.; Wu, J.; Zhao, C.; Hao, H.; Liu, H.; Zhang, L.; Nie, L.; Qin, H.; Wang, M.; et al. Establishment and validation of a pseudovirus neutralization assay for SARS-CoV-2. *Emerg. Microbes Infect.* **2020**, *9*, 680–686. [CrossRef]
21. Ju, B.; Zhang, Q.; Ge, X.; Wang, R.; Yu, J.; Shan, S.; Zhou, B.; Song, S.; Tang, X.; Yu, J.; et al. Potent human neutralizing antibodies elicited by SARS-CoV-2 infection. *bioRxiv* **2020**. [CrossRef]
22. Trombetta, C.M.; Remarque, E.J.; Mortier, D.; Montomoli, E. Comparison of hemagglutination inhibition, single radial hemolysis, virus neutralization assays, and ELISA to detect antibody levels against seasonal influenza viruses. *Influ. Other Respir. Viruses* **2018**, *12*, 675–686. [CrossRef]
23. Manenti, A.; Maciola, A.K.; Trombetta, C.M.; Kistner, O.; Casa, E.; Hyseni, I.; Razzano, I.; Torelli, A.; Montomoli, E. Influenza Anti-Stalk Antibodies: Development of a New Method for the Evaluation of the Immune Responses to Universal Vaccine. *Vaccines* **2020**, *8*, 43. [CrossRef] [PubMed]
24. Manenti, A.; Maggetti, M.; Casa, E.; Martinuzzi, D.; Torelli, A.; Trombetta, C.M.; Marchi, S.; Montomoli, E. Evaluation of SARS-CoV-2 neutralizing antibodies using a CPE-based colorimetric live virus micro-neutralization assay in human serum samples. *J. Med Virol.* **2020**. [CrossRef] [PubMed]
25. Thompson, C.; Grayson, N.; Paton, R.; Lourenço, J.; Penman, B.; Lee, L.N.; Odon, V.; Mongkolsapaya, J.; Chinnakannan, S.; Dejnirattisai, W.; et al. Neutralising antibodies to SARS coronavirus 2 in Scottish blood donors—A pilot study of the value of serology to determine population exposure. *medRxiv* **2020**. [CrossRef]
26. Zufferey, R.; Nagy, D.; Mandel, R.J.; Naldini, L.; Trono, D. Multiply attenuated lentiviral vector achieves efficient gene delivery in vivo. *Nat. Biotechnol.* **1997**, *15*, 871–875. [CrossRef]
27. Zufferey, R.; Dull, T.; Mandel, R.J.; Bukovsky, A.; Quiroz, D.; Naldini, L.; Trono, D. Self-Inactivating Lentivirus Vector for Safe and Efficient In Vivo Gene Delivery. *J. Virol.* **1998**, *72*, 9873–9880. [CrossRef] [PubMed]
28. Böttcher, E.; Matrosovich, T.; Beyerle, M.; Klenk, H.-D.; Garten, W.; Matrosovich, M. Proteolytic Activation of Influenza Viruses by Serine Proteases TMPRSS2 and HAT from Human Airway Epithelium. *J. Virol.* **2006**, *80*, 9896–9898. [CrossRef]

29. Temperton, N.; Chan, P.K.; Simmons, G.; Zambon, M.C.; Tedder, R.S.; Takeuchi, Y.; Weiss, R.A. Longitudinally Profiling Neutralizing Antibody Response to SARS Coronavirus with Pseudotypes. *Emerg. Infect. Dis.* **2005**, *11*, 411–416. [CrossRef] [PubMed]
30. Grehan, K.; Ferrara, F.; Temperton, N. An optimised method for the production of MERS-CoV spike expressing viral pseudotypes. *MethodsX* **2015**, *2*, 379–384. [CrossRef]
31. Stewart, S.A.; Dykxhoorn, D.M.; Palliser, D.; Mizuno, H.; Yu, E.Y.; An, N.S.; Sabatini, D.M.; Chen, I.S.; Hahn, W.C.; Sharp, P.A.; et al. Lentivirus-delivered stable gene silencing by RNAi in primary cells. *RNA* **2003**, *9*, 493–501. [CrossRef]
32. Kundi, M. One-hit models for virus inactivation studies. *Antivir. Res.* **1999**, *41*, 145–152. [CrossRef]
33. Ou, X.; Liu, Y.; Lei, X.; Li, P.; Mi, D.; Ren, L.; Guo, L.; Guo, R.; Chen, T.; Hu, J.; et al. Characterization of spike glycoprotein of SARS-CoV-2 on virus entry and its immune cross-reactivity with SARS-CoV. *Nat. Commun.* **2020**, *11*, 1–12. [CrossRef] [PubMed]
34. Shajahan, A.; Supekar, N.T.; Gleinich, A.; Azadi, P. Deducing the N- and O-glycosylation profile of the spike protein of novel coronavirus SARS-CoV-2. *Glycobiology* **2020**. [CrossRef] [PubMed]
35. Geraerts, M.; Willems, S.; Baekelandt, V.; Debyser, Z.; Gijsbers, R. Comparison of lentiviral vector titration methods. *BMC Biotechnol.* **2006**, *6*, 34. [CrossRef] [PubMed]
36. Material not intended for publication: No. Author. Affiliation, City, State. FACS analysis, 2020.
37. Amanat, F.; Stadlbauer, D.; Strohmeier, S.; Nguyen, T.H.O.; Chromikova, V.; McMahon, M.; Jiang, K.; Arunkumar, G.A.; Jurczyszak, D.; Polanco, J.; et al. A serological assay to detect SARS-CoV-2 seroconversion in humans. *Nat. Med.* **2020**, *26*, 1033–1036. [CrossRef] [PubMed]
38. Cicchetti, D.V. Guidelines, criteria, and rules of thumb for evaluating normed and standardized assessment instruments in psychology. *Psychol. Assess.* **1994**, *6*, 284–290. [CrossRef]
39. Bland, J.M.; Altman, U.G. Measuring agreement in method comparison studies. *Stat. Methods Med. Res.* **1999**, *8*, 135–160. [CrossRef]
40. Bootz, A.; Karbach, A.; Spindler, J.; Kropff, B.; Reuter, N.; Sticht, H.; Winkler, T.H.; Britt, W.J.; Mach, M. Protective capacity of neutralizing and non-neutralizing antibodies against glycoprotein B of cytomegalovirus. *PLoS Pathog.* **2017**, *13*, e1006601. [CrossRef]
41. Jiang, S.; Hillyer, C.; Du, L. Neutralizing Antibodies against SARS-CoV-2 and Other Human Coronaviruses. *Trends Immunol.* **2020**, *41*, 355–359. [CrossRef]
42. Milani, G.P.; Montomoli, E.; Bollati, V.; Albetti, B.; Bandi, C.; Bellini, T.; Bonzini, M.; Buscaglia, M.; Cantarella, C.; Cantone, L.; et al. SARS-CoV-2 infection among asymptomatic homebound subjects in Milan, Italy. *Eur. J. Intern. Med.* **2020**, *78*, 161–163. [CrossRef]
43. Perera, R.A.; Mok, C.K.; Tsang, O.T.; Lv, H.; Ko, R.L.; Wu, N.C.; Yuan, M.; Leung, W.S.; Mc Chan, J.; Chik, T.S.; et al. Serological assays for severe acute respiratory syndrome coronavirus 2 (SARS-CoV-2), March 2020. *Eurosurveillance* **2020**, *25*, 2000421. [CrossRef]
44. Seow, J.; Graham, C.; Merrick, B.; Acors, S.; Steel, K.J.; Hemmings, O.; O'Bryne, A.; Kouphou, N.; Pickering, S.; Galao, R.; et al. Longitudinal evaluation and decline of antibody responses in SARS-CoV-2 infection. *MedRxiv* **2020**. [CrossRef]
45. Molesti, E.; Cattoli, G.; Ferrara, F.; Böttcher-Friebertshäuser, E.; Terregino, C.; Temperton, N. The production and development of H7 Influenza virus pseudotypes for the study of humoral responses against avian viruses. *J. Mol. Genet. Med. Int. J. Biomed. Res.* **2013**, *7*, 315–320. [CrossRef]
46. Li, Q.; Liu, Q.; Huang, W.; Li, X.; Wang, Y. Current status on the development of pseudoviruses for enveloped viruses. *Rev. Med. Virol.* **2018**, *28*, e1963. [CrossRef]
47. Li, W.; Moore, M.J.; Vasilieva, N.; Sui, J.; Wong, S.K.; Berne, M.A.; Somasundaran, M.; Sullivan, J.L.; Luzuriaga, K.; Greenough, T.C.; et al. Angiotensin-converting enzyme 2 is a functional receptor for the SARS coronavirus. *Nature* **2003**, *426*, 450–454. [CrossRef]
48. Case, J.B.; Rothlauf, P.W.; Chen, R.E.; Liu, Z.; Zhao, H.; Kim, A.S.; Bloyet, L.-M.; Zeng, Q.; Tahan, S.; Droit, L.; et al. Neutralizing antibody and soluble ACE2 inhibition of a replication-competent VSV-SARS-CoV-2 and a clinical isolate of SARS-CoV-2. *Cell Host Microbe* **2020**. [CrossRef] [PubMed]
49. Alberini, I.; Del Tordello, E.; Fasolo, A.; Temperton, N.; Galli, G.; Gentile, C.; Montomoli, E.; Hilbert, A.K.; Banzhoff, A.; Del Giudice, G.; et al. Pseudoparticle neutralization is a reliable assay to measure immunity and cross-reactivity to H5N1 influenza viruses. *Vaccine* **2009**, *27*, 5998–6003. [CrossRef] [PubMed]

50. Molesti, E.; Wright, E.; Terregino, C.; Rahman, R.; Cattoli, G.; Temperton, N. Multiplex Evaluation of Influenza Neutralizing Antibodies with Potential Applicability to In-Field Serological Studies. *J. Immunol. Res.* **2014**, *2014*, 457932. [CrossRef] [PubMed]
51. Wang, W.; Butler, E.N.; Veguilla, V.; Vassell, R.; Thomas, J.T.; Moos, M.; Ye, Z.; Hancock, K.; Weiss, C.D. Establishment of retroviral pseudotypes with influenza hemagglutinins from H1, H3, and H5 subtypes for sensitive and specific detection of neutralizing antibodies. *J. Virol. Methods* **2008**, *153*, 111–119. [CrossRef] [PubMed]
52. Garcia, J.-M.; Lagarde, N.; Ma, E.S.; De Jong, M.D.; Peiris, J.M. Optimization and evaluation of an influenza A (H5) pseudotyped lentiviral particle-based serological assay. *J. Clin. Virol.* **2010**, *47*, 29–33. [CrossRef]
53. Wright, E.; Temperton, N.; Marston, D.A.; McElhinney, L.M.; Fooks, A.R.; Weiss, R.A. Investigating antibody neutralization of lyssaviruses using lentiviral pseudotypes: A cross-species comparison. *J. Gen. Virol.* **2008**, *89*, 2204–2213. [CrossRef]
54. Logan, N.; McMonagle, E.; Drew, A.A.; Takahashi, E.; McDonald, M.; Baron, M.; Gilbert, M.; Cleaveland, S.; Haydon, D.T.; Hosie, M.J.; et al. Efficient generation of vesicular stomatitis virus (VSV)-pseudotypes bearing morbilliviral glycoproteins and their use in quantifying virus neutralising antibodies. *Vaccine* **2016**, *34*, 814–822. [CrossRef] [PubMed]
55. The United States Pharmacopeial Convention. *Design and Development of Biological Assays*; The United States Pharmacopeial Convention: Rockville, MD, USA, 2010; Volume 1032, pp. 1–36.
56. The United States Pharmacopeial Convention. *Biological Assay Validation*; The United States Pharmacopeial Convention: Rockville, MD, USA, 2010; Volume 1033, pp. 1–25.